Atom transfer radical polymerisation -towards the synthesis of a fully-functional photorefractive polymer

Christopher Anthony Wyres

The University of Aston in Birmingham

September 2000

The University of Aston in Birmingham

Atom transfer radical polymerisation -towards the synthesis of a fully-functional photorefractive polymer

Christopher Anthony Wyres

A thesis submitted for the degree of Doctor of Philosophy

September 2000

Summary

Atom transfer radical polymerisation (ATRP) of styrene in xylene solution initiated with 1-phenylethyl bromide and mediated by CuBr/N-propyl-2-pyridinemethanimine catalyst complex was studied. The polymerisation was ill-controlled, yielding polymers with broad molecular weight distributions and values of number average molecular weight considerably higher than the theoretical values calculated from 100% initiator efficiency. The degree of control afforded over the polymerisation was enhanced by use of a more soluble catalyst complex, CuBr/N-octyl-2-pyridinemethanimine. Furthermore, the use of a more polar solvent, diglyme, generated a homogeneous catalyst complex that facilitated the production of polymers having narrow molecular weight distributions ($1.10 < PDi < 1.20$).

The kinetics of the atom transfer radical polymerisation of methyl methacrylate at 90°C in diglyme solution initiated with ethyl-2-bromo*iso*butyrate and mediated by CuBr/N-octyl-2-pyridinemethanimine was studied and the orders of the reaction were established. The effect on the rate of polymerisation of the ratio of CuBr:N-octyl-2-pyridinemethanimine was also determined.

The temperature dependencies of the rate of polymerisation of methyl methacrylate in diglyme solution and xylene solution were studied, and were found to be non-linear and dependent upon the polarity of the solvent.

The use of highly polar aprotic solvents, such as N,N-dimethylformamide and dimethylsulphoxide, was found to be detrimental to the degree of control afforded over the polymerisation of methyl methacrylate. This was circumvented by use of a 5-fold excess, over that conventionally used, of catalyst complex.

The atom transfer radical polymerisation of (4-nitrophenyl)-[3-[N-[2-(methacryloyloxy)ethyl]carbazolyl]]diazene in dimethyl sulphoxide solution was studied. Although homopolymerisation yielded only oligomers, copolymerisation of this monomer with methyl methacrylate was found to be readily achievable.

Keywords: ATRP, Styrene; Methyl methacrylate; Polar solvents; Fully-functional photorefractive polymer.

To those who have educated me.

Acknowledgements

Sincere thanks to Dr Allan Amass, for not only granting me this opportunity, but also for all of his advice and support over the last four years, some of which was beyond the call of duty. I would also like to thank Dr I. Marcia Hohn and Dr Eammon Colclough of DERA for all of their support, particularly as they have subsequently engineered a position for me within their organisation.

I acknowledge the hard work of the support staff in the department and thank them for their effort: Steve Ludlow, for always getting the best deal and for paying me in beer for all the odd-jobs that I've done for him; Roger and Ian in workshops, for repairing those vacuum pumps even though I was one of Amass' lot; Mike Lea for fixing every piece of electrical equipment that we managed break in the lab; Alex Stewart, for his glassblowing services and his constant reminders about how amateur my attempts to construct glassware were; Mike Perry, for running the fastest NMR service in the West Midlands and for constantly reminding me what a poor season Newcastle United were having.

I would like to say cheers to my fellow lab-mates, past and present, for making my time at Aston enjoyable; Graeme for those afternoons down the pub, Iris for teaching us all the wrong Chinese words, Hassen for invaluable discussions about football and occasionally chemistry, Tristan for translating the local dialect into English, Pete for proving that man can survive on pizza alone, Wendy for warning us when Allan was in a "good" mood, James, Colin, Rob, Nigel, Adrian, and all the French exchange students.

I would also like to thank my family for all the support, I could not have done it without you! I particularly thank Melanie for putting up with me for this long.

Contents

List of figures

List of schemes

List of tables

1. Introduction

1.1 The photorefractive effect

The photorefractive (PR) effect is defined as the spatial modulation of the index of refraction due to charge distribution in an optically non-linear material. It is generally believed that the effect is comprised of four basic processes:

(1) The photogeneration of charge carriers by a spatially modulated light intensity.
(2) The transport of the charge carriers away from the sight of generation, either by thermal diffusion or electric drift.
(3) The trapping of the charge carriers in sites distant from the sites of generation, resulting in charge separation and hence the formation of a space-charge field.
(4) The formation of a phase grating, as a result of the modulation of the index of refraction by the space-charge field.

Therefore, the necessary components of a photorefractive material are a photoionisable charge generator, a charge transporting medium, charge trapping sites, and a dependence of the index of refraction upon space-charge field. Figure 1.1 illustrates the microscopic processes and the optical standing wave pattern that result from the intersection of two coherent beams of light in such a material.

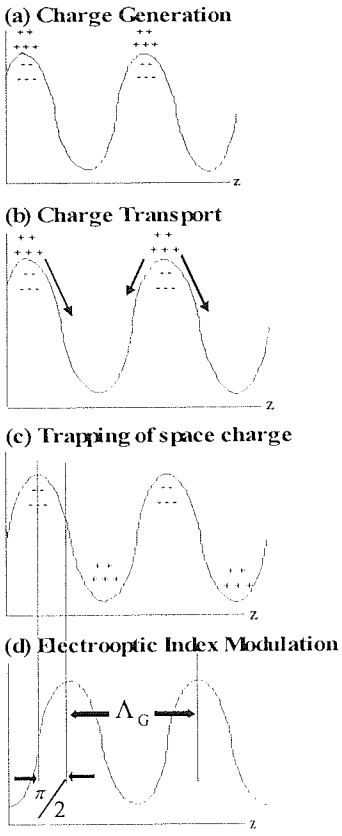

Figure 1.1. Schematic view of the processes involved in the formation of a photorefractive grating.

The spatially modulated intensity pattern manifested in the intersection region is comprised of light and dark planes and possesses a spatial wavelength, Λ_G, which is given by

$$\Lambda_G = \frac{\lambda_0}{2n\sin\left[\left(\theta_2 - \theta_1\right)/2\right]} \tag{1.1}$$

where n is the index of refraction of the material, λ_0 is the optical wavelength in free space, and θ_1 and θ_2 are the internal angles of incidence of the two writing beams relative to the sample normal. The magnitude of the grating wavevector, K_G, is given by

$$K_G = \frac{2\pi}{\Lambda_G} \tag{1.2}$$

If the direction of this grating wavevector is taken as the direction normal to the light and dark planes and this is the z-axis, then the optical intensity follows the offset sinusoidal pattern illustrated in figure 1.1(a). Charges are photogenerated at the light intensity maxima by absorption of the optical radiation, are transported away from the sites of generation and become resident in trapping centres, forming a non-uniform space-charge distribution. It is generally accepted that the charge generating step involves the separation of electrons and holes and that the transport of these species occurs via a field-induced hopping mechanism[1]. As illustrated in figure 1.1.(b) and (c), there is a net migration of charge from regions of high intensity to those of low intensity, creating a spatial pattern of charges that follows that of the light intensity pattern. According to Poisson's equation of electrostatics,

$$\nabla \overline{E} = \frac{\rho}{\varepsilon_0} \tag{1.3}$$

(where $\overline{E}$ is the average energy of the particles, ρ is the charge density, ε_0 is the permittivity of the medium, and ∇ is a product of the wavefunction) the charge distribution produces a sinusoidal space-charge electric field analogous to that shown in figure 1(d). Furthermore, as Poisson's equation relates the spatial gradient of the electric field to the charge distribution, such that the electrostatic field is integral over the charge density, if the charge density is sinusoidal then the field must be cosinusoidal. Thus, the resulting internal electric field is shifted in space 90° relative to the trapped charge, or one quarter of the grating wavelength. Ultimately, the space-charge electric field induces a spatial modulation of the refractive index via the linear electro-optic effect, a second-order nonlinear optical response in which the index of refraction at a particular point in the material is linearly proportional to the value of the electric field at that point. The relationship between the magnitude of the index modulation, Δn, and the magnitude of the space-charge field, E_{sc}, is described by equation 1.4

$$\Delta n = -(1/2) n^3 r_e E_{sc} \tag{1.4}$$

where r_e is the effective electro-optic coefficient for the geometry under consideration.

The sinusoidally varying modulation of the index of refraction results in the production of a phase grating which has the ability to diffract light. This imparts a distinct property to photorefractive materials. The optical energy of the two incident beams can exchange in an asymmetric manner, with one beam gaining energy and the other beam losing energy. In fact this forms the basis of a simple test, two-beam coupling gain, conclusively distinguishing photorefractivity from the numerous other mechanisms of grating formation, such as photochromism, thermochromism, thermorefraction, generation of excited states etc[1].

Two-beam coupling gain experiments are conducted using a system similar to that illustrated in figure1.2.

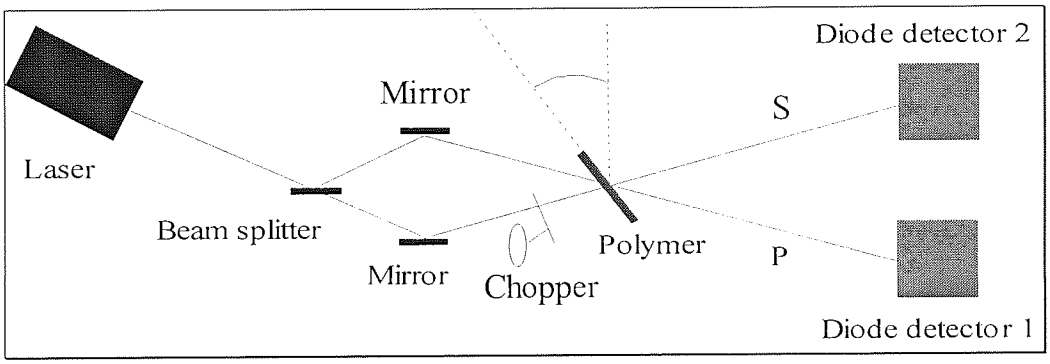

Figure 1.2. Typical experimental setup utilised for two beam coupling experiments.

As stated previously, the basis of the test is reliant upon the material's ability, or inability, to form a phase grating capable of diffracting light. If the material is indeed photorefractive, the two coherent incident beams intersecting on the material will be diffracted into each other, resulting in an asymmetric energy exchange. By monitoring this optical energy exchange, the optical gain coefficient, Γ, can be deduced from[1,2]

$$\Gamma = \frac{1}{L}\ln\left(\frac{1+\alpha}{1-\beta\alpha}\right) \tag{1.5}$$

where $\alpha = \Delta I_s(L)/I_sL$, $\Delta I_s(L)$ is the intensity change of the signal beam, I_sL is the total signal beam intensity emerging from the sample, L is the path length of the writing beam, and $\beta = I_s(0)/I_p(0)$, is the ratio of the incident beam intensities. Thus, the magnitude of the optical gain coefficient is used as a measure of photorefractivity. For

materials that do not induce such a process, conclusive evidence is provided that the grating arising is from a non-photorefractive mechanism. This distinction arises as unlike phase gratings arising from the photorefractive effect, those occurring as a consequence of other effects do not display a non-zero spatial phase shift between the index of refraction grating and the optical intensity pattern. It is noteworthy, that in certain cases the optical gain exhibited may not exceed the absorption coefficient of the material. Hence, although the phase grating is shown to be photorefractive in nature, such materials do not yield a net optical gain.

The presence of a non-zero spatial phase shift between the index of refraction grating and the optical intensity pattern is crucial in applications of photorefractive materials, as many utilise this phenomenon to furnish the required response for the given application.

1.2. Applications of photorefractive materials

The index gratings which may be written into a photorefractive material constitute "volume phase holograms". The capability of photorefractive materials to readily permit the writing and erasure of such holograms with light, makes them capable of real-time holography and gives rise to numerous potential and actual applications in fields such as image processing, signal processing, holographic data storage and optical interconnections for computing[1,3,4].

Some of the most interesting and promising applications of photorefractive materials encompass the field of holography. More specifically, three-dimensional depth resolved holography utilising photorefractive materials has been shown to be a valuable method of real-time 3-D imaging, providing rapid whole-field acquisition and high depth and transverse spatial resolution images. The fact that the technique has the capability to record high quality images through turbid media, means that it has many applications, such as biomedical imaging through tissue[5], and imaging through water and the atmosphere[6].

The technique is reliant upon the photorefractive ability of the material to "undo" the distortions created when light passes through a turbid media. A schematic of this process is shown below.

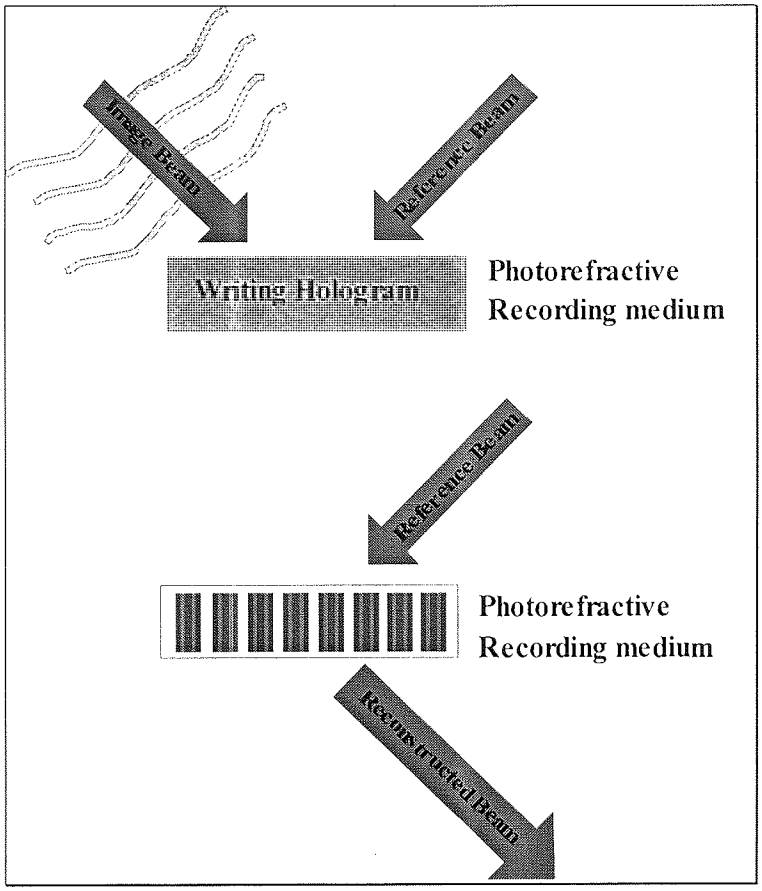

Figure 1.3. Schematic of photorefractive holography.

The photorefractive medium is utilised to record the hologram via the photorefractive effect. The hologram is then reconstructed by blocking the image beam and letting the reference beam diffract off the refractive index pattern to record an image at the camera. Alternatively, this can be achieved by the use of a different wavelength source and subsequently Bragg-matching the read-out beam to the refractive index pattern. Through either method, any incoherent light present in the object beam is filtered out and consequently does not contribute to the hologram.

Depth-resolved images can be generated by photorefractive holography, allowing the separation of the different layers of a three-dimensional object according to their corresponding depths within the surface(s) of the object. The effect utilises the different path lengths travelled by light reflecting from the different depths within an object to separate the layers. The typical experimental set-up used for this process is shown in figure 1.4.

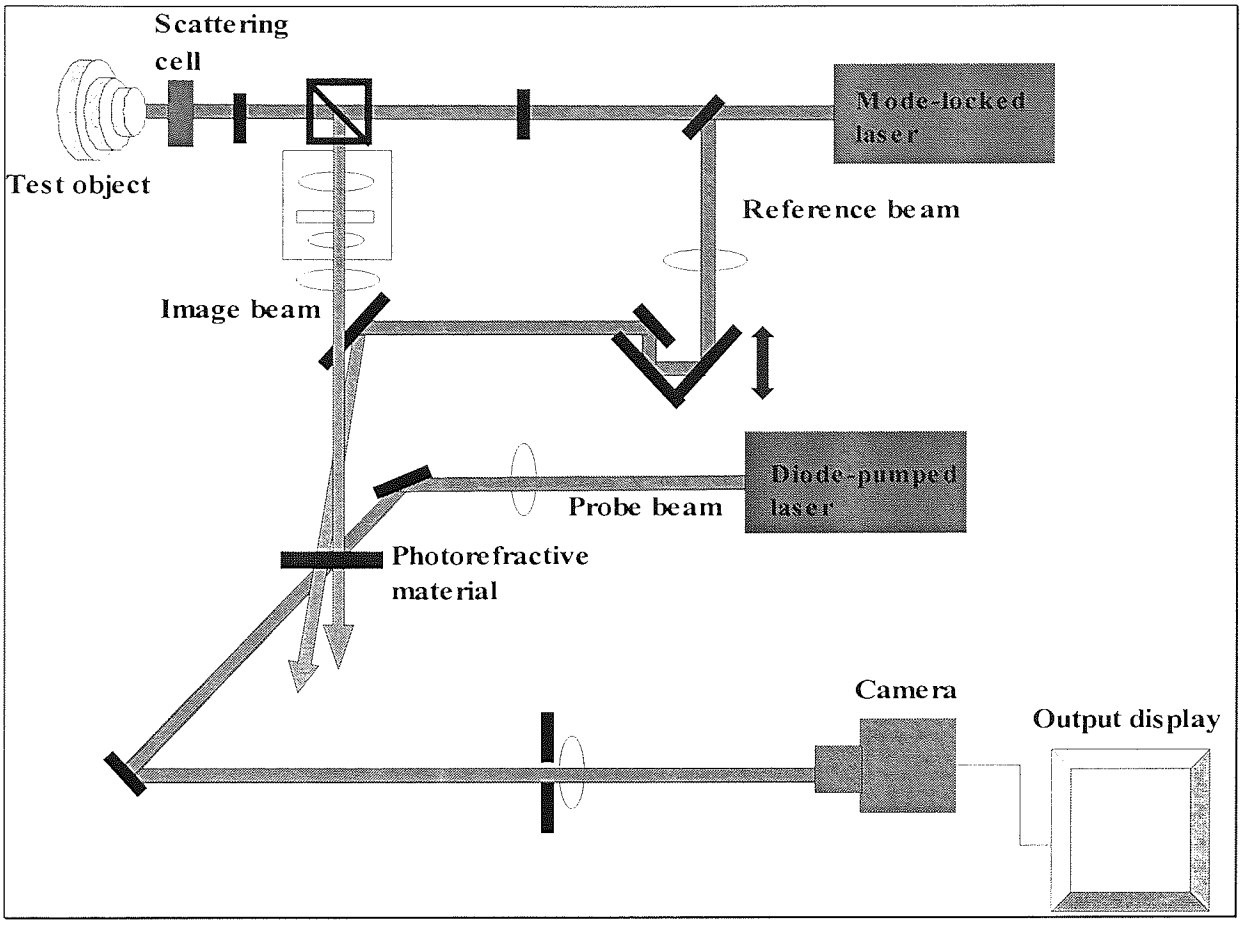

Figure 1.4. Typical set-up utilised for photorefractive holography.

The different depths in the object are recorded by matching the object and the reference beam lengths to within the coherence length of the laser, and can be individually selected by adjusting the path length of the reference beam. The images are resolved by scanning the reference beam path length with a probe beam, which is subsequently read by the camera.

It is apparent from past and current research that the realisation of actual and potential applications of photorefractive materials will allow significant technological advances to be made in a vast range of fields. However, this can and will only be achieved through the development of precise understanding of the microscopic processes comprising the photorefractive effect and via the tailoring and optimisation of the properties of the materials utilised to furnish the desired effect.

1.3. Photorefractive materials

The photorefractive effect was first observed over 30 years ago in ferroelectric single crystals, such as $LiNbO_3$[7, 8]. In the 25 years following this discovery, research focused almost exclusively upon inorganic materials[1], such as ferroelectric crystals ($LiNbO_3$, $LiTaO_3$, $BaTiO_3$), semiconductors (GaAS, InP, CdF_2) and sillenites ($Bi_{12}SiO_{20}$). However, the difficulty of crystal growth and sample preparation has limited the widespread use of these materials. Thus, more recently, the focus of research in this field has switched to alternative materials.

1.3.1. Photorefractive polymers

Polymers have emerged as the most suitable candidate for the construction of photorefractive materials, owing to their relative ease of preparation, amenability to structural modification, and inherent processability.

As stated previously, the necessary components of a photorefractive material are a photoionisable charge generator, a charge transporting medium, charge trapping sites, and a dependence of the index of refraction upon space-charge field (i.e. electrooptic nonlinearity). Hence, a polymer must contain moieties capable of such processes, to be able to furnish a PR effect. PR polymers are thus typically comprised of photoionisable charge generators, photoconductive species, and a nonlinear optical chromophore. At present, the nature of the charge trapping sites in polymeric materials is not explicitly understood, and hence the deliberate incorporation of such a species is not undertaken. However, it is assumed that impurities and structural defects within the polymer matrix perform this role.

Two fundamentally different strategies have been developed for the preparation of PR polymers: composite materials, involving doping of the required functionalities into a polymeric host, and fully-functionalised polymers, that have all functional species covalently bound to the polymeric backbone.

1.3.1.1. Composite materials

Composite PR polymeric materials are comprised of a polymer host doped with the appropriate functional molecules required to furnish a PR effect. The simplest materials consist of an inert polymer doped with a charge generating species, charge conducting species and nonlinear optical (NLO) chromophores. However, it is usually

desirable to incorporate at least one of the required functionalities into the polymeric host to minimise the inert volume in the material. The two most prominent approaches that have emerged utilise either NLO active polymers, or photoconductive polymers, as the host matrix.

1.3.1.1.1. Doped materials based on non-linear optical hosts

The first example of a PR polymer[9] was comprised of a cross-linkable, NLO epoxy polymer, bisphenol-A-diglycidylether-4-nitro-1,2-phenylenediamine (I), doped with 30wt% of the hole transporting agent diethylaminobenzaldehydediphenyl hydrazone (II). Two beam coupling experiments illustrated that the performance of this material was poor, generating an optical gain of $0.33cm^{-1}$, in comparison to an absorption coefficient of $10cm^{-1}$. Although a net optical gain was not observed, the possibility of preparing polymeric PR materials had nevertheless been illustrated.

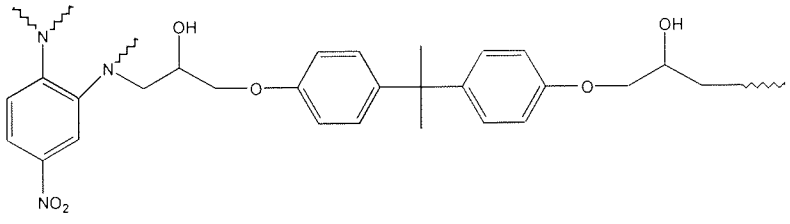

(I)

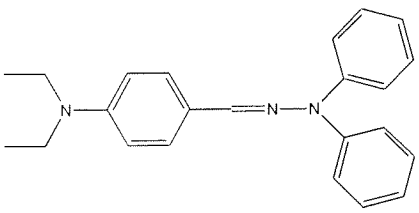

(II)

The linear epoxy polymer, bisphenol-A-diglycidylether-4-nitro-4'-aminotolan (III), doped with 30wt% diethylaminobenzaldehydediphenylhydrazone (II), has also been reported to display a weak photorefractive effect[10]. However, a net optical gain was not exhibited ($\Gamma = 1.8cm^{-1}$, $\alpha = 18cm^{-1}$).

The only other example of a PR material based upon a NLO polymer host, for which conclusive evidence of PR properties has been reported[11], was composed of a copolymer of methyl methacrylate and (N-methyl-4-nitroanilino)-2-N-ethylmethacrylate (IV), doped with 30wt% of the hole transporting agent diethylaminobenzaldehydediphenylhydrazone (II) and 0.6wt% of the charge generating agent C_{60} fullerene. However, as in the previous examples of this class of PR materials, a net gain was not observed ($\Gamma = 0.6cm^{-1}$, $\alpha = 3.4cm^{-1}$).

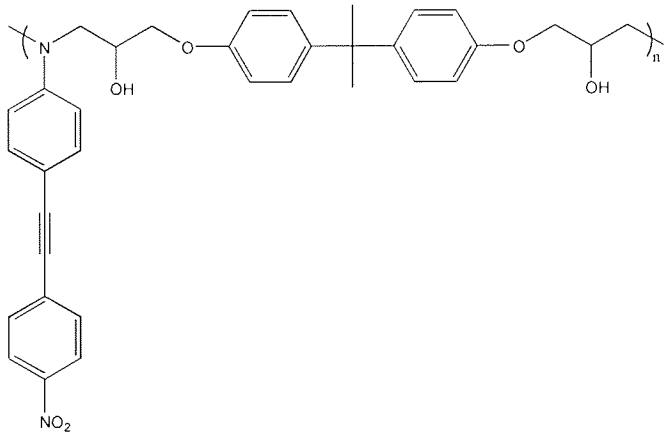

(III)

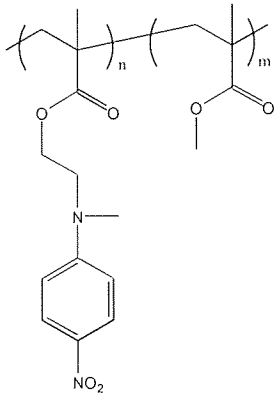

(IV)

1.3.1.1.2. Doped materials based on charge-transporting polymers

Research conducted on charge-conducting polymers as hosts for PR polymer mixtures, has focused almost exclusively on poly(N-vinylcarbazole) (PVCz). The performance of composites utilising other charge-conducting polymer hosts, such as poly[(4-n-butoxyphenyl)ethylsilane][12], has been comparatively limited thus far.

The first PR polymer reported to exhibit net optical gain consisted of PVCz (V), doped with 33wt% of the NLO chromophore 3-fluoro-4-(diethylamino)-(E)-β-nitrostyrene (VI) and 1.3wt% of the sensitiser 2,4,7-trinitro-9-fluorenone (VII). The net optical gain of 7.2 cm^{-1}, although relatively low, was in excess of that expected from the electro-optic PR effect alone. An extensive study of the effect of chromophore structure upon the performance of the resultant materials[13], revealed that the lowering of the glass transition temperature (T_g), by the plasticising effect of the dopants, greatly enhanced the performance of the materials. The orientational enhancement effect[14] was subsequently proposed to explain this phenomenon, prompting a flurry of activity, focusing upon enhancement of the mobility of the chromophore by lowering the T_g of the host material.

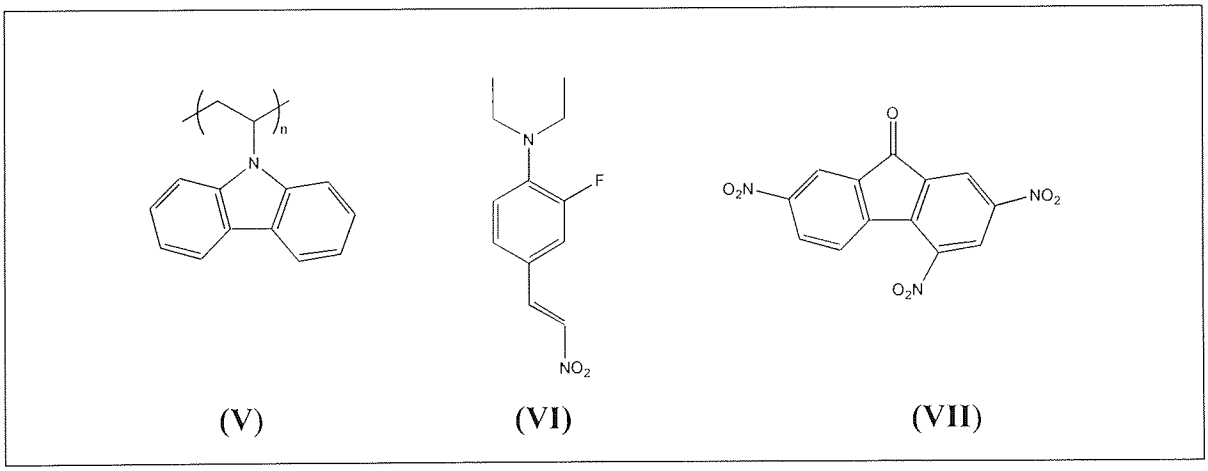

(V) (VI) (VII)

Two distinct strategies have emerged as methods of optimising the performance of PR composites via the orientational enhancement effect; addition of plasticisers, and utilisation of a charge-conducting polymer having a lower T_g. Both approaches have led to significant improvement in the performance of polymeric PR materials.

The introduction of plasticisers to the PR polymer composite has proved the most popular approach, as it is a much simpler technique that allows a vast array of

materials to be prepared and surveyed in a relatively short period of time. Most studies have focused on the use of N-ethylcarbazole as the plasticising agent[15, 16], with optimum performance being found for materials having a T_g approximately equal to room temperature[16]. A PVCz composite[17] doped with 33wt% of the NLO chromophore 2,5-dimethyl4-(p-nitrophenylazo)anisole (VIII), 1.3wt% of 2,4,7-trinitrofluorenone, and 20wt% of N-ethylcarbazole, was found to exhibit a net optical gain of 207cm^{-1}. The remarkable performance of this material led to the construction of a prototype optical pattern recognition system[18].

A similar level of performance has been reported for composites comprised of low T_g polysiloxanes bearing pendant carbazole groups (IX), doped with 43 wt% of the NLO chromophore (VIII) and 1 wt% trinitrofluorenone[19]. The net optical gain observed (220 cm^{-1}) and excellent optical quality of this material facilitated the construction of a digital data recording device[20].

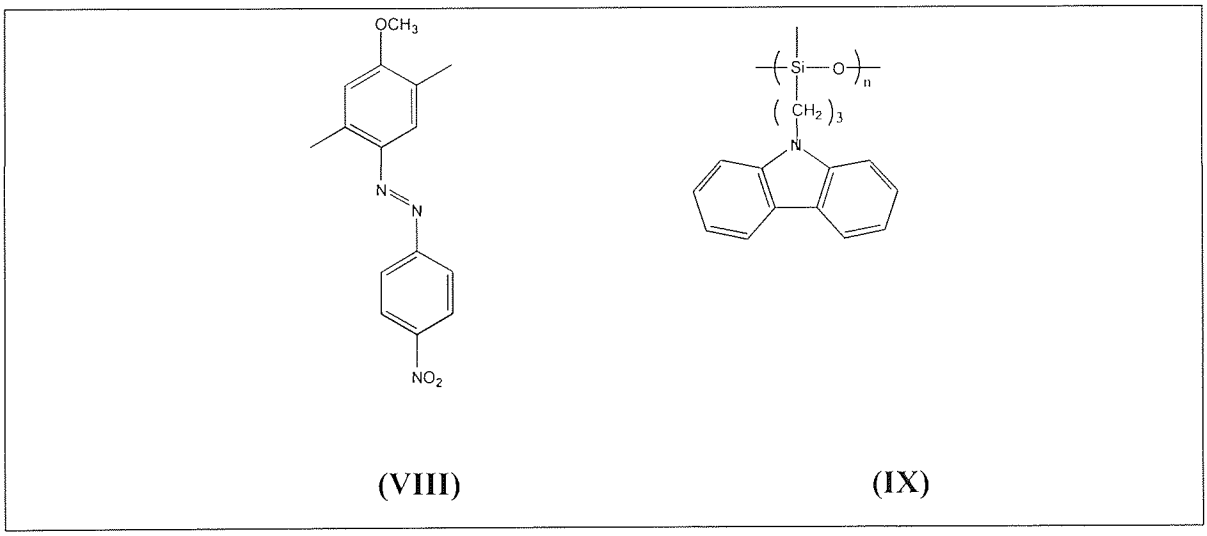

(VIII) **(IX)**

Despite the excellent PR properties observed for composite materials, they are not suitable for many applications, owing to their inherent lack of meta-stability. The principal cause of this low shelf-life (typically a few days[21]) is crystallisation of the dopants that leads to phase separation and loss of optical transparency. Several strategies have been employed to overcome this problem, such as utilisation of lower chromophore concentrations, liquid chromophores, and liquid plasticisers[22]. However, all attempts to construct crystallisation resistant composites have resulted in materials exhibiting significantly poorer PR properties.

1.3.1.2. Fully-functionalised PR polymers

The critical problem of phase separation in composite PR polymers can be overcome by synthesis of a single component system, bearing all functionalities necessary to furnish a PR effect, a fully-functionalised PR polymer. The construction of such materials is presently the main focus of research in this field.

The first reported fully-functional PR polymer was a polyurethane having charge generating, charge conducting and NLO chromophore species linked into the chain (X)[23]. However, the PR effect in these materials, although observable, was too weak to quantify. Subsequent attempts[24, 25] to improve the properties of these materials by alteration of the component ratios also proved futile, achieving a maximum optical gain of only 0.88cm^{-1} in comparison to an absorption coefficient of 194 cm^{-1}.

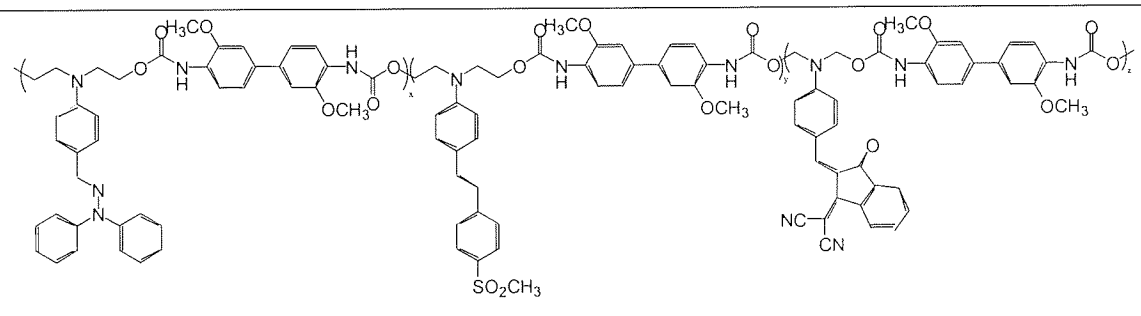

(X)

Net optical gain for fully-functional PR polymers was initially observed for a low T_g polyurethane, comprised of bifunctional charge conducting carbazole NLO chromophores linked by alkyl chains (XI)[26]. Although the net gain was only 6 cm^{-1}, it was nonetheless significant, proving that high performance single component PR polymers were viable.

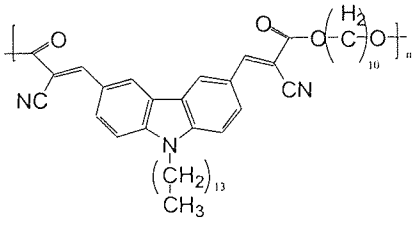

(XI)

The largest net optical gain for a fully-functional PR polymer, 198cm^{-1}, was reported for a conjugated phenylenevinylene polymer, bearing a tris(bipyridyl)ruthenium charge sensitising complex in the backbone and having

pendant (4-sulphonylmethyl)-p-aminostibene NLO chromophores (XII)[27, 28]. It is believed that the high performance of this material is a due to the extremely high efficiency of charge generation efficiency exhibited by the tris(bipyridyl)ruthenium complex, combined with the high photoconductivity afforded by the conjugated backbone.

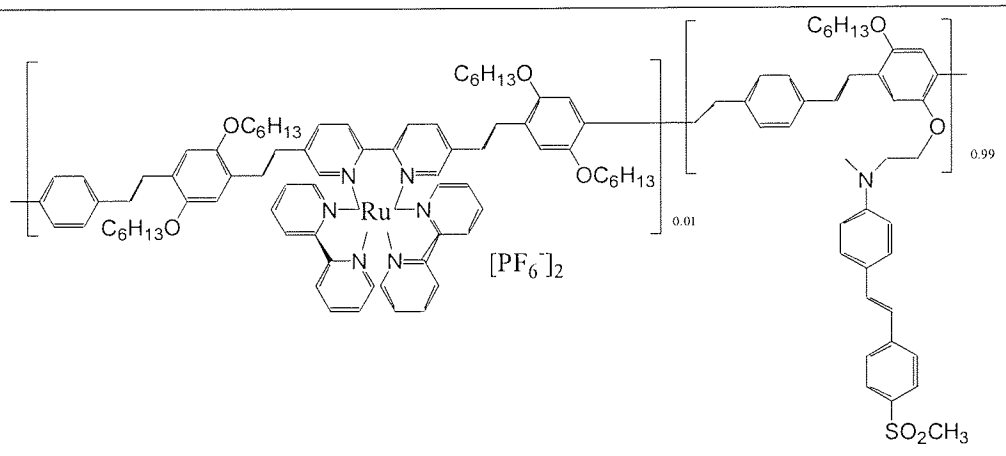

(XII)

Attempts to improve the performance of this material by lowering the T_g, or exchanging the charge generating complex have thus far proved ineffective[29].

The fully-functionalised PR polymers described thus far, all suffer from a common problem. The functionalities required to furnish a PR effect are borne by separate monomer units, limiting their concentration in the resultant polymer. It is probable that this limits the ultimate performance of the material. It is believed that a polymer having all functionalities incorporated in each repeat unit would thus circumvent this problem. Only one example of such a material has appeared in the literature to date, poly{(4-nitrophenyl)-[3-[N-[2-(methacryloyloxy)ethyl]-carbazolyl]]diazene} (XIII)[30]. However, although the existence of a PR effect was conclusively proven by 2BC experiments, the magnitude of the gain coefficient was not reported. Moreover, it is anticipated that the performance of this class of material will be comparable to that of PVCz based composites.

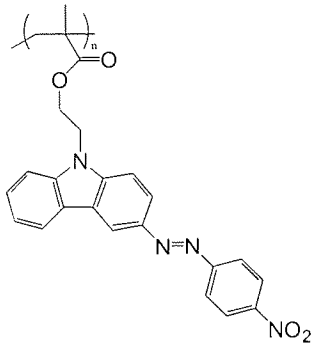

(XIII)

In summary, significant progress has been made in the field of photorefractive polymers over the last six years. The performance of these materials is still not comparable to those of their inorganic counterparts, but it is anticipated that further advances in the near future will facilitate the realisation of this goal. It is felt that such advances would in part be afforded by the development of techniques capable of synthesising PR polymers of precisely controlled architecture.

1.4. Polymer synthesis

1.4.1. Introduction

The synthesis of polymers can be achieved by a wide variety of techniques, all of which can be categorised into one of two distinct groups, depending upon the reactions and mechanisms involved in the polymerisation process; step growth, or condensation polymerisations and chain growth, or addition polymerisations. This distinction was first made by Carothers[31]. Step growth polymerisation proceeds by the combination of monomers, dimers and oligomers and generally involves the elimination of a small molecule such as H_2O, CO_2 or NH_3. Chain growth polymerisation proceeds via the successive addition of monomer to a propagating chain end, with the overall process being comprised of three distinct stages: (i) initiation, the generation of the active centre; (ii) propagation, the repeated addition of monomer to the active centre; (iii) termination, the seizure of the kinetic chain growth process by neutralisation or transfer of the active centre. There are numerous species that can induce chain growth

polymerisation and hence this category can be further subdivided according to the nature of the active centre generated. The main sub-categories are free-radical polymerisation[32], anionic polymerisation[33], cationic polymerisation[34], coordinative polymerisation, such as Ziegler-Natta[35] and metathesis systems[36], and group transfer polymerisation[37]. Of these, free-radical polymerisation is the most universal, allowing the polymerisation of a vast range of vinyl monomers in a wide range of media, without the need for stringent purification of the reagents utilised. Free-radical polymerisation is thus the most industrially important polymerisation process.

1.4.2. Free-radical polymerisation

A free-radical is an electrically neutral atomic or molecular species possessing an unpaired electron. Such species are capable of reacting with the π-bond of olefinic monomers to generate a chain carrier, which under appropriate conditions is capable of propagating a macromolecular chain. The mechanism of the chain growth process occurs in three distinct stages, as illustrated in scheme 1.1.

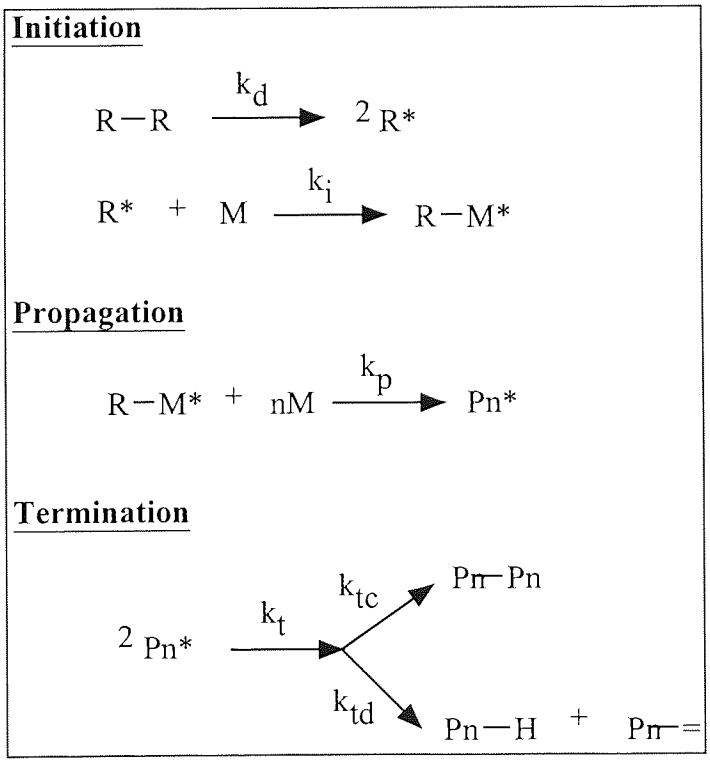

Scheme 1.1. Mechanism of free-radical polymerisation.

The initiation step is comprised of two stages; initiator decomposition, generating the primary radicals, followed by attack on a monomer unit to form the chain

carrier. Generally, the rate of decomposition of the initiator is slow in comparison to the rate of addition of a primary radical to a monomer and the rate of termination. The rate of initiation, R_i, is thus represented by equation 1.1, where the factor 2 is utilised to express the production of two primary radicals from the thermolysis of each molecule of initiator, and *f* the efficiency of initiation.

$$R_i = \frac{d[RM^*]}{dt} = 2k_d f[I] \qquad (1.1)$$

Typical examples of initiators generating radicals by thermal decomposition are benzoyl peroxide and α,α'-azobisisobutyronitrile (AIBN). Radicals can also be generated by photolysis, redox reactions or by ionising radiation (α, -β-, γ-, or X-rays). However, thermolysis is the most commonly used technique and hence the following description will only describe the case for this.

The generated chain radicals grow, or propagate, by rapid successive additions of monomer units. The velocity of the propagation step, k_p, is assumed to be independent of both the size of the chain radical and of the medium, i.e. monomer concentration and nature of any diluent. Thus the rate of bimolecular propagation is assumed to be constant for each step and hence the rate of polymerisation, R_p, can be described by equation 1.2.

$$R_p = \frac{d[M]}{dt} = k_p[P_n^*][M] \qquad (1.2.)$$

[M] is the concentration of monomer and [Pn*] is the concentration of propagating radicals.

Monomer addition occurs predominantly in a head-to-tail fashion to ensure retention of the most stable radical. The reactivity of the chain radical is thus determined by the resonance stabilisation from the α-substituents. It is therefore found that k_p increases in the order styrene < methacrylate < acrylate.

Termination of the propagating chains generally occurs by interaction of any pair of radicals to form inactive dead polymer chains, although it may occur by transfer reactions. As termination is a bimolecular process, the rate of termination, R_t, can be expressed by

$$R_t = k_t[P_n*]^2 \tag{1.3}$$

where k_t is the rate constant of termination, which comprises both the rate constant of termination for combination, k_{tc}, and the rate constant of termination for disproportionation, k_{td} (i.e. $k_t = k_{tc} + k_{td}$) . In most free-radical polymerisations, the half-life of decomposition of the initiator is such that primary radicals are continually generated throughout the course of the polymerisation, and hence if the rate of termination is less than the rate of initiation, the concentration of active centres will continuously increase. In the extreme case, this may propagate to explosive proportions. However, in most polymerisations a steady-state predominates, where the concentration of active centres can be regarded as being constant. Under such circumstances $R_i = R_t$. $[P_n*]$ is typically of the order of 10^{-8} mol dm^{-3}. Moreover, as the rate of formation of radicals is counterbalanced by their rate of destruction, for a polymerisation utilising thermolysis of a molecule to generate radicals,

$$2k_d f[I] = k_t[P_n*]^2 \tag{1.4}$$

Thus an expression for the concentration of active centres can be derived.

$$[P_n*] = \left(\frac{k_d f[I]}{k_t}\right)^{1/2} \tag{1.5}$$

Substitution of this expression into equation 1.4, gives the following equation for the overall rate of polymerisation.

$$R_p = k_p\left(\frac{k_d f[I]}{k_t}\right)^{1/2}[M] \tag{1.6}$$

From this it can be seen that when the efficiency of initiation is high, the rate is proportional to the monomer concentration and the square root of the initiator concentration. However, when f is low, it becomes a function of the monomer concentration and hence R_p is proportional to $[M]^{3/2}$.

Using the above model it is possible to derive expressions for the kinetic chain length, $\bar{\nu}$, which is a measure of the average number of monomer units adding to an active centre during its lifetime. Under steady-state conditions

$$\bar{\nu} = \frac{R_p}{R_i} = \frac{R_p}{R_t} = \frac{k_p^2[M]^2}{2k_tR_p} \qquad (1.7)$$

As $\bar{\nu}$ is inversely proportional to the rate of polymerisation, an increase in the temperature and a consequent increase in the rate of polymerisation results in a decrease in the kinetic chain length. Moreover, $\bar{\nu}$ is also inversely proportional to the radical concentration and hence a certain degree of control over the chain length can be exercised by manipulation of the initiator concentration. However, the nature of the polymerisation, particularly the continuous generation of active centres and the unavoidable occurrence of termination reactions, precludes the exercise of a high level of control comparable to that achievable with other techniques.

The average degree of polymerisation, $\overline{Dp}$, is related to the kinetic chain length by equation 1.8, where q is a scaling factor dependent upon the mechanism of termination.

$$\overline{Dp} = q\bar{\nu} \qquad (1.8)$$

For termination by combination, q = 2, but where termination occurs by disproportionation q = 1. However, in certain cases $\overline{Dp}$ is not within these limits and hence it is apparent that another mode of termination is occurring. This alternative mechanism is referred to as chain transfer.

Chain transfer occurs through the transfer of activity to another species, as illustrated in scheme 1.2.

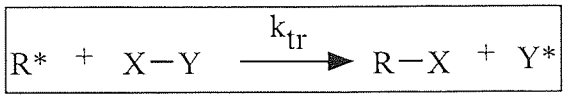

Scheme 1.2. Chain transfer process.

When the product is sufficiently active another chain will emanate and hence chain transfer has no effect on the rate of polymerisation. Chain transfer is essentially a competitive process between transfer and propagation where the effectiveness of a given agent, the chain transfer constant, C, is defined as k_{tr}/k_p. The magnitude of C is dependent upon the nature of the transfer agent and the monomer. It is also dependent upon temperature, as the activation energies of the transfer and propagation processes are generally different.

There are several types of chain transfer that can occur. Transfer to monomer, other than the conventional initiation or propagation steps, generally occurs through hydrogen abstraction, as illustrated in scheme 1.3. However, in most cases the effect is so small that it goes relatively unnoticed. For example in the polymerisation of styrene at 60°C such transfer occurs on average only once for every 10^5 growth steps[32].

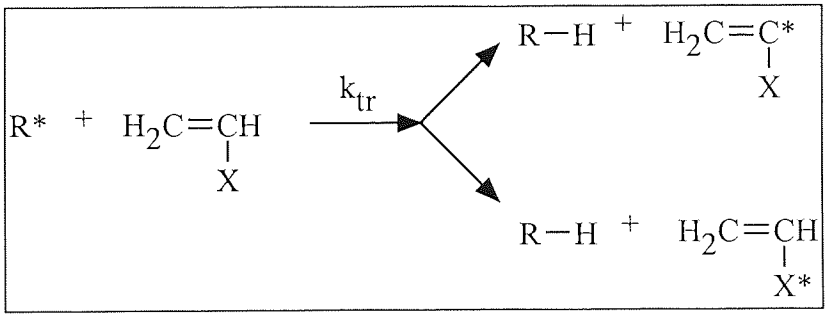

Scheme 1.3. Transfer to monomer.

For allylic monomers the effect is considerable and is regarded as degradative transfer. The large magnitude of the effect arises from the formation of the resonance stabilised allylic radical by abstraction of the α-hydrogen, as shown in scheme 1.4.

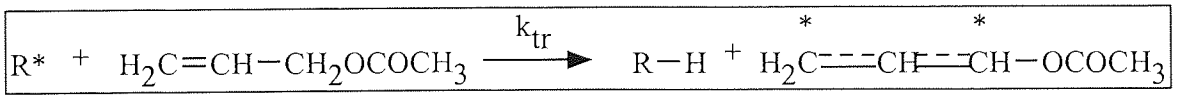

Scheme 1.4. Allylic radical formation.

Transfer to polymer can also occur, but is generally only manifested in the latter stages of the polymerisation when the concentration of polymer is relatively high in comparison to the monomer concentration. As shown in scheme 1.5, such reactions lead to structural branching and consequently result in broadening of the molecular weight distribution. This reaction is known to occur readily in the high pressure polymerisation of ethylene[38].

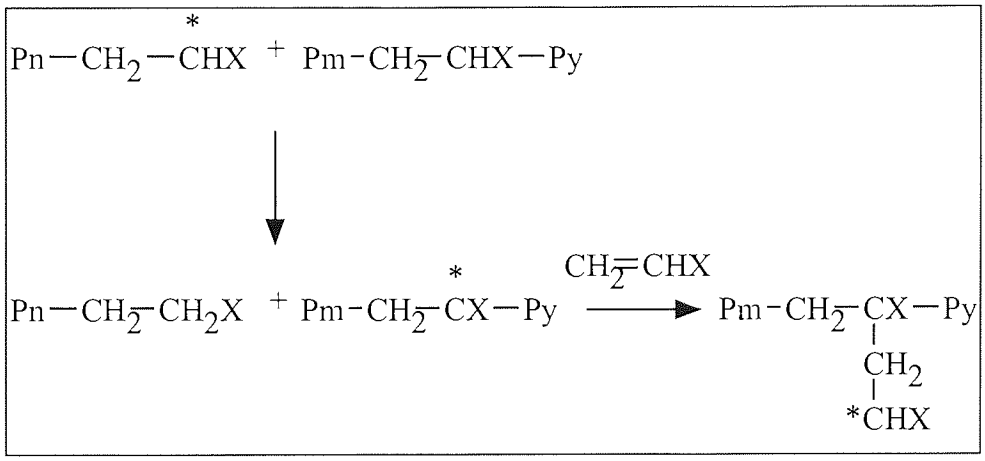

Scheme 1.5. Transfer to polymer.

When polymerisations are conducted in solution as opposed to the undiluted state, or bulk polymerisation, marked effects on the chain length can be observed. Solvents can act as transfer agents, with the magnitude of their effect dependent upon the concentration of the solvent, the strength of the bond involved in the abstraction step, and the stability of the radical formed. The principle effect is a decrease in the average degree of polymerisation, with telomerisation occurring when the process is particularly prominent. The influence of the transfer process upon the $\overline{Dp}$ can be estimated from a simplified form of the Mayo equation, which assumes that the predominant mode of transfer is that to solvent.

$$\frac{1}{\overline{Dp}} = \left(\frac{1}{\overline{Dp}}\right)_0 + C_s\frac{[S]}{[M]} \qquad (1.9.)$$

Examples of chain transfer constants to styrene at 60°C for some agents are listed in table 1.1.

Solvent	$10^4 * C_s$
Benzene	0.023
n-Heptane	0.42
CCl_4	90
CBr_4	22000
n-Butyl mercaptan	210000

Table 1.1. Examples of chain transfer constants[39].

Initiator efficiency can be effected by transfer processes. Radicals can attack initiator molecules, as shown in scheme 1.6, leading to incorporation of initiator fragments as end groups. Although the process may lead to initiation of new chain carriers, when it is predominant, such as in the case of organic peroxides, it leads to poor initiator efficiency. The effect is not pronounced for azo initiators, which are hence preferred for kinetic studies.

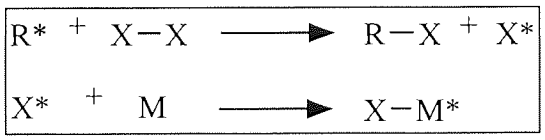

Scheme 1.6. Transfer to initiator.

The effect is very pronounced for certain classes of initiators. Such compounds are referred to as inifers (*ini*tiator-trans*fer* agents) and include organosulphur compounds[51]. Inifers result in degradative transfer and they can be used for the production of low molecular weight chains with functional end groups. However, other compounds, such as alkyl mercaptans, are more commonly used for controlling the molecular weight of polymers. Indeed, many reports of the use of such compounds have appeared in the literature[40].

When the radical produced by chain transfer is relatively stable and the rate of re-initiation of polymerisation is slow, the transfer agent will retard the rate of polymerisation. Nitrobenzene is a compound well known to exhibit such behaviour. Moreover, in extreme cases when the transfer agent is particularly efficient, it may completely suppress polymerisation by converting the primary radicals into inactive species. Such compounds are called inhibitors, with diphenyl picryl hydrazyl being an

example[41], and are commonly utilised to prevent autopolymerisation during the transport and storage of monomers.

In summary, it is apparent that free-radical polymerisation is an extremely useful technique, with the neutrality of the species involved facilitating the polymerisation of a vast range of monomers. However, it is clear that its use for the synthesis of macromolecules of precisely controlled architecture is precluded by the unavoidable occurrence of termination and transfer reactions.

1.4.3. Living radical polymerisation

1.4.3.1. Characteristics of living polymerisation

A living polymerisation is defined as a polymerisation in which propagation proceeds in the absence of termination or transfer reactions and the growing chain ends remain active even after all monomer has been consumed. For such a polymerisation, in which the rate of initiation is fast compared to the rate of propagation, and hence the growth of all polymer chains occurs at the same rate, the resultant polymers will display narrow molecular weight distributions. The molecular weight distribution will then have a Poisson distribution[42] given by;

$$\frac{\overline{M_w}}{\overline{M_n}} = 1 + \frac{\overline{M_n}}{\left(\overline{M_n} + 1\right)^2} \qquad (1.10)$$

Moreover, where the efficiency of the initiation step is complete, such that each initiating molecule generates one discrete propagating chain, the number average degree of polymerisation will be given by;

$$\overline{Dp_n} = \frac{[M]_0 - [M]_t}{[I]_0} \qquad (1.11)$$

Thus, for reactions with a high rate of initiation relative to the rate of propagation, the molecular weight increases linearly with monomer conversion. Conversely, if the rate of

initiation is slow then the resultant polymers will possess a broad molecular weight distribution.

In a living polymerisation, the chain ends remain active after the consumption of all monomer, and hence the additional polymerisation will be induced if more monomer is added. However, in reality this concept is unachievable, as all chain ends will eventually isomerise, react with their surroundings or otherwise decompose, regardless of their nature. Therefore, a living polymerisation is practically defined as one in which the chain ends remain active long enough to allow any further synthesis to be completed.

The first example of such a polymerisation, the anionic polymerisation of styrene initiated by sodium napthalide (scheme 1.7), was reported by Szwarc[43]. The polymerisation was conducted by initially adding sodium to a solution of napthalene in THF to produce the green napthyl radical-anion, and then subsequently adding styrene. Upon addition of styrene, the solution becomes red due to the transfer of an electron from the napthyl radical-anion to the monomer, producing the styryl radical-anion. The subsequent combination of two of these radical-anions results in the formation of dianions, which propagate from both ends. The persistence of the red colour after consumption of all the monomer attests to the living nature of this polymerisation. Moreover, further evidence of the living nature of this polymerisation was obtained by the observation of a molecular weight increase upon the addition of a second batch of monomer to the completed polymerisation.

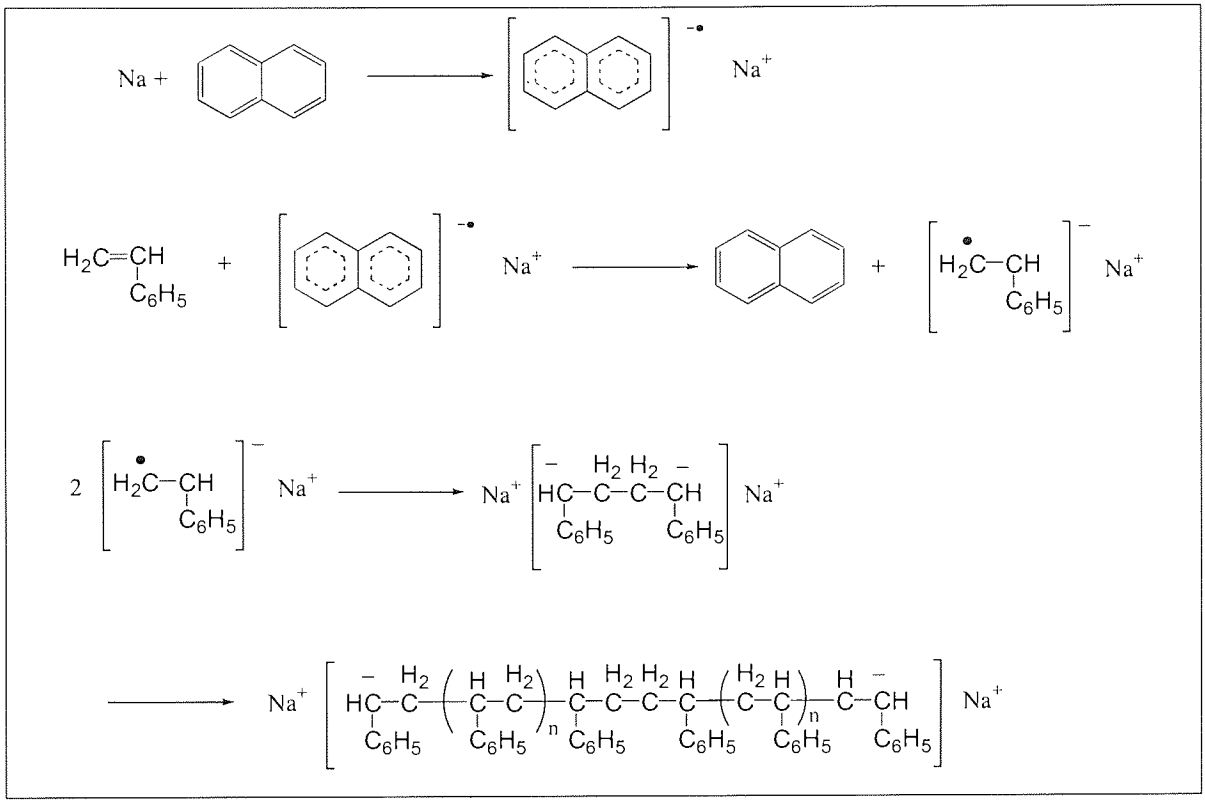

Scheme 1.7. Living anionic polymerisation of styrene.

Since this discovery, living polymerisation has become well established in the areas of anionic polymerisation[44], cationic polymerisation[45] and group transfer polymerisation[46]. However, more recently, due to the limitations of the aforementioned techniques, living radical polymerisation has emerged as the predominant area of research activity in this field. Whilst this technique cannot be considered as truly living, due to the unavoidable occurrence of radical termination and transfer reactions, it is nevertheless capable of yielding well defined polymers and copolymers which, after depletion of all monomer, are capable of further growth upon addition of more monomer. However, it is possible to argue that the occurrence of irreversible termination, albeit of a negligible or undetectable quantity, is unavoidable in all currently known polymerisation systems. Hence, it is presently correct to categorise radical polymerisations displaying similar behaviour as living polymerisations.

1.4.3.2. Early developments – a model for living radical polymerisation

The first report of the possibility of a living radical polymerisation appeared in 1957[47]. The principle was based upon the intermittent irradiation of an emulsion polymerisation with a light source, which when utilised produced ultrahigh molecular

weight polymers displaying extremely narrow molecular weight distributions ($1.01 < \overline{M_w}/\overline{M_n} < 1.13$). Subsequently, other possibilities were proposed for radical polymerisations of some organised monomers complexed with guest compounds such as perhydrotriphenylene[48], of ethylene initiated with triethyl aluminium/γ-butyrolactone/tert-butyl perisobutyrate[49], and of methyl methacrylate in the presence of zinc chloride[50]. However, none of these studies presented or furnished any significant evidence of a living radical polymerisation.

The first real progress towards the realisation of a living radical polymerisation was made by Otsu, whom proposed the iniferter (*ini*tiator-trans*fer* agent-*ter*minator) concept[51, 52], which is notably similar to Kennedy's inifer theory for cationic polymerisation[53]. The concept, as shown in scheme 1.8, was based upon the reversible dissociation of a polymer end group into a primary reactive propagating radical and a more stable secondary radical species that cannot initiate polymerisation, but only recombine with a primary radical. Otsu proposed that under the correct conditions, such that there is a reservoir of dormant species in equilibrium with a minute concentration of radicals, the continued dissociation and recombination of the two radical species would allow polymerisation to proceed with a minimum of irreversible termination reactions.

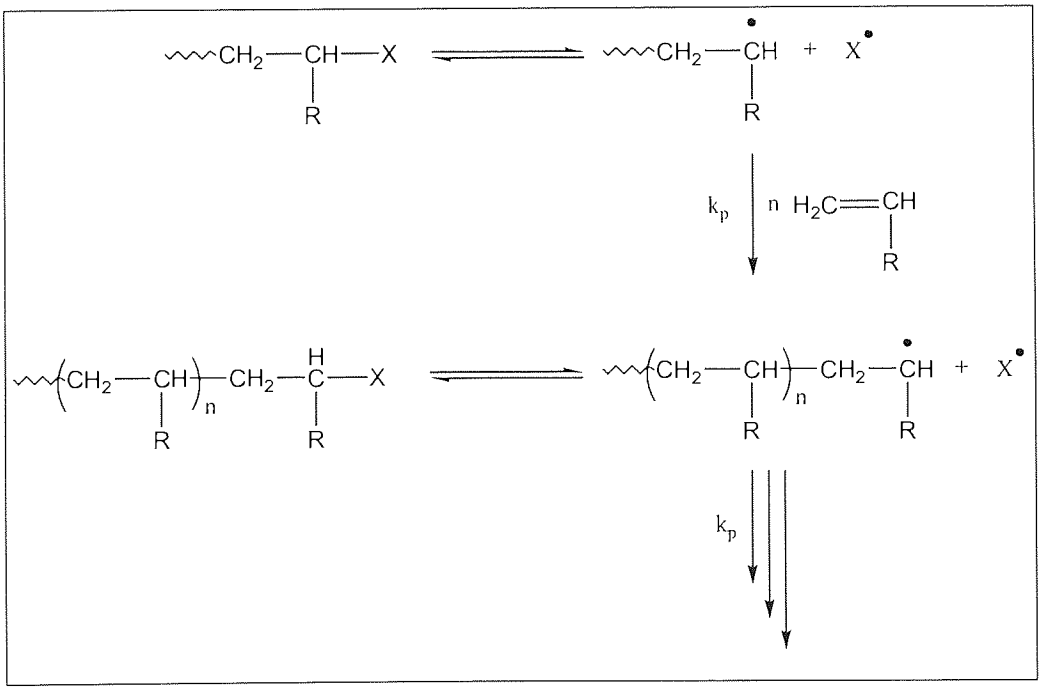

Scheme 1.8. The iniferter concept.

Otsu[52] and Braun[54] initially reported the use of carbon-centred radicals based upon arylmethanes as suitable reversible end-capping agents. Otsu also illustrated that tetraalkylthiuram disulphides and dithiocarbamates could be used as photoiniferters[52, 55] and subsequently that tetramethylene disulphide could be used as a thermal iniferter[56] for the polymerisation of styrene. However, despite the effectiveness of these techniques for the synthesis of homopolymers, block co-polymers and star polymers, none yielded polymers displaying narrow molecular weight distributions comparable to those achievable by the well-established ionic living polymerisation techniques. Nevertheless, the principle of reversible deactivation of propagating radicals had been proven and an ideal model for controlled/living radical polymerisation developed.

Currently, there are three general approaches towards generating an equilibrium between dormant chains and active propagating radicals, as shown in scheme 1.9.

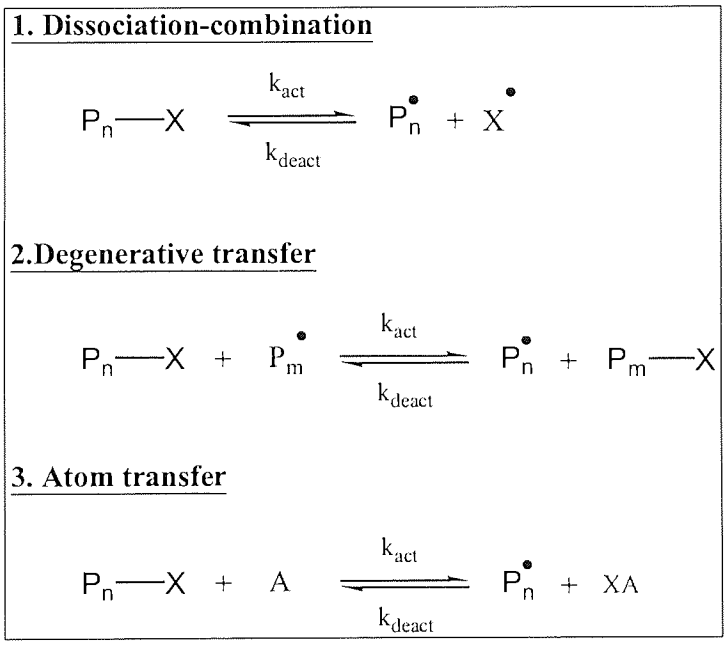

Scheme 1.9. Approaches to controlled/living radical polymerisation.

The first approach is analogous to Otsu's model, involving the reversible dissociation and combination of propagating and stable radicals, and is referred to as stable free radical polymerisation. The second approach is based upon a thermodynamically neutral exchange process between propagating radicals and dormant species, typically referred to as degenerative transfer. The third example, although essentially the same as the first approach, is based upon the catalysed, reversible

cleavage of the covalent bond in the dormant species via a redox process. This process is currently known as atom transfer radical polymerisation.

1.4.3.3. The persistent radical effect

Despite the explicit differences between the three aforementioned approaches, they are all dominated by the same four processes; activation, deactivation, propagation and termination. Hence it is not surprising that the control over the polymerisation in each case is evolved via the same mechanism, known as the persistent radical effect[57, 58, 59].

Considering the ideal case of a polymerisation involving only reversible radical formation, propagation and termination, and ignoring additional side reactions and chain length dependencies of rate constants, the following process can be envisaged. Activation of the dormant chains results in formation of transient propagating radicals and less reactive persistent species in equal concentrations and at the same rate. The persistent species do not react with themselves, but only cross-couple with the transient radicals to reform dormant chains. However, the highly reactive transient radicals are less selective and can undergo propagation, cross-couple with the persistent species to reform dormant chains, or irreversibly self-terminate. Owing to the stoichiometry of the equilibrium, occurrence of the self-termination reaction generates an excess of the persistent species. As the polymerisation proceeds, this excess increases continuously. Thus, the cross-coupling reaction of the transient radicals with the persistent radicals becomes more and more favourable compared to the self-termination reaction. In this manner, the self-termination reaction is inhibited, allowing the polymerisation to proceed in a controlled manner with only a negligible amount of termination.

1.4.3.4. Stable free-radical polymerisation

As previously stated, initial attempts to control radical polymerisations utilised iniferters, such as arylmethanes[52] and disulphide derivatives[55, 56]. However, the usefulness of these systems for the synthesis of polymers having a narrow molecular weight distribution is limited by the slow rate of propagation, the ability of the iniferter fragment to initiate new chains at any time during the course of the polymerisation and the loss of the activity of the iniferter fragment. Nevertheless, these systems established the concept of living radical polymerisation.

Catalytic chain transfer polymerisation, utilising organocobalt complexes, has been shown in some cases to proceed in a controlled manner, with molecular weight evolving with increasing conversion of monomer[60]. Davis et al have illustrated that this living character is a result of reversible end-capping of the polymer chains by stable organocobalt radicals[61]. However, although such systems are effective under the correct conditions, they are predominantly used to attenuate the molecular weight of polymers in free-radical polymerisation by the conventional catalytic chain transfer process.

The pioneering work of Solomon and Rizzardo on the use of stable nitroxyl radicals as reversible end-capping agents in vinyl polymerisation[62, 63] has led to a flurry of activity in this field in recent years. In particular, Georges et al have widely reported the use of 2,2,6,6-tetramethylpiperidinyloxy (TEMPO) for the pseudo living radical polymerisation of styrene initiated by benzoyl peroxide[64, 65]. The optimisation of this technique allowed the production of polystyrenes having narrow molecular weight distributions ($1.15 < \overline{M_w}/\overline{M_n} < 1.3$). The exact nature of the mechanism of the polymerisation, shown in scheme 1.10, has been a topic of great debate, but was confirmed by extensive studies, using electron spin resonance techniques[66, 67, 68], to be similar to the initial "model for living radical polymerisation" proposed by Otsu et al (scheme 1.8.). It is of note that these studies also revealed a low stationary concentration of propagating species in these polymerisations ($[Pn^*] \approx 10^{-8}M$), which is one of the principal factors permitting the synthesis of narrow polydispersity resins.

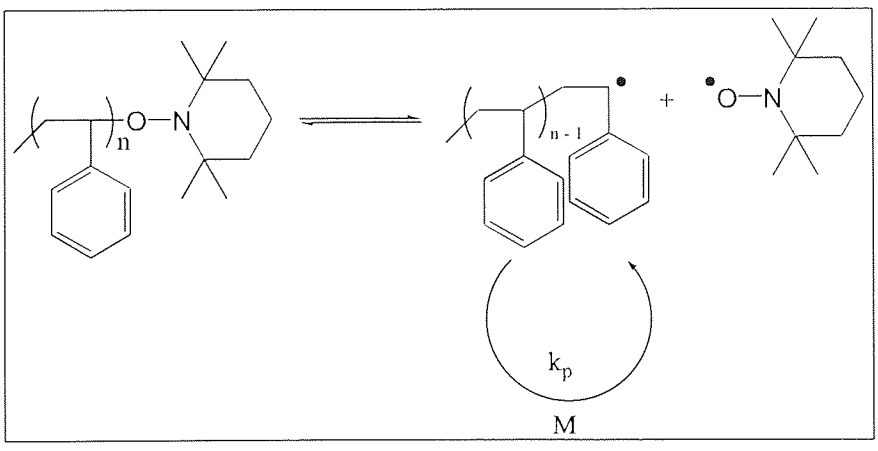

Scheme 1.10. mechanism of TEMPO mediated polymerisation of styrene.

The typically high temperatures required to induce homolysis of the -C-ON bond (125-140°C) and unsuitably long polymerisation times, have raised concerns over

the effect thermal polymerisation plays in the initiation of the polymer chains[69,70]. Indeed, Hawker et al have shown that such controlled polymerisations can be conducted in the absence of conventional radical initiators[71].

In an attempt to compensate for such detrimental behaviour, Georges et al studied the effect of the addition of some known inhibitors of styrene autopolymerisation[72], such as camphor sulphonic acid[73] and 2-fluoro-1-methylpyridinium-p-toluenesulphonate[74], to the TEMPO mediated polymerisation of styrene. It was found that the additives accelerated the rate of polymerisation by consumption of TEMPO[75], but that this effect was manifested at the expense of the level of control afforded over the polymerisation. However, optimisation of the ratio of the additive to TEMPO allowed the production of polymers displaying molecular weight distributions comparable to those observed for polymers synthesised in the absence of such additives.

Other attempts to overcome the problems associated with the polymerisation of styrene at elevated temperatures, focused upon the use of nitroxides other than TEMPO, which have been shown to form weaker -C-ON bonds[76]. Nitroxides such as N,N-di-*tert*-butyl nitroxide (DTBN)[77], pyrrodinyloxyl[78] and N-*tert*-butyl-1-diethylphosphono-2,2-dimethoxypropyl nitroxyl (DEPN)[79], have all been reported as effective alternatives for the controlled polymerisation of styrene. However, none of these examples afforded any significant advantages over TEMPO for the controlled polymerisation of this monomer.

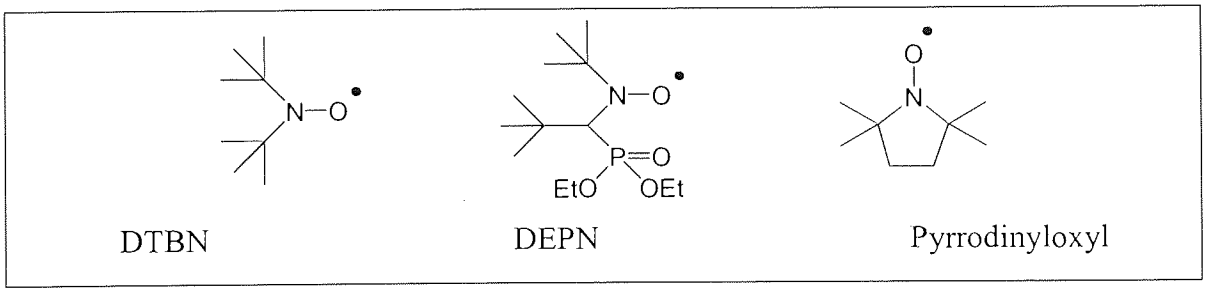

Whilst TEMPO and other nitroxide derivatives have been shown to be particularly useful for the controlled polymerisation of styrene and its derivatives[80, 81], they have not been widely reported as being applicable for the well-controlled polymerisation of other categories of vinyl monomers. The only exception is DEPN, which has been utilised to control the polymerisation of n-butyl acrylate[77]. However, Hawker et al have recently published a report claiming the development of a universal alkoxyamine (XIV) for "living" free-radical polymerisation[82].

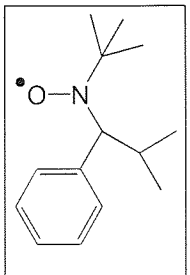

(XIV)

Indeed, whilst this adduct has been shown to be effective for the homo and copolymerisation of a wide range of monomers, it has also been found to be incompatible with some functional monomers such as acrylic acid and glycidyl acrylate. Despite this, it is apparent from reports such as this that the presently accepted limitations of nitroxide-mediated "living" free-radical polymerisation can and will be overcome by the use of stable nitroxides of different structures.

1.4.3.5. Degenerative transfer

An ideal degenerative transfer process consists of a thermodynamically neutral exchange process between a growing radical and a dormant species bearing a fragment structurally similar to the active macroradical. To achieve this, the polymer-transfer agent bond must be resistant to homolytic cleavage, but of sufficient lability to allow a rapid exchange process. In cases where this is not apparent, a unimolecular process will occur.

Matyjaszewski et al reported the successful control of the polymerisation of styrene utilising 1-phenylethyl iodide as the degenerative transfer agent[199]. The process operates by the mechanism shown in scheme 1.11, which is initiated by conventional radical initiators such as benzoyl peroxide or AIBN.

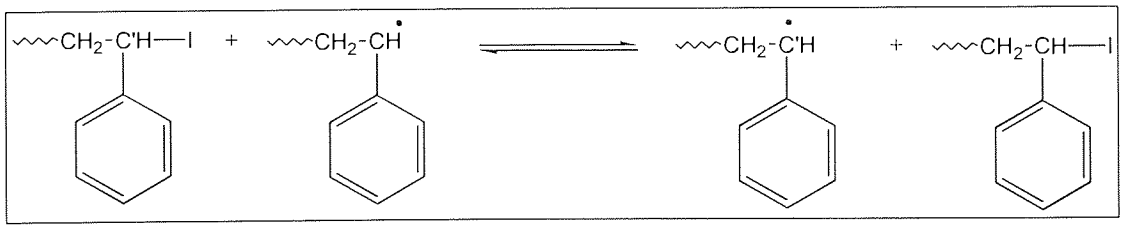

Scheme 1.11. Iodine transfer polymerisation.

RAFT (*R*eversible *A*ddition-*F*ragmentation chain *T*ransfer) is the most recent example of a controlled/living radical polymerisation technique to be reported[83, 84]. The process as illustrated in scheme 1.12, utilises thiocarbonylthio compounds similar to

those used by Otsu as iniferters[52], to confer living polymerisation characteristics. However, unlike iniferters RAFT agents exhibit rates of addition and fragmentation that are fast relative to the rate of propagation, and expel radicals capable of reinitiating polymerisation.

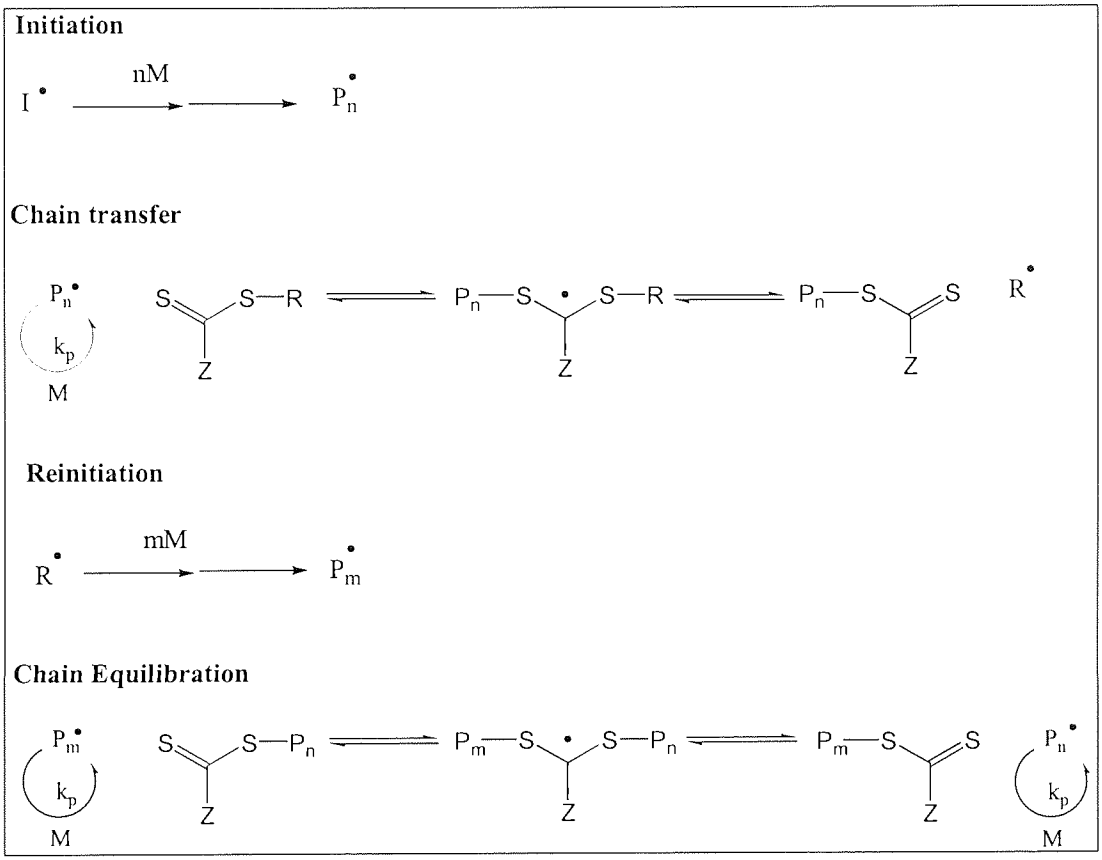

Scheme 1.12. RAFT.

The different behaviour of RAFT agents and iniferters is attributed to the difference in reactivity of the respective thiocarbonyl bonds. The thiocarbonyl group of iniferters is known to be less susceptible to chain transfer than that of RAFT agents, due to the delocalisation of the non-bonded electron pair on the nitrogen with the thiocarbonyl group[85]. Such characteristics preclude involvement in reversible addition-fragmentation reactions. To circumvent such problems Rizzardo et al utilised compounds with substituents which activate, or more importantly do not deactivate the thiocarbonyl bond. Examples are shown in scheme 1.13, with compounds where Z is an activating group such as aryl or alkyl, or derivatives where the lone pair of electrons on the nitrogen is involved in an aromatic system, such as pyrrole or imidazole, proving the most effective.

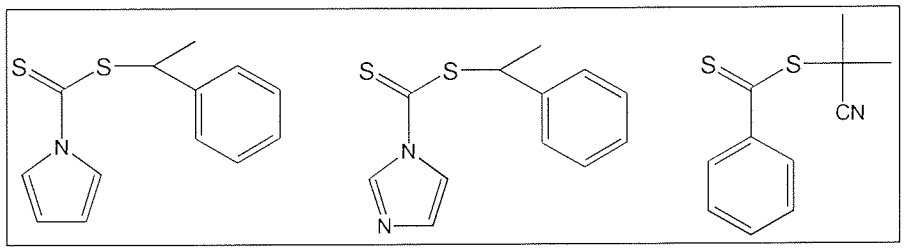

Scheme 1.13. Typical RAFT agents.

Unlike all other examples of controlled/"living" radical polymerisation reported to date, RAFT polymerisation appears thus far to be a universal technique. The homopolymerisation of styrenic, methacrylic and acrylic monomers, as well as functional monomers such as acrylic acid, p-styrenesulphonic acid and dimethylaminoethyl methacrylate amongst others, initiated with conventional free-radical initiators (e.g. AIBN), has been reported to yield resins with narrow molecular weight distributions ($1.02 < \overline{M_w}/\overline{M_n} < 1.3$) over a wide molecular weight range (5,000-500,000 g mol^{-1})[83, 84]. The controlled synthesis of a variety of copolymers as well as homo and copolymers of more complex architectures (star, graft etc.) has also been reported[86]. Moreover, the technique seems unaffected by the reaction temperature or the medium in which the polymerisation is conducted, and hence appears so far to exhibit a level of versatility comparable to that of conventional free-radical polymerisation.

1.4.3.6. Atom transfer radical polymerisation

Atom transfer radical polymerisation (ATRP) is essentially an extension of the well-known atom transfer radical addition reactions widely utilised in organic chemistry[87]. It can be defined as the reversible abstraction of a halide atom from a dormant pseudo-alkyl halide, by a transition metal complex, to form a propagating radical and an oxidised metal species. The basic mechanism of this process is shown in scheme 1.14, and is reliant upon the ability of the metal to shuttle between two oxidation states, via a one-electron redox cycle.

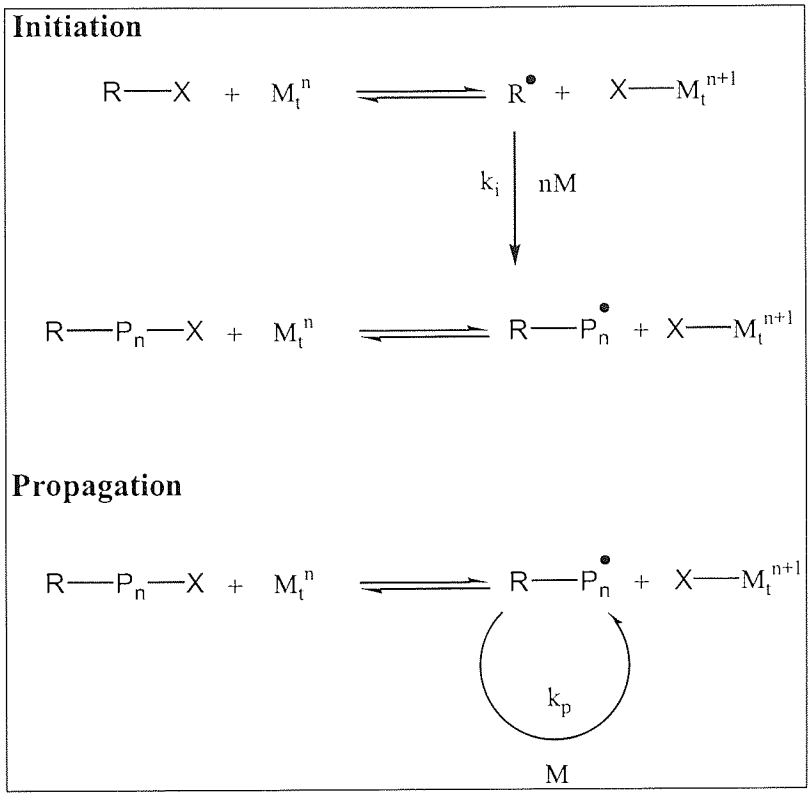

Scheme 1.14. ATRP.

A wide range of transition metal complexes have been utilised to mediate ATRP of various monomers. Table 1.2 lists some of these examples. As the focus of this study is copper halide/α-diimine mediated ATRP, a more thorough discussion of this catalyst system is present in the text following table 1.2. Hence, only one example of copper halide mediated ATRP is listed. It is also noteworthy that copper halide/α-diimine has been the most intensely studied ATRP catalyst system to date.

Transition metal complex	Initiator	Monomers	Ref. no.
$CuX(\alpha\text{-diimine})_2$	Alkyl halide	Styrene, methacrylates, acrylates	88
$Ru(PPh_3)_3Cl_2$	Alkyl halide/ $MeAl(ODBP)_2$	Methacrylates.	89, 90, 91
$RuH_2(PPh_3)_4$	Alkyl halide	Methyl methacrylate	92
$FeCl_2(PR_3)_3$	Alkyl halide	Styrene, methyl methacrylate	93
$FeC_5H_5(CO)_2I$	Alkyl iodide/$Ti(O\textit{i}\text{-Pr})_4$	Styrene	94
$Ni\{o,o'(CH_2Nme_2)C_6H_3\}Br$	Alkyl halide	Methacrylates	95
$NiBr_2(PPh_3)_2$	Alkyl halide	Methacrylates, acrylates	96
$NiBr_2(Pn\text{-}Bu_3)_2$	Alkyl halide	Methacrylates, acrylates	97
$Pd(OAc)_2/PPh_3$	CCl_4	Methyl methacrylate	98
$RhCl_3(PPh_3)_3$	Alkyl halide	Methyl methacrylate	99
$ReO_2I(PPh_3)_2$	Alkyl iodide	Styrene	100

Table 1.2. Transition metal complexes utilised in ATRP.

$Cu^{(I)}$halide/α-diimine mediated ATRP was first reported in 1995, for $Cu^{(I)}Cl$ complexed by 2,2'-bipyridyl[101]. However, owing to the heterogeneous nature of the catalyst complex the polymerisation of styrene, methyl methacrylate and methyl acrylate were ill controlled[102, 103], yielding polymers with relatively broad molecular weight distributions (Pdi > 1.5). It was subsequently found that the 4,4'-substitution of the 2,2'-bipyridyl rings with long alkyl chains afforded a more soluble catalyst complex

in hydrocarbon solution[104]. This facilitated the production of polymers having predetermined degrees of polymerisation ($DP_n = \Delta[M]/[I]_0$) and narrow molecular weight distributions ($1.05 < PDi. < 1.20$)[105, 106].

An alternative α-diimine ligand to 4,4'-alkyl-2,2'-bipyridyl for $Cu^{(I)}Br$ mediated ATRP was proposed by Haddleton et al. N-Propyl-2-pyridylmethanimine (XV) was reported to yield a homogeneous catalyst complex in hydrocarbon solution, which afforded a high degree of control over the polymerisation of methyl methacrylate[107]. It was subsequently reported that the solubility of the catalyst complex could be increased by increasing the length of the pendant alkyl chain on the ligand[108]. Surprisingly, this was found to have no effect upon the level of control afforded over the polymerisation, which is in stark contrast to that observed for increases in the solubility of the 2,2'-bipyridyl $Cu^{(I)}$ halide catalyst complex.

A variety of other ligands has been utilised for copper halide mediated ATRP; 1,10-phenanthrolines[109, 110] (XVI), picolylamines[111] (XVII and XVIII), multidentate amines[112] (XVIIII, XX, XXI), and sparteine[113] (XXII). However, none offer significant advantages over the two previously mentioned examples.

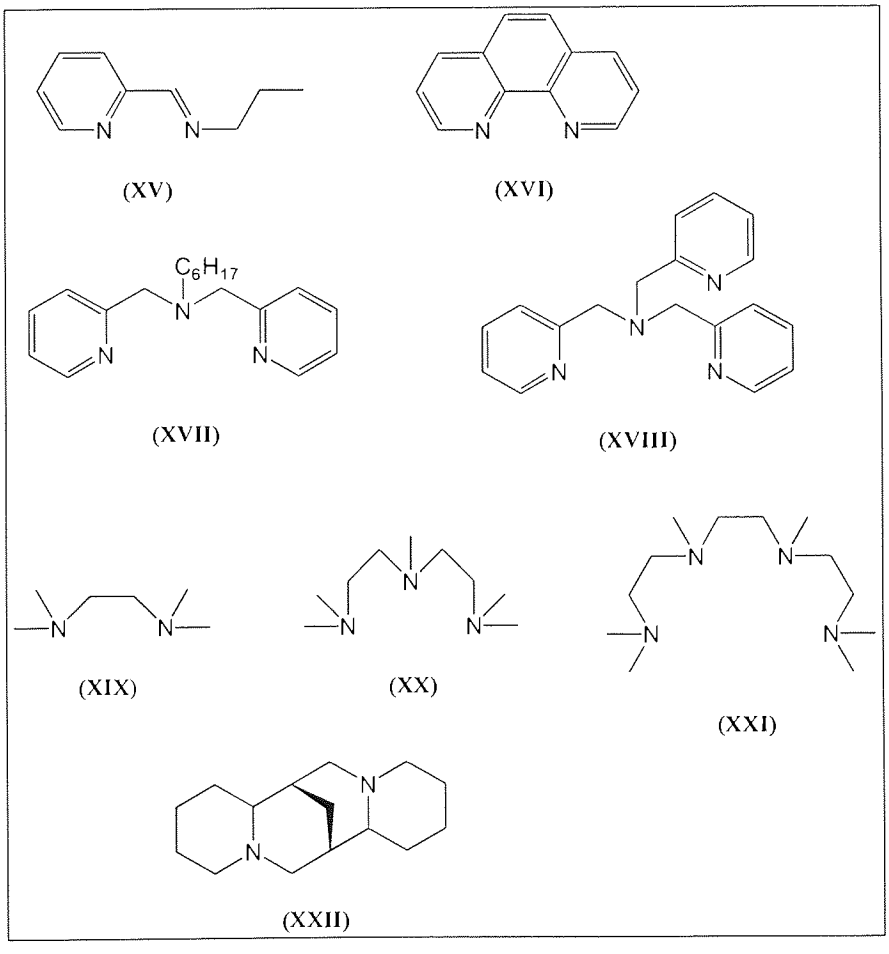

Alkyl halides (chloride or bromide) are typically used as initiators in copper halide/α-diimine mediated ATRP. The selection of the appropriate molecule, which yields a suitably high ratio of the rate of initiation to the rate of propagation, is essential for controlled polymerisation. Alkyl halides that closely resemble the halogen end-capped chain end are generally utilised. For example, 1-phenylethyl bromide is commonly used for the ATRP of styrene. Moreover, arenesulphonyl chlorides have been reported to be a class of universal initiators, capable of effectively initiating the polymerisation of styrenic, methacrylic and acrylic monomers[114]. In each case, near-complete initiation is observed, as the highly reactive arylsulphonyl radicals generated cannot self-terminate. However, the polymer radicals generated are susceptible to termination and unless a suitable concentration of deactivator is present at the outset termination reactions will develop.

The precise mechanism of copper halide/α-diimine mediated ATRP has been of great debate. It is generally accepted that the copper halide is complexed by 2 equivalents of the ligand, and that abstraction of a halogen atom from a dormant chain, to form a chain radical, results in rearrangement from a tetrahedral $Cu^{(I)}$ complex to a distorted square based pyramidal $Cu^{(II)}$ complex, as shown in scheme 1.15. It is assumed that the cationic copper(α-diimine)$_2$ complexes are complexed by a halide counteranion. However, Matyjaszewski et al have recently reported that this may not be the case, suggesting that a $[CuX_2]^-$ species actually fulfils the role of counteranion[115].

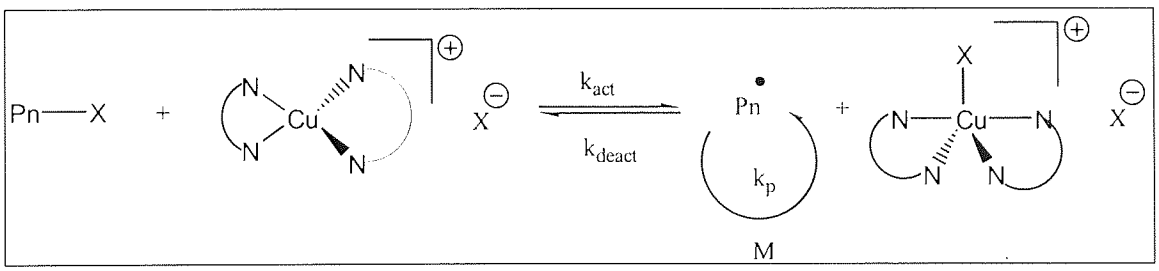

Scheme 1.15. Mechanism of copper halide/α-diimine mediated ATRP.

Although the exact nature of the copper complexes is not known, the formation of $Cu^{(II)}$ complexes during ATRP has been confirmed by electron paramagnetic resonance spectroscopy[116]. Furthermore, the formation of an excess of deactivator (5% $Cu^{(II)}$ relative to $Cu^{(I)}$) during the incipient stages of the polymerisation was also

observed, suggesting the persistent radical effect is operational. Further evidence for this phenomenon was provided using the GPC curve resolution method[117].

There is powerful evidence to suggest that the assumed ATRP equilibrium is operational, but no direct evidence of the nature of the propagating species has been reported. This is primarily owing to the paramagnetic nature of the catalytic species precluding the direct observation of radicals by electron spin resonance or electron paramagnetic resonance spectroscopy. Nevertheless, there is considerable indirect evidence that reinforces this claim.

The most powerful piece of evidence supporting the radical nature of the propagating species in ATRP is reverse-ATRP[118]. This technique utilises conventional radical initiators, such as AIBN, in conjunction with $Cu^{(II)}$halide/α-diimine complexes to enter the ATRP equilibrium from the opposite side to that from which it is conventionally approached. This illustrates that free-radicals are efficiently scavenged by the $Cu^{(II)}$ deactivating species, and that the resultant adducts can participate in ATRP. However, although this confirms that radicals can be involved in the initiation step, it does not prove that the propagating species formed after the initial deactivation are also free-radicals.

Further substantial evidence for propagation via a free-radical species is provided by the similarity of regio- chemo- and stereo-selectivities observed for polymers synthesised by ATRP and free-radical polymerisation[119]. Moreover, atom transfer radical copolymerisation reactivity ratios for numerous sets of monomers have also been observed to be identical to those known for free-radical polymerisation[120].

The addition of scavengers or initiators that are selective for a particular active site is a common ploy for distinguishing between ionic, radical, and coordination mechanisms. As ATRP has been shown to be effective in the presence of water and small quantities of nucleophiles, polymerisation involving cationic or anionic intermediates can be excluded. Furthermore, the termination of the ATRP of styrene upon addition of galvinoxyl, strongly suggests that radicals are involved. However, the possible deactivation of the catalyst by such species cannot be discounted.

It is noteworthy that Haddleton et al reported that the rate of polymerisation of methyl methacrylate was accelerated in the presence of phenols, which are commonly used inhibitors of free-radical polymerisation[119]. On the basis of this, it was suggested that ATRP could not proceed via radical intermediates[121]. However, phenols have

previously been shown to be ineffective retarders of polymerisation in the absence of oxygen[122]. It is also probable that the rate acceleration is manifested as a result of the reduction of $Cu^{(II)}$ deactivating species by phenol, given that a similar reaction of hydroquinone with silver halides is well known, and is commonly utilised in the photographic development process[123].

Considering the evidence concerning the mechanism of ATRP, it is currently reasonable to assume that it can be described by scheme 1.15. Thus, assuming that the propagating species are radicals, the rate of polymerisation can be described by equation 1.12.

$$Rp = -\frac{d[M]}{dt} = k_p[Pn^*][M] \qquad (1.12)$$

Where Rp = the rate of polymerisation.

[M] = the concentration of monomer.

t = time.

k_p = the rate constant of radical propagation.

[Pn*] = the concentration of propagating species.

The steady-state assumption for the concentration of propagating radicals is expressed by

$$\frac{d[Pn^*]}{dt} = k_{act}[PnX]\left[Cu^{(I)}/2L\right] - k_{deact}[Pn^*]\left[Cu^{(II)}X/2L\right] = 0 \qquad (1.13)$$

and thus,

$$[Pn^*] = \frac{k_{act}[PnX]\left[Cu^{(I)}/2L\right]}{k_{deact}\left[Cu^{(II)}X/2L\right]} \qquad (1.14)$$

Where k_{act} = the rate constant of activation.

k_{deact} = the rate constant of deactivation.

[PnX] = the concentration of dormant chains.

$[Cu^{(I)}/2L]$ = the concentration of activating species.

$[Cu^{(II)}X/2L]$ = the concentration of deactivating species.

Substitution of equation 1.14 into equation 1.12, under the assumptions that the rate of initiation is faster than the rate of propagation and that the equilibrium between dormant and active species is rapid and shifted to the dormant species, yields

$$Rp = -\frac{d[M]}{dt} = k_p \frac{k_{act}[PnX][Cu^{(I)}/2L]}{k_{deact}[Cu^{(II)}X/2L]}[M] \qquad (1.15)$$

which can be simplified to

$$Rp = k_p[Pn^*][M]k_pK_{eq}[PnX]_0 \frac{[Cu^{(I)}/2L]}{[Cu^{(II)}X/2L]}[M] \qquad (1.16)$$

Where $K_{eq} = k_{act}/k_{deact}$ and $[PnX]_0$ = the initial concentration of initiator.

Several reports detailing thorough investigations of the ATRP of various monomers have appeared in the literature. The rate of propagation has been reported to be first order with respect to the concentration of monomer, initiator and $Cu^{(I)}$halide[105, 124]. Determination of the external order of the reaction with respect to $Cu^{(II)}$ deactivator has proved elusive, owing to its in situ formation via the persistent radical effect. Even when polymerisation is conducted in the presence of an initial concentration of deactivator in excess of that typically formed, more deactivator is still generated[116]. The concentration of propagating species has been estimated to be of the order of 10^{-8}M [105, 108, 124]. This is comparable to that observed for other living radical polymerisation techniques, and is suitably low to ensure termination is negligible. The equilibrium constant has been estimated to be in the region of 10^{-8} [105, 124], with the constituent rate constants of activation and deactivation estimated as approximately 10^{-1} $M^{-1}s^{-1}$ and 10^7 $M^{-1}s^{-1}$ respectively[88]. Moreover, the activation frequency has been estimated and has been shown to be the principle reason for the formation of narrow polydispersity polymers from an early stage of the polymerisation[117].

1.5. Synthetic applications of ATRP

ATRP has the potential ability to facilitate the synthesis of polymers of precisely controlled architecture, composition and functionality. The realisation of such potential would result in advances in current materials technology, and hence this is providing a driving force for the current intensive activity in this field.

1.5.1. Functional polymers

It is generally assumed that the propagating species in ATRP are free radicals and therefore it is assumed that the technique will display similar versatility to that of conventional free-radical polymerisation, allowing the polymerisation of a vast range of monomers.

The homopolymerisation of numerous methacrylic and acrylic monomers bearing pendant functional groups, such as glycidyl acrylate[125], 2-hydroxyethyl acrylate[126] and methacryloyl-1,2:5,6-di-O-isopropylidene-D-glucofuranose[127], has been conducted using the conventional copper halide/4,4'-dialkyl-2,2'-bipyridyl catalyst system. Haddleton has also reported the use of the CuBr/N-(n-pentyl)-2-pyridinemethanimine catalyst system for the polymerisation of 5'-methacryloyluridine and 5'-methacryloyladenosine[128]. The structures of these monomers are shown in Scheme 1.16.

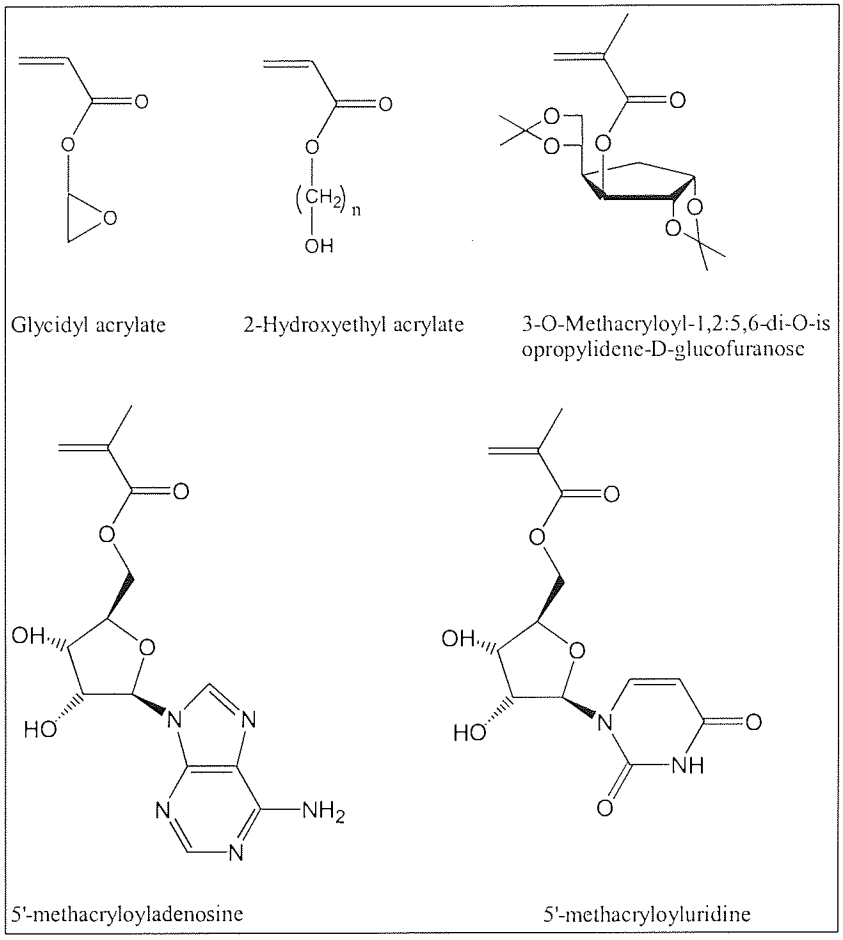

Scheme 1.16. Monomers bearing pendant functional groups polymerised by ATRP.

More interestingly, the ATRP of monomethoxy-capped oligo(ethylene oxide)[129] and sodium methacrylate[130] in aqueous media at ambient temperatures mediated by CuBr/2,2'-bipyridyl has been reported. The polymerisations proceeded at much faster rates than that observed for comparable polymerisations in conventionally used non-polar solvents, with resultant polymers surprisingly displaying narrow molecular weight distributions ($\overline{M_w}/\overline{M_n}$ <1.20). It is thought that the rate acceleration is due to the preferential formation of the desired monomeric catalyst, Cu(I)(2,2'-bipyridyl)$_2$ in aqueous media.

ATRP has also been utilised for the synthesis of polyacrylonitrile displaying extremely narrow molecular weight distributions[131, 132]. However, the resultant polymers had molecular weights that were considerably higher than the corresponding values calculated from 100% initiator efficiency, and the pseudo first-order kinetic plots displayed significant curvature. The authors were unsure of the reason for this behaviour, but suggested that alteration of the metal or ligand may facilitate better

control. Indeed, this approach has proved successful for the ATRP of 4-vinyl pyridine[133] and methacrylamides[134, 135], where the use of PMDETA and Me_6TREN respectively as ligands, as opposed to 2,2'-bipyridyl, dramatically improved the control over the polymerisation.

It is of note that vinyl acetate, vinyl chloride and acrylic and methacrylic acid have so far not been polymerised directly by ATRP. Carboxylic acid groups appear particularly detrimental to ATRP. A study by Haddleton et al[136] suggested that increasing the ratio of the acid to CuBr/N-(n-butyl)-2-pyridinemethanimine catalyst above unity results in poisoning of the active catalytic species and broadening of the molecular weight distribution displayed by the resultant polymers. The only manner in which these problems can be circumvented is by polymerisation of monomers having the acid function protected[137], which can subsequently be deprotected to yield the desired acid functionality.

1.5.2. Telechelic polymers

The synthesis of telechelic polymers by ATRP can be achieved by two routes; post-polymerisation modification of end groups, or by use of initiators bearing functional groups. In polymerisations where transfer is negligible, all chains will bear the initiator fragment. Thus, if an initiator bearing a given functionality is utilised, end-functional polymers can be synthesised in a single step. This approach has been widely utilised for the synthesis of polymers incorporating allyl[138], hydroxy[139, 140], nitro and amino[141], and thipohene[142] functional end-groups amongst others.

Polymers synthesised by ATRP generally possess a terminal halogen group, which makes them amenable to further reactions. The halogen end-group has been transformed by post-polymerisation reactions, into a variety of functional groups. These include allyl[143, 144], azido and amino groups[145, 146], although the transformation of the halogen to virtually any end-group can be envisaged. Moreover, when difunctional initiators are used, such as dibromo-p-xylene, α,ω-difunctional polymers can be synthesised, as the polymers will possess halogen groups at either end of the chain. This principle could also be applied to any multifunctional initiator, provided the retention of the halogen end-groups is possible during the polymerisation.

1.5.3. Co-polymers

ATRP can be utilised for the synthesis of statistical, alternating, block and graft copolymers. The kinetic parameters for the atom transfer copolymerisation of any given two monomers have been found to be similar to those observed in conventional free-radical polymerisation[147]. The statistical copolymerisations of n-butyl acrylate with methyl methacrylate[148], n-butyl methacrylate with methyl methacrylate[149], styrene with n-butyl methacrylate[150], and styrene with N-cyclohexylmaleimide[151], have been reported and all were found to agree with this (i.e. the reactivity ratios in conventional free-radical polymerisation and ATRP are interchangeable).

Gradient copolymers of styrene and n-butyl acrylate, in which the sequence distribution of the repeat units varies in a well-defined way as function of chain length, have been synthesised by ATRP[152]. Moreover, alternating copolymers of N-substituted maleimides with styrene have also been synthesised[153], further indicating the versatility of ATRP.

Block copolymers can be synthesised by ATRP by two methods; sequential monomer addition, or by use of macroinitiators. The former of these two methods is the most simple, involving addition of a second monomer after consumption of the first. The one-pot synthesis of acrylate-methacrylate block copolymers was achieved in this way[154]. However, the latter of the two aforementioned techniques appears the preferred route, as it allows tailoring of the nature of the catalyst and medium to the synthesis of the second block.

The alterations generally concern interchange of the halogen end group from a Br to a Cl, by a process deemed "halogen exchange"[155, 156]. The exchange is moderated by changing the catalyst from CuBr to CuCl, with Cl then replacing Br as the end-cap due to its greater affinity to form a bond with carbon. Matyjasewski illustrated this technique to be particularly effective for the synthesis of ABA triblock copolymers of methyl methacrylate and methyl acrylate using a difunctional initiator[157], where CuBr/bis(bromopropionyloxy)ethane is the preferred couple for the synthesis of well defined poly(methyl acrylate) blocks. If the Br end-groups of the central poly(methyl acrylate) block are not replaced by Cl, the initiation of the second methyl methacrylate block is slow and incomplete and resultant polymers display broad bimodal molecular weight distributions. A variety of other thermoplastic elastomers have also been prepared by ATRP, utilising butyl acrylate, methyl acrylate, or 2-ethylhexyl acrylate as

the central soft block, with styrene, methyl methacrylate, or acrylonitrile as the hard A blocks[158, 159].

Macroinitiators prepared by polymerisation techniques other than ATRP have also been utilised for block copolymer synthesis. Polymers synthesised by living carbocationic polymerisation are perhaps the most amenable to this transformation, as they generally possess halogen end-groups. For example, polystyrene-polyisobutene, poly(methyl methacrylate)-poly(isobutene), poly(methyl acrylate)-poly(isobutene), AB and ABA block copolymers have been prepared by use of mono or α,ω-difunctional polyisobutene Cl end-capped macroinitiators[160, 161, 162].

The use of polymers prepared by other techniques as macroinitiators for ATRP generally requires the modification of the end-group to that resembling an ATRP initiator. The synthetic procedures utilised for this, are normally trivial, but must nonetheless be very efficient.

The transformation of polymers synthesised by living anionic polymerisation to ATRP macroinitiators, as shown in scheme 1.17, can be achieved by first reacting the anionic chain end with styrene oxide and then subsequently reacting the product with bromoisobutyrylbromide (BriBBr). Macroinitiators such as polystyrene and polystyrene-polyisoprene have been found to be efficient for the synthesis of AB and ABA block copolymers respectively, with styrene, methyl acrylate, butyl acrylate, methyl methacrylate and acrylonitrile[163].

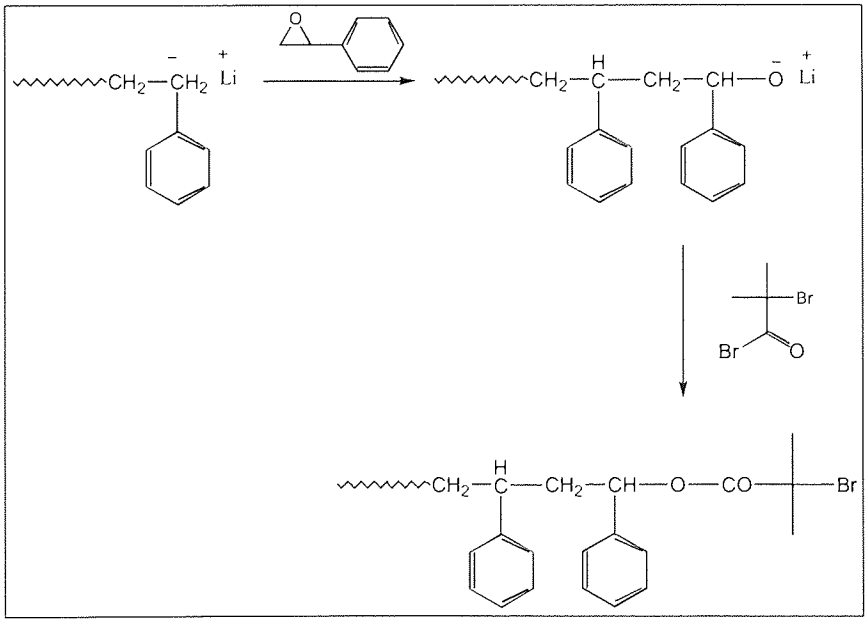

Scheme 1.17. Transformation of anionic polymerisation to ATRP.

Polynorbornene synthesised by living ring-opening methathesis polymerisation (ROMP) mediated by a Schrock carbene complex, has also been transformed into and used as a macroinitiator for ATRP of a variety of monomers[164], as shown in scheme 1.18. It is anticipated that this technique will be compatible with other polycyclics synthesised by ROMP, and hence will facilitate the synthesis of a variety of new materials.

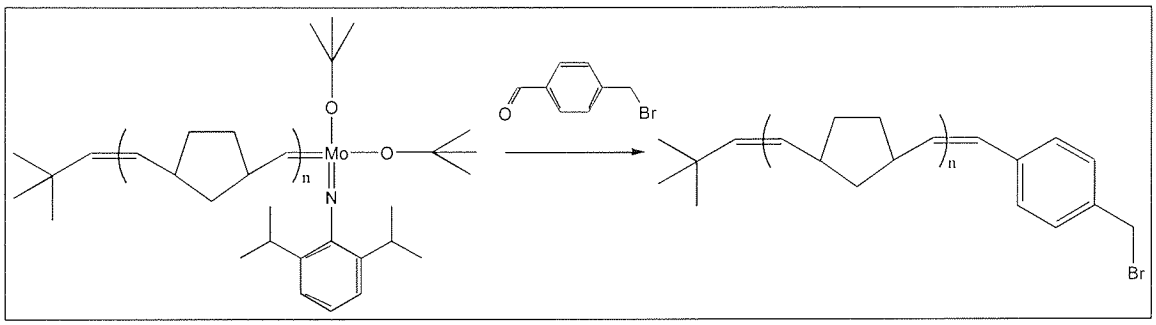

Scheme 1.18. Transformation of ROMP to ATRP.

Similar techniques have been developed for the synthesis of ABA copolymers with a central block that has been synthesised by step growth polymerisation, such as polysulphone or polyesters[165]. In fact, any polymer with an amino or hydroxy end-group can be modified, by reaction with 2-bromopropionyl bromide or similar, to form a macroinitiator for ATRP. For example, the use of poly(oxyethylene) in this role has been widely reported[166, 167, 129].

Inorganic/organic hybrid materials can also be synthesised by the macroinitiator method. Poly(dimethylsiloxane) benzyl chloride functionalised macroinitiators can be used for the synthesis of di and triblock copolymers with styrene and a variety of acrylates[168].

Most recently, radical telomerisation has emerged as a facile route to macroinitiators of vinyl polymers that can only be synthesised by conventional free-radical polymerisation. The transfer agent is utilised to incorporate end-groups into the polymer that are capable of initiating ATRP. Block copolymers of vinyl acetate with styrene[169] and n-butyl acrylate[170], and poly(vinylidene fluoride) with styrene[171] have been synthesised in this manner. Other attempts to synthesise similar materials employed functionalised azo-initiators to furnish polymers with end-groups capable of initiating ATRP[172]. However, this route yields polymers with much broader molecular weight distributions.

1.5.4. Multi-armed polymers

Multiarmed or branched polymers are of great interest because of their potential to form unique spatial shapes, lower degrees of chain entanglements and lower viscosity in comparison with their linear counterparts. There are numerous ways to prepare such polymers by ATRP.

The simplest procedure involves the use of multifunctional initiators with three or more initiating sites as the central core from which the growing chains radiate. A range of different molecules have been utilised to synthesise star polymers, shown in scheme 1.19, ranging from simple trifunctional initiators, such as 1,3,5-(2'-bromo-2'methylpropionato)benzene[173] and 1,1,1-tris(4-(2-bromoisobutyryloxy)phenyl) ethane[174], to more complex tetra, hexa and octafunctional initiators based on calixarenes[175, 176], hexaphenyl benzenes[177], cyclotriphosphazenes[174], and cyclosiloxanes[174]. Star polymers with much higher numbers of arms radiating from a central dendritic core have also been synthesised[178]. An extravagant attempt to synthesise star polymers with 45 or more arms using a hyperbranched polyglycerol macroinitiator has also been reported[179].

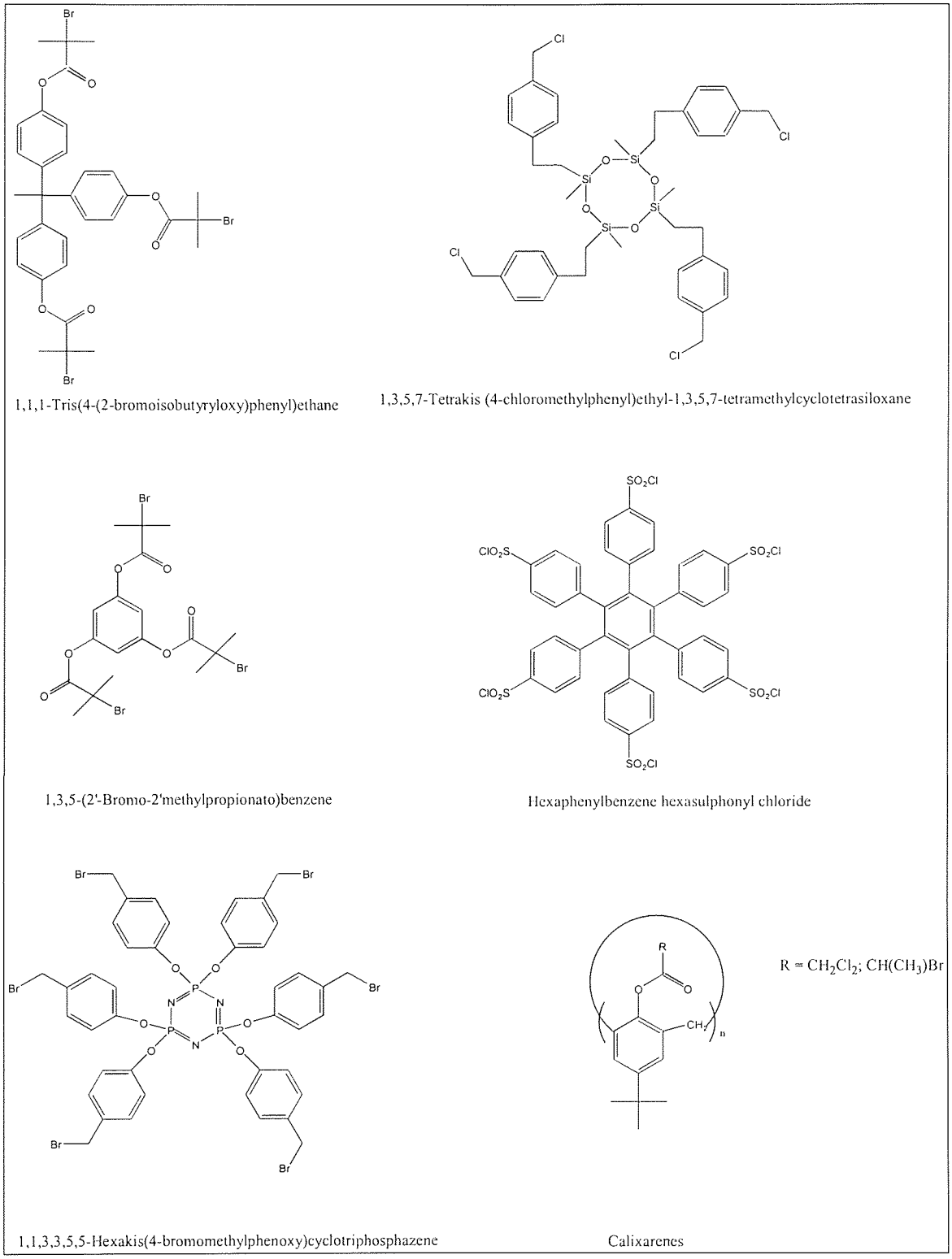

Scheme 1.19. Multifunctional initiators for ATRP.

Densely grafted, or brush polymers, can also be synthesised by ATRP. The preferred route, illustrated in scheme 1.20, involves grafting from a macroinitiator with branch points at every repeat unit in the backbone[180].

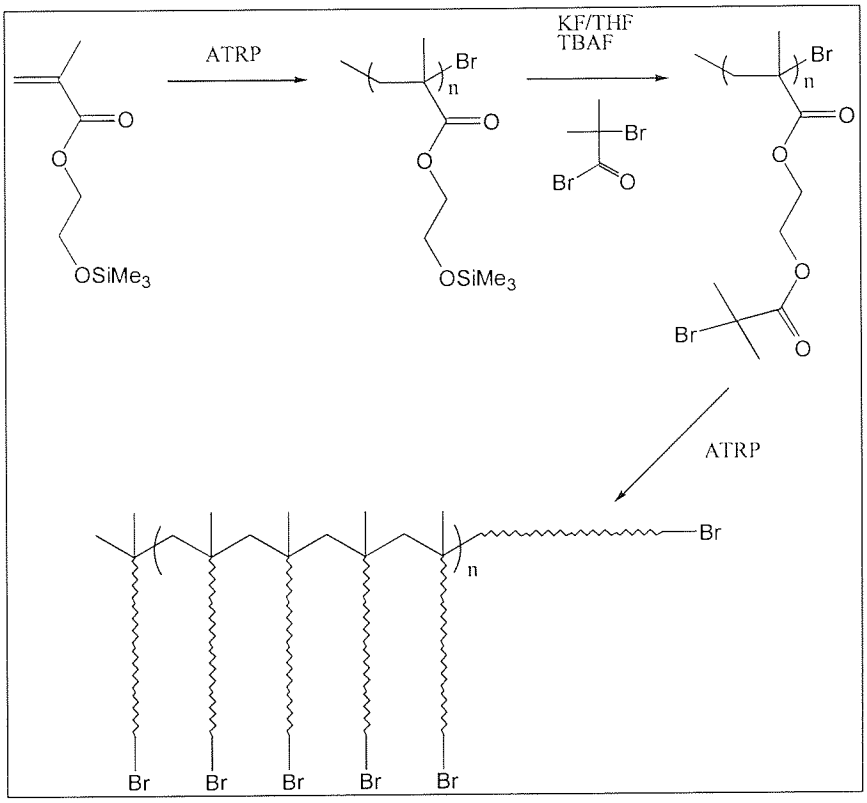

Scheme 1.20. Synthesis of graft polymers by ATRP.

Hyperbranched polymers can be prepared by self-condensing vinyl polymerisation[181], shown in scheme 1.21, which utilises bifunctional monomers in which one of the functionalities can be activated by an external trigger to cause the free-radical polymerisation of the other. Such monomers thus bear both a vinyl group and an initiator group.

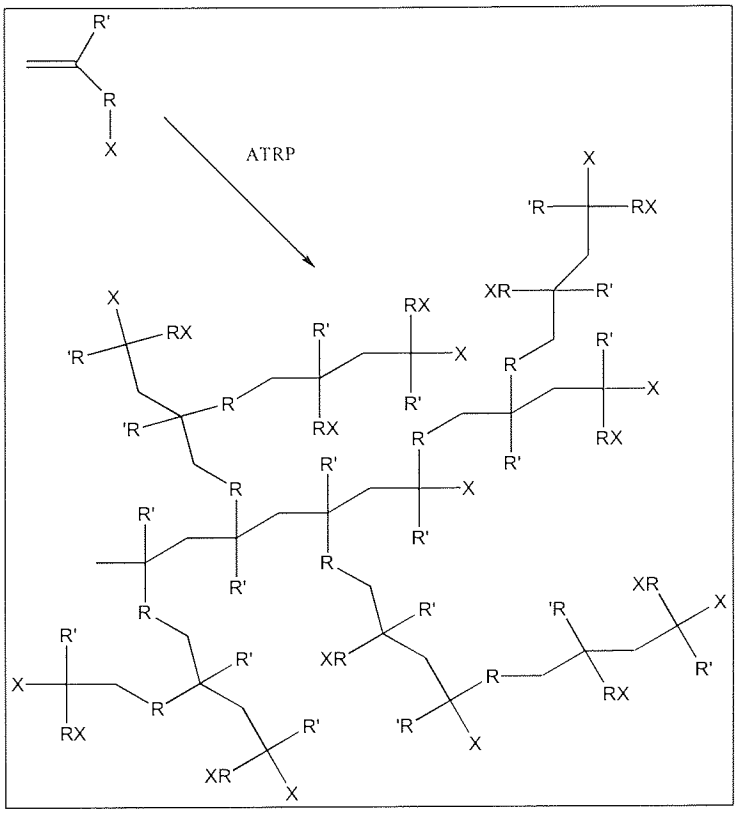

Scheme 1.21. Self-condensing vinyl polymerisation.

p-Chloromethylstyrene[182] and 2-(2-bromopropionyloxy)ethyl acrylate[183, 184, 185] have been shown to be suitable candidates for this process. However, both polymerisations are subject to problems, such as biradical termination reactions, which if prolific generate a large excess of the deactivator and thus retard the polymerisation. Matyjaszewski sought to overcome this problem by use of zero-valent copper as a reducing agent for copper(II) deactivating species. Moreover, whilst this allows the polymerisations to be driven to higher conversion, it does not prevent the detrimental termination reactions. Hence, without further improvements this technique cannot be utilised to produce well-defined polymers with controlled degrees of branching. However, it does have the potential to facilitate the synthesis of dendritic polymers in a single step.

1.6. Scope of the project

It is evident that ATRP offers the potential to synthesise a wide range of speciality materials. The ultimate aim of this project is to develop an effective ATRP catalyst system for the polymerisation of methacrylic monomers bearing bifunctional photoconductive NLO chromophores. It is anticipated that this could then be utilised for the synthesis of multi-armed PR polymers of precisely controlled architecture.

The scope of this project is to develop an effective ATRP catalyst system for the polymerisation of methacrylic monomers, using suitable commercially available model monomers. The kinetics and the effects of the concentrations of the various components upon the polymerisation are to be studied, to facilitate the development of a thorough understanding of the polymerisation system. This knowledge may then be utilised for the optimisation of the reaction conditions for the polymerisation of the model monomers, and subsequently the target monomers.

2. Experimental

2.1. Vacuum techniques

The vacuum line, illustrated in figure 2.1, was constructed of pyrex glass and consisted of a single manifold (A) with a series of B19 ground glass joints connected to this by PTFE greaseless taps. The manifold was connected to a mercury diffusion pump and an Edwards rotary vacuum pump via a main tap. Two liquid nitrogen cold traps were present to prevent vapours generated in the system from entering and contaminating the vacuum pump. The mercury diffusion pump and the rotary vacuum pump were used in combination to reduce the internal pressure of the system to approximately 10^{-4}mm Hg, which was measured using a mercury "vacustat" gauge. A nitrogen supply was also connected to the system to allow manipulation of materials under an inert atmosphere.

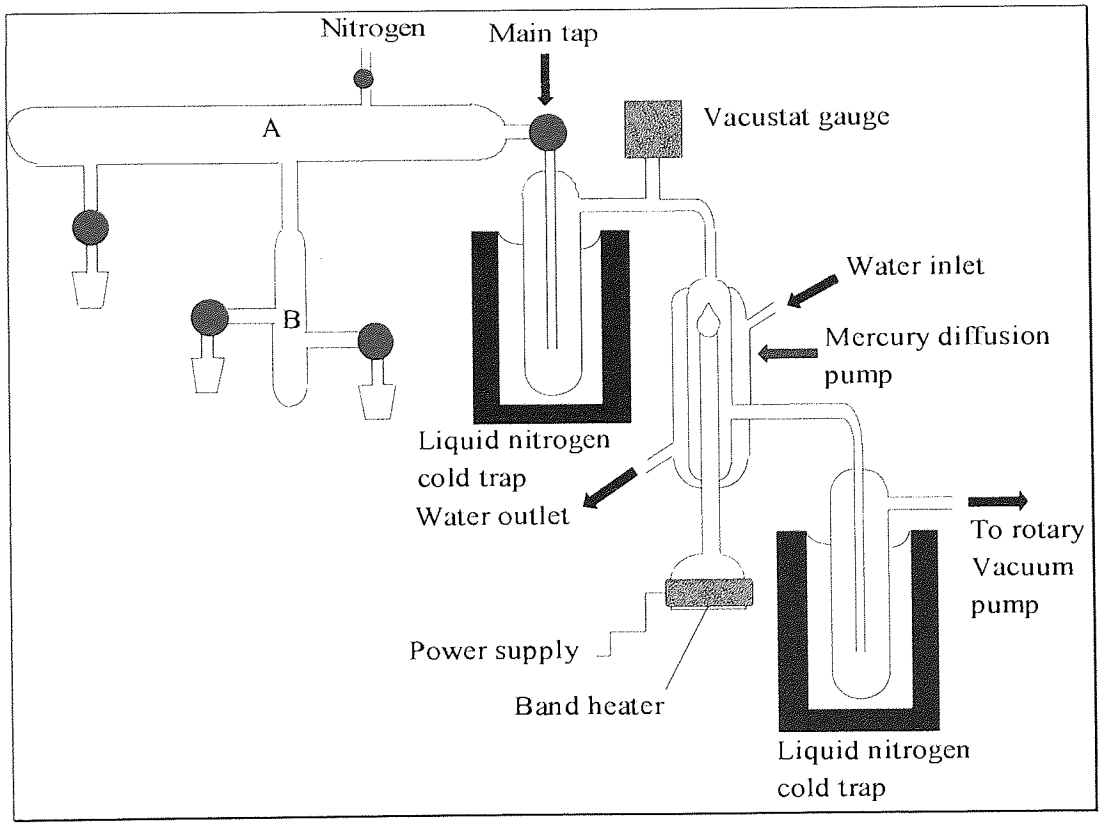

Figure 2.1. Vacuum line.

2.1.1. Freeze-thaw degassing

In order to remove unwanted dissolved gases from solution and facilitate distillation of materials under vacuum, liquids were degassed by a freeze-pump-thaw degassing process. The flask containing the material was connected to the vacuum line, the main tap opened and the manifold evacuated. The material was then frozen by immersing the flask in liquid nitrogen. When frozen, the tap on the flask containing the material was opened and the flask evacuated. Once the pressure in the system had reached its minimum value again, the tap on the flask was closed and the contents of the flask allowed to warm to room temperature, releasing trapped gases. The contents of the flask were then frozen once more, the tap on the flask was opened and the flask re-evacuated to remove the released gases. When the pressure in the system reached a minimum value, the tap on the flask was closed and the material allowed to warm to room temperature. The procedure was repeated until no further gas was released during the thawing stage of the process.

2.1.2. Trap-to-trap distillation

The vacuum line was utilised to transfer degassed liquids to a second vessel by a trap-to-trap distillation procedure. The flask containing the degassed liquid and the receiver flask were attached to the vacuum line and the manifold evacuated. The receiver flask was immersed in liquid nitrogen and then subsequently evacuated by opening the tap on this flask. When the pressure reached a minimum level the main tap was closed to isolate the manifold from the pump. The tap on the flask containing the degassed liquid was then opened allowing the material to distil. When the desired amount of material had been collected in the receiver flask the taps on the flasks were closed and the main tap opened to remove any remaining vapours from the manifold.

2.2. Argon dry box

A dry-box supplied by Halco engineering Ltd was utilised to allow storage and manipulation of materials under an inert atmosphere. The apparatus consisted of a main compartment with access gloves and a double door posting port. The main compartment was maintained under an argon atmosphere which was constantly re-circulated through moisture and oxygen absorbent columns containing 3A molecular sieve and BASF

R311 catalyst respectively. The double door posting port allowed equipment and materials to be transferred to and from the port without breaching the atmosphere within the main compartment. Transfer of materials into the main compartment was achieved by sealing the door connecting the main compartment and the port, placing the desired articles in the port, sealing the outer door of the port and then subsequently subjecting the port to three cycles of evacuation and filling with argon. The door connecting the main compartment to the port was then opened and the articles transferred from the port into the main compartment. The removal of articles from the main compartment was achieved by the reverse of this procedure.

2.3. Materials and purification

2.3.1. Styrene

Styrene, 99% purity, was purchased from the Aldrich Chemical Company and stored in a refrigerator until required. The product was supplied with 0.005% by weight of the commercial auto-polymerisation inhibitor 4-tert-butyl catechol, which was removed by standing 250ml of the liquid over 20g of sodium hydroxide pellets. Styrene was subsequently distilled under high vacuum by the trap to trap distillation technique (section 2.1.2), directly from this flask into a vacuum flask containing 10g of calcium hydride over which it was stored in a refrigerator until required. Monomer was then distilled under high vacuum directly from this flask into the polymerisation vessel as required.

2.3.2. Methyl methacrylate

Methyl methacrylate, 99% purity, was purchased from Aldrich and purified by a procedure identical to that described for styrene.

2.3.3. Xylene

A solution of mixed isomers of xylene, 98% purity, was purchased from Fisher Scientific and purified by first standing over anhydrous magnesium sulphate and then subsequently over calcium hydride. When required the appropriate quantity of xylene was distilled under high vacuum directly into the reaction vessel by the trap to trap distillation technique described in section 2.1.2.

2.3.4. Diglyme

Diglyme, 99+% purity (anhydrous), was purchased from Aldrich and used without further purification. The material was stored and handled exclusively in the argon dry box.

2.3.5. Dimethyl sulphoxide

Dimethyl sulphoxide, 99+% purity (anhydrous), was purchased from Aldrich and used without further purification. The material was stored and handled in the argon dry box.

2.3.6. N,N'-Dimethyl formamide

N,N'-Dimethyl formamide 99% (HPLC grade) was purchased from Fisher Scientific and stored in a vacuum flask over calcium hydride. When required, the appropriate quantity was distilled under high vacuum from this flask into the desired reaction vessel.

2.3.7. N,N'-Dimethylacetamide

Dimethylacetamide, 99+% purity (anhydrous), was purchased from Aldrich and used without further purification. The material was stored and manipulated exclusively in the argon dry box.

2.3.8. 1-Phenyl ethyl bromide

1-Phenyl ethyl bromide, 98% purity, was purchased from Lancaster Synthesis and used without further purification. The material was stored and manipulated in the argon dry box.

2.3.9. Ethyl-2-bromoisobutyrate

Ethyl-2-bromoisobutyrate 98% was purchased from Lancaster and used without purification. The material was stored and manipulated in the argon dry box.

2.3.10. Copper (I) bromide

Copper(I) bromide, 99.999% certified purity, was purchased from the Aldrich chemical company and used without further purification.

2.3.11. Copper (II) bromide

Copper (II) Bromide, 99.999% certified purity, was purchased from Aldrich and used without further purification.

2.3.12. Methanol

Methanol, SLR grade, was purchased from Fisher Scientific and used without further purification.

2.3.13. Hexane

Hexane, SLR grade, was purchased from Fisher Scientific and used without further purification.

2.3.14. Tetrahydrofuran

Tetrahydrofuran, HPLC grade, was purchased from Fisher Scientific and used without further purification.

2.3.15. Magnesium sulphate

Magnesium sulphate, 98% purity (anhydrous), was purchased from Aldrich and stored in an oven at 200°C until required.

2.3.16. Calcium Hydride

Calcium hydride, 97% purity, was purchased from Avocado Chemicals and used without further purification.

2.3.17. Carbazole

Carbazole, 98% purity, was purchased from Lancaster and used without further purification.

2.3.18. 2-Chloroethanol

2-Chloroethanol, 98% purity, was purchased from Lancaster and used without further purification.

2.3.19. Potassium hydroxide

Potassium hydroxide, 97% purity, was purchased from Lancaster and used without further purification.

2.3.20. 4-Nitro aniline

4-Nitro aniline, 98% purity, was purchased from the Acros Chemical Company and used without further purification.

2.3.21. Hydrochloric acid

Hydrochloric acid, 35% aqueous solution, was purchased from Fisher scientific and used without further purification.

2.3.22. Sodium nitrite

Sodium nitrite, 98% purity, was purchased from the Acros Chemical Company and used without further purification.

2.3.23. Water

Water, HPLC grade, was purchased from Fisher Scientific and used without further purification.

2.3.24. Sodium lauryl sulphate

Sodium lauryl sulphate, 95% purity, was purchased from the Aldrich and used without further purification.

2.3.25. Dichloromethane

Dichloromethane, SLR grade, was purchased from Fisher and used without further purification.

2.3.26. N-(2-hydroxyethyl) carbazole

N-(2-hydroxyethyl) carbazole was synthesised by the procedure described in section 2.5.1.

2.3.27. Methacryloyl chloride

Methacryloyl chloride, 97% purity, was purchased from the Lancaster chemical company and used without further purification.

.2.3.28. Triethylamine

Triethylamine, 98% purity was purchased from the Lancaster chemical company and used without further purification.

2.3.29. (4-Nitrophenyl)-[3-[N-(2-hydroxyethyl)carbazolyl]]diazene

(4-Nitrophenyl)-[3-[N-(2-hydroxyethyl)carbazolyl]]diazene was synthesised by the procedure described in section 2.5.2.

2.3.30. Sodium carbonate

Sodium carbonate, 98% purity, was purchased from the Lancaster chemical company and used without further purification.

2.3.31. (4-Nitrophenyl)-[3-[N-[2-(methacryloyloxy)ethyl] carbazolyl]] diazene

(4-Nitrophenyl)-[3-[N-[2-(methacryloyloxy)ethyl] carbazolyl]] diazene was synthesised by the procedure described in section 2.5.3.

2.3.32. 2-Pyridinecarboxaldehyde

2-Pyridine carboxaldehyde, 99% purity, was purchased from the Aldrich chemical company and used without further purification.

2.3.33. n-Alkyl amines

Propylamine, butylamine and octylamine, all 99% purity, were purchased from the Lancaster chemical company and used without further purification.

2.3.34. Diethyl ether

Diethyl ether, SLR grade, was purchased from Fisher scientific and used without further purification.

2.3.35. Ethanol

Ethanol, 99% purity, was supplied by the Fisher chemical company and used without further purification.

2.3.36. N-(n-alkyl)-2-pyridinemethanimines

N-(n-propyl)-2-pyridinemethanimine, N-(n-butyl)-2-pyridinemethanimine, N-(n-octyl)-2-pyridinemethanimine were synthesised by the procedure described in section 2.4.

2.4. The synthesis of N-alkyl-2-pyridinemethanimines

N-propyl-2-pyridinemethanimine, N-butyl-2-pyridinemethanimine and N-octyl-2-pyridinemethanimine were synthesised by the condensation of the appropriate n-alkyl amine with pyridine-2-carboxaldehyde in a Schiff's base reaction. The general synthetic procedure utilised is described as follows.

10mL of pyridine-2-carboxaldehyde (0.105 mol) was dissolved in 80mL of diethyl ether. 0.12 mol of the appropriate amine was added dropwise with stirring to the solution over 10 minutes, after which 5g of anhydrous magnesium sulphate was added. The mixture was stirred for a further 30 minutes. The magnesium sulphate was then removed by filtration and the solvent, and any unreacted amine, subsequently removed by rotoevaporation. The resultant golden-yellow oil was stored in a a sealed flask in a freezer until required.

2.5 The synthesis of (4-nitrophenyl)-[3-[N-[2-(methacryloyloxy)ethyl] carbazolyl]]diazene

The synthesis of (4-nitrophenyl)-[3-[N-[2-(methacryloyloxy)ethyl] carbazolyl]] diazene (MOECarb) was achieved by a modified procedure of that reported by Ho et al[30]. The overall reaction scheme consists of three steps and is summarised in scheme 2.1.

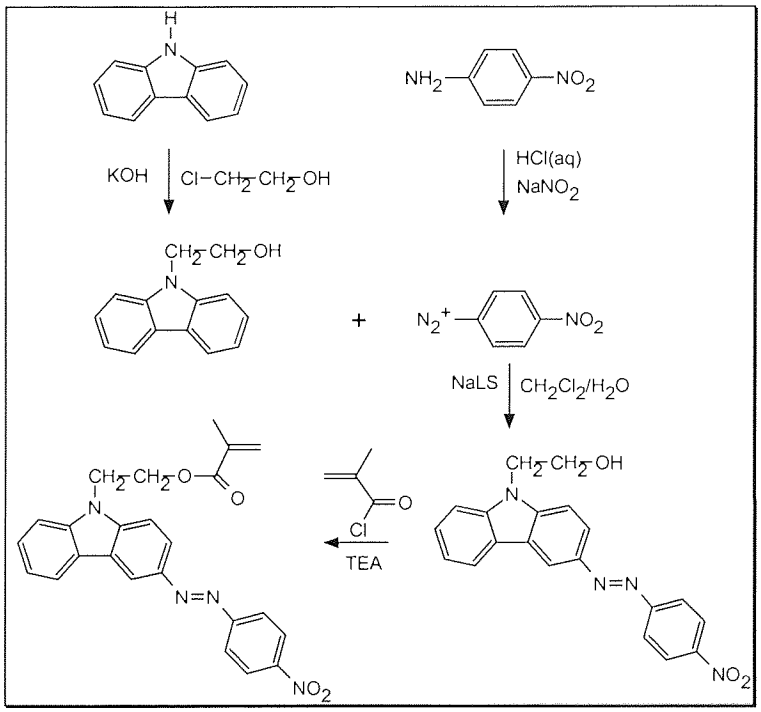

Scheme 2.1. Reaction scheme for the synthesis of MOECarb.

As illustrated, N-(2-hydroxyethyl) carbazole was obtained by the alkylation of carbazole and then coupled with 4-nitrobenzenediazonium chloride in a two phase water-dichloromethane mixture. Esterification of (4-nitrophenyl)-[3-[N-(2-hydroxyethyl)carbazolyl]]diazene with methacryloyl chloride gave the desired monomer. The respective methods by which each step was conducted are described in sections 2.5.1, 2.5.2, 2.5.3.

2.5.1. The synthesis of N-(2-hydroxyethyl) carbazole

14.0g (0.25 mol) of powdered potassium hydroxide was weighed into a 250ml single necked round bottomed flask. 80ml of DMF was added to this and the mixture

stirred at room temperature for 15 minutes. 6.6g (0.040mol) of carbazole was then added and the mixture stirred at room temperature for 45 minutes. 4.0g (0.050 mol) of 2-chloroethanol was added slowly and the resultant mixture stirred overnight. The mixture was then poured into 1.5 L of water and allowed to stand for approximately 30 minutes to allow the precipitation of the product to reach completion. The resultant white solid was filtered, washed with copious amounts of distilled water and air-dried. The product was then purified by dissolving in ethanol, filtering off the insoluble residue and reprecipitating in distilled water. The white solid was filtered, air-dried and subsequently dried under vacuum at 50°C.

2.5.2. The synthesis of (4-nitrophenyl)-[3-[N-(2-hydroxyethyl)carbazolyl]]diazene

2.8g (0.020 mol) of 4-nitro aniline was weighed into a 1L three-necked round bottomed flask and dissolved in a solution of concentrated HCl (10ml) in water (300ml). The mixture was then cooled in an ice bath until the temperature was below 5°C. 1.6g (0.022 mol) Sodium nitrite dissolved in 10mL of water was then added slowly to the mixture, whilst the temperature of the reaction mixture was maintained below 5°C. The resultant solution was stirred for 30 minutes and the low temperature maintained, after which 1.0g of sodium lauryl sulphate was added followed by a solution of N-(2-hydoxyethyl)carbazole (8.4g, 0.04 mol) in dichloromethane (300mL). The mixture was stirred vigorously at room temperature for 24 hours after which 200mL of ethanol was added and the DCM layer removed by rotoevaporation. The red precipitate was filtered, washed with copious amounts of water, air dried and finally dried under vacuum at 50°C.

2.5.3. The synthesis of (4-nitrophenyl)-[3-[N-[2-(methacryloyloxy)ethyl] carbazolyl]] diazene

3.6g (0.01 mol) of (4-nitrophenyl)-[3-[N-(2-hydroxyethyl)carbazolyl]]diazene was weighed into a 250mL three-necked round bottomed flask, followed by 1.2g (0.012 mol) of triethylamine. The mixture was dissolved in 100mL of tetrahydrofuran and a solution of methacryloyl chloride (1.5mL, 0.011mol) in tetrahydrofuran (5mL) subsequently added slowly over a 30 minute period. The mixture was then stirred overnight at room temperature. The solvent was removed by rotoevaporation and the residue washed with approximately 200mL of a one weight percent solution of sodium carbonate in water. The red solid was filtered, washed with water and air-dried.

2.6 Polymerisation techniques

2.6.1 Batch reactions

All batch polymerisations were conducted in a vessel such as that shown in figure 2.2.

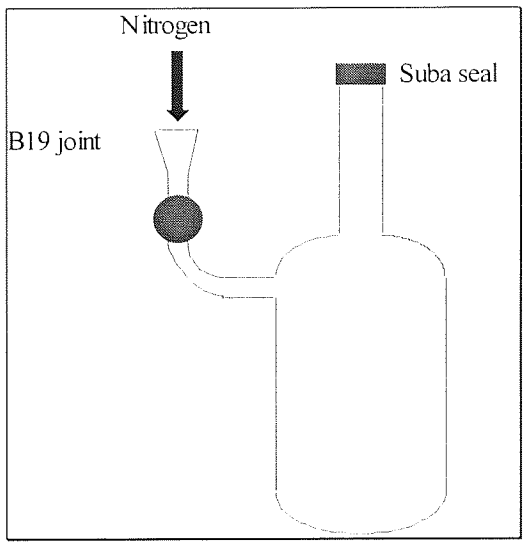

Figure 2.2. Batch polymerisation vessel.

The required quantity of $Cu^{(I)}Br$ was weighed into the reaction vessel followed by the appropriate amount of the N-alkyl-2-pyridinemethanimine ligand. The vessel was sealed with a rubber septum and attached to the vacuum line. The contents of the flask were then subjected to one freeze-pump-thaw degassing cycle. The mass of the flask was recorded and the appropriate amount of monomer distilled directly into the vessel under high vacuum by the technique described in section 2.1.2. For polymerisations utilising xylene and/or DMF as the solvent, the appropriate quantity of solvent was distilled into the reaction vessel under high vacuum by the trap-to-trap distillation technique. The reaction mixture was then subjected to three freeze-pump-thaw degassing cycles (section 2.1.1) after which the vessel was charged with nitrogen at atmospheric pressure. The vessel was then transferred to the argon dry box and the desired amount of initiator (1-PEBr or 2-EiBBr) and a magnetic stirrer bar were added.

For polymerisations utilising solvents other than xylene or DMF, the reaction mixture was subjected to three freeze-thaw degassing cycles immediately after the

addition of the monomer. Again, the vessel was charged with nitrogen at atmospheric pressure after completion of the final freeze-thaw degassing cycle and transferred to the argon dry box where the appropriate quantities of solvent (diglyme, DMSO, DMA), initiator (1-PEBr or 2-EiBBr) and a magnetic stirrer bar were added.

In all cases the solutions prepared were immediately immersed in an oil bath, maintained at the desired reaction temperature, and stirred continuously under a gentle nitrogen purge maintaining the reaction vessel at atmospheric pressure. After the desired time period the reactions were halted by dissolving the solution in approximately 50-fold excess of tetrahydrofuran. The samples were then placed in a fume cupboard and the solvents and residual monomer allowed to evaporate. The residue was subsequently dried to constant weight in a vacuum oven at 45°C. The percentage conversion of monomer was then calculated by gravimetry, as described in section 2.7.3. The polymer samples were purified by dissolving in tetrahydrofuran and precipitating in a non-solvent such as methanol or hexane, for polystyrene and poly(methyl methacrylate) respectively.

2.6.2 Sampling reactions

Sampling reactions were conducted in a polymerisation vessel fitted with an Omnifit® "column bleed valve", as illustrated in figure 2.3. This enabled the samples to be withdrawn from the reaction mixture without breaching the atmosphere within the vessel.

In all cases the reaction mixtures were prepared by a procedure identical to that described for batch polymerisations in section 2.4.1, except that the omnifit valve was used in place of a rubber septum. Samples withdrawn from the reaction liquor were treated by the same procedure as that described for the termination and subsequent analysis of batch reactions.

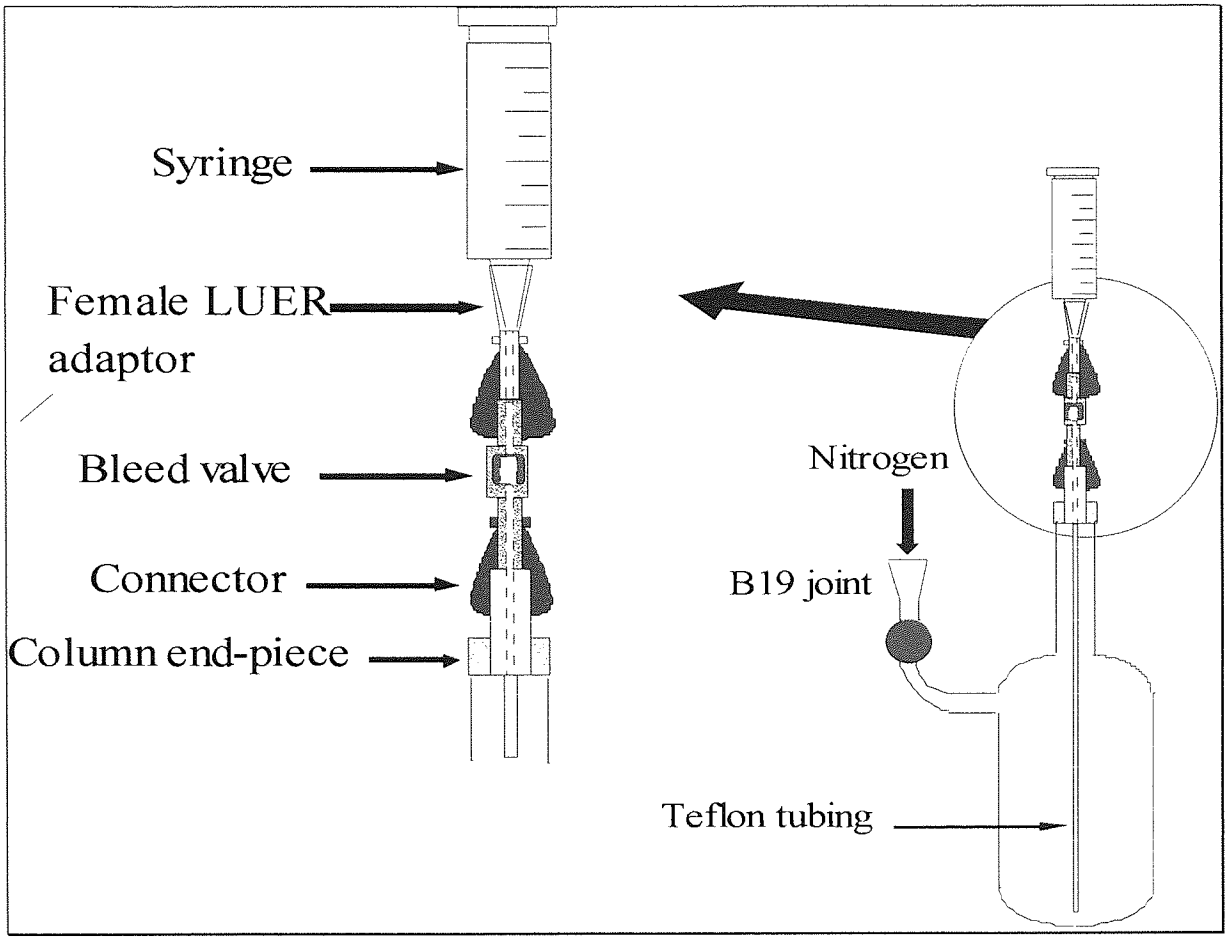

Figure 2.3. Sampling vessel.

2.6.3. Polymerisation of (4-nitrophenyl)-[3-[N-[2-(methacryloyloxy)ethyl] carbazolyl]] diazene

2.6.3.1. Free-radical polymerisation of (4-nitrophenyl)-[3-[N-[2-(methacryloyloxy)ethyl]carbazolyl]]diazene

The conventional free-radical polymerisation of (4-nitrophenyl)-[3-[N-[2-(methacryloyloxy)ethyl]carbazolyl]]diazene was conducted by preparing a 10(w/w)% solution of the monomer in DMSO and adding to this the appropriate quantity of the initiator 2,2'-azoisobutyronitrile, such that the ratio of initiator to monomer was 1:200. This solution was subjected to three freeze-thaw degassing cycles and subsequently charged with nitrogen. The vessel was immersed in an oil bath, maintained at 90°C, and stirred continuously under a gentle nitrogen purge maintaining the reaction vessel at

atmospheric pressure. The polymerisation was allowed to proceed for 48 hours, after which it was stopped by pouring the solution into ethanol. The resultant red precipitate was filtered under vacuum, washed with ethanol to remove any remaining residual monomer, air-dried and subsequently dried under vacuum at 50°C.

2.6.3.2 ATRP of (4-nitrophenyl)-[3-[N-[2-(methacryloyloxy)ethyl]carbazolyl]] diazene

The ATRP of (4-nitrophenyl)-[3-[N-[2-(methacryloyloxy)ethyl]carbazolyl]] diazene was conducted by an identical procedure to that described for styrene and methyl methacrylate in section 2.4.2. The only exception to this procedure was that during the preparation of the reaction mixture the solvent was added prior to the freeze-thaw degassing cycles, to facilitate removal of trapped gases from the solid monomer.

2.6.3.3 Atom transfer radical copolymerisation of MMA and (4-nitrophenyl)-[3-[N-[2-(methacryloyloxy)ethyl] carbazolyl]] diazene

The co-polymerisation of methyl methacrylate and (4-nitrophenyl)-[3-[N-[2-(methacryloyloxy)ethyl]carbazolyl]] diazene was conducted by a procedure similar to that described in section 2.4.3.2 for the homopolymerisation of (4-nitrophenyl)-[3-[N-[2-(methacryloyloxy)ethyl]carbazolyl]] diazene. The exception to this procedure was that the required quantity of MMA was distilled into the vessel after freeze-thaw degassing of the (4-nitrophenyl)-[3-[N-[2-(methacryloyloxy)ethyl]carbazolyl]]diazene/catalyst solution.

2.7. Analysis techniques

2.7.1. Gel permeation chromotography

Gel permeation chromatography (GPC), which is also commonly referred to as size exclusion chromatography (SEC), is a technique used for determining the molecular weight distribution of a given polymer sample. The mechanism is reliant upon the fractionation of the sample into its constituent molecules according to their hydrodynamic volume. This separation is achieved by passing a solution of the sample

through a series of columns containing a stationary phase of highly cross-linked polystyrene beads having a controlled distribution of pore sizes. Separation is effected by the sieving action of the stationary phase, with molecules entering or being excluded from pores according to their hydrodynamic volume. Thus, molecules having a greater hydrodynamic volume will be eluted from the columns more rapidly than molecules with a lesser hydrodynamic volume, as they are excluded from a greater fraction of pores than their smaller counterparts.

2.7.1.1. Apparatus

Figure 2.4 shows a schematic illustration of the gel permeation chromatograph used. A Knauer HPLC pump was used to pump the mobile phase, HPLC grade THF, through the system at a rate of 1mL min^{-1}. THF solutions of the polymer, ~ 0.25% w/v, were prepared and introduced into the system via the injector. The sample was then pumped through the column set, before passing through the Knauer differential refractometer, U. V. detector and subsequently to waste. The column set was supplied by Polymer Laboratories and consisted of a pre-column filter, a mixed B column and a μ-PL gel column with an exclusion limit of 10^3 Å. The columns were contained in a thermostatically controlled oven, which maintained the temperature at 40°C, to circumvent errors due to fluctuations in temperature. The outputs of the detectors were passed to a Polymer Laboratories DCU and analysed using PL Caliber® software.

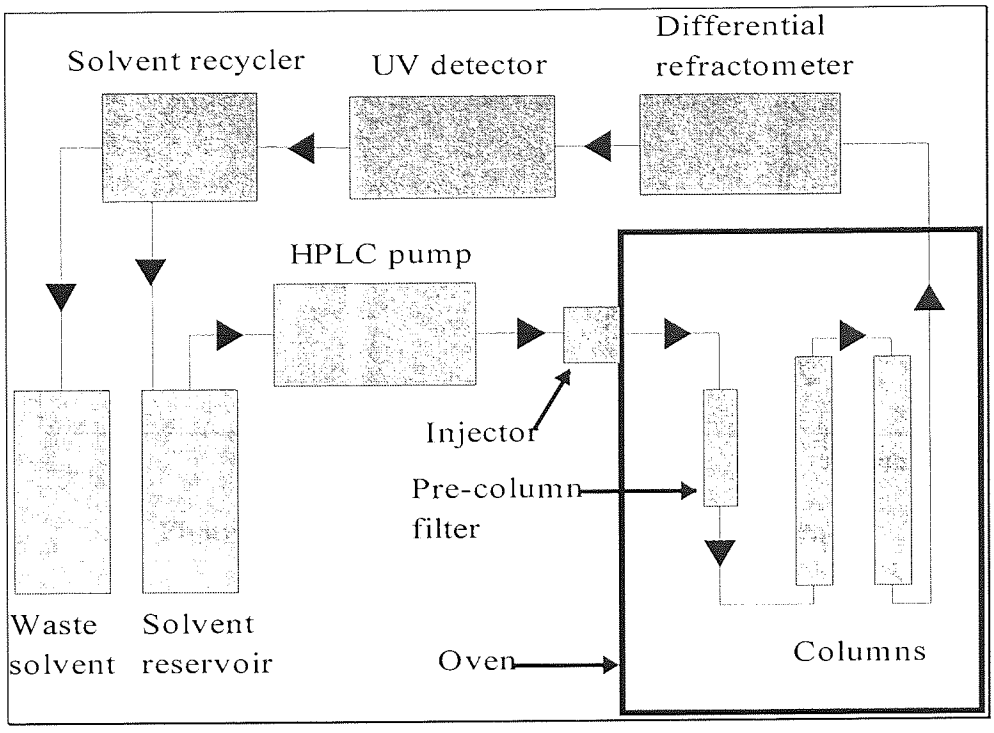

Figure 2.4. Gel permeation chromatograph

2.7.1.2. Theory

A typical gel permeation chromatogram is illustrated in figure 2.5. When a differential refractometer is used as the detector then the difference in refractive index (Δn) between the solvent and the polymer solution in the solvent at any given elution volume, is proportional to the height, h, at that point. Hence the difference in refractive index is dependent on the concentration of polymer in the eluent and the weight fraction of polymer at that elution volume.

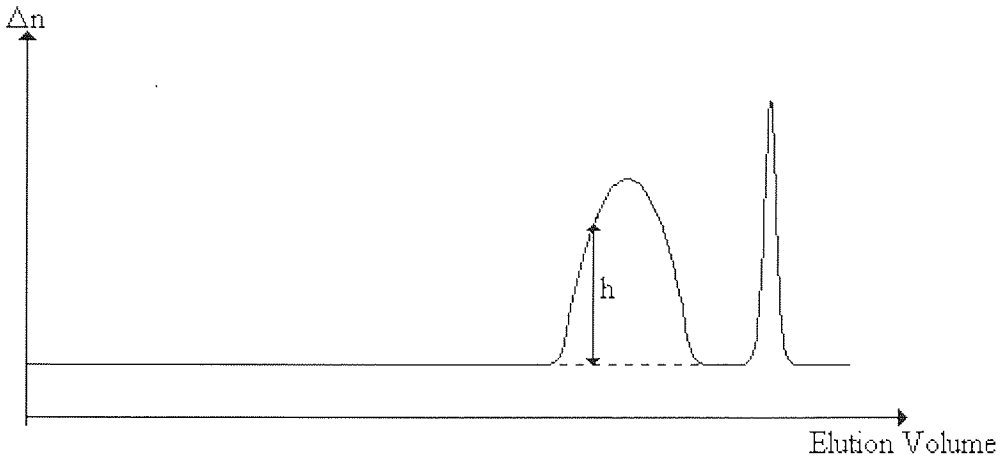

Figure 2.5. Typical gel permeation chromatogram.

The number average ($\overline{M_n}$) and weight average ($\overline{M_w}$) molecular weights of a polymer can be defined as;

$$\overline{M_n} = \frac{\Sigma N_i M_i}{\Sigma N_i} \text{ and } \overline{M_w} = \frac{\Sigma N_i M_i^2}{\Sigma N_i M_i} \qquad (2.1)$$

where N_i = number of molecules of molecular weight M_i.
If W_i is the weight fraction of polymer at molecular weight M_i then;

$$W_i \propto N_i M_i \text{ and } N_i \propto \frac{W_i}{M_i} \qquad (2.2)$$

and;

$$\overline{M_n} = \frac{\Sigma W_i}{\Sigma W_i/M_i} \text{ and } \overline{M_w} = \frac{\Sigma W_i M_i}{\Sigma W_i}. \qquad (2.3)$$

Given the above relationships the molecular weights can be calculated from the SEC trace by;

$$\overline{M_n} = \frac{\Sigma h_i}{\Sigma h_i/M_i} \text{ and } \overline{M_w} = \frac{\Sigma h_i M_i}{\Sigma h_i}. \qquad (2.4)$$

To determine the relationship between the molecular weight of eluted polymer (M_i) and the elution volume, a series of polystyrene standards of known molecular weight and molecular weight distribution ($\overline{M_w}/\overline{M_n}$) were analysed. A calibration curve was thus constructed by plotting the logarithm of the molecular weight against the observed elution volume and a 3rd order polynomial equation describing this

relationship was subsequently obtained. Figure 2.6 shows the calibration curve utilised, which was then utilised to construct a molar mass distribution curve for the polymer under study.

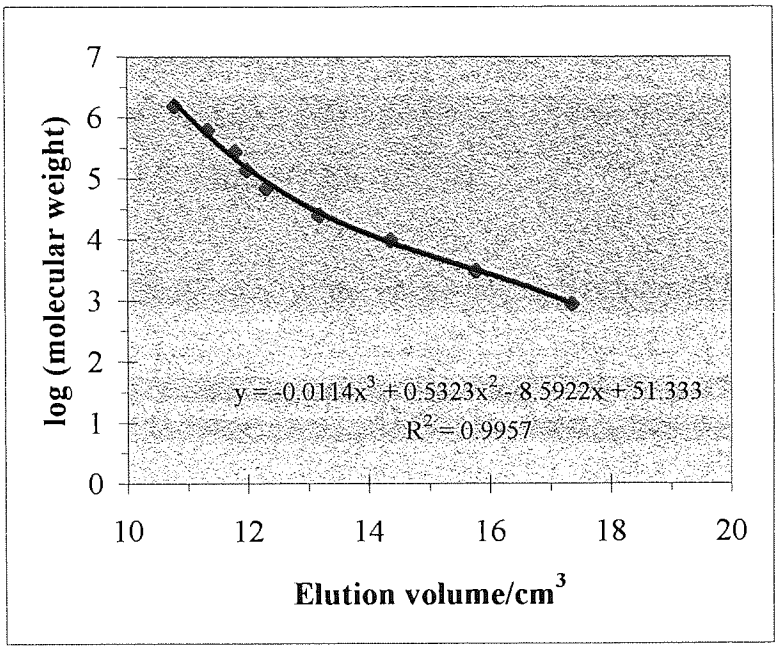

Figure 2.6. GPC calibration curve for polystyrene standards.

However, as different polymers swell to different extents in a given solvent, the hydrodynamic volume of chains of the polystyrene standard and the polymer under study of a given molecular weight may differ, and hence if the polymer under study is not polystyrene, then the molecular weight values derived are not necessarily absolute values. This problem can be circumvented and absolute values obtained for polymers other than the calibrant by using the universal calibration method. This compensation relies upon the fact that the hydrodynamic volume of a polymer molecule in solution is proportional to its intrinsic viscosity $[\eta]$, and molecular weight. Thus, two polymers eluting at the same elution volume must have the same hydrodynamic volume and therefore;

$$[\eta_1] M_1 = [\eta_2] M_2 \qquad (2.5)$$

where $[\eta_1]$ and $[\eta_2]$ are the intrinsic viscosity's of the two polymers

and M_1 and M_2 their molecular weights.

The intrinsic viscosity of a polymer is related to its molecular weight by the equation

$$[\eta] = KM^{\alpha} \tag{2.6}$$

where K and α are the Mark-Houwink constants for polymers in different solvents. Hence for co-eluting polymers

$$K_1 M_1^{\alpha 1} M_1 = K_2 M_2^{\alpha 2} M_2 . \tag{2.7}$$

Thus the absolute molar mass value of the unknown can be obtained from

$$\log M_2 = \frac{(1+\alpha_1)}{(1+\alpha_2)} \log M_1 + \frac{1}{(1+\alpha_2)} \log\left(\frac{K_1}{K_2}\right) \tag{2.8}$$

if the Mark Houwink constants are known for both the calibrant standard and the polymer under study.

2.7.2. Gravimetry

The extent of monomer conversion achieved for a given polymerisation sample was determined by gravimetric analysis. The technique is reliant upon the evaporation of residual monomer and other volatile components from the sample, to leave a given mass of polymer and a known mass of non-volatile reaction components. Thus, the percentage of monomer converted to polymer can be calculated from

$$C = \frac{(M_R - M_{NV})}{M_M} \times 100\% \tag{2.9}$$

where C is the %conversion, M_R is the total mass of residue, M_{NV} is the mass of known non-volatiles and M_M is the initial mass of monomer. For samples withdrawn from a homogeneous polymerisation solution the quantities were calculated according to the ratio of the volume of sample withdrawn to that of the volume of the entire reaction mixture. The accuracy of the technique is thus dependent upon the accuracy of the measurement of the volume of the sample withdrawn.

2.7.3 Nuclear magnetic resonance spectroscopy

Fourier transform high resolution ^{1}H and ^{13}C N.M.R. were conducted using a Bruker AC 300 spectrometer. The spectra recorded corresponded to solutions of the samples in deuterated chloroform containing a small quantity of tetramethylsilane as reference. The P.E.N.DA.N.T. pulse technique was utilised for ^{13}C analysis and thus methyl and methine carbons appear as positive peaks and methylene and quaternary carbons appear as negative peaks. All spectra were analysed using WinNMR software supplied by Bruker.

2.7.4 Infra red spectroscopy

Fourier transform infra red spectroscopy was conducted on a Perkin Elmer Paragon 1000 spectrophotometer. The spectra recorded correspond to films of the pure sample liquid sandwiched between NaCl discs.

3. Atom transfer radical polymerisation of styrene

3.1. Introduction

The ultimate aim of this work, as stated previously, was to develop an ATRP technique that facilitates the synthesis of photorefractive polymers of precisely controlled architecture. The proposed target polymers consist of a poly(methacrylate) backbone bearing pendant bifunctional charge-conducting, non-linear optical chromophores, and hence it is imperative that the developed technique is compatible with and has the capacity to afford a high degree of control over the polymerisation of such methacrylic monomers. However, considering the relative reactivity of this class of monomers, it was decided that, prior to the utilisation of the technique for the polymerisation of methacrylic monomers, a suitable technique would first be developed for the polymerisation of a less reactive category of monomer. In accord with this, styrene was selected as the most suitable candidate.

Upon commencing this work numerous reports of the ATRP of styrene mediated by copper halide/α-diimine complexes had appeared in the literature. Most notably, Matyjaszewski had described the transformation of the heterogeneous CuBr/2,2'-bipyridyl catalyst complex to that of a homogeneous system. This transformation was achieved by the synthesis and utilisation of 4,4'-alkyl substituted bipyridyl ligands. However, whilst this method is effective, the synthesis of the appropriate ligands is time-consuming and relatively expensive.

Subsequently, Haddleton et al reported N-propyl-2-pyridinemethanimine (PPMI) to be an effective alternative to bipyridyl ligands for ATRP, facilitating the production of a homogeneous reaction mixture and hence allowing a reaction profile to be developed by the sampling of a single reaction over a given time period. Furthermore, the synthesis of such compounds was reported to be achievable by a relatively simple, quick and cost-effective procedure. The use of PPMI in the ATRP of styrene was thus investigated.

3.2. N-propyl-2-pyridinemethanimine/CuBr mediated ATRP of styrene

3.2.1. Synthesis of N-propyl-2-pyridylmethanimine

N-Propyl-2-pyridylmethanimine (PPMI) was synthesised by the condensation of propylamine with 2-pyridinecarboxaldehyde by the procedure described in section 2.4. The reaction proceeded to quantitative conversion producing the desired product in high yield (96%).

The product was analysed by infra-red spectroscopy (figure 3.1) and ^{1}H and ^{13}C NMR spectroscopy (figure 3.2 and 3.3 respectively) in accordance with the procedures described in section 2.7.3 and 2.7.4 respectively.

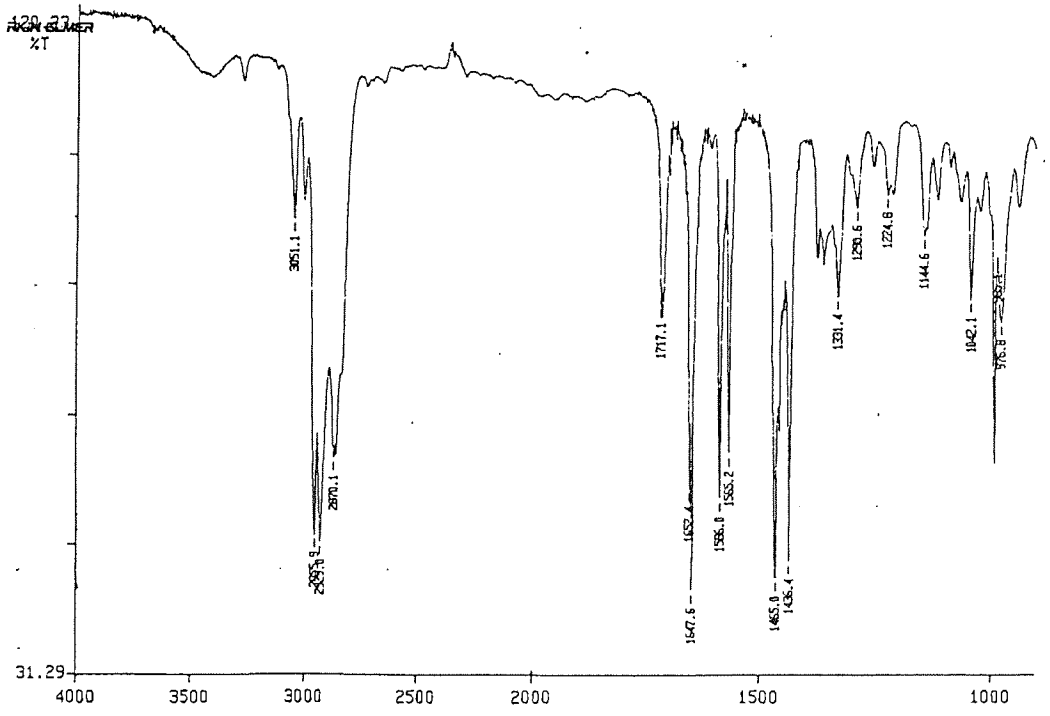

Figure 3.1 Infra-red spectrum of PPMI.

The infra-red spectrum illustrated in figure 3.1 indicates a successful synthesis. In particular, the presence of peaks at 1649cm^{-1} (-C=N- stretch) and 1586cm^{-1} (pyridine derivative) are indicative of the desired product. Moreover, the absence of a major peak at approximately 1700cm^{-1} (aromatic aldehyde –C=O stretch) indicates that all of the 2-pyridinecarboxaldehyde was consumed in product forming reactions or was removed during the purification of the product.

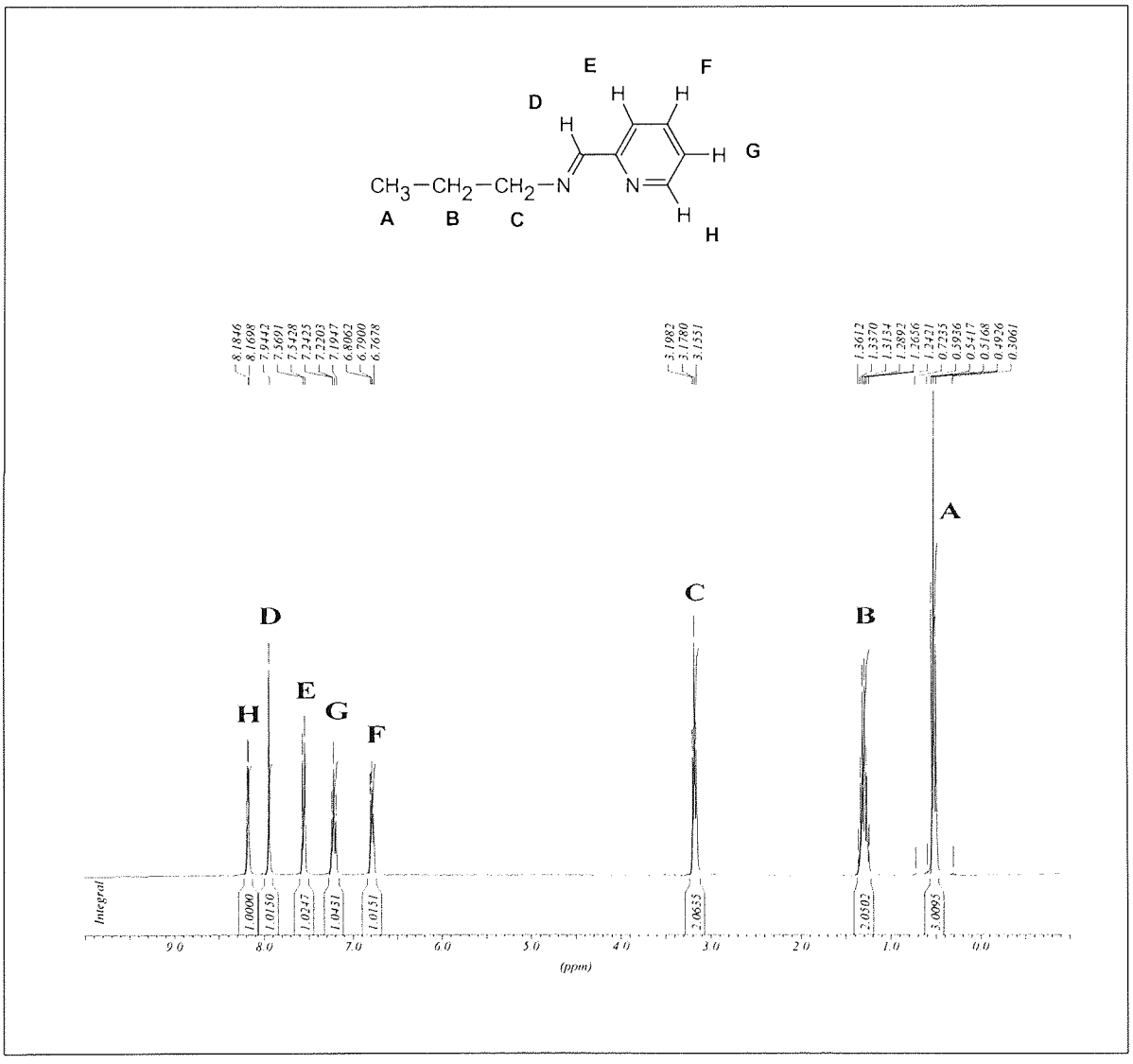

Figure 3.2 ^{1}H NMR of PPMI.

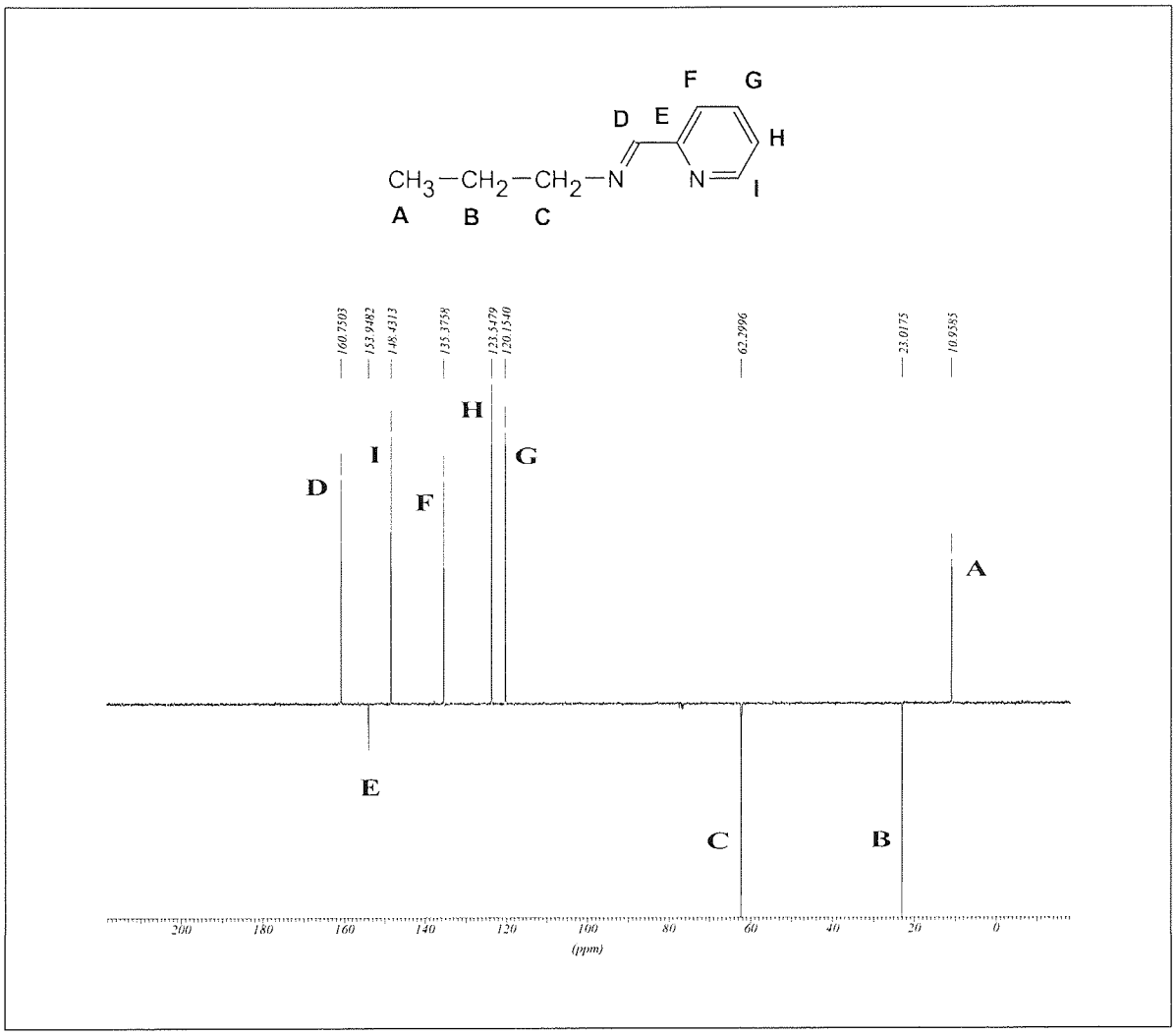

Figure 3.3. ^{13}C NMR of PPMI.

3.2.2 Polymerisation of styrene mediated by CuBr/PPMI

A mixture of styrene/CuBr/PPMI/1-PEBr in a molar ratio of 100:1:3:1 in xylene solution (50% v/v with styrene) was prepared by the procedure described in section 2.6. However, it was noted that this mixture was not, homogeneous, as expected, but that a quantity of the $Cu^{(I)}Br$ remained insoluble even upon heating to the reaction temperature (100°C). A series of batch polymerisations was therefore conducted by the procedure described in 2.6.1, as it would have been difficult to withdraw a representative sample from such a solution. Any attempts remove samples would also result in the alteration of the concentrations of the components remaining in the reaction mixture and thus alter the profile of the polymerisation.

The results of the polymerisations are listed in table 3.1. In each case conversion was determined by gravimetric analysis, as described in section 2.7.2, and the resultant polymers analysed by GPC., as described in section 2.7.1. Additionally the polymer recovered from the reaction ceased after 3 hours was also analysed by ^{1}H NMR spectroscopy (figure 3.4) as outlined in section 2.7.4.

Reaction Time /Hours	%Conversion	$\ln([M]_0/[M]_t)$	$\overline{M_n}$	$\overline{M_w}/\overline{M_n}$
3.0	29	0.3423	3540	1.35
5.5	41	0.5276	4810	1.34
7.5	53	0.7550	6350	1.44
9.0	60	0.9163	7270	1.66

Table 3.1. Dependence of conversion, molecular weight and molecular weight distribution on the time of reaction for styrene polymerisation at 100°C mediated by CuBr/PPMI/1-PEBr.

Figure 3.4 clearly illustrates the successful synthesis of linear polystyrene chains. Furthermore, it is also apparent that the reaction was initiated by the 1-phenylethyl moiety, as the corresponding methyl unit is clearly visible on the spectrum (1.04 ppm). It is also possible to suggest from this spectrum that the chain is end-capped by a bromine group, as the α-proton of the terminal repeat unit is visible down-field (4.40 ppm) of the corresponding main-chain protons (1.87 ppm). This is consistent with the de-shielding effect of a neighbouring atom such as bromine. It is thus apparent that the polymer synthesised is consistent with that expected for the ATRP of styrene initiated with 1-PEBr and mediated by CuBr/PPMI. Moreover, from the ratio of the areas of the peaks corresponding to the methyl group of the initiator fragment, A, and the main-chain methylene groups and α-protons, B and C respectively, the number-average molecular weight can be estimated as 2900 g mol^{-1}, which is in agreement with that estimated by GPC ($\overline{M_n}$ = 3540).

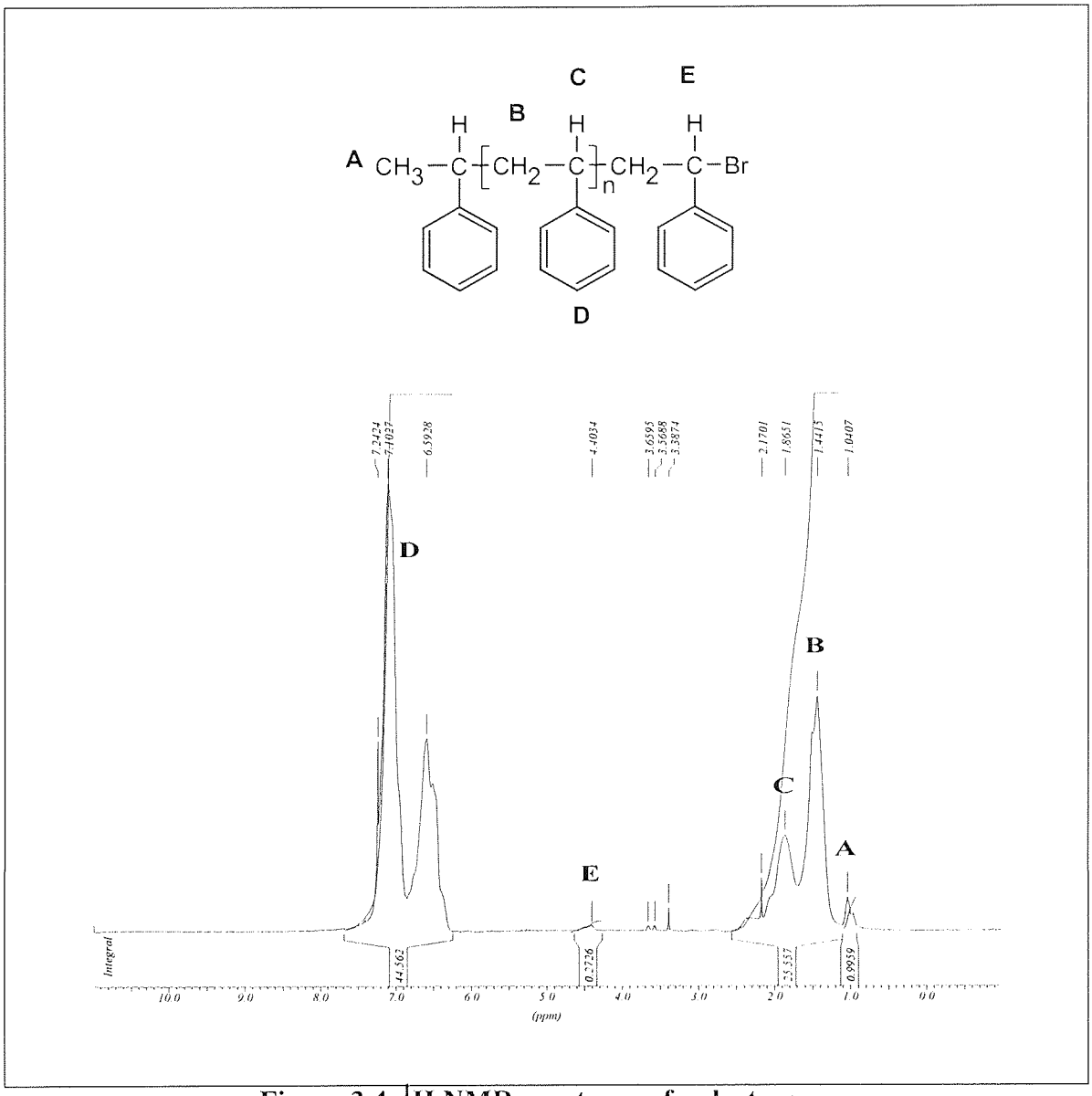

Figure 3.4. ^{1}H NMR spectrum of polystyrene.

The results of the polymerisations listed in table 3.3 illustrate that the conversion of monomer to polymer increases with time, and that the molecular weight also increases with conversion (figure 3.5 and 3.6). However, it is notable that the observed values of the number average molecular weight deviate from the values calculated from 100% initiator efficiency ($\overline{Mn}_{th}$) using equation 3.1,

$$\overline{Mn}_{th} = \left[\frac{[M]_0}{[I]_0} \times MW_m \times C\right] + MW_i \qquad (3.1)$$

where $[M]_0$ is the initial monomer concentration, $[I]_0$ is the initial concentration of the initiator, MW_m is the molecular weight of the monomer, C is the level of monomer conversion and MW_i is the molecular weight of the initiator. Furthermore, the molecular weight distribution broadens as the polymerisation proceeds (figure 3.5 and 3.6) suggesting that the degree of control afforded over the polymerisation is low and possibly decreases over the course of the polymerisation.

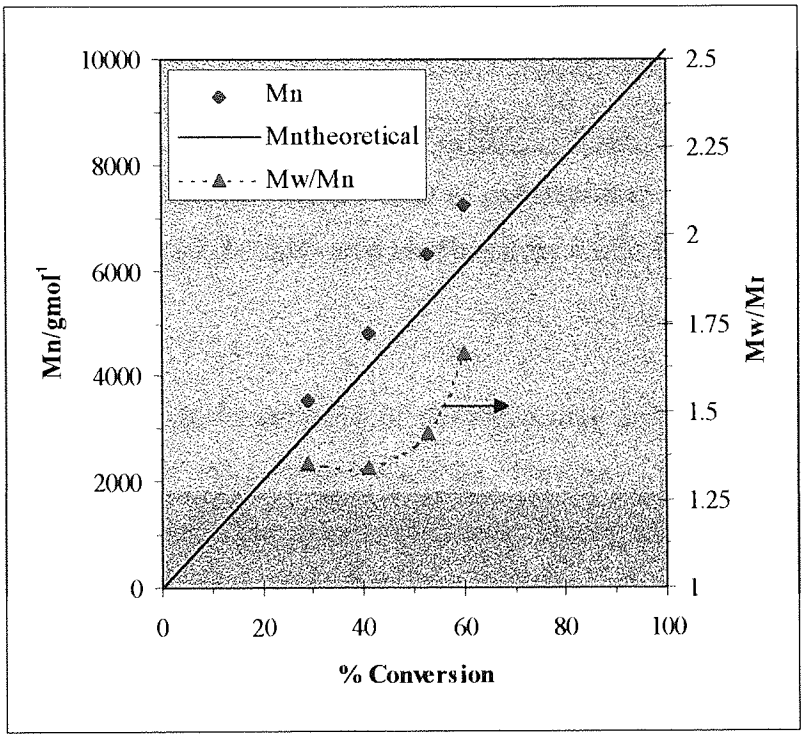

Figure 3.5. The dependence of molecular weight and molecular weight distribution on monomer conversion for the polymerisation of styrene initiated by 1-PEBr and mediated by CuBr/PPMI.

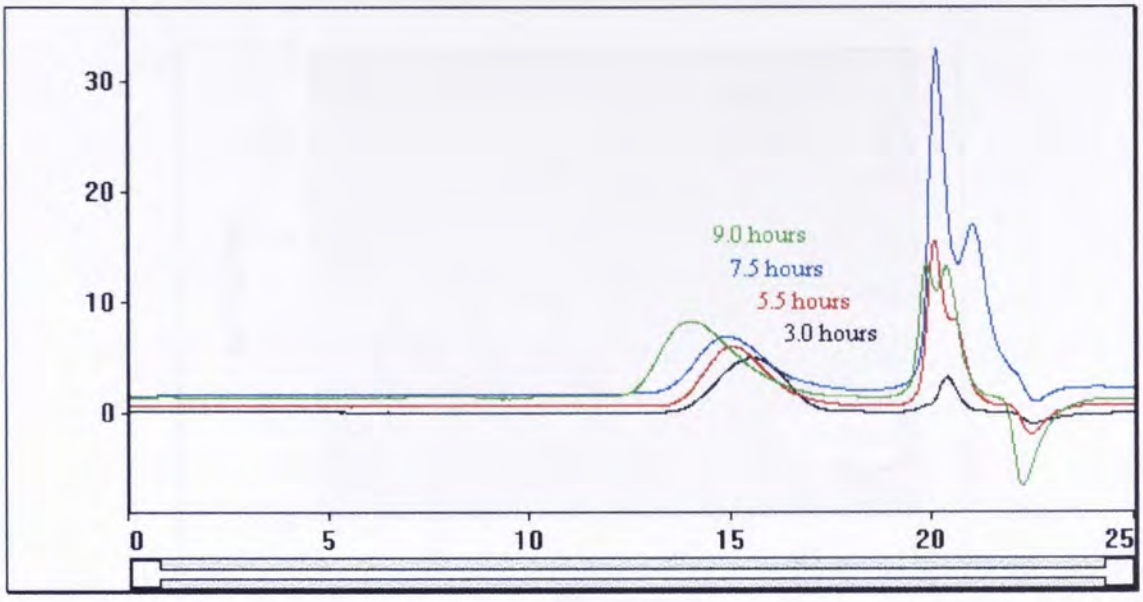

Figure 3.6. Gel permeation chromatograms of polystyrenes synthesised by ATRP initiated by 1-PEBr and mediated by CuBr/PPMI.

It is possible that the broadening of the molecular weight distribution may be due to the occurrence of termination reactions. However, this is contrary to the suggestion of the semilogarithmic pseudo first-order kinetic plot (figure 3.7) which is surprisingly linear, illustrating that the concentration of active species remains approximately constant throughout the course of the polymerisation. This linear relationship is consistent with a "living"/controlled polymerisation and also suggests that the reaction is first-order with respect to monomer concentration.

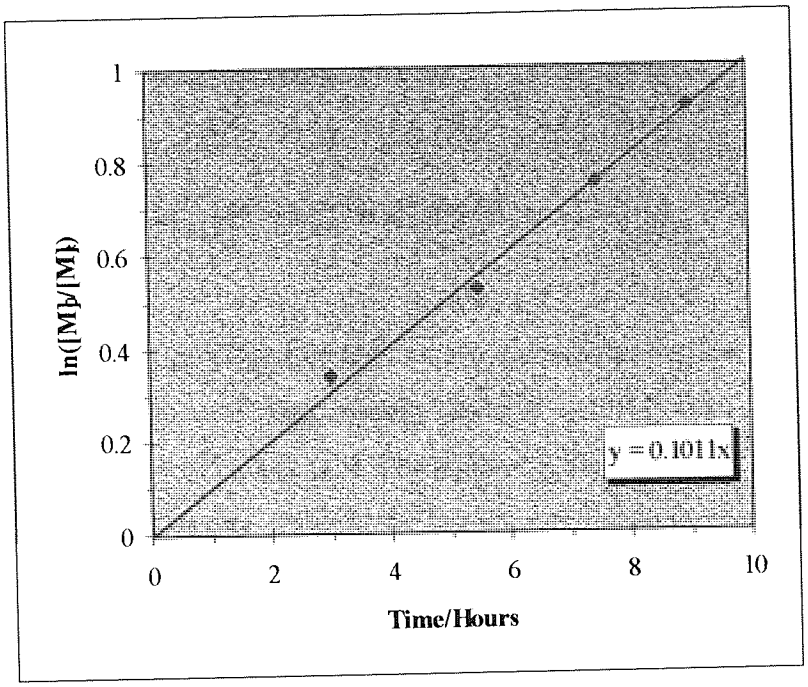

Figure 3.7. Pseudo first-order kinetic plot for the polymerisation of styrene initiated by 1-PEBr and mediated by CuBr/PPMI.

Considering the proposed reaction mechanism for ATRP (Scheme 1.14) and assuming that the rate of initiation is fast compared to the rate of propagation and also that an insignificant level of termination is occurring, the following rate expressions can be derived (equations 3.2 and 3.3).

$$K_{eq} = \frac{k_{act}}{k_{deact}} = \frac{[Pn^*]/[Cu(II)X]}{[Cu(I)]/[Pn-X]} \qquad (3.2)$$

$$Rp = \frac{-d[M]}{dt} = k_{app}[M] = k_p[Pn^*][M] = k_p K_{eq}[Pn-X]\frac{[Cu(I)]}{[Cu(II)X]}[M] \qquad (3.3)$$

K_{eq} is the equilibrium constant for the formation of the active centre, k_{act} and k_{deact} are the rate constants of activation and deactivation respectively, [Pn*] is the concentration of propagating species, [Cu(II)X] and [Cu(I)] are respectively the concentrations of copper(II) and copper(I) species, [Pn-X] is the concentration of dormant halogen end-capped chains, Rp is the rate of polymerisation, [M] the concentration of monomer, k_{app}

is the apparent rate constant of polymerisation and k_p is the rate constant of propagation. Integration of equation 3.3 yields equation 3.4.

$$\ln\frac{[M]_0}{[M]_t} = k_{app}t = k_p[Pn*]t \qquad (3.4)$$

Thus, assuming that the propagating species are indeed free-radical in nature then the steady-state concentration of propagating species ([Pn*]) can be estimated by combination of the value of k_{app} (k_{app} = dln[M]/dt = 2.81 x 10^{-5} s^{-1} ; i.e. the gradient of the semilogarithmic plot, figure 3.6) and the known rate constant of radical propagation for styrene at 100°C (k_p = 1255 $M^{-1}s^{-1}$)[186]. The concentration of propagating species is thus equal to 2.24 x10^{-8} M. This value is comparable to that observed by Matyjasewski et al for the copper halide/4,4'-dinonyl-2,2'-bipyridyl mediated ATRP of styrene[105] and Georges et al for the TEMPO mediated polymerisation of styrene[67]. Hence the concentration of radicals is suitably low to ensure propagation is favoured over the undesirable termination reactions synonymous with free-radical polymerisation. However, it is of note that this is inconsistent with the observed broadening of the molecular weight distribution with the progression of the polymerisation, which suggests that a considerable degree of termination is occurring.

As stated previously a quantity of the CuBr remained insoluble even when the solution was heated to the reaction temperature (100°C) and stirred continuously. This may have led to inefficient catalysis and therefore a low degree of control being exerted over the polymerisation and hence the resultant broadening of the molecular weight distribution as the reaction proceeded.

From these initial experiments it is apparent that PPMI/CuBr complexes are not wholly soluble in xylene/styrene mixtures and that the inherent heterogeneous nature of the catalyst leads to inefficient catalysis. Furthermore, to enhance the level of control afforded over the polymerisation, it is evident that the attainment of a more soluble and ultimately homogeneous catalyst complex is desirable.

3.3. The effect of the length of the alkyl chain on N-alkyl-2-pyridylmethanimine ligands

It has been widely suggested in the literature that the degree of control afforded over the polymerisation in copper halide/α-diimine mediated ATRP can be enhanced by increasing the solubility of the catalyst complex. Matyjasewski[105] and Percec[104] have reported that the solubility of 2,2'-bipyridyl/copper$^{(I)}$ halide complexes in hydrocarbon solvents can be improved by substitution of an alkyl chain at the 4,4' positions of the bipyridyl rings. Therefore the effect of extending the length of the pendant alkyl chain on N-propyl-2-pyridylmethanimine on the solubility and catalytic activity of the resultant CuBr complexes was investigated.

3.3.1. The synthesis of N-butyl-2-pyridylmethanimine and N-octyl-2-pyridylmethanimine

N-butyl-2-pyridylmethanimine (BPMI) and N-octyl-2-pyridinemethanimine (OPMI) were synthesised by the procedure described in section 2.4. As in the case of PPMI, BPMI and OPMI were obtained in a high yield (97% and 98% respectively) and were analysed by infra-red spectroscopy and by ^{1}H and ^{13}C NMR spectroscopy as described in sections 2.7.3 and 2.7.4 respectively. The infra-red and NMR spectra, along with the corresponding peak assignments, for BPMI and OPMI, are shown in appendix 1 and 2 respectively.

3.3.2. The effect of the length of the pendant alkyl chain on the N-alkyl-2-pyridylmethanimine ligands upon the polymerisation of styrene at 100°C mediated by CuBr/ N-alkyl-2-pyridylmethanimine

Reaction mixtures of styrene/CuBr/N-alkyl-2-pyridylmethanimine/1-PEBr in a molar ratio of 100:1:3:1 in 50% v/v xylene solution were prepared by the procedure described in section 2.6. In the case of BPMI, as was noted for polymerisations utilising CuBr/PPMI catalyst complexes, the reaction mixture was heterogeneous and contained a small amount of undissolved catalyst complex, visible even upon heating to the reaction temperature (100°C). Therefore, a series of batch polymerisations were conducted so as to avoid the complications outlined previously, which are associated with the periodic sampling of a heterogeneous reaction mixture. No such problems were encountered for OPMI and hence a profile of the polymerisation was drawn-up by

periodic sampling of a single reaction. The results of these polymerisations are listed in tables 3.2 and 3.3 respectively.

Reaction Time /Hours	%Conversion	$\ln([M]_0/[M]_t)$	$\overline{M_n}$	$\overline{M_w}/\overline{M_n}$
3	20	0.2231	2360	1.30
4	25	0.2877	2730	1.29
7	46	0.6162	4940	1.29
15	67	1.1394	7150	1.27

Table 3.2. Results of the ATRP of styrene at 100°C initiated with 1-PEBr and mediated by CuBr/BPMI.

Reaction Time /Hours	%Conversion	$\ln([M]_0/[M]_t)$	$\overline{M_n}$	$\overline{M_w}/\overline{M_n}$
2	6	0.0619	1178	1.28
5	13	0.1393	1721	1.21
7	25	0.2877	2703	1.25
15	47	0.6349	4873	1.20
20	69	1.1712	7175	1.23
24	84	1.8326	8646	1.19
36	91	2.4079	9419	1.21

Table 3.3. Results of the ATRP of styrene at 100°C initiated with 1-PEBr and mediated by CuBr/OPMI.

The results illustrate that the degree of control afforded over the polymerisation in both cases is superior to that observed for the CuBr/PPMI mediated ATRP of styrene. As shown in figure 3.8, the molecular weights of the polymers are in close agreement with the theoretical values, calculated using equation 3.1, and the molecular weight distributions are considerably narrower than those observed for polymers prepared with the aforementioned system. Moreover, the polymers synthesised in the polymerisation

utilising OPMI as the ligands displayed narrower molecular weight distributions than those synthesised in polymerisations utilising BPMI as ligands. It is thus apparent that increasing the solubility of the catalyst complex increases the level of control afforded over the polymerisation.

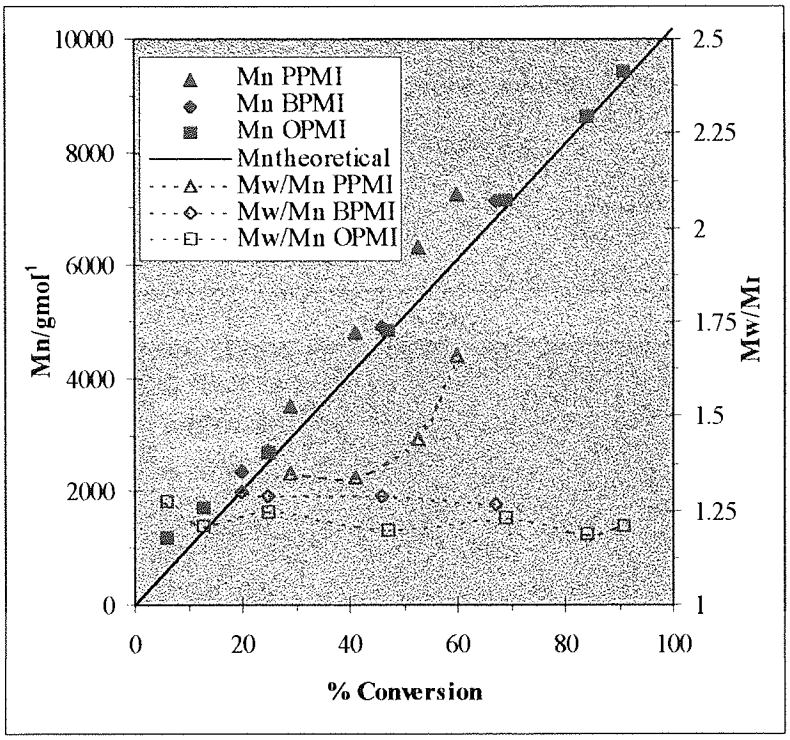

Figure 3.8. The effect of the length of the pendant alkyl chain on the ligand on the evolution of molecular weight and molecular weight distribution with monomer conversion.

The rate of polymerisation was found to decrease with increasing alkyl chain length on the ligand, as shown in figures 3.9 and 3.10. This is surprising, as increasing the solubility of the catalyst complex would be expected to lead to an increase in the concentration of active catalytic species and in turn to result in an increase in the concentration of propagating species and hence an increase in the rate of polymerisation. However, the observed decrease in the rate of polymerisation can be associated with an increase in the efficiency of the atom transfer process induced by the greater solubility of the BPMI and OPMI catalyst complexes relative to the PPMI analogues. In particular, if the solubility of the deactivating species is enhanced, then the rate of deactivation of the propagating species will increase. This effect will in turn

lead to a lower concentration of active propagating species and hence a lower rate of polymerisation. Furthermore, the lowering of the concentration of the propagating species would result in a decrease in the probability of the occurrence of bimolecular termination reactions during the course of the polymerisation and thus favour the production of polymers displaying narrower molecular weight distribution. This is consistent with the higher degree of control afforded over the polymerisation which is observed for polymerisations utilising the more soluble BPMI and OPMI catalyst complexes compared to the less soluble PPMI analogue.

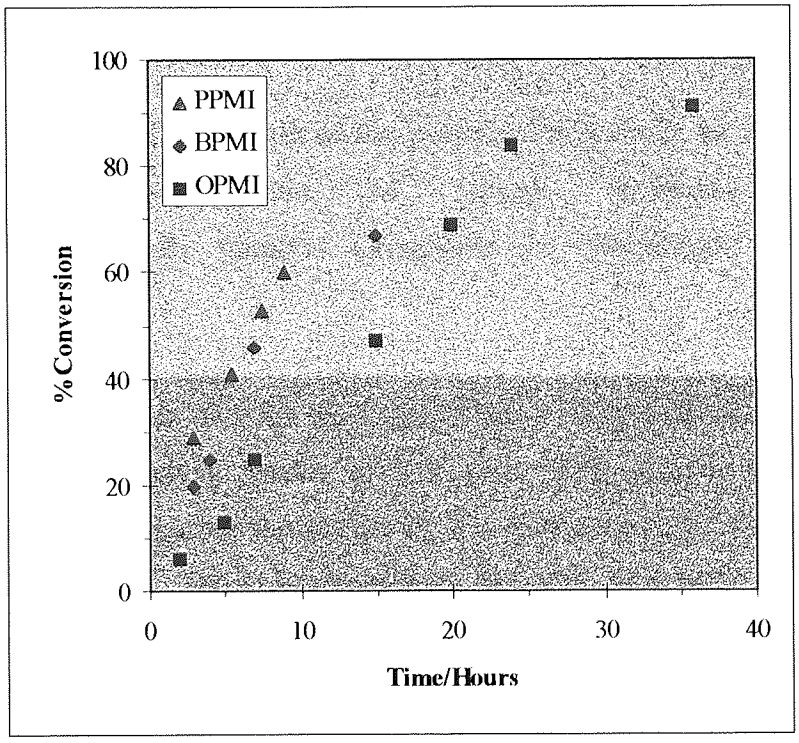

Figure 3.9. The effect of the length of the pendant alkyl chain on the ligand upon the rate of monomer conversion for the polymerisation of styrene mediated by alkyl pyridinemethanimine/CuBr catalyst complexes in conjunction with 1-PEBr initiator.

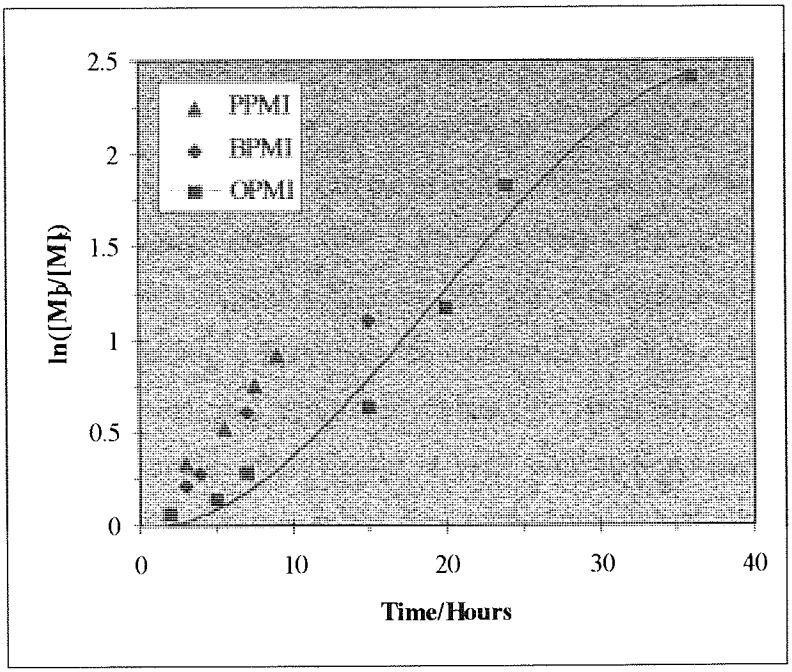

Figure 3.10. The effect of the length of the pendant alkyl chain on the ligand upon the rate of polymerisation of styrene mediated by alkyl pyridinemethanimine/CuBr catalyst complexes in conjunction with 1-PEBr initiator.

The semilogarithmic plot for the CuBr/OPMI mediated polymerisation (figure 3.10) is sigmoidal in nature, which is indicative of a gradual increase in the concentration of the propagating species during the early stages of the reaction, until a "steady-state" is achieved. The concentration of propagating species and the rate of polymerisation then decrease.

Considering the mechanism of $Cu^{(I)}Br/\alpha$-diimine mediated ATRP (scheme 1.14), the curvature of the plots in the initial stages may be due to a relatively slow initiation process, but may also be indicative of the formation of a steady-state concentration of deactivating $Cu^{(II)}Br_2/2L$ and propagating species via the persistent radical effect1[187, 57, 59].

The following profile can be envisaged considering the persistent radical effect. The reaction of $Cu^{(I)}Br/2L$ with the initiator results in the formation of active initiating and propagating species and $Cu^{(II)}Br_2/2L$, with the concentration of each of the former species increasing with time. Owing to the relatively low concentration of $Cu^{(II)}Br_2/2L$ in the early stages of the polymerisation, the rate of deactivation is slow and hence the time the chain-ends spend in the active form is relatively long facilitating bimolecular

termination reactions and the irreversible formation of an excess of $Cu^{(II)}Br_2/2L$. As this process continues the concentration of $Cu^{(II)}Br_2/2L$ species gradually increases and therefore the rate of the deactivation process increases, leading to an decrease in the rate of termination and thus an increase the concentration of chains participating effectively in a dynamic ATRP equilibrium. After a given period of time, the concentration of $Cu^{(II)}Br_2/2L$ is sufficiently large to sustain an efficient deactivation process, suppressing termination and maintaining a maximum concentration of active centres allowing the polymerisation to proceed in a controlled manner under steady-state conditions. The apparent deviation from this steady-state at high conversion observed in figure 3.9 probably coincides with a decrease in the concentration of potentially active chain-ends via termination reactions. However, it is also probable that the decrease in the rate of polymerisation is manifested as a result of monomer consumption or the conversion of the catalyst to inactive states

Whilst the sigmoidal nature of the semilogarithmic plots can in part be rationalised by contemplation of the persistent radical effect, it is not entirely consistent with the acceleration of the rate of polymerisation in the incipient stages of the polymerisation. If indeed an excess of deactivating species is formed in the initial stages of the polymerisation, a retardation of the rate, not the manifested increase, would be expected. It is therefore possible that the observed acceleration in rate coincides with a decrease in the concentration of the deactivating species. Moreover, although an exact mechanism for such a process is unclear, it can be speculated that the decrease in concentration arises either from a decrease in the solubility of the deactivating species, or transformation of this species into something quite different. Furthermore, given the magnitude of the rate of acceleration it is not inconceivable that the excess Cu(II) deactivating species are transformed into Cu(I) activating species.

The role of the persistent radical effect appears to be of paramount importance for the evolution of control over the polymerisation. It is apparent that, via this mechanism, control is evolved at the expense of initiator efficiency, with the termination reactions required to generate the excess of $Cu^{(II)}Br_2/2L$ resulting in the destruction of propagating centres. However, as illustrated in figure 3.8, the effect is so small that it does not detract from the degree of control afforded over the polymerisation, with close correlation existing between observed molecular weight values and theoretical molecular weight values calculated from 100% initiator efficiency.

In summary, the use of OPMI as a complexing ligand produces a highly soluble near homogeneous catalyst complex in xylene/styrene solution and hence makes the system amenable to kinetic study. However, despite this the molecular weight distributions are still broader than those reported in the literature for comparable systems. It is thus apparent that the attainment of a more soluble catalyst system is desirable to allow the synthesis of polymers having even narrower molecular weight distributions.

3.4. Effect of solvent

In an attempt to produce a more soluble catalyst system, the effect of using a more polar solvent was investigated. Diglyme (2-methoxyethyl ether) was chosen as it has a suitably high boiling point (163°C).

The ATRP of styrene was conducted as described previously, except that xylene was replaced with diglyme as the solvent. A mixture of styrene/CuBr/OPMI/1-PEBr in a ratio of 100:1:3:1 respectively was prepared in diglyme solution such that the volume ratio of styrene:diglyme was 1:1. The reaction mixture appeared entirely homogeneous at both room and reaction temperature (100°C) and hence the profile of the polymerisation was followed by periodic sampling of the reaction mixture, as described in section 2.6.2. The results of the polymerisation are displayed in table 3.4. In each case monomer conversion was determined by gravimetry and molecular weight values by GPC, as described in sections 2.7.2 and 2.7.1 respectively.

Reaction time/ Hours	%Conversion	$\ln([M]_0/[M]_t)$	$\overline{M_n}$	$\overline{M_w}/\overline{M_n}$
6	12.8	0.1369	1550	1.27
16	29.7	0.3524	3190	1.22
20	38.9	0.4926	4130	1.21
25	55.0	0.7985	5600	1.17
30	64.4	1.0328	6510	1.16
48	79.3	1.5750	8190	1.12

Table 3.4. Dependence of conversion, molecular weight and molecular weight distribution on the time of reaction for the polymerisation of styrene conducted in diglyme solution, initiated by 1-PEBr and mediated by CuBr/OPMI.

The results in table 3.4 display that the molecular weight distribution of the polymers narrows considerably as the reaction proceeds, as would be expected for a controlled polymerisation. Figure 3.11 compares the dependence of molecular weight and molecular weight distribution on conversion for the two separate polymerisations conducted in xylene and diglyme solutions. It is evident that the use of diglyme as a solvent results in a much higher degree of control being afforded over the polymerisation than that observed for polymerisations conducted in xylene solution, with the corresponding molecular weight distributions of comparable samples being much narrower.

As shown in figure 3.12, the increase in the solubility of the catalyst complex has resulted in a considerable decrease in the rate of polymerisation. This is consistent with the previous observations upon generating a more soluble catalyst system, and thus it is possible that the lower rate of polymerisation is due to an increase in the solubility of the deactivating $Cu^{(II)}Br_2/2L$ complex, as suggested previously. However, it is also possible that such a marked decrease is caused by diglyme in some way hindering the interaction of the active catalyst and the dormant bromine end-capped chain.

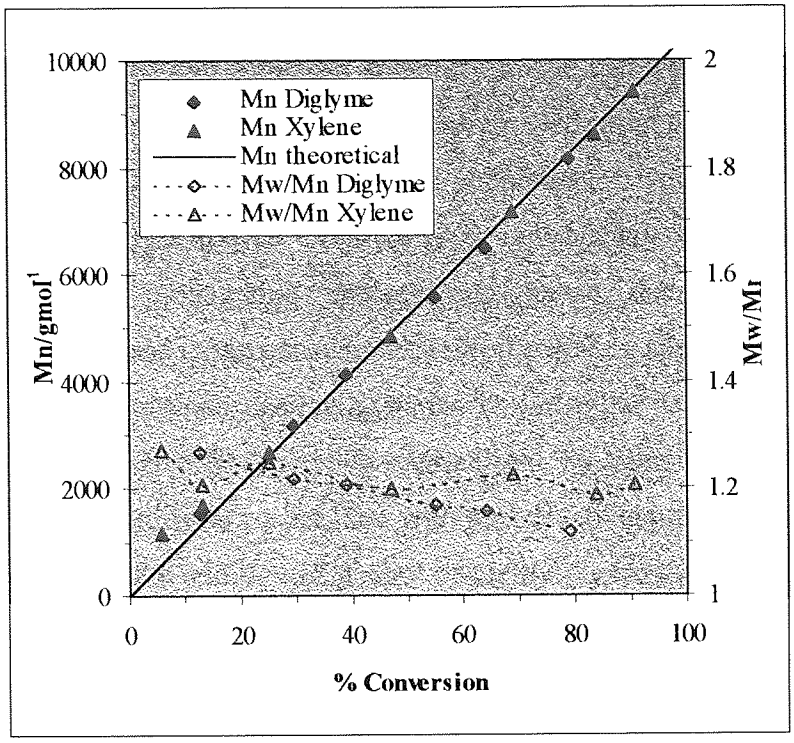

Figure 3.11. The effect of solvent selection on the dependence of molecular weight and molecular weight distribution on monomer conversion for the polymerisation of styrene initiated by 1-PEBr and mediated by CuBr/OPMI.

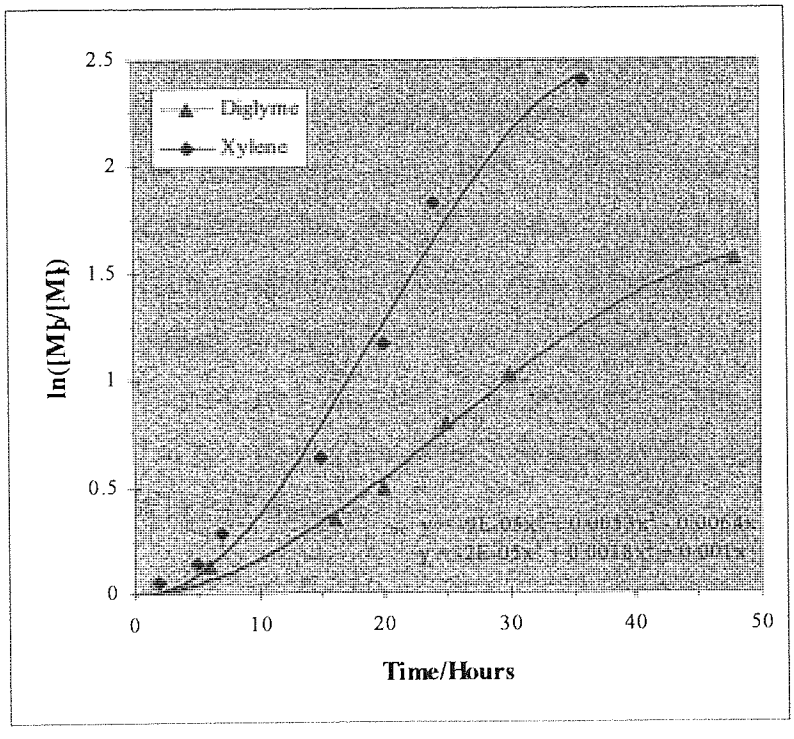

Figure 3.12. The effect of solvent on the rate of polymerisation of styrene initiated by 1-PEBr and mediated by CuBr/OPMI.

The lower rate of polymerisation observed in diglyme may simply be due to solvation effects, whereby the enhanced solubility of the catalyst complex in diglyme solution confers the existence of a greater solvation shell around the catalyst complex than that apparent in xylene solution. Such a phenomenon would hinder interaction between the active catalyst and the bromine end-capped chain, effectively decreasing the concentration of propagating species and hence decreasing the rate of polymerisation. A decrease in the concentration of propagating species is also consistent with the production of polymers displaying narrower molecular weight distributions.

Alternatively, this effect may be rationalised by considering diglyme as a species which has the ability to co-ordinate with and deactivate the catalyst. Haddleton et al have reported that the addition of phenol or methyl hydroquinone to the ATRP of methyl methacrylate conducted in xylene solution results in an increase in the rate of polymerisation, where the role of the phenol is defined as displacing an α-diimine ligand to form the active catalytic species[119, 121]. Matyjasewski has also reported that the active catalytic species in the ATRP of MMA appears to be a one to one ligand to $Cu^{(I)}Br$ complex[129], with such species having a vacant co-ordination site which in some way facilitates propagation. However, contrary to this it has been reported that the active catalytic species in the ATRP of styrene appears to be a two to one ligand to $Cu^{(I)}Br$ complex[105]. Indeed if this is the case then the co-ordination of diglyme with the Cu centre and the consequent displacement of a ligand will result in deactivation of the active catalyst and thus decrease the rate of polymerisation.

Regardless of the mechanism by which diglyme lowers the rate of polymerisation, it is apparent that this effect facilitates the production of polymers displaying narrower molecular weight distributions than those observed for polymers synthesised in xylene solution. Furthermore, it can be assumed that this is a direct consequence of the lowering of the concentration of propagating species and hence a decrease in the likelihood of termination reactions. It is thus evident that diglyme is the preferred solvent for the ATRP of styrene.

4. ATRP of Methyl methacrylate

4.1. Introduction

The ultimate goal of this work is to develop a technique capable of precisely controlling the polymerisation of methacrylic monomers bearing pendant functional groups. However, as such monomers are expensive and are time consuming to prepare, the development of a controlled polymerisation technique is best achieved using an accurate but simple, less expensive model monomer. Methyl methacrylate (MMA) was selected for this purpose and hence this chapter details the development and study of an effective ATRP technique for this monomer.

ATRP of methyl methacrylate has been widely reported in the literature (see section 1.4.3.5). At the time of commencing this work, Haddleton et al had previously reported that the polymerisation of MMA initiated by ethyl-2-bromoisobutyrate could be effectively controlled by a CuBr/N-propyl-2-pyridinemethanimine catalyst complex[107]. However, as illustrated in chapter 3, the use of N-propyl-2-pyridinemethanimine as a ligand results in the formation of a heterogeneous catalyst complex in hydrocarbon solution. Whilst this may still allow the control of the polymerisation of MMA, it is highly undesirable for kinetic studies of the polymerisation process. Furthermore, preliminary studies on the ATRP of styrene (chapter 3) revealed that the use of a more soluble catalyst complex, namely CuBr/OPMI, results in a greater degree of control being afforded over the polymerisation. Thus, the studies detailed within this chapter utilise the highly soluble CuBr/OPMI catalyst complex, as it makes the polymerisation amenable to kinetic study and imparts the potential to effect a high degree of control over the polymerisation.

4.2. The development of an effective ATRP system for MMA

4.2.1. ATRP of MMA initiated by 1-PEBr at 100°C

The suitability of the ATRP system developed for styrene for the controlled polymerisation of methyl methacrylate (MMA), was assessed by conducting the polymerisation of MMA under the same conditions as those described for styrene. Thus,

a mixture of MMA/CuBr/OPMI/1-PEBr in a ratio of 100:1:3:1 respectively, in diglyme solution (50% v/v with MMA), was prepared by the procedure described in section 2.6.2 and subsequently heated to 100°C. However, it is of note that owing to the higher density of MMA than styrene, the concentrations of the respective components of the reaction mixture are slightly higher than those utilised for the ATRP of styrene. Thus $[MMA]_0$ = 4.76 mol dm^{-3}, $[CuBr]_0$ = 0.0476 mol dm^{-3}, $[OPMI]_0$ = 0.143 mol dm^{-3} and $[1\text{-}PEBr]_0$ = 0.0476 mol dm^{-3}.

A profile of the polymerisation was drawn-up by sampling of the reaction liquor at timed intervals. In each case the level of monomer conversion was determined by gravimetry and the corresponding molecular weight values determined by G.P.C. as described in sections 2.7.2 and 2.7.1 respectively. Table 4.1 lists the results obtained. The theoretical $\overline{Mn}$ values ($\overline{Mn_{th}}$) were calculated using equation 3.1.

Time/ Minutes	%Conversion	$\overline{M_{nth}}$	$\overline{M_n}$	$\overline{M_w}$	$\overline{M_w}/\overline{M_n}$
30	8.5	1035	2130	4250	1.99
60	14.1	1595	4200	6460	1.54
90	23.8	2565	5280	8540	1.62
120	26.7	2855	7370	11000	1.49
180	30.4	3225	11660	17654	1.51

Table 4.1. Effect of time on the level of monomer conversion, molecular weight and molecular weight distribution for the ATRP of MMA at 100°C initiated by 1-PEBr and mediated by CuBr/OPMI.

It is apparent from the results obtained that 1-PEBr is an ineffective initiator for the ATRP of MMA. The resultant polymers display broad molecular weight distributions, indicative of a low level of control over the polymerisation and consistent with an undesirably slow rate of initiation relative to the rate of propagation. Furthermore, as illustrated in table 4.1, the observed values of $\overline{Mn}$ are considerably higher than the theoretical values calculated for 100% initiator efficiency. This is again indicative of inefficient initiation. Figure 4.1 shows the GPC traces for the series of polymers isolated in this experiment.

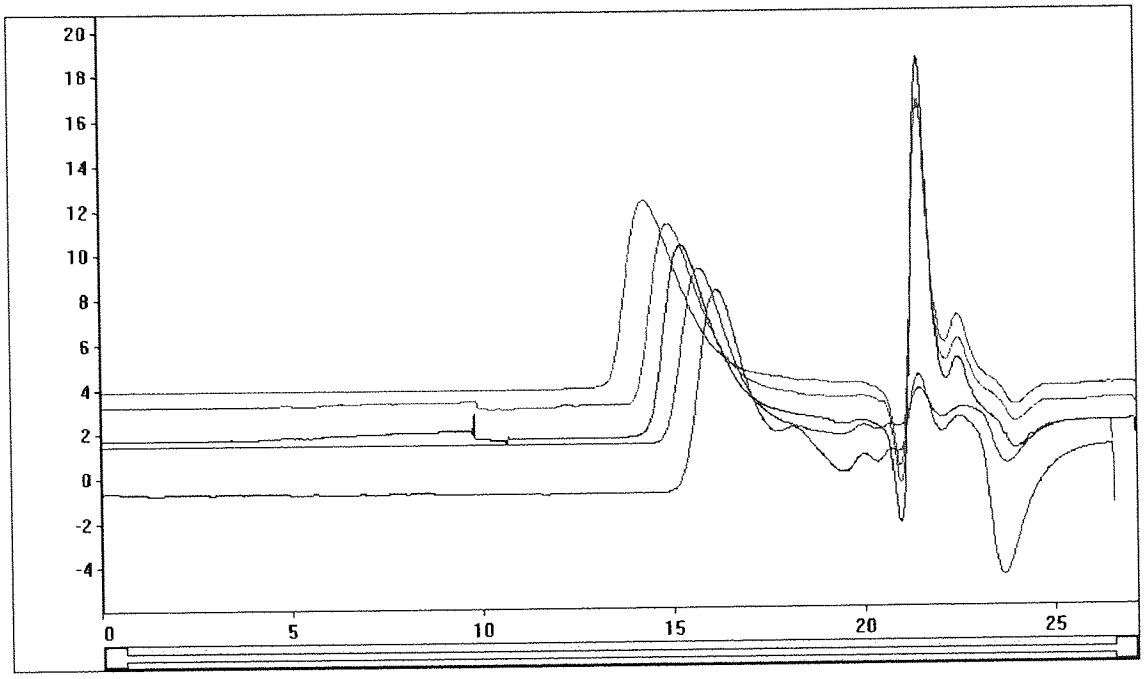

Figure 4.1. Gel permeation chromatogram for the ATRP of MMA initiated by 1-PEBr.

4.2.2. ATRP of MMA initiated by ethyl-2-bromoisobutyrate

In an attempt to produce an efficient initiation system for the ATRP of MMA, ethyl-2-bromoisobutyrate (2-EiBBr) was utilised as an alternative to 1-PEBr. This molecule was chosen as it is analogous to a Br end-capped poly(methyl methacrylate) chain, and thus should yield a rate of initiation comparable to the rate of propagation. Furthermore, its use as an initiator for the ATRP of MMA has been reported in the literature[107, 124]. Polymerisation was conducted by a procedure identical to that described for the previous case (section 4.1.1), and thus $[MMA]_0$ = 4.76 mol dm^{-3}, $[CuBr]_0$ = 0.0476 mol dm^{-3}, $[OPMI]_0$ = 0.143 mol dm^{-3} and $[1\text{-}PEBr]_0$ = 0.0476 mol dm^{-3} in diglyme solution (50% v/v with MMA). The results of the polymerisation are listed in table 4.2.

Time /Minutes	%Conversion	$\overline{M_{nth}}$	$\overline{M_n}$	$\overline{M_w}$	$\overline{M_w}/\overline{M_n}$
20	16.4	1835	2670	3230	1.21
80	61.5	6345	6580	8670	1.32
140	84.4	8635	9130	11390	1.25
175	92.4	9435	10070	13140	1.31

Table 4.2. Results of the ATRP of MMA at 100°C initiated by 2-EiBBr and mediated by CuBr/OPMI.

The results illustrate that 2-EiBBr is a more effective initiator of the polymerisation of MMA than 1-PEBr, resulting in polymers displaying narrower molecular weight distributions and molecular weights close to the theoretical values calculated from 100% initiator efficiency. Moreover, the pseudo first-order kinetic plot (figure 4.2.) is linear indicating that the concentration of propagating species is approximately constant during the course of the polymerisation, which suggests that the polymerisation proceeds in a controlled manner.

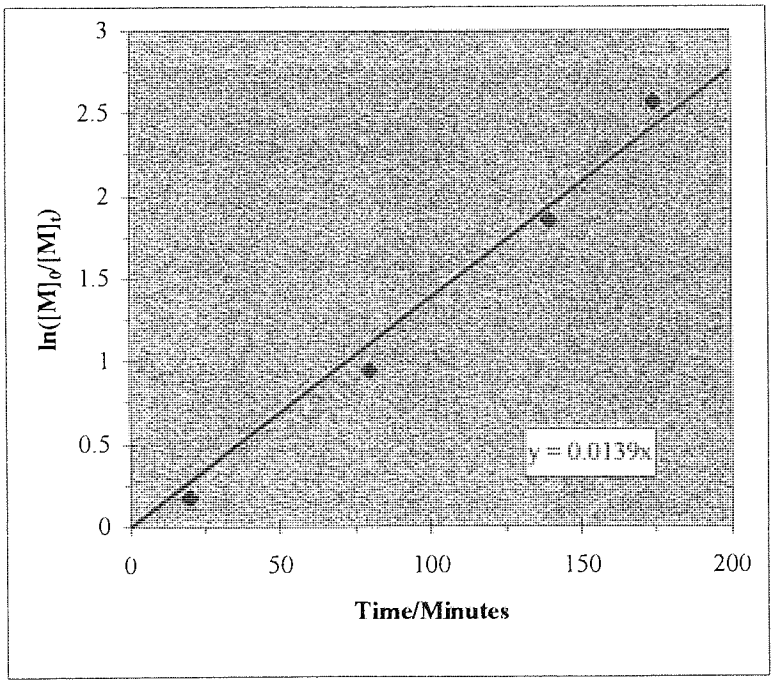

Figure 4.2. Pseudo first-order kinetic plot for the ATRP of MMA at 100°C.

However, it is of note that the polymers display broader molecular weight distributions than those observed for the analogous polymerisation of styrene (section 3.3; $1.1 < \overline{Mw} / \overline{Mn} < 1.2$), and hence it is apparent that a lower degree of control is afforded over the polymerisation of MMA than styrene under these experimental conditions. This difference may in part be due to the differences in the respective rate constants of initiation, propagation and termination for the two monomers, as well as differences in the equilibrium constants for the activation and deactivation processes involved in these reactions. Moreover, it is probable that the broader molecular weight distributions observed for the polymerisation of MMA, are also a direct consequence of the more significant occurrence of transfer and other undesirable side reactions than observed in the polymerisation of styrene.

The structure of one of the polymer samples isolated ($\overline{Mn} = 2670$, $\overline{Mw} / \overline{Mn} = 1.21$) was examined by ^{1}H NMR spectroscopy, as described in section 2.7.3. Figure 4.3 shows the NMR spectrum and the corresponding peak assignments.

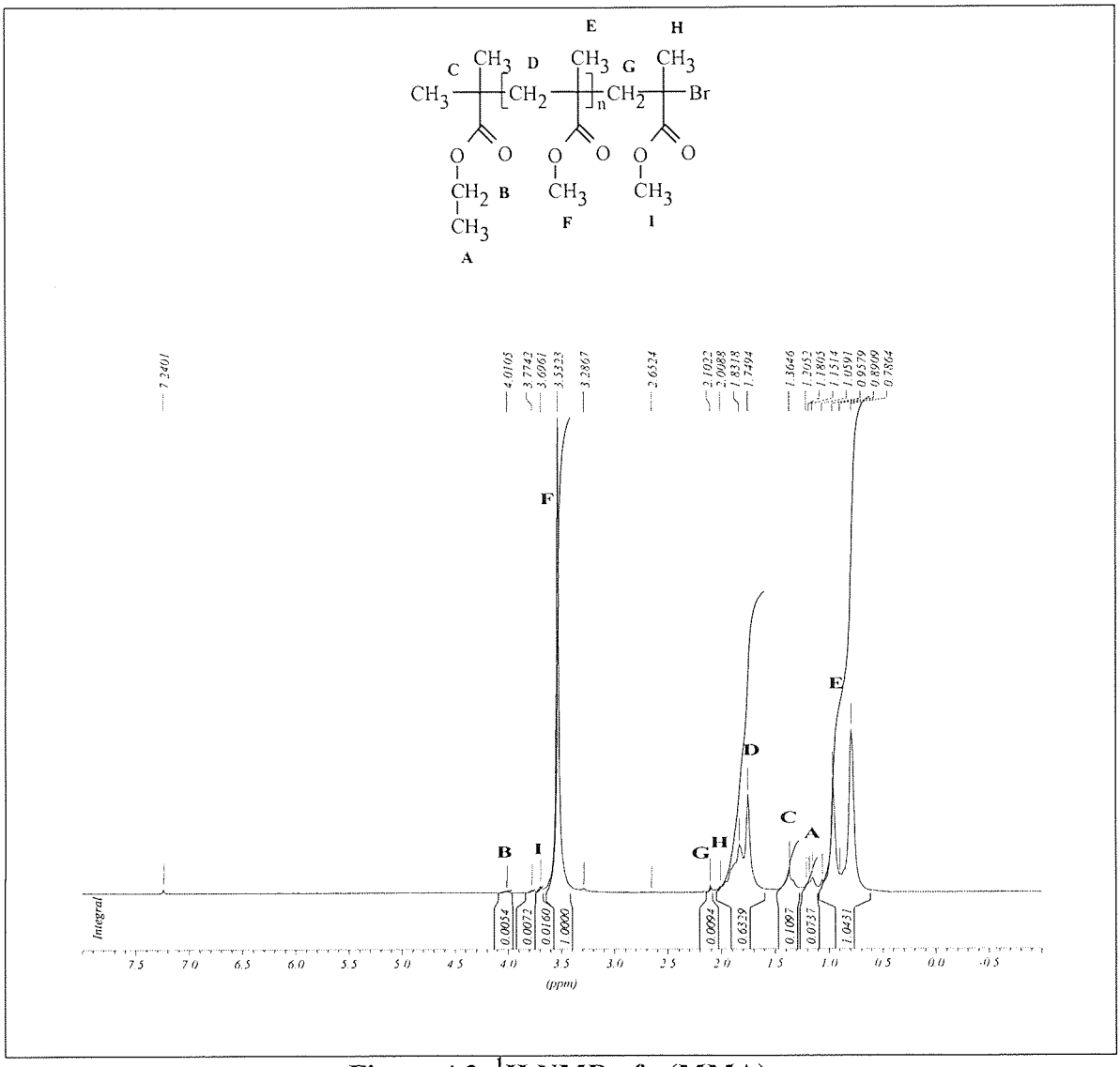

Figure 4.3. ^{1}H NMR of p(MMA).

It is apparent from the ^{1}H NMR spectrum shown in figure 4.3 that 2-EiBBr has initiated the polymerisation, with peaks corresponding to the constituent portions of the initiator fragment clearly visible. Furthermore, the molecular weight value calculated from the ratio of the integrated peak areas corresponding to the initiator methyl group (C) and the main chain methyl group (E) is 2113 g mol^{-1}, which is in agreement with that determined by GPC ($\overline{Mn}$ = 2670).

Confirmation that the polymer chains possessed Br-headgroups was achieved by utilising a quantity of this sample as a macroinitiator of the polymerisation of MMA. This was undertaken by preparing a diglyme solution (50%v/v) of MMA/CuBr/OPMI and the polymer sample, in a ratio of 100:1:3:1 respectively, by the standard procedure described in section 2.6.1. The solution was then heated to 90°C and maintained at this

temperature for 3 hours. The resultant polymer was then isolated, purified and analysed by GPC. The results of this experiment are listed in table 4.3, with the corresponding chromatograms shown in figure 4.4, and clearly indicate that reinitiation and extension of the macroinitiator chains has occurred. Furthermore, it is also apparent from the GPC traces that there is no evidence for any macroinitiator remaining unused.

	$\overline{M_n}$	$\overline{M_w}$	$\overline{M_w}/\overline{M_n}$
Macroinitiator	2670	3230	1.21
Polymer	9830	12960	1.32

Table 4.3. Molecular weight values of macroinitiator and reinitiated polymer.

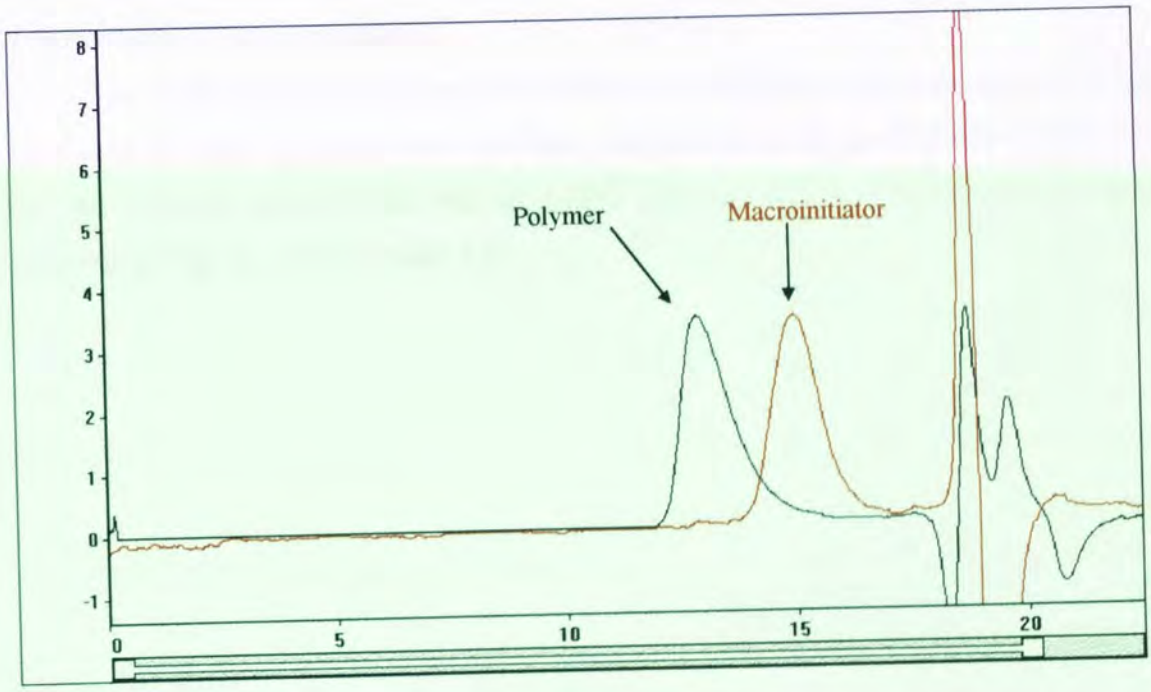

Figure 4.4. Gel permeation chromatogram of macroinitiator and reinitiated polymer.

4.3. The effect of temperature

4.3.1. The effect of temperature upon the rate of polymerisation and the molecular weight distribution of the resultant polymers

As stated previously, the ATRP of MMA at 100°C led to the production of polymers displaying broader molecular weight distributions than those observed for the ATRP of styrene at the same temperature. It is possible that this is attributable to differences in the respective k_p/k_t ratios of the two monomers. However, it is also notable that the significance of transfer and other undesirable side reactions becomes much more apparent at elevated temperatures, and thus it is probable that this is also a cause of the broader molecular weight distribution at these temperatures. Considering this, it would be undesirable to raise the temperature further, despite the fact that this would increase the ratio of propagation to termination. Hence, the effect of decreasing the temperature upon the kinetics and the level of control afforded over the polymerisation was investigated.

A series of polymerisations was conducted at different temperatures, utilising in each case the same procedure and the same concentrations of components as that used for the polymerisation conducted at 100°C (section 4.2.2). The results of these polymerisations are listed in table 4.4.

Temp./ °C	Time/ Minutes	%Conv.	$\overline{M_{nth}}$	$\overline{M_n}$	$\overline{M_w}$	$\overline{M_w}/\overline{M_n}$	$\ln\frac{[M]_0}{[M]_t}$
100	20	16.4	1835	2670	3230	1.21	0.182
	80	61.5	6345	6580	10130	1.32	0.955
	140	84.4	8635	9130	11390	1.25	1.858
	175	92.4	9435	10070	13140	1.31	2.577
90	30	22.9	2485	2590	3340	1.29	0.260
	60	40.7	4265	4430	5400	1.22	0.523
	90	51.9	5385	5460	6610	1.21	0.732
	120	61.1	6305	6370	7700	1.19	0.944
	180	75.3	7725	7930	9360	1.18	1.398
	210	79.8	8175	8550	10180	1.19	1.604
	240	86.6	8855	9010	10540	1.17	2.001
	300	90.9	9285	9470	11270	1.19	2.397
80	30	23.2	2515	2660	3410	1.28	0.264
	90	42.4	4415	5030	6410	1.27	0.552
	125	54.2	5615	5070	6800	1.34	0.781
	190	65.9	6785	6350	8180	1.29	1.076
	220	67.5	6945	7090	8980	1.27	1.124
	250	70.5	7245	7280	9120	1.25	1.221
60	30	10.5	1245	1460	1850	1.27	0.111
	75	15.5	1745	1790	2200	1.23	0.168
	200	31.9	3385	3290	4110	1.25	0.384
	255	39.2	4115	3860	4750	1.23	0.498
	310	45.0	4745	4680	5990	1.28	0.598
	380	55.5	5745	5720	7220	1.26	0.810
	460	61.2	6315	6100	7810	1.28	0.947
35	195	16.4	1835	2120	2650	1.25	0.179
	300	27.6	2955	3010	3700	1.23	0.323
	500	43.3	4525	4670	5980	1.28	0.567
	750	52.8	5475	5690	7170	1.26	0.751
	1215	66.0	6795	7030	8930	1.27	1.079

Table 4.4. The effect of temperature on the ATRP of MMA initiated by 2-EiBBr and mediated by CuBr/OPMI.

The results in table 4.4 illustrate that all polymerisations produced polymers having values of $\overline{Mn}$ close to the calculated values ($\overline{Mn_{th}}$) and narrow molecular weight distributions. It is notable that the polymerisation conducted at 90°C yielded polymers displaying the narrowest molecular weight distributions. The gel permeation chromatograms for the series of polymers isolated in this experiment are illustrated in

figure 4.5. The corresponding chromatograms for the polymerisations conducted at the other temperatures are shown in appendix 4(a).

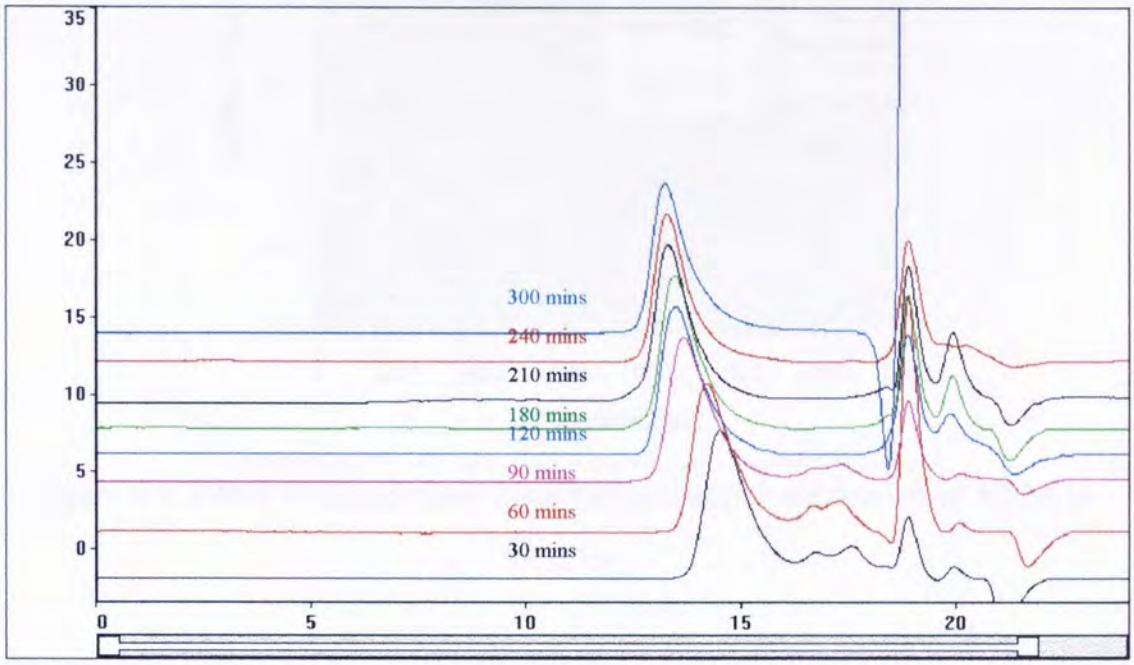

Figure 4.5. Gel permeation chromatograms for the ATRP of MMA at 90°C.

Figure 4.6 illustrates the effect of temperature upon the rate of polymerisation. The rate of polymerisation decreases with decreasing temperature, as expected, with the data for the polymerisation at each temperature producing a straight line fit. This is in each case, indicative of a constant concentration of propagating species and in combination with the molecular weight data listed in table 4.4, suggests that the polymerisation proceeds in a controlled manner over the entire temperature range studied. It is of note that these results are in agreement with those reported by Haddleton et al[119].

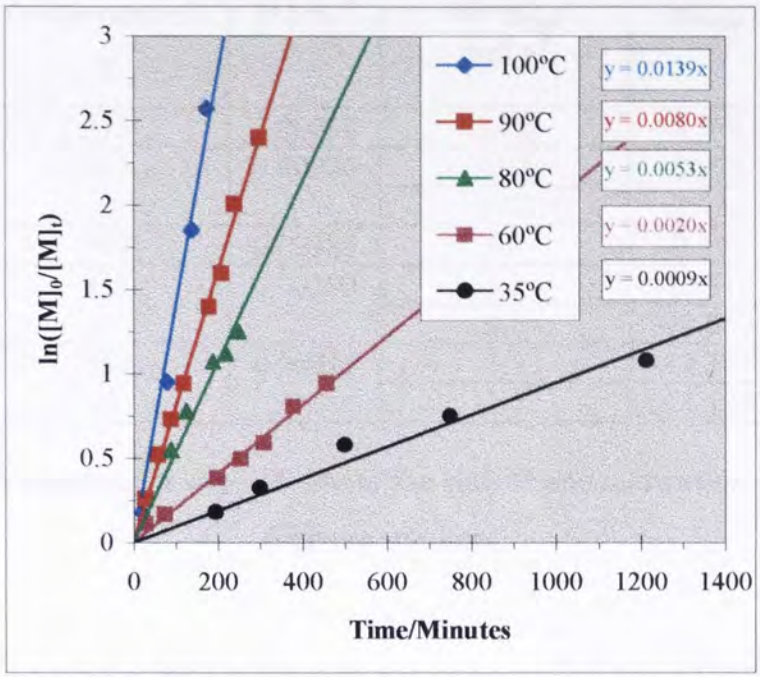

Figure 4.6. Effect of temperature upon the rate of polymerisation of MMA in diglyme.

4.3.2. Determination of the activation energy of the ATRP of MMA

It is widely accepted that many reactions have rate constants that follow the Arrhenius equation

$$\ln k = \ln A - \frac{E_a}{RT} \qquad (4.1)$$

where k is the rate constant,

A is the pre-exponential factor,

R is the molar gas constant (8.314 $JK^{-1}mol^{-1}$),

T is the temperature (K),

and E_a is the activation energy.

The rate constant under study is regarded as following this relationship if a plot of lnk against 1/T is linear and the gradient of the straight line produced is thus equal to $-E_a/R$. In order to assess the temperature dependence of the rate of polymerisation of MMA in diglyme solution, the Arrhenius parameters for the apparent rate constant of polymerisation, k_{app}, were determined (Table 4.5) and the corresponding plot constructed (figure 4.7). The values of k_{app} used are those derived from the relevant pseudo first-order kinetic plots illustrated in figure 4.6. The data for the additional repeat experiments listed in table 4.5 is listed in appendix 4(b).

Temperature/ K	$1/T/K^{-1}$	$10^5 * k_{app}$/ mol s^{-1}	lnk_{app}
373	0.00268	23.2	-8.370
363	0.00276	13.3	-8.923
		13.2	-8.933
353	0.00283	8.8	-9.334
333	0.00300	3.3	-10.310
		3.5	-10.260
308	0.00325	1.5	-11.107
		1.5	-11.107

Table 4.5. Temperature dependence of the rate of polymerisation of MMA in diglyme solution.

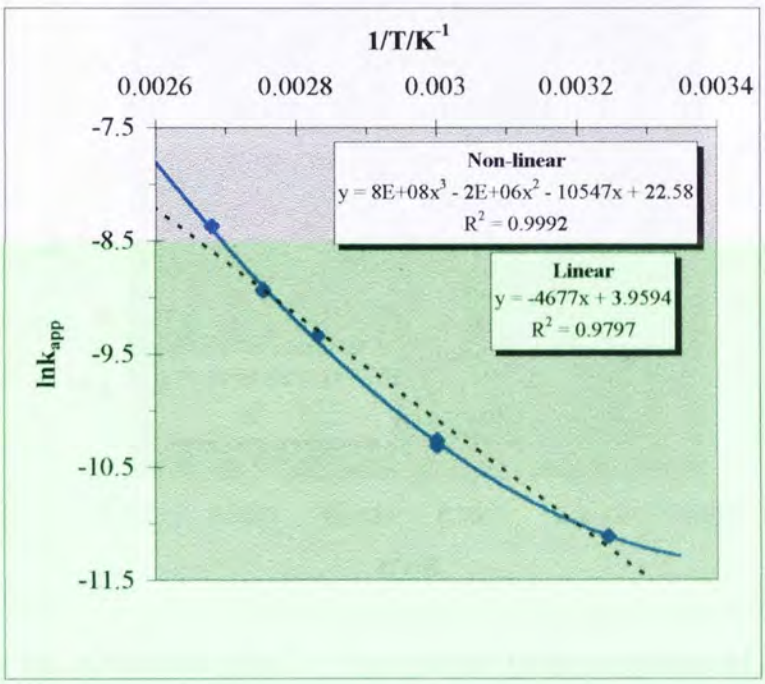

Figure 4.7. Arrhenius plot for the ATRP of MMA in diglyme solution.

As illustrated in figure 4.7, the Arrhenius plot does not yield a straight line, although it is possible to make a reasonable linear approximation comparable to those reported in the literature. However, it is evident that the temperature dependence of the apparent rate constant of polymerisation for the system studied is distinctly unlike a typical Arrhenius plot. Moreover, owing to the linearity of the Arrhenius plot for the known rate constants of radical propagation of methyl methacrylate[188] over the same temperature range (i.e. constant E_a), as shown in figure 4.8, and given that the

relationship between the enthalpy of the equilibrium, the apparent activation energy and the activation energy of propagation can be expressed by

$$\Delta H^{\circ}_{eq} = \Delta E^{\neq}_{app} - \Delta E^{\neq}_{prop} \qquad (4.2)$$

it is possible to infer that the enthalpy of the equilibrium decreases with decreasing temperature. However, it is more probable that the non-linearity of the plot arises due to a shift in position of the equilibrium with temperature. This would be particularly evident if the temperature dependency of the rate constants of activation and deactivation were different.

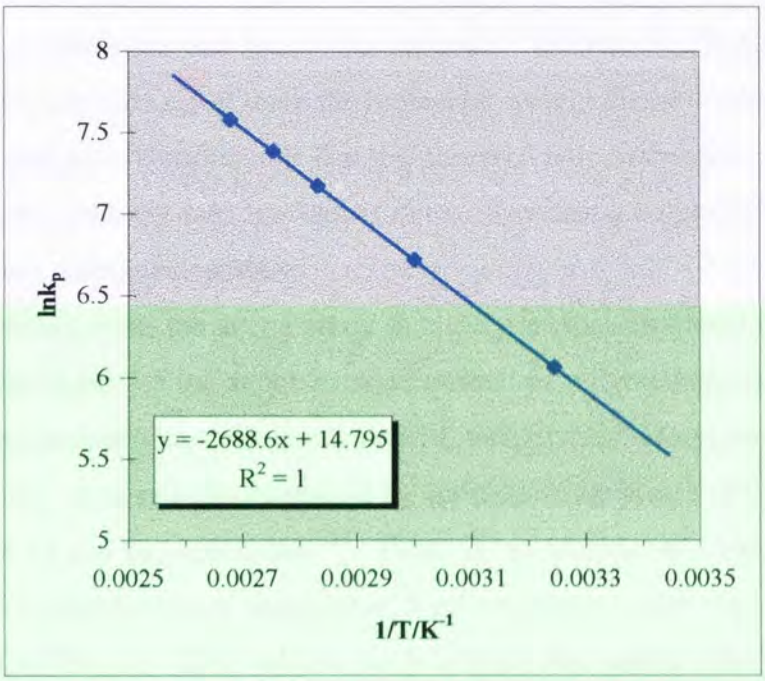

Figure 4.8. Arrhenius plot for free-radical polymerisation of MMA.

Indeed there is some evidence in the literature which lends support to this theory. In particular, Matyjasewski et al have reported that the UV-Vis absorbance of the band corresponding to the suspected active catalytic species in ATRP increases with decreasing temperature[189]. However, it is notable that this increase appears to be at the expense of the band corresponding to $Cu^{(II)}Br_2$/4,4'-dinonyl-2,2'-bipyridyl complex. This apparent change in the concentrations of the activating and deactivating catalytic species would thus alter the magnitude of the equilibrium constant ($K_{eq} = k_{act}/k_{deact}$),

such that it would increase with decreasing temperature, which in turn would fit with the proposed theory.

The observed effect on the equilibrium constant could also be manifested if the solubility of the deactivator is dependent upon temperature. If the solubility of this complex decreases with decreasing temperature, the effective concentration of deactivator and therefore the rate of deactivation would decrease with temperature, and hence confer the observed effect on the temperature dependence of the apparent rate constant of polymerisation. It is of note that a similar effect upon the rate of the polymerisation was observed for alterations in the solubility of the catalytic complex in the ATRP of styrene (section 3.2). Furthermore, Haddleton et al reported a comparable effect upon the ATRP of MMA[108]. However, it is notable that contrary to that found for the ATRP of styrene (section 3.2), the results of the above study indicate that the polymerisation temperature and hence the proposed variance in the solubility of the catalyst complex, has little effect upon the molecular weight distribution of the resultant polymers. It is thus highly improbable that the observed non-Arrhenius-like temperature dependence of the apparent rate constant is due to decreasing solubility of the catalyst complex with decreasing temperature.

It is apparent from the above study that the principal problems of studying the temperature dependence of the apparent rate constant of polymerisation arise from the variation of the concentration of deactivator with temperature. Matyjasewski et al have reported that this problem can be overcome by addition of an excess of $Cu^{(II)}Br_2$ prior to commencement of the polymerisation[124]. Thus, in an attempt to compensate for the variation in the concentration of deactivator, a polymerisation was conducted in which an excess of $Cu^{(II)}Br_2$/2L (20% relative to $[CuBr]_0$) was added. The results of this experiment are listed in table 4.6.

Time/Minutes	%Conversion
30	7.9
60	8.6
90	11.0
120	11.8
180	18.1
240	59.3
360	76.2

Table 4.6. Results of the polymerisation of MMA in the presence of 20% $Cu^{(II)}Br_2/2L$.

The resultant pseudo first-order kinetic plot, shown in figure 4.9, is clearly non-linear, suggesting that this method is unsuitable for the catalytic system under study. However, regardless of this, it is evident from this plot that although the excess deactivator suppresses propagation in the early stages of polymerisation, the rate of polymerisation gradually increases until it is comparable to that of a polymerisation conducted in the absence of an initial excess of $Cu^{(II)}Br_2/2L$ deactivator. It is thus apparent that the concentration of the deactivator decreases, such that the value of the equilibrium constant K_{eq}, where $K_{eq} = k_{act}/k_{deact}$, is comparable to that of the polymerisation conducted without added $Cu^{(II)}Br_2/2L$.

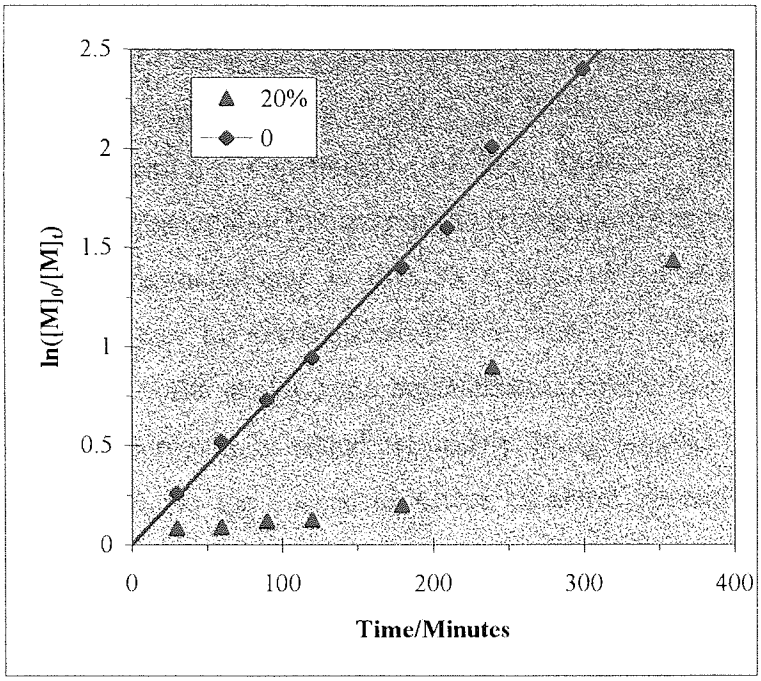

Figure 4.9. Effect of the addition of initial excess of $Cu^{(II)}Br_2$ on the rate of polymerisation.

Moreover, given the magnitude of the effect it is not inconceivable that the excess deactivator is converted into activating $Cu^{(I)}$ species. However, the manifestation of such an effect would require the operation of a process of interconversion of $Cu^{(II)}$ and $Cu^{(I)}$ species in addition to that in the assumed ATRP equilibrium. If indeed this is true, then the ATRP process can be represented by scheme 4.1. The steady-state concentration of $Cu^{(II)}Br_2/2L$ would therefore be dependent upon not only the rates of activation and deactivation of the chains, but also upon the rate of conversion of $Cu^{(II)}$ into $Cu^{(I)}$ species.

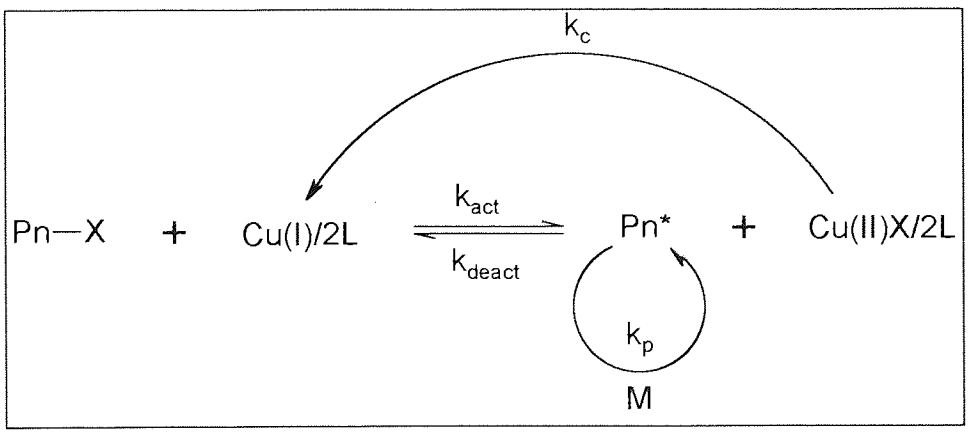

Scheme 4.1. Redefined ATRP process.

As the concentration of deactivator regulates the concentration of propagating species and consequently the apparent rate constant of polymerisation, it is evident that this will also be dependent upon the magnitude of k_c. Thus, considering the observed non-Arrhenius-like temperature dependence of the apparent rate constant of polymerisation and the corresponding linearity of the temperature dependence of k_p, it is possible that the observed behaviour is due to a non-Arrhenius-like temperature dependence of k_c. This can be rationalised if the ratio of k_c/k_{act} increases with decreasing temperature; i.e. the steady-state concentration of $Cu^{(II)}Br_2$ decreases with decreasing temperature. Moreover, as stated previously, Matyjasewski has reported that the conversion of $Cu^{(II)}Br_2$ to the suspected active catalytic species becomes more prominent as the temperature is decreased, suggesting that the proposed theory is indeed correct. However, given this evidence it is difficult to speculate upon a precise mechanism for this process, but it does nevertheless confirm its existence.

Although the Arrhenius plot clearly yields a non-linear fit, to allow comparison of the data with that reported in the literature the apparent activation energy was calculated from the linear approximation (E_{app} = 39 kJ mol^{-1}). It is of note that the value is considerably lower than most of the values quoted in the literature, which are listed in table 4.7. However, the value determined is in close agreement with that reported by Haddleton et al for the ATRP of MMA conducted in the presence of methyl hydoquinone[119]. This similarity may be coincidental, but it is possible that diglyme operates in a similar manner to that described for methyl hydroquinone and phenol[119, 190], displacing a ligand from the Cu(I) center and creating a vacant co-ordination site which facilitates propagation. Haddleton reported that this action was responsible for lowering the activation energy of the process relative to that of a control system without additional co-ordinating ligands other than the required α-diimines.

Author	Catalyst complex / initiator / solvent	E_a/ $kJmol^{-1}$	Reference
Percec	(CuCl/4,4'-di(5-nonyl)-2,2'-bipyridine)/p-toluenesulphonyl chloride/p-xylene	106.0	114
Matyjasewski	(CuCl/4,4'-di(5-nonyl)-2,2'-bipyridine)/p-toluenesulphonyl chloride/diphenyl ether	62.9	124
Haddleton	(CuBr/N-butyl-2-pyridinemethanimine)/2-EiBBr/toluene	60.3	119
Haddleton	(CuBr/N-butyl-2-pyridinemethanimine)/2-EiBBr/toluene/phenol	44.9	119

Table 4.7. Values of E_a reported in the literature.

To determine if this phenomenon is operational, the series of polymerisations were repeated in xylene solution, as it is unlikely that this non-polar molecule will co-ordinate strongly to the copper centre. The series of pseudo first-order kinetic plots constructed are illustrated in figure 4.10 and the corresponding Arrhenius parameters listed in table 4.8. The full data sets for this series of polymerisations are contained in appendix 5. It is of note that the data for the polymerisation conducted at 35°C has been excluded from this series, as the reaction solution was visibly heterogeneous.

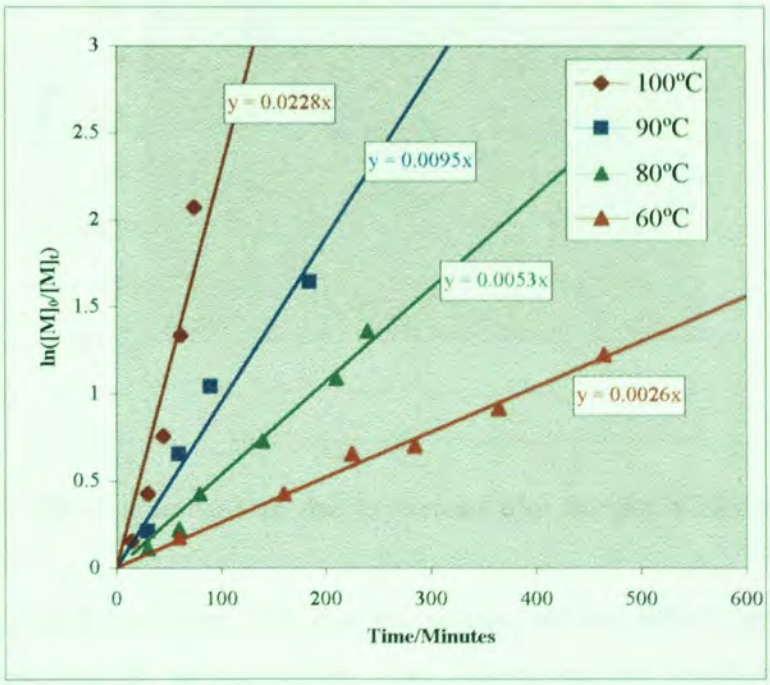

Figure 4.10. Effect of temperature upon the rate of polymerisation of MMA in xylene.

Temperature		$1/T/K^{-1}$	k_{app}/ $x10^{-5}$ mol s^{-1}	lnk_{app}
°C	K			
100	373	0.00268	38.33	-7.866
90	363	0.00276	15.83	-8.75
80	353	0.00283	8.83	-9.335
60	333	0.00300	4.33	-10.047

Table 4.8. Temperature dependence of the rate of polymerisation of MMA in xylene.

From the data listed in table 4.9, the corresponding Arrhenius plot (figure 4.11) was constructed. For comparative purposes, the Arrhenius plot for the ATRP of MMA in diglyme solution is also illustrated in figure 4.11.

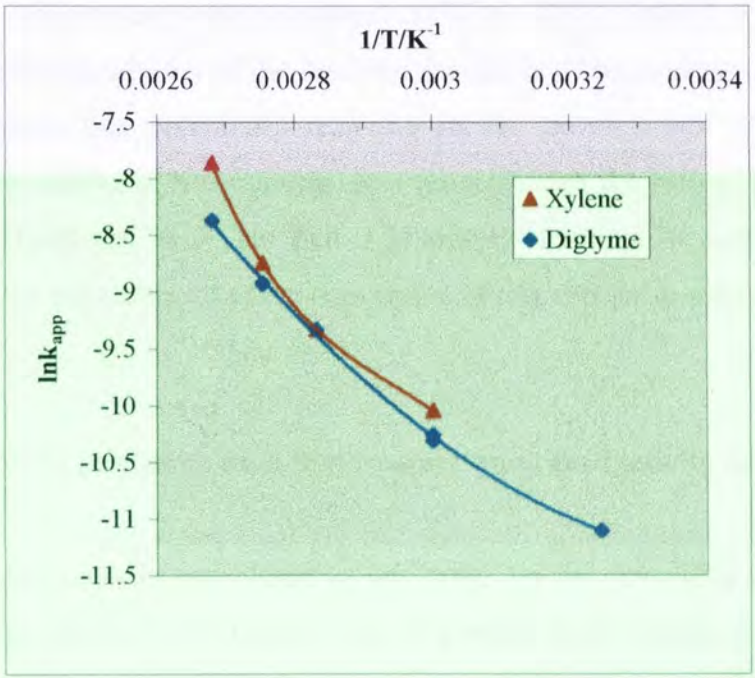

Figure 4.11. Effect of solvent on the Arrhenius plot for the ATRP of MMA.

It is apparent from figure 4.11 that the solvent utilised affects the temperature dependence of the rate of polymerisation, with polymerisations conducted in xylene proceeding at noticeably faster rates than those conducted in diglyme. This is in agreement with that found for the effect of solvent upon the ATRP of styrene (section 3.3). Furthermore, it was also noted for the ATRP of styrene that the solubility of the

catalyst complex in xylene solution appeared inferior to that observed in diglyme solution. Therefore, it is possible that the difference in the temperature dependencies of the ATRP of MMA in xylene and diglyme solutions respectively, is due to differences in the solubility of the catalyst complex in these solvents. Moreover, the faster rates of polymerisation observed in xylene solution may thus be due to a lower solubility of the deactivator in this solvent than in diglyme. However, it is also probable that these differences are due to solvent dependency of k_c or K_{eq}, with the more polar solvent diglyme inhibiting the conversion of $Cu^{(II)}$ into $Cu^{(I)}$ species. This would also be consistent with the effect of solvent observed in the ATRP of styrene.

Regardless of the reason for the rate of polymerisation being greater in xylene than diglyme, it is attestation that diglyme does not perform a similar role to that reported for phenol[119]. However, it is of note that Haddleton et al utilised a combination of ligand and solvent (N-(n-pentyl)-2-pyridylmethanimine/toluene), in the study of the effect of phenols, which is unlikely to have generated a homogeneous catalyst complex over the entire temperature range examined (90°C to -15°C). Indeed, it is evident from this study that the dissolution of the catalytic species is of paramount importance, with failure to achieve this potentially resulting in the development of fundamentally imprecise representations. Nevertheless, it is probable that the role of phenol is not as described by Haddleton et al, but that it is simply involved in consumption of the deactivator or the enhancement of the conversion of this species to activating species.

4.3.3. The effect of polymerisation temperature upon the tacticity of the resultant polymer

ATRP is generally considered as occurring via the reversible abstraction by a transition metal species of a halide from a pseudo-alkyl halide, to form a freely propagating radical and an oxidised metal species. If this were indeed the case, then it would be expected that the resultant polymers would possess structures comparable to those of polymers synthesised by conventional free-radical polymerisation.

In free-radical polymerisation, the orientation of approach of the incoming monomer is unaffected by the stereostructure of the propagating chain. The propagating radical is considered to be a freely rotating planar sp^2 carbon centre, and the configuration of the sp^3 centre that results on adding monomer is only determined by the addition of another monomer unit. This mechanism is commonly referred to as

Bernoulli-trial propagation and leads to a situation whereby the configuration of the adding monomer can occur in one of two ways. The two possible results of the addition are illustrated in scheme 4.2, and are referred to as isotactic and syndiotactic placements respectively.

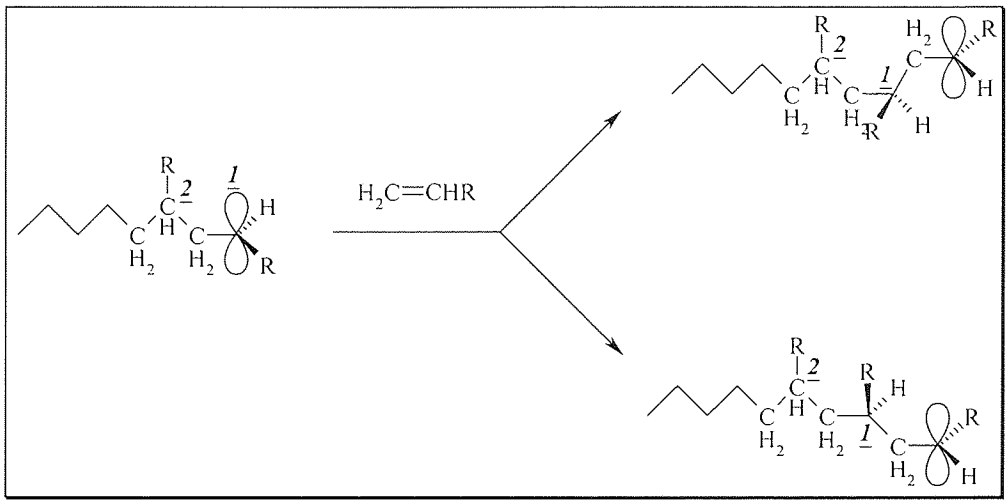

Scheme 4.2. Stereoregulation in free-radical polymerisation.

It is apparent that either of the two modes of addition can occur during a given propagation step, and hence the stereoregularity of polymers arising from a freely propagating species, such as a radical, is a function of the relative rates of these two modes of addition. Considering the outcomes of the two individual modes of addition, it is apparent that substituents in an isotactic placement will experience greater repulsion and steric hindrance than those in a syndiotactic placement. Therefore, the magnitude of the enthalpy and entropy of activation of a syndiotactic placement are less than those corresponding to an isotactic placement, and hence the syndiotactic configuration is the more favoured. Furthermore, due to this, the magnitude of the relative rates of the two modes of addition is temperature dependent, decreasing temperature resulting in further preference for the syndiotactic placement. Thus, for polymerisations involving propagation via a free-radical species, the degree of isotactic placements should decrease with decreasing reaction temperature.

In an attempt to clarify the nature of the propagating species involved in ATRP, the microstructures of polymers synthesised at various temperatures via this technique (section 4.3.1), were determined by ^{1}H N.M.R. spectroscopy, as described in section 2.7.3. For the purpose of these measurements, three consecutive constituent monomer

units within the chains were considered as defining a configuration. The three possible configurations of such triads are illustrated in scheme 4.3.

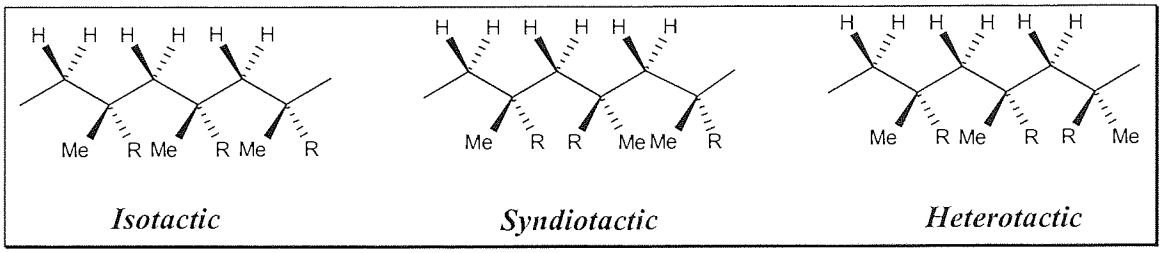

Scheme 4.3. Stereoregular triads for p(MMA).

In ^{1}H N.M.R. spectroscopy, the signal corresponding to the α-methyl group of p(MMA) can be analysed to determine the stereoregularity of a given polymer sample. Moreover, as the three equivalent protons of this group are sensitive to the chemical environment, the signal corresponding to this group is resolved into three distinct peaks, with each corresponding to one of the three possible triad sequences. Therefore, the relative degrees of isotactic, heterotactic and syndiotactic placements comprising a given polymer sample can be determined.

Figure 4.12 shows the ^{1}H N.M.R. spectra of three polymer samples prepared at 100, 90 and 35°C respectively. Only the signal corresponding to the α-methyl groups of the respective polymers is illustrated. The three peaks in each spectrum correspond to isotactic, heterotactic and syndiotactic placements, from higher to lower chemical shifts respectively.

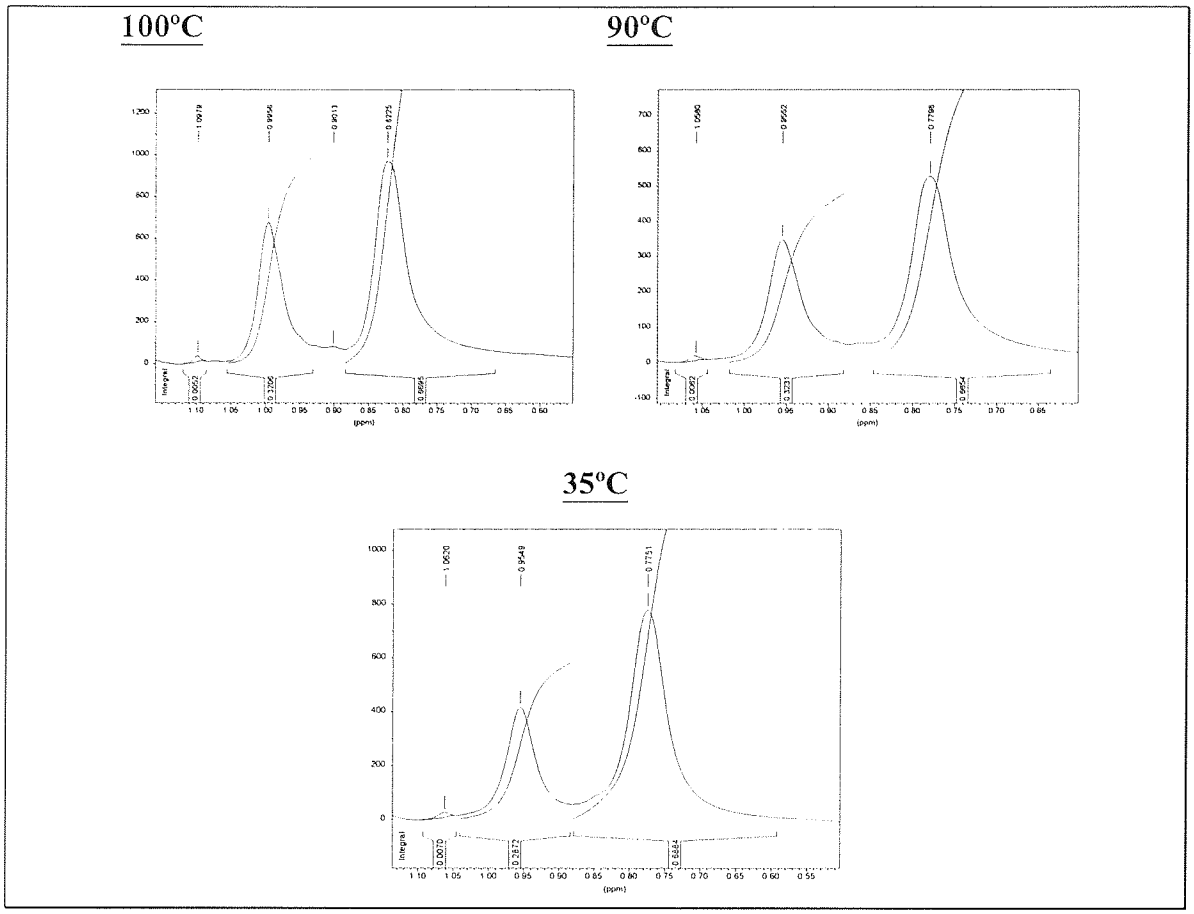

Figure 4.12. ^{1}H N.M.R. spectra of p(MMA) samples prepared at various temperatures.

Temperature/°C	Isotactic	Syndiotactic	Heterotactic
100	0.005	0.670	0.321
90	0.006	0.665	0.323
35	0.007	0.688	0.287

Table 4.9. The effect of temperature upon the tacticity of the resultant polymers.

The results suggest a reverse of the expected trend, with the degree of isotactic placements increasing, albeit slightly, with decreasing temperature. However, due to the inherent sensitivity of the technique, it is not possible to estimate the area of the peaks, particularly that corresponding to isotactic placements, with the desired precision. Hence, it is difficult to draw any real conclusions from this evidence, other than that the

polymers display stereochemistries consistent with those of polymers synthesised by free-radical polymerisation[191]. Therefore, it is possible to speculate that the propagating species in ATRP are free-radicals. However, it is of note that similar results can be observed for any freely propagating species regardless of their nature.

4.4. Kinetics of the ATRP of MMA at 90°C

4.4.1. The effect of the initial concentration of monomer

It is evident from the linearity of the series of plots of $\ln([M]_0/[M]_t)$ against time (see figure 4.6) that the rate of polymerisation is first-order with respect to the concentration of monomer. This is in good agreement with all reports in the literature[107, 108, 114].

4.4.2. The effect of the initial concentration of initiator

A series of reactions were conducted to study the effect on the polymerisation of varying the concentration of the initiator 2-EiBBr. The initial concentrations of monomer and catalyst complex were kept constant; $[MMA]_0 = 4.76$ mol dm^{-3}, $[CuBr]_0 = 0.0476$mol dm^{-3}, $[OPMI]_0 = 0.143$ mol dm^{-3}. The polymerisations were followed by sampling of the reaction liquor at timed intervals, as described in section 2.6.2. In each case, monomer conversion was determined by gravimetry, and molecular weight values by GPC, as described in sections 2.7.1 and 2.7.2 respectively.

The full data sets for this series of experiments are shown in appendix 6. However, it is of note that for each experiment, the resultant polymers displayed narrow molecular weight distributions ($\overline{Mw}/\overline{Mn} < 1.3$) and values of number average molecular weight comparable to the theoretical values calculated using equation 3.1. This suggested that effective control was afforded over each polymerisation. Moreover, plots of $\ln([M]_0/[M]_t)$ against time were constructed for each experiment, as illustrated in figure 4.13., and linear fits were obtained for each concentration further suggesting that a high level of control was afforded over each polymerisation.

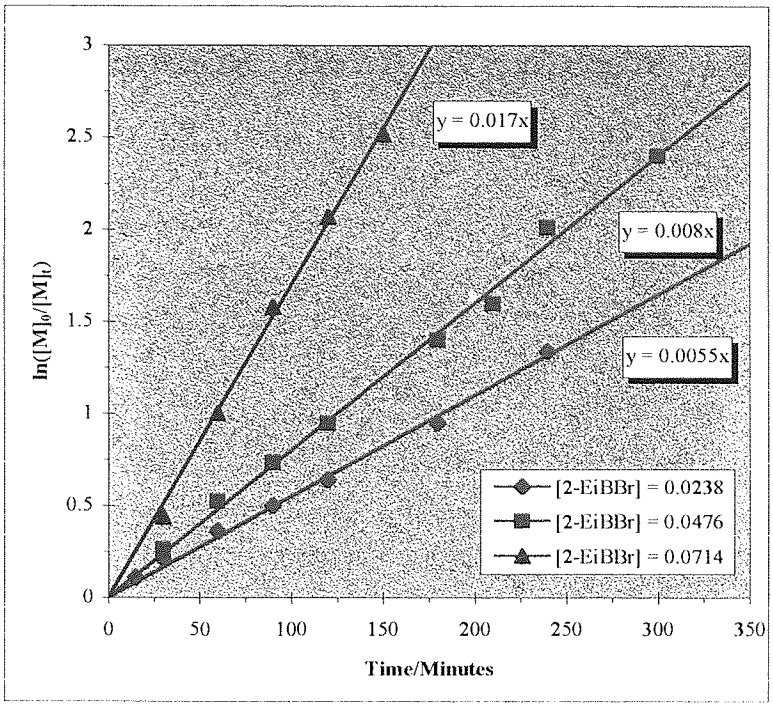

Figure 4.13. The effect of the initial concentration of 2-EiBBr upon the rate of polymerisation.

The apparent rate constant of polymerisation for each experiment was obtained from the gradient of the respective plots (figure 4.13). The dependence of the apparent rate constant of polymerisation on the initial concentration of 2-EiBBr is shown in table 4.10.

$[2\text{-EiBBr}]_0$/ mol dm^{-3}	$10^5 * k_{app}/s^{-1}$	$10^8 * [Pn^*]$/ mol dm^{-3}	$\ln[2\text{-EiBBr}]_0$	$\ln k_{app}$
0.0238	9.2	5.69	-3.74	-9.29
0.0476	13.3	8.23	-3.04	-8.93
0.0714	28.4	17.57	-2.64	-8.17

Table 4.10. Dependence of the apparent rate constant of polymerisation on the initial concentration of 2-EiBBr.

The order of the reaction with respect to initiator was estimated from a plot of $\ln k_{app}$ against $\ln[2\text{-EiBBr}]_0$, shown in figure 4.14. The straight line through the data points has a gradient of 0.97, which approximates to a first-order dependence of the

apparent rate constant on the initial concentration of 2-EiBBr. This is in agreement with the values reported in the literature. However, it is of note that the straight line is a poor fit through the data.

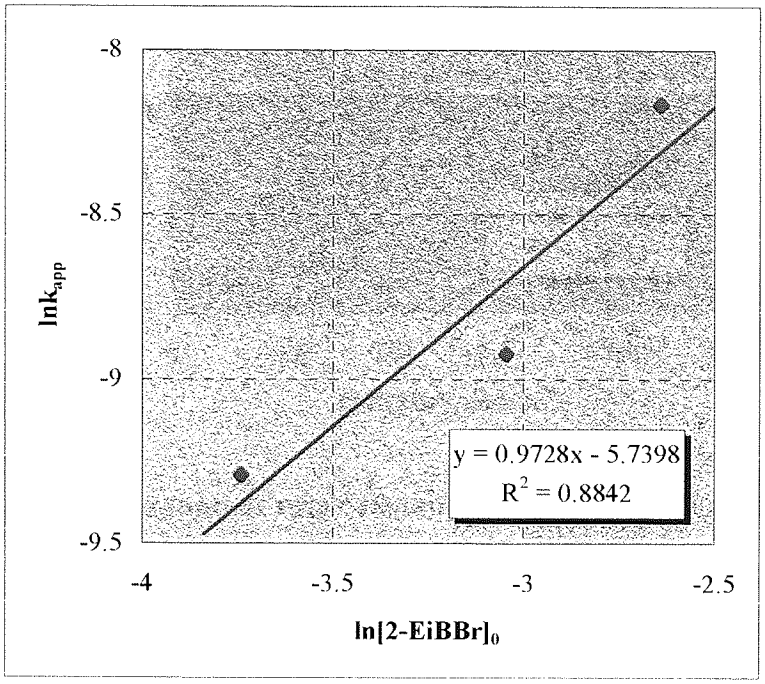

Figure 4.14. Graph of $\ln k_{app}$ against $\ln[2\text{-EiBBr}]_0$.

A plot of the measured apparent rate constant against the initial concentration of 2-EiBBr is shown in figure 4.15. The linearity of this plot again suggests that there is a first-order dependence of the apparent rate constant upon the initial concentration of 2-EiBBr. However, it is of note that there appears to be a threshold concentration of initiator of 0.005 mol dm^{-3} necessary for polymerisation to occur. This may result from the formation of an appropriate steady-state concentration of $Cu^{(II)}Br_2$ via the persistent radical effect, which involves consumption of active centres via termination reactions.

In an attempt to compensate for this, a plot of $\ln k_{app}$ against $\ln([2\text{-EiBBr}]_0 - [I_x])$ was constructed, where $[I_x]$ is the threshold concentration. However, it is of note that this plot appearred inferior to that of $\ln k_{app}$ against $\ln[2\text{-EiBBr}]_0$ (figure 4.14.), producing a poorer fit through the data and suggesting a much larger deviation from a first-order dependence of the apparent rate constant upon the concentration of initiator.

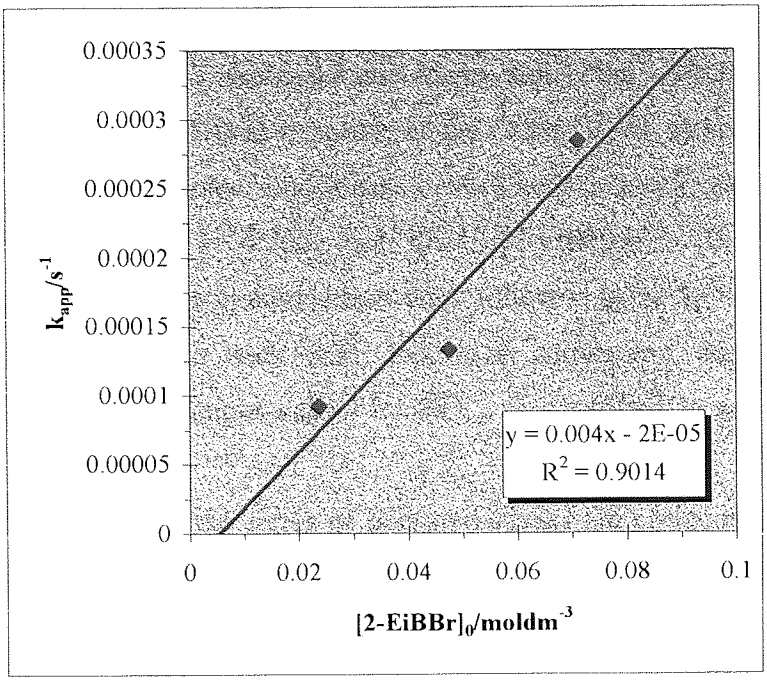

Figure 4.15. Graph of apparent rate constant of polymerisation against initial concentration of 2-EiBBr.

It is possible that the inappropriateness of the plot of $\ln k_{app}$ against $\ln([2\text{-EiBBr}]_0 - [I_x])$ is due to variations in the concentrations of $Cu^{(II)}Br_2$ formed during the polymerisation at each initial concentration of initiator. Moreover, it is evident that increasing the initial concentration of initiator results in an increase in the rate of polymerisation, which is manifested by an increase in the concentration of propagating species. Increasing the concentration of propagating species will increase the probability of the occurrence of biradical termination reactions, and hence the level of deactivator required to sustain effective control over the polymerisation will also increase. As the polymers prepared in each experiment display comparably narrow molecular weight distributions, it is apparent that this is indeed the case. Thus, it is clear that, as suggested, variation in the steady-state concentrations of deactivator in each experiment is the principal cause of the inappropriateness of the plot of $\ln k_{app}$ against $\ln([2\text{-EiBBr}]_0 - [I_x])$. However, it is evident that if the variation in the concentration of the deactivator is only small, as it appears to be in this case, then its effect upon the dependence of the apparent rate constant upon the initial concentration of initiator will be negligible.

4.4.3. The effect of the initial concentration of catalyst

A series of reactions were conducted to study the effect on the rate of polymerisation of varying the concentration of the CuBr/OPMI catalyst complex. The initial concentrations of monomer and initiator were kept constant, as was the ratio of OPMI to CuBr; $[MMA]_0$ = 4.762 mol dm^{-3}, $[2\text{-EiBBr}]_0$ = 0.0476 mol dm^{-3}, $[OPMI]_0$:$[CuBr]_0$ = 3:1. The polymerisations were followed by sampling of the reaction liquor at timed intervals. In each case, monomer conversion was determined by gravimetry, and molecular weight values by GPC, as described in sections 2.7.2 and 2.7.1 respectively.

The full data sets for the series of polymerisations are contained in appendix 7, but it is noteworthy that each experiment produced polymers displaying relatively narrow molecular weight distributions ($\overline{Mw}$ / $\overline{Mn}$ < 1.35). However, it is also of note that polymers synthesised at the highest concentration of CuBr ($[CuBr]_0$ = 0.0952 mol dm^{-3}) displayed molecular weights which deviated slightly from the corresponding values calculated from 100% initiator efficiency. The pseudo first-order kinetic plots of $\ln([M]_0/[M]_t)$ against time constructed for the series of polymerisations are shown in figure 4.16.

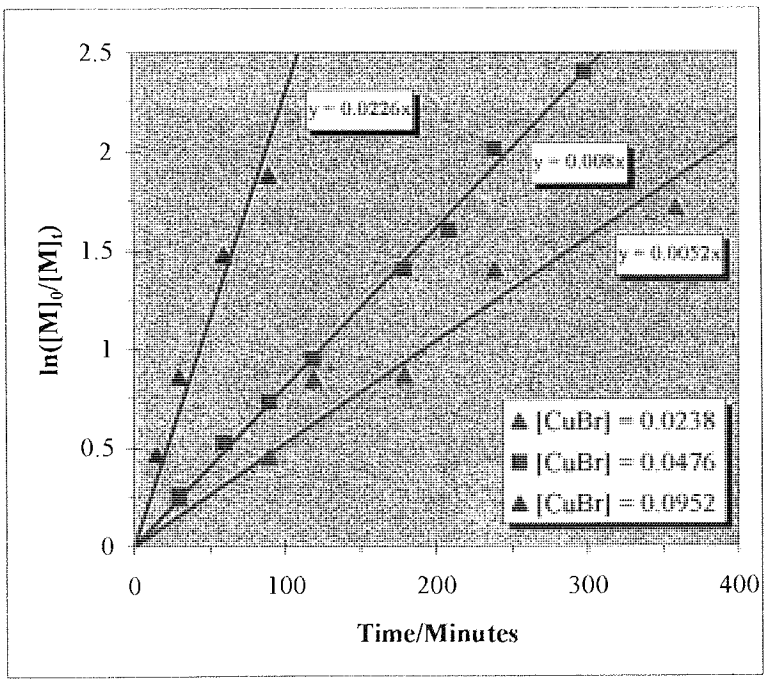

Figure 4.16. The effect of the initial concentration of CuBr upon the rate of polymerisation.

The apparent rate constant of polymerisation for each experiment was derived from the gradients of the plots in figure 4.16. The dependence of the apparent rate constant upon the initial concentration of CuBr is listed in table 4.11.

$[CuBr]_0$/ mol dm^{-3}	$10^5 k_{app}$/ s^{-1}	10^8 [Pn*]/ mol dm^{-3}	$\ln[CuBr]_0$	$\ln k_{app}$
0.0238	8.7	5.4	-3.74	-9.35
0.0476	13.3	8.2	-3.04	-8.93
0.0952	37.7	23.3	-2.35	-7.88

Table 4.11. Dependence of the apparent rate constant of polymerisation upon the initial concentration of CuBr.

The order of the reaction with respect to the initial concentration of CuBr can be estimated from a plot of $\ln k_{app}$ against $\ln[CuBr]_0$, shown in figure 4.17. The straight line through the points has a gradient of 1.06, which suggests that the apparent rate constant has a first-order dependence upon the initial concentration of CuBr. This is in agreement with results reported in the literature[124].

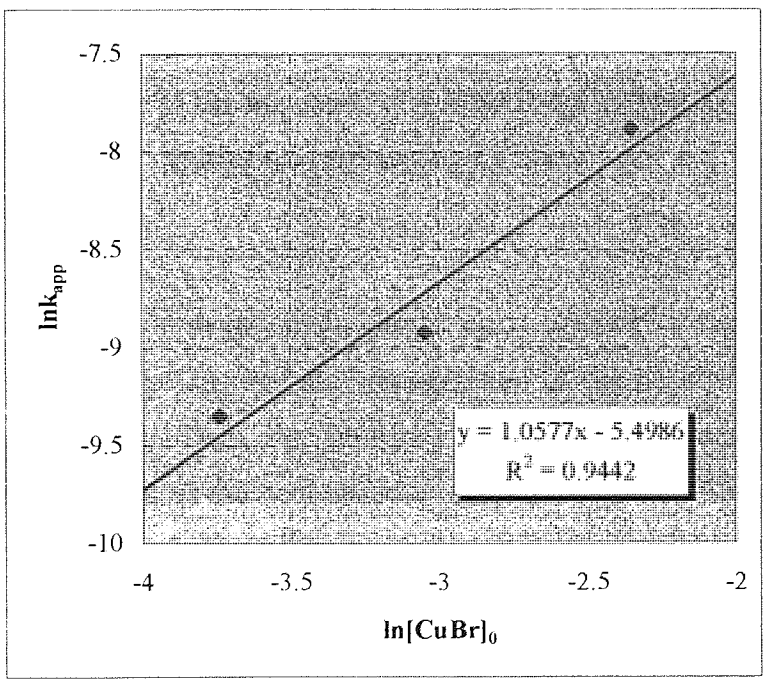

Figure 4.17. Graph of $\ln[CuBr]_0$ against $\ln k_{app}$.

Figure 4.18. shows a plot of the apparent rate constant of polymerisation against the initial concentration of CuBr. The straight line through the data suggests a first-order dependence, which is in agreement with that determined above. However, it is interesting to note that there appears again to be a threshold concentration of catalyst ($[CuBr]_x$ = 0.0095 mol dm^{-3}) required for polymerisation to occur, which is similar to that observed for the plot of the apparent rate constant of polymerisation against the initial concentration of initiator.

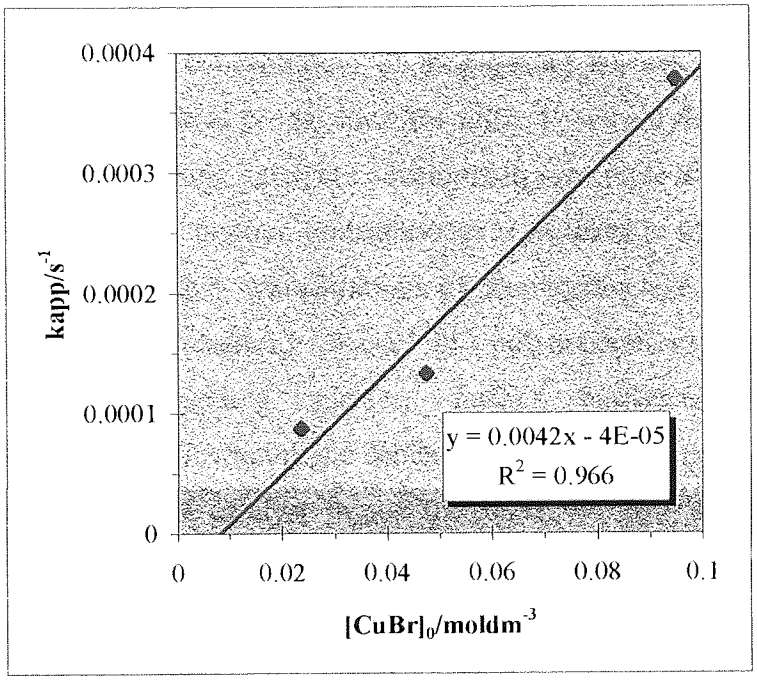

Figure 4.18. Dependence of the apparent rate constant of polymerisation upon the initial concentration of CuBr.

The observation of a threshold concentration is probably a consequence of the formation of an appropriate steady-state concentration of the deactivator $Cu^{(II)}Br_2$, as proposed in section 4.4.1. Thus, the similarity between the corresponding plots of apparent rate constant against the concentration of initiator and $Cu^{(I)}Br$ respectively is not entirely unexpected, as both $Cu^{(I)}Br$ and initiator are irreversibly consumed in the formation of the appropriate quantity of $Cu^{(II)}Br_2$. However, it is of note that it was shown in section 4.3.2 that $Cu^{(II)}$ species can be transformed into $Cu^{(I)}$ species, by a process outside of the confines of the general ATRP equilibrium.

In an attempt to compensate for the apparent threshold concentration a plot of $\ln k_{app}$ against $\ln([CuBr]_0 - [CuBr]_x)$ was constructed. However, this plot produces a poor fit through the data and suggests a much larger deviation from a first-order dependence of the apparent rate constant upon the concentration of catalyst than the plot of $\ln k_{app}$ against $\ln[CuBr]_0$ (figure 4.17.).

Similarly to that found in section 4.4.2 for the plot of $\ln k_{app}$ against $\ln([2\text{-EiBBr}]_0 - [I_x])$, it is possible that the inappropriateness of the plot of $\ln k_{app}$ against $\ln([CuBr]_0 - [CuBr]_x)$ is due to variations in the concentrations of $Cu^{(II)}Br_2$ formed during the polymerisation, at each initial concentration of catalyst. However, this is not entirely surprising, as the concentration of propagating species, calculated from the known rate constant of radical propagation for methyl methacrylate (k_p= 1616 mol s^{-1})[188], increases with increasing catalyst concentration (see table 4.11.), and hence it is probable that a higher concentration of deactivator is required to effect control over the polymerisations having higher concentrations of propagating species. It is also likely that more termination reactions occur in polymerisations involving higher concentrations of propagating species, further emphasising the possible inappropriateness of plots illustrating the dependence of the apparent rate constant upon the initial concentration of catalyst minus the threshold concentration of catalyst. However, it is of note that similar to that observed for the effect of varying the initial concentration of initiator, the level of termination in each experiment is negligible and has little influence on the molecular weight distributions of the resultant polymers. Its slight effect upon the kinetics of the polymerisation is therefore surprising, particularly as it is evident that any excess $Cu^{(II)}$ generated can be transformed back into $Cu^{(I)}$.

4.4.4. The effect of the initial ratio of OPMI to CuBr

The effect of the ratio of the initial concentrations of ligand to CuBr upon the rate of polymerisation at 90°C in diglyme solution was investigated. A series of experiments was conducted in which the initial concentration of OPMI was varied whilst the concentrations of MMA, CuBr, 2-EiBBr and diglyme were kept constant; $[MMA]_0$ = 4.76 mol dm^{-3}, $[CuBr]_0$ = 0.0476 mol dm^{-3}, $[2\text{-EiBBr}]_0$ = 0.0476 mol dm^{-3}, Diglyme = 50% v/v with MMA. The polymerisations were followed by periodic sampling of the reaction liquor and monomer conversion determined in each case by gravimetry. The results for the polymerisations are listed in appendix 8.

The pseudo first-order kinetic plots for the series of polymerisations are shown in figure 4.19, and clearly illustrate that with the exception of the polymerisation conducted with a $[OPMI]_0:[CuBr]_0$ equal to 0.5:1, all polymerisations proceeded at a similar rate. The corresponding values of the apparent rate constants of polymerisation are listed in table 4.12.

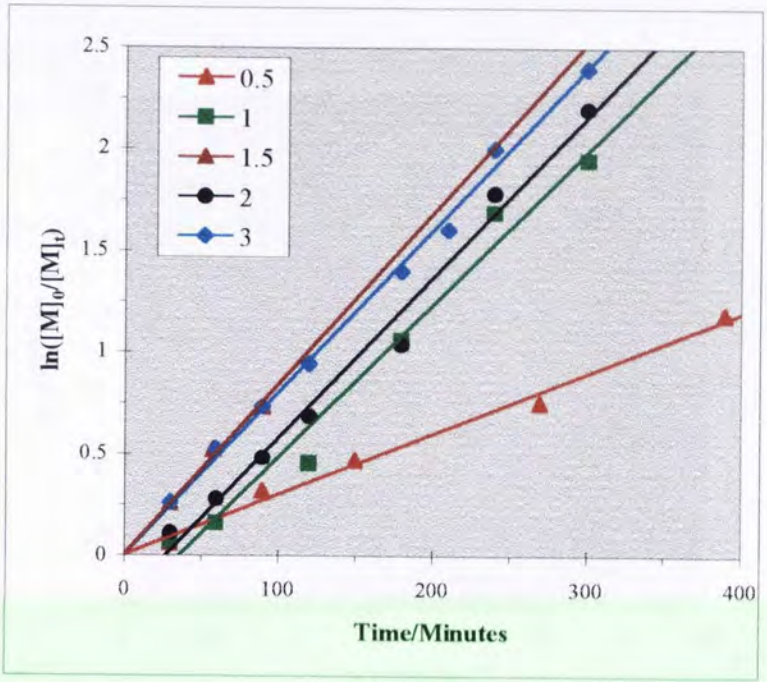

Figure 4.19. The effect of the ligand to CuBr ratio upon the rate of polymerisation.

$[OPMI]_0:[CuBr]_0$	$10^5 * k_{app}/s^{-1}$
0.5	5.0
1.0	12.5
1.5	14.0
2.0	13.2
3.0	13.3

Table 4.12. Dependence of the apparent rate constant of polymerisation upon the ratio of $[OPMI]_0:[CuBr]_0$.

A plot of the apparent rate constant against $[OPMI]_0:[CuBr]_0$ is shown in figure 4.20, illustrating that the rate of polymerisation is unaffected by increasing the ratio of

OPMI to CuBr above 1:1. It is of note that the observed trend is in agreement with that reported by Matyjasewski et al[124], but that it is in contrast to that reported by Haddleton et al[108], who reported that the kinetically optimum ratio of ligand to CuBr was 2:1. However, it is probable that this disparity emanates from the utilisation of BPMI as a complexing ligand by Haddleton et al which, as reported in section 3.2, was found to generate a less soluble catalyst complex than OPMI.

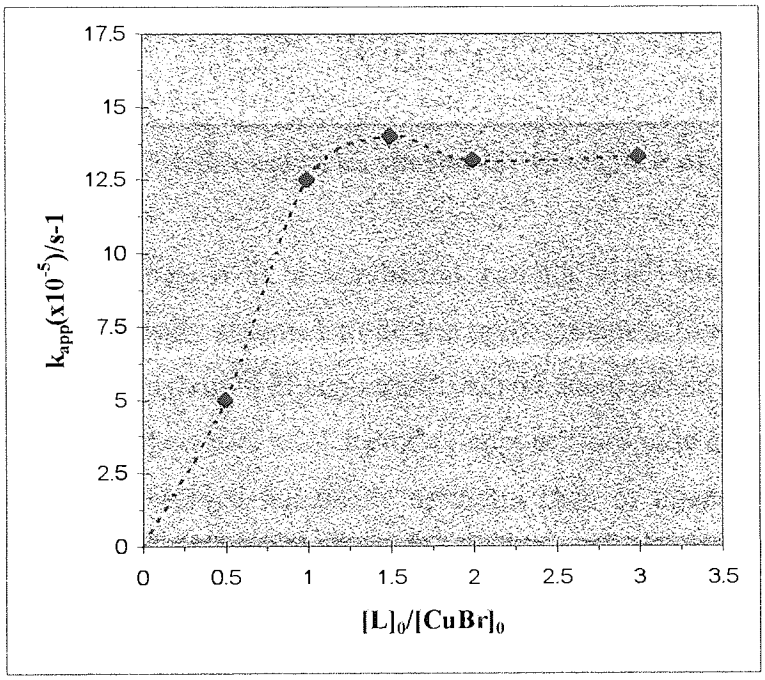

Figure 4.20. The effect of $[OPMI]_0$:$[CuBr]_0$ upon the rate of polymerisation.

As the kinetically optimum ratio of OPMI to CuBr appears to be 1:1, it is possible to assume that the active catalytic species is a 1:1 complex of OPMI and CuBr. Some of the possible species this includes are illustrated in scheme 4.4.

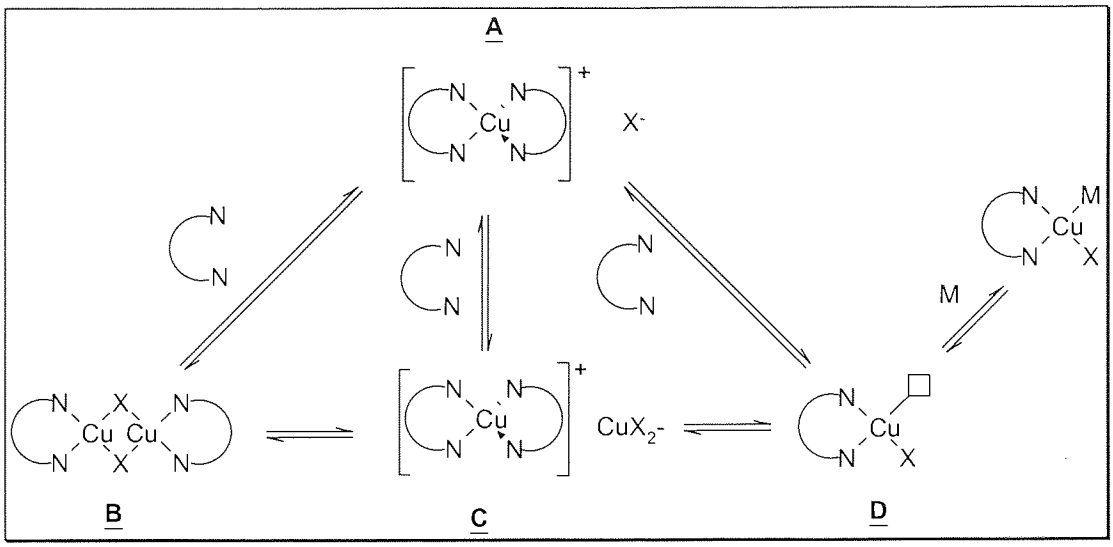

Scheme 4.4. Possible catalytic species for the ATRP of MMA.

The species denoted A is a tetrahedral cationic $Cu^{(I)}$ complex with a Br^- counteranion and is generally assumed to be the predominant active catalytic species. Such complexes have been thoroughly characterised and documented in the literature[190]. However, this particular species is a 2:1 ligand to copper(I)bromide complex and hence does not adhere to the observed kinetically optimum ratio of ligand to CuBr of 1:1. Moreover, it has been reported that this complex only predominates in polar solvents, with the halogen bridged dimer, B, predominating in non-polar solvents typically utilised in ATRP[192, 193]. As such species are 1:1 ligand to CuBr complexes it is possible that they constitute the active catalytic species in ATRP conducted in non-polar solvents. However, it is equally probable that complex D is the active catalytic species. Indeed, Haddleton et al have reported substantial evidence to support this theory. They have proposed that additives such as phenols[121, 190, 119] or benzoic acid[136] interact with the copper centre, displacing a ligand and creating a vacant co-ordination site which facilitates propagation. Whilst this hypothesis is reasonable, more recent evidence reported by Matyjaszewski et al strongly suggests that complex C is the predominant species present in non-polar solvent solutions[189]. As the ratio of ligand to Cu in this complex equates to 1:1, it is apparent that this observation is in agreement with the results of the above study. Furthermore, it is of note that the aforementioned publication by Matyjaszewski et al also states that no dimeric halogen-bridged compounds were detected, perhaps eliminating such species from the possibilities. However, considering all the evidence, it is still not possible to speculate upon the exact nature of the active

catalytic species for the ATRP of MMA. It is conceivable that all of the above species, as well as many others, may coexist in an extremely complex dynamic equilibrium.

4.5. Study of the initial period of the polymerisation by GPC

The role of the persistent radical effect in establishment of the appropriate quantity of deactivator has been discussed in the previous sections. However, no direct evidence for the occurrence of this phenomenon has thus far been provided. In an attempt to verify its occurrence, the initial period of the polymerisation was studied, as it is suspected that this is the period during which the process occurs predominantly.

A solution of MMA/CuBr/OPMI/2-EiBBr in diglyme (50% v/v with MMA) was prepared by the procedure described in section 2.6.2, such that $[MMA]_0 = 4.76$ mol dm^{-3}, $[CuBr]_0 = 0.0235$ mol dm^{-3}, $[OPMI]_0 = 0.0705$ mol dm^{-3} and $[2\text{-EiBBr}]_0 = 0.0235$ mol dm^{-3}. The solution was then heated to 90°C and samples removed at timed intervals. In each case the samples were quenched by dissolving in a fifty-fold excess of THF, the volatiles evaporated off and the resultant residue analysed by GPC.

The molecular weight data for the series of polymers isolated are listed in table 4.13 and the corresponding gel permeation chromatograms illustrated in figure 4.21.

Time/Minutes	$\overline{M_n}$	$\overline{M_w}$	$\overline{M_p}$	PDi
2	5190	6520	7510	1.26
4	4810	6910	8590	1.44
6	4580	6880	9370	1.50
8	4690	7080	10330	1.51
10	5390	7610	5980	1.41
12	5860	8310	7360	1.42
14	6960	9180	8620	1.32
30	7810	9970	9770	1.28
60	10680	13710	14570	1.28
120	14480	18550	20290	1.28
180	17350	23040	23770	1.33

Table 4.13. Molecular weight data for polymers isolated for the study of the initial period of the polymerisation.

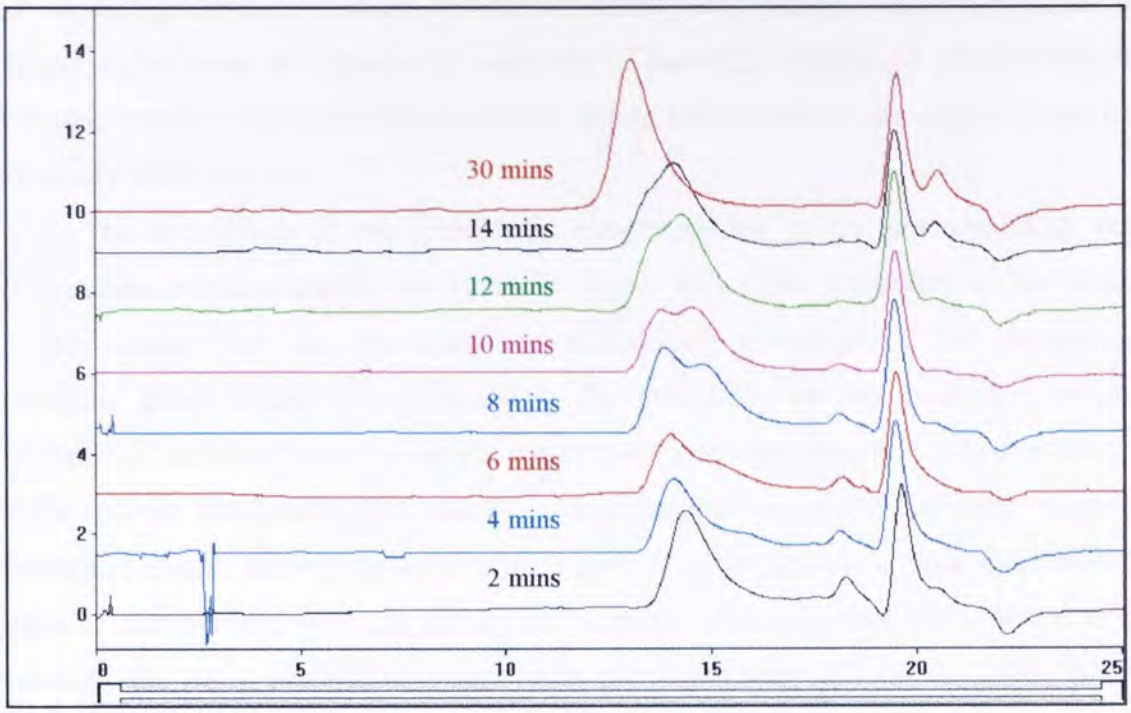

Figure 4.21. Gel permeation chromatograms for the series of polymers isolated from the initial 30 minutes of the polymerisation period.

As clearly shown in figure 4.21, the first sample isolated after two minutes has a unimodal molecular weight distribution, whereas subsequent samples withdrawn over the ensuing 12 minutes display distinctly bimodal molecular weight distributions. The sample isolated after 30 minutes displays a unimodal molecular weight distribution, as did all the subsequent samples withdrawn after much longer reaction times, the results for which are listed in table 4.13.

This phenomenon, as previously suggested, is a consequence of the formation of the appropriate quantity of deactivator via the persistent radical effect. It is envisaged that during the early stages of the polymerisation the concentration of deactivator is low and hence the rate of deactivation of the active species is slow, favouring propagation. Consequently, relatively high molecular weight chains are formed rapidly at the beginning of the polymerisation. However, due to the low concentration of deactivator, the time the chain ends spend in the active form is relatively large, facilitating bimolecular termination reactions and the irreversible formation of dead polymer chains and an excess of the deactivator. As the polymerisation proceeds, the concentration of deactivator increases and hence the rate of deactivation also increases, such that after a given period of time the concentration of deactivator is sufficient to suppress termination and allow the polymerisation to proceed in a controlled manner. Therefore,

the remaining dormant halogen end-capped chains can undergo further propagation without succumbing to termination reactions. Thus their degree of polymerisation increases, whereas that of the dead polymer chains formed during the establishment of this steady-state does not.

The occurrence of this process is clearly visible in the corresponding gel permeatation chromatograms illustrated in figure 4.21. The formation of the dead polymer chains and the subsequent controlled polymerisation of the remaining potentially active chains is manifested in the bimodality of the molecular weight distributions, with the higher molecular weight peak corresponding to the dead polymer chains and the lower molecular weight peak corresponding to the surviving halogen end-capped chains. Moreover, the continued growth of the remaining potentially active chains is also evident, with the corresponding peak emerging after four minutes and becoming the more predominant peak with increasing time. Eventually after thirty minutes the molecular weight of these chains surpasses that of the dead polymer chains, the corresponding peak for which appears insignificant at this and subsequent stages of the polymerisation. It is of note that the disappearance of the peak corresponding to the dead polymer chains is in agreement with the results of all the aforementioned polymerisations, for which no residual dead polymer chains were detected. However, this is not surprising, as the proportion of chains undergoing termination during such polymerisations is low, and has been estimated to be approximately 5%[195].

The results of this study are in good agreement with those reported by Matyjaszewski and Fukuda[117], whom observed a similar phenomenon for the chain extension of a bromine end-capped polystyrene macroinitiator. Furthermore, the observed decrease in $\overline{Mn}$ during the incipient stages of the polymerisation period studied is comparable to that predicted by theoretical simulations described by Matyjaszewski[196]and Fischer[59]. However, it is notable that no reports of comparable direct experimental evidence of the phenomenon observed in this study have appeared in the literature to date.

Chapter 5. ATRP of methyl methacrylate in polar solvents

5.1. Introduction

The ATRP of methyl methacrylate, as outlined in chapter 4, is readily achievable in relatively non-polar solvents such as xylene and diglyme. However, the extension of this system to the synthesis of the desired photorefractive polymers is somewhat limited, as the target polymers and monomers are only sparingly soluble in such solvents. Only polar aprotic solvents, such as dimethyl sulphoxide (DMSO) and N,N-dimethylformamide (DMF), provide effective dissolution of these monomers. Therefore, the extension of the developed CuBr/OPMI ATRP catalyst system to the polymerisation of methacrylic monomers in such solvents was investigated, using methyl methacrylate as a simple model monomer.

5.2. Effect of solvent

The polymerisation of MMA in DMSO and DMF solutions at 90°C was investigated. The same recipe as that utilised in chapter 4 for polymerisations in diglyme and xylene was adhered to, such that $[MMA]_0$ = 4.76 mol dm^{-3}, $[CuBr]_0$ = 0.0476 mol dm^{-3}, $[OPMI]_0$ = 0.143 mol dm^{-3}, $[2\text{-EiBBr}]_0$ = 0.0476 mol dm^{-3}, and the volume ratio of solvent to MMA was 1:1. The polymerisations were followed by periodic sampling of the reaction liquor, as described in section 2.6.2. In each case, monomer conversion was determined by gravimetry and molecular weight values by GPC, as described in sections 2.7.2 and 2.7.1 respectively.

Figure 5.1 illustrates the effect of solvent on the extent of monomer conversion with time. The full data sets for the polymerisations in DMSO and DMF are listed in appendix 9. The data for polymerisations conducted in non-polar solvents is shown for comparative purposes. It is notable that, when the polymerisations are conducted in polar solvents conversion does not exceed 40%, even with prolonged heating. Furthermore, as shown in figure 5.2, the number-average molecular weight values for polymers synthesised in polar solvents do not correlate with the theoretical values calculated from 100% initiator efficiency ($Mn_{theoretical}$). The molecular weight

distributions of polymers synthesised in DMF are also considerably broader than those for polymers synthesised in the other solvents.

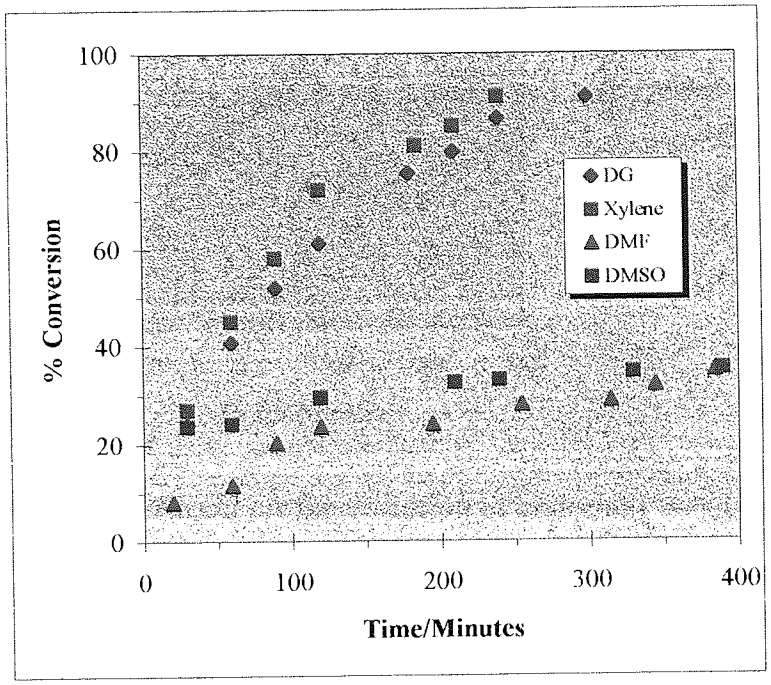

Figure 5.1. Effect of solvent on the extent of monomer conversion with time.

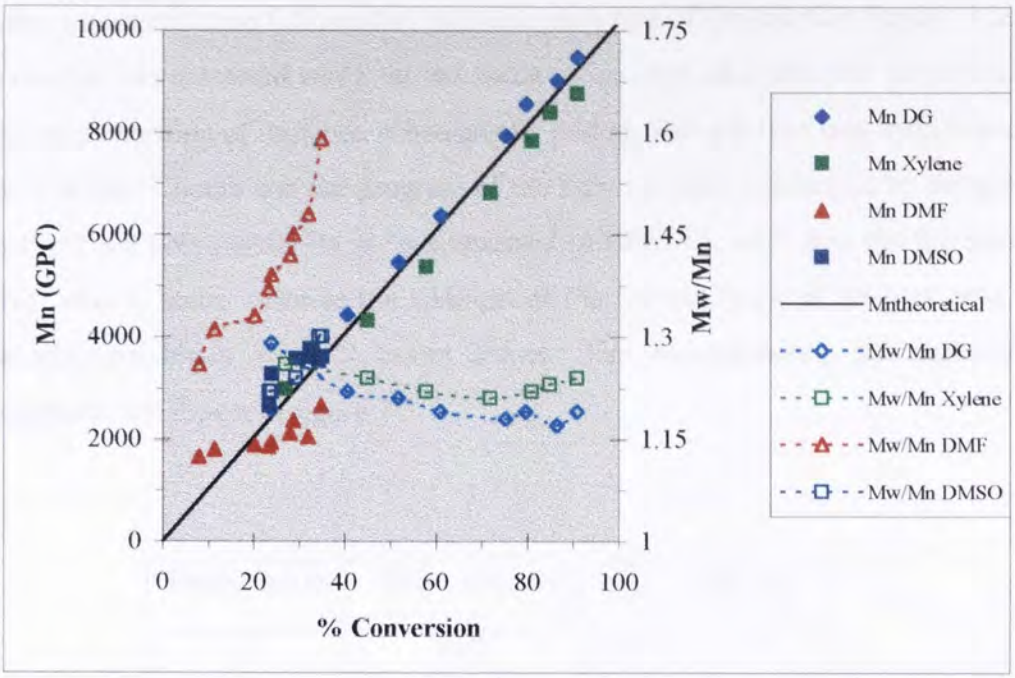

Figure 5.2. Effect of solvent on the evolution of molecular weight and molecular weight distribution with conversion.

It is possible that the limited level of monomer conversion achievable and the lack of control over polymerisations conducted in polar solvents are due to interaction of the solvent with the copper centre, which may result in conversion of the active catalytic complex to an inactive state. Indeed, Vairon[197] and Matyjaszewski[132, 133] have also made similar observations. However, it is also probable that the polymerisation is inhibited by an excess of deactivator, formed via termination reactions.

5.3. Effect of the addition of a second batch of initiator

To determine if the active catalyst complex is consumed during the polymerisation of MMA in polar solvents, an experiment was conducted in which a second batch of initiator was added to the reaction mixture when the level of conversion reached 35%.

A solution of MMA/CuBr/OPMI/2-EiBBr in DMSO was prepared as described for previous identical experiments (section 5.2), such that $[MMA]_0$ = 4.76 mol dm^{-3}, $[CuBr]_0$ = 0.0476 mol dm^{-3}, $[OPMI]_0$ = 0.143 mol dm^{-3}, $[2\text{-EiBBr}]_0$ = 0.0476mol dm^{-3}, and the volume ratio of DMSO to MMA was 1:1. The solution was heated to 90°C and

the ensuing polymerisation followed by periodic sampling of the reaction liquor. After 6 hours a sample was extracted and a second batch of initiator, of equimolar proportion to the initial concentration of initiator, subsequently added. The solution was maintained at 90°C for a further 5 hours and the progress of the polymerisation followed by sampling. The results of the polymerisation are summarised in table 5.1, with data for the sample withdrawn after 6 hours, prior to the addition of the second batch of initiator, and the final sample withdrawn after 11 hours shown. The corresponding gel permeation chromatograms are shown in figure 5.3.

Time/Hours	%Conversion	$\overline{M_n}$	$\overline{M_w}/\overline{M_n}$
6	35.3	3710	1.29
11	39.3	3960	1.33

Table 5.1. Results of the polymerisation of MMA in DMSO involving addition of a second batch of initiator.

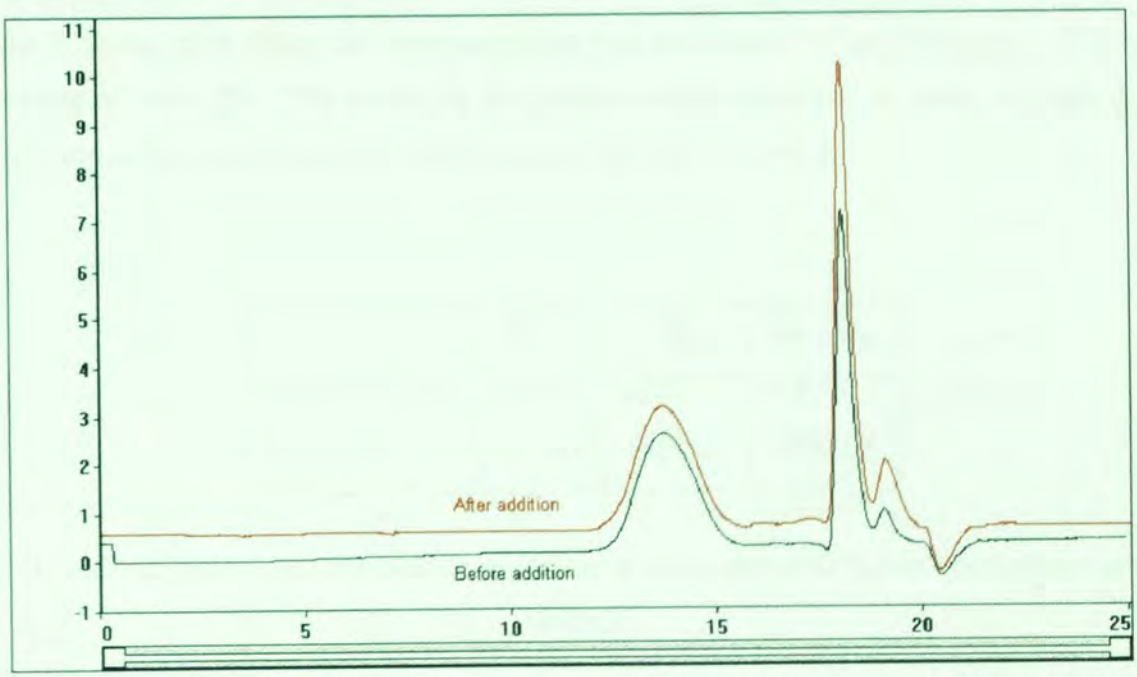

Figure 5.3. Gel permeation chromatograms of p(MMA) before and after addition of a second batch of monomer.

It is evident from the results that the addition of a second batch of initiator resulted in a negligible amount of polymerisation. This indicates that the termination of polymerisation in polar solvents is due to consumption of, or suppression of the activity of, the active catalytic species.

5.4. Reinitiation experiment

It is apparent from the above experiment that the active catalyst complex is consumed during the initial stages of the polymerisation. However, the negligible effect of the addition of a second batch of initiator does not confirm whether the termination of chain growth processes in polar solvents is also due to loss of chain-end functionality. In an attempt to determine this, an experiment was conducted in which a p(MMA) sample, prepared in DMSO solution, was used as a macroinitiator of the polymerisation of MMA in diglyme, a solvent previously found to be compatible with this technique. Thus, a solution of MMA/CuBr/OPMI/macroinitiator in diglyme was prepared, where $[MMA]_0$ = 4.76 mol dm^{-3}, $[CuBr]_0$ = 0.0238 mol dm^{-3}, $[OPMI]_0$ = 0.0714 mol dm^{-3}, $[macroinitiator]_0$ = 0.0238 mol dm^{-3}, and the volume ratio of diglyme to MMA was 1:1. The solution was heated to 90°C and maintained at this temperature for 4 hours, after which the polymerisation was terminated by pouring into a 50-fold excess of cold THF. The results of the polymerisation are listed in table 5.2, and the corresponding gel permeation chromatograms shown in figure 5.4.

	$\overline{M_n}$	$\overline{M_w}$	$\overline{M_w}/\overline{M_n}$
Macroinitiator	3280	4000	1.22
Polymer	53150	102790	1.93

Table 5.2. Results of reinitiation experiment using macroinitiator synthesised in DMSO.

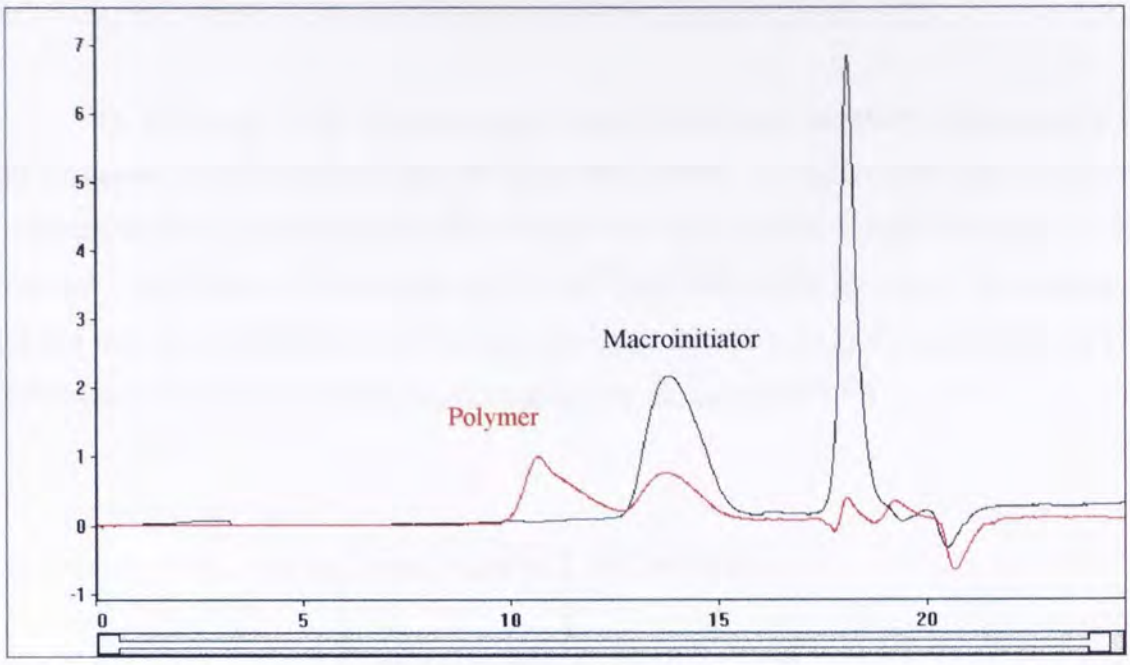

Figure 5.4. Gel permeation chromatograms of macroinitiator and resultant polymer.

It is evident from the chromatograms shown in figure 5.4 that the macroinitiator contained a high proportion of residual dead polymer chains, indicating that a significant number of the chains synthesised in polar solvents do not possess terminal Br head-groups. This is contrary to that found for chains synthesised in comparatively non-polar solvents, such as diglyme, which were found to be efficient macroinitiators (see figure 4.4). It is therefore apparent that the use of polar solvents not only results in deactivation of the active catalyst, but also causes significant loss of chain-end functionality. It is possible that the two processes are synonymous, with bimolecular termination reactions leading to the formation of an excess of the Cu(II) deactivating species, which will suppress polymerisation. Moreover, as illustrated in section 4.3.1, excess deactivator can be re-converted into Cu(I) activating species and hence such behaviour would be unexpected. However, as intimated in section 4.3.2, the rate of this conversion reaction may be dependent upon the polarity of the solvent, decreasing with increasing solvent polarity. It is therefore probable that polar aprotic solvents suppress this reaction and hence any excess deactivator that is generated becomes persistent. Its continued generation would thus eventually lead to a situation whereby polymerisation is suppressed, or in the extreme case inhibited, as is observed.

5.5. Polymerisation in the presence of an initial excess of deactivator

To determine if the formation of a large excess concentration of deactivator is the principal cause of the termination of polymerisation, an experiment was conducted in which an initial excess of $Cu^{(II)}Br_2$ deactivator was present; where $[MMA]_0 = 4.76$ mol dm^{-3}, $[Cu^{(I)}Br]_0 = 0.0476$ mol dm^{-3}, $[Cu^{(II)}Br_2]_0 = 0.00952$ mol dm^{-3}, $[2\text{-EiBBr}]_0 = 0.0476$ mol dm^{-3}, $[OPMI]_0 = 0.1714$ mol dm^{-3}, and DMSO was in a volume ratio of 1:1 with MMA. The results of the polymerisation are shown in table 5.3.

Time/Minutes	%Conversion
30	1.8
60	4.5
120	7.2
180	8.3
240	7.9
300	8.8

Table 5.3. Results of the polymerisation of MMA in DMSO in the presence of an initial excess of deactivator.

It is evident from the results that only a negligible amount of polymerisation occurred, illustrating that the $Cu^{(II)}Br_2$ has suppressed the polymerisation. This is contrary to that found for an identical polymerisation conducted in diglyme solution which, after an initial period of retardation, proceeded at a much faster rate. Moreover, it is thus evident that as suspected, the transformation of Cu(II) to Cu(I) is inhibited in polar aprotic solvents, and that this is the primary cause of the premature cessation of the polymerisation in such solvents.

5.6. Effect of increasing the initial concentration of ligand

The previous experiments illustrated that the formation of a high persistent concentration of deactivator is the principal cause of the premature termination of the polymerisation in polar solvents. This high concentration arises from the inhibition of the conversion of this species back into Cu(I). Moreover, Klumpermann recently suggested in a seminal paper that this transformation is mediated by the ligand, as it preferentially stabilises the lower oxidation state[198]. In order to investigate this, a polymerisation in DMSO solution was conducted at 90°C in the presence of a high concentration of ligand, greatly in excess of that routinely utilised for the formation and dissolution of the desired catalyst; where $[MMA]_0$ = 4.76 mol dm^{-3}, $[CuBr]_0$ = 0.0476 mol dm^{-3}, $[OPMI]_0$ = 1.19 mol dm^{-3}, $[2\text{-EiBBr}]_0$ = 0.0476 mol dm^{-3}, and the volume ratio of DMSO to MMA was 1:1. The high concentration of OPMI utilised generates a ligand to CuBr ratio of 25:1, as opposed to the standard ratio of 3:1. The results of the polymerisation are listed in table 5.3.

Time/Minutes	%Conversion	$\overline{M_n}$	$\overline{M_w}/\overline{M_n}$
10	39.4	3750	1.36
20	63.7	5760	1.52
40	81.4	6200	1.87
60	91.6	6390	1.90

Table 5.3. Results of the polymerisation in the presence of a high concentration of OPMI.

The results clearly indicate that in contrast to the polymerisation conducted with the conventional concentration of ligand (0.143 mol dm^{-3}), in which the level of monomer conversion did not exceed 40%, the use of a higher concentration of ligand allows the polymerisation to be driven towards completion. However, there is a notable broadening of the molecular weight distribution with the progression of the polymerisation. It is probable that this is due to the occurrence of termination or other reactions involving the loss of chain-end functionality. Regardless of this, it is evident from this experiment that the use of a higher concentration of ligand profoundly affects

the polymerisation. It can be speculated, that the excess ligand drives the transformation of the generated Cu(II) back into Cu(I), preventing the formation of a high persistent concentration of deactivator and hence ensuring the progression of the polymerisation. Moreover, it is possible to project from this that further increases in the concentration of ligand may effect a higher degree of control over the polymerisation. However, this is undesirable, as it is probable that the volume of ligand required to achieve this would be in excess of that of the solvent and hence would inhibit the dissolution of the target monomers and polymers.

5.7. Effect of zerovalent copper

The use of zerovalent copper in CuBr catalysed ATRP has been reported to facilitate faster rates of polymerisation[199]. The role of copper(0) is to scavenge excess deactivator, converting it, as well as itself, to Cu(I) activating species. As the formation of excess deactivator appears to be a fundamental problem with polymerisations in polar aprotic solvents, the use of Cu(0) in such polymerisations was investigated.

A solution was prepared which contained equimolar amounts of $Cu^{(I)}Br$ and Cu(0) powder, where $[MMA]_0 = 4.76$ mol dm^{-3}, $[CuBr]_0 = 0.0476$ mol dm^{-3}, $[Cu(0)]_0 = 0.0476$ mol dm^{-3}, $[OPMI]_0 = 0.286$ mol dm^{-3}, $[2\text{-EiBBr}]_0 = 0.0476$ mol dm^{-3}, and the volume ratio of DMSO to MMA was 1:1. The solution was heated to 90°C and samples withdrawn at periodic intervals. In each case, conversion was determined by gravimetry and molecular weight values by GPC, as described in sections 2.7.2 and 2.7.1 respectively. The results of the polymerisation are listed in table 5.4.

Time/Minutes	%Conversion	$\overline{M_n}$	$\overline{M_w}/\overline{M_n}$
2.5	23.9	9430	1.62
5.0	47.9	9370	1.71
7.5	61.5	9510	1.68
10.0	72.3	9590	1.73
12.5	77.2	9480	1.76
15.0	85.3	9620	1.76
20.0	94.1	9530	1.80

Table 5.4. Results of the ATRP of MMA with Cu(0)/Cu$^{(I)}$Br.

The results indicate that the addition of Cu(0) allows the polymerisation to be driven towards completion, presumably by scavenging any deactivator formed. However, it is clear that this process is so efficient that the persistent concentration of deactivator is insufficient to control the polymerisation, and hence the resultant polymers display broad molecular weight distributions. The polymerisation thus resembles a redox initiated free-radical polymerisation, with the number average molecular weight of the polymers formed not increasing with monomer conversion. This is illustrated in figure 5.5, showing the gel permeation chromatograms of the first and last samples.

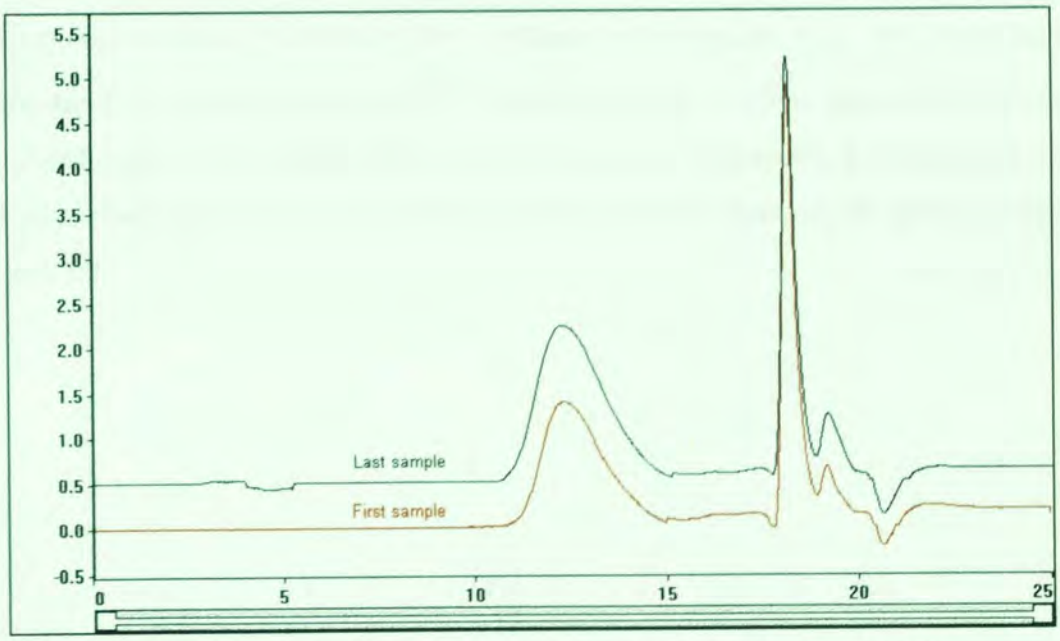

Figure 5.5. GPC traces of polymers synthesised using Cu(0).

Although the use of Cu(0) in this instance, resulted in an uncontrolled polymerisation, the experiment provides further evidence that the termination of chain growth processes in polar solvents is due to formation of a large excess of deactivator.

5.8. Effect of initial concentration of catalyst

A series of experiments was conducted to study the effect on the polymerisation of MMA in polar solvents of varying the initial concentration of the CuBr/OPMI catalyst complex. The initial concentrations of monomer and initiator were kept constant, as was the ratio of CuBr to OPMI; $[MMA]_0$ = 4.76 mol dm^{-3}, $[2\text{-EiBBr}]_0$ = 0.0476 mol dm^{-3}, $[OPMI]_0$:$[CuBr]_0$ = 3:1, solvent (DMSO or DMF) to MMA volume ratio of 1:1. The polymerisations were followed by sampling of the reaction liquor at timed intervals, as described in section 2.6.2. In each case, monomer conversion was determined by gravimetry and molecular weight values by GPC, as described in sections 2.7.2 and 2.7.1 respectively. The full data sets for the polymerisations are listed in appendix 10.

The effect of the initial concentration of the catalyst complex upon the extent and rate of monomer conversion in DMSO solution are shown in figure 5.6. It is evident that increasing the initial concentration of the catalyst complex increases the extent of monomer conversion attainable. Furthermore, as shown in figure 5.7, the level of control also increases with increasing initial concentration of catalyst complex, with the highest concentration facilitating the synthesis of polymers with relatively narrow molecular weight distributions and $\overline{M_n}$ values which are in close agreement with those calculated from 100% initiator efficiency ($M_{n\ theoretical}$). Moreover, a comparable effect was also observed for polymeriations conducted in DMF solution, as shown in figures 5.8 and 5.9.

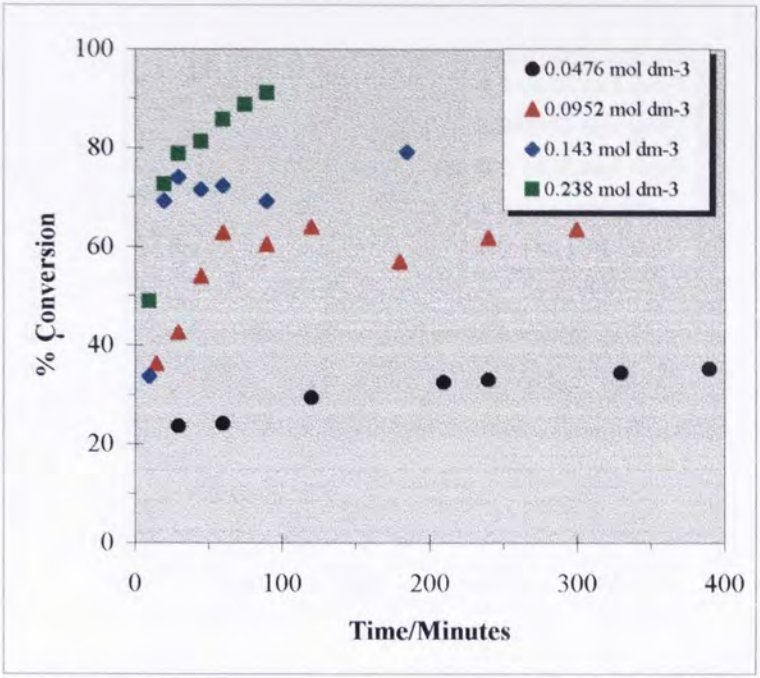

Figure 5.6. Effect of initial catalyst concentration upon the rate of monomer conversion in DMSO.

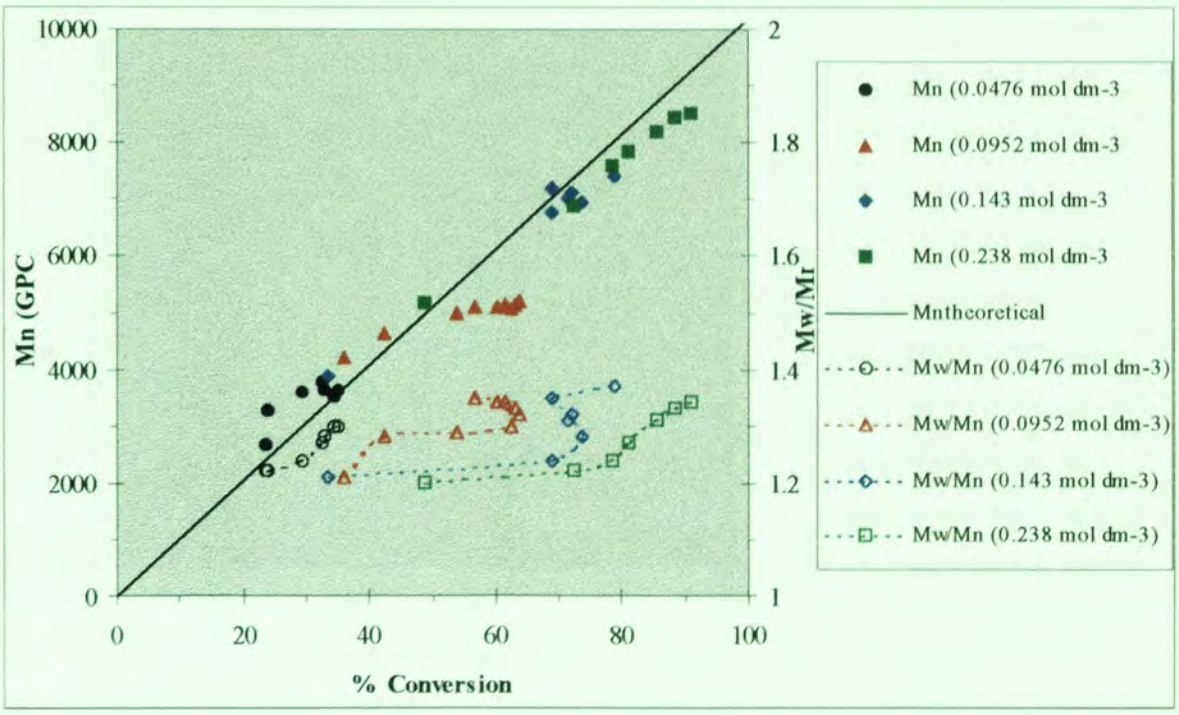

Figure 5.7. Effect of initial catalyst concentration upon the evolution of molecular weight and polydispersity with conversion in DMSO.

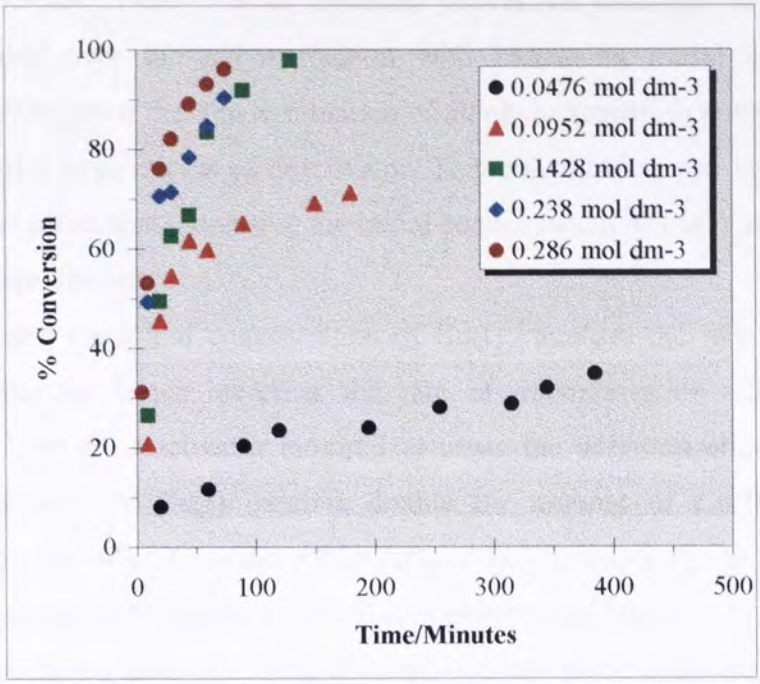

Figure 5.8. Effect of initial catalyst concentration upon the rate of monomer conversion in DMF.

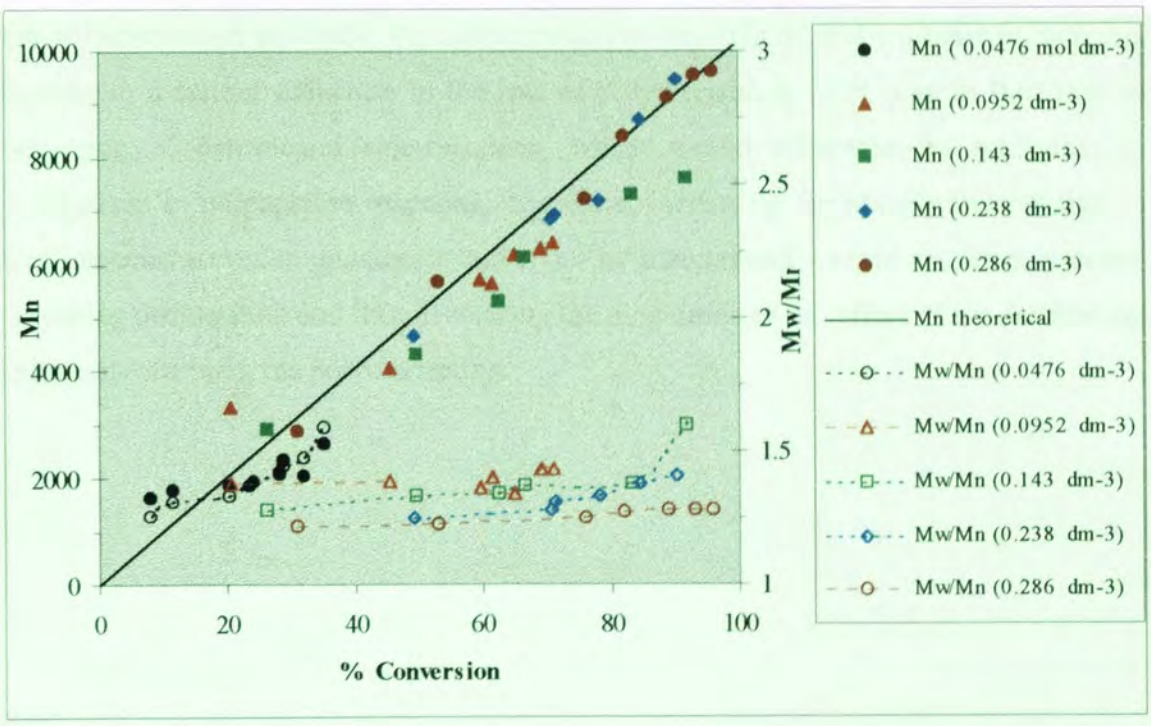

Figure 5.9. Effect of initial catalyst concentration upon the evolution of molecular weight and polydispersity with conversion in DMF.

The increase in the level of monomer conversion attainable and the degree of control afforded over the polymerisation with increasing initial concentration of catalyst, is further proof that the termination of all chain growth in polar solvents is due to formation of a large excess of deactivator. This phenomenon can be rationalised by considering the effect that increasing the initial concentration of Cu(I) activating species has upon the equilibrium.

Increasing the initial concentration of Cu(I) increases the rate of activation of dormant chains and hence increases the rate of polymerisation. However, it also increases the level of deactivator required to cease the polymerisation. Doubling the initial concentration of Cu(I) requires double the amount of Cu(II) to cease the polymerisation (i.e. 20% of 2 is more than 20% of 1). Therefore, the level of conversion achievable increases with increasing initial concentration of catalyst.

The increasing level of control afforded over the polymerisation with increasing initial concentration of Cu(I), can be viewed as a product of the maintenance of an optimal dynamic equilibrium between dormant and active species. The relatively high persistent concentration of deactivator formed ensures that the time the chain-ends spend in the active form is low, thus hindering bimolecular termination. However, as the polymerisation proceeds, the concentration of deactivator will continue to increase, leading to a further reduction in the rate of polymerisation. This may in turn lead to favouring of detrimental side-reactions, which would otherwise be negligible in comparison to propagation reactions. Therefore, increasing the initial concentration of Cu(I) species serves to counteract this effect by maintaining a rapid exchange process, favouring propagation and thus decreasing the magnitude of the effect of the detrimental side-reactions upon the polymerisation.

Chapter 6. The synthesis and polymerisation of (4-nitrophenyl)-[3-[N-[2-(methacryloyloxy)ethyl]carbazolyl]]diazene

6.1. Introduction

As previously stated, the ultimate goal of this work is to synthesise fully-functional photorefractive polymers of precisely controlled architecture. A fully-functional photorefractive polymer is one in which all functionalities required to furnish a photorefractive effect are covalently attached to the polymeric backbone. A suitable candidate monomer must therefore contain both a non-linear optical chromophore and a charge-conducting group. However, a vinyl monomer possessing both of these functionalities as separate pendant groups would be highly sterically hindered, and consequently unpolymerisable. A monomer having a bifunctional pendant group capable of fulfilling both of these requirements is thus inherently more suitable. (4-Nitrophenyl)-[3-[N-[2-(methacryloyloxy)ethyl]carbazolyl]]diazene, which possesses a pendant bifunctional charge-conducting non-linear optical chromophore, is an example of such a monomer. Hence, its synthesis and polymerisation by the developed ATRP catalyst system was investigated.

6.2. The synthesis of (4-nitrophenyl)-[3-[N-[2-(methacryloyloxy)ethyl]carbazolyl]] diazene

The synthesis of (4-nitrophenyl)-[3-[N-[2-(methacryloyloxy)ethyl]carbazolyl]] diazene (MOECarb) was achieved by the three step procedure outlined in section 2.5. The overall reaction scheme is illustrated in scheme 6.1.

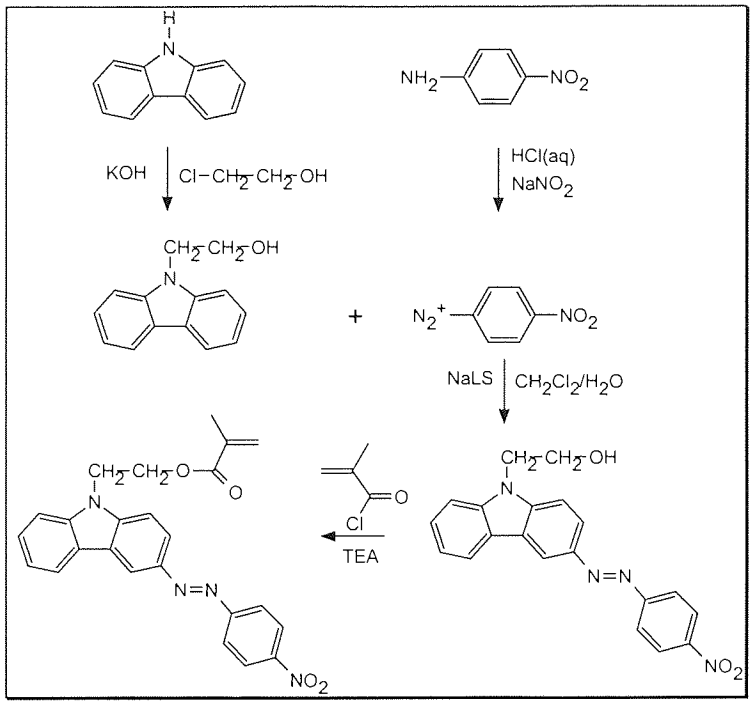

Scheme 6.1. Reaction scheme for the synthesis of MOECarb.

As illustrated, N-(2-hydroxyethyl)carbazole was obtained by the alkylation of carbazole and this subsequently coupled with 4-nitrobenzenediazonium chloride in a two phase water-dichloromethane mixture. Esterification of (4-nitrophenyl)-[3-[N-(2-hydroxyethyl)carbazolyl]]diazene with methacryloyl chloride gave the desired monomer. The results of the respective steps and the characterisation of the corresponding compounds are described in the following sections.

6.2.1. The synthesis of N-(2-hydroxyethyl)carbazole

N-(2-hydroxyethyl)carbazole was synthesised by the procedure outlined in section 2.5.1. The white, cotton wool like solid was isolated in high yield (94%) and analysed by ^{1}H N.M.R. spectroscopy. The resulting spectrum and the corresponding peak assignments are shown in figure 6.1.

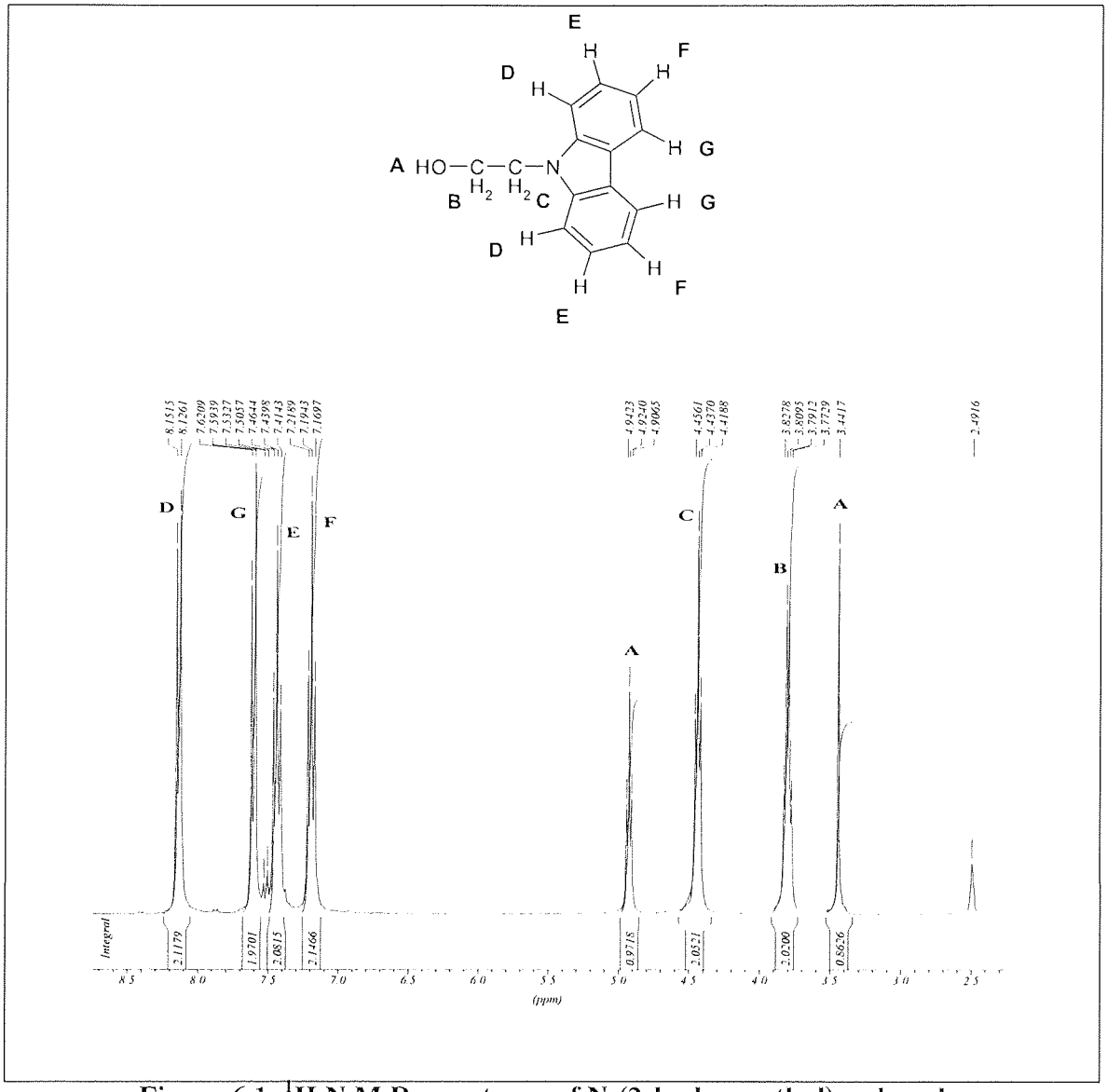

Figure 6.1. ^{1}H N.M.R. spectrum of N-(2-hydroxyethyl)carbazole.

6.2.2. The synthesis of (4-nitrophenyl)-[3-[N-(2-hydroxyethyl)carbazolyl]] diazene

(4-Nitrophenyl)-[3-[N-(2-hydroxyethyl)carbazolyl]] diazene was synthesised by the procedure described in section 2.5.2. The red powdery product (86% yield) was analysed by ^{1}H N.M.R., the spectrum for which is shown in figure 6.2. The corresponding peak assignments are also shown in figure 6.2 and although exact assignments have not been made for all of the protons, sufficient have been identified to confirm the structure of the desired product.

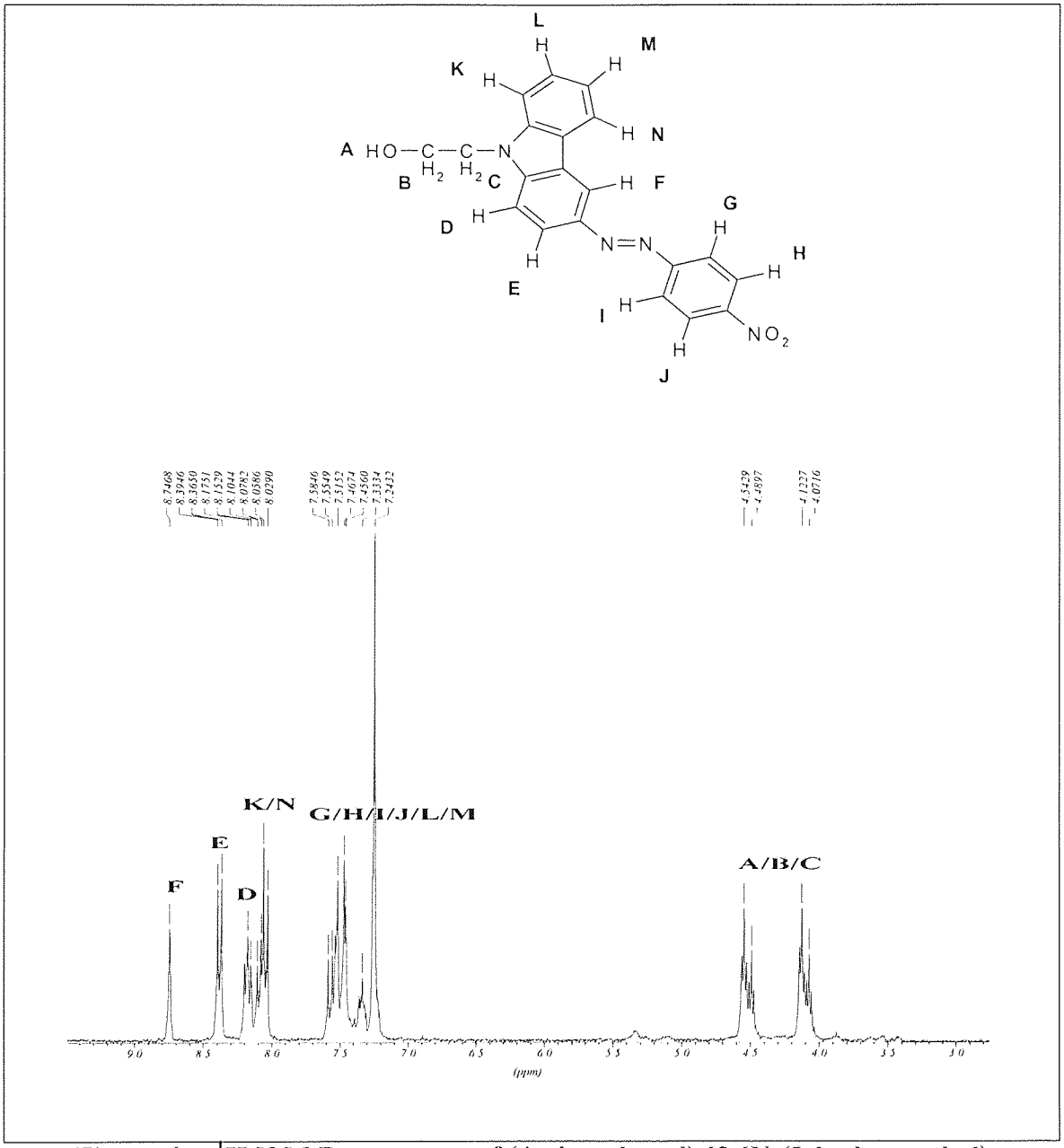

Figure 6.2. ^{1}H N.M.R. spectrum of (4-nitrophenyl)-[3-[N-(2-hydroxyethyl) carbazolyl]] diazene.

6.2.3. The synthesis of (4-nitrophenyl)-[3-[N-[2-(methacryloyloxy)ethyl] carbazolyl]]diazene

(4-nitrophenyl)-[3-[N-[2-(methacryloyloxy)ethyl]carbazolyl]]diazene was synthesised by the procedure described in section 2.5.3. The product was isolated in high yield (89%) and its structure confirmed by ^{1}H N.M.R. spectroscopy. The spectrum and the corresponding peak assignments are shown figure 6.3.

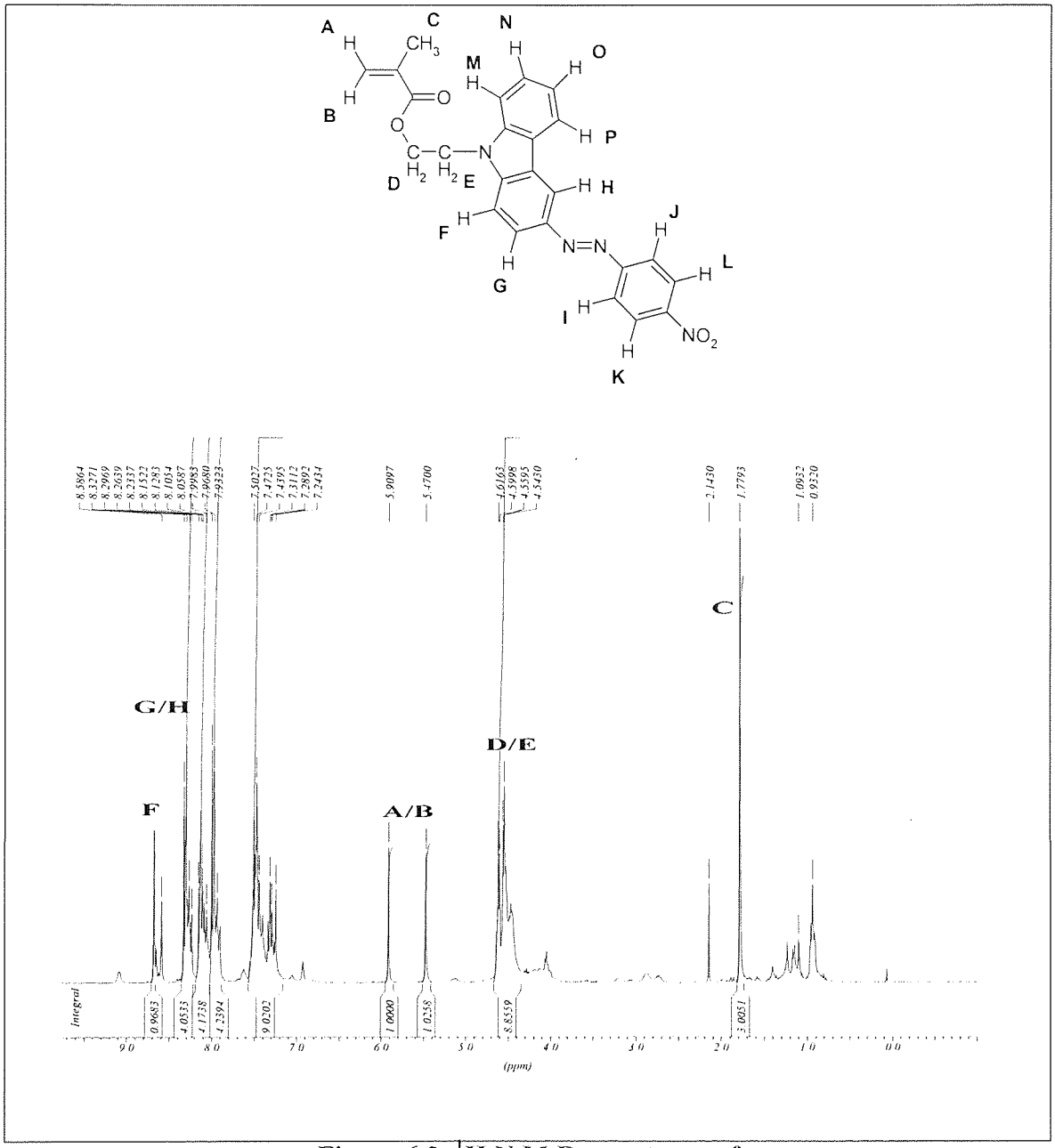

Figure 6.3. ^{1}H N.M.R. spectrum of (4-nitrophenyl)-[3-[N-[2-(methacryloyloxy)ethyl] carbazolyl]] diazene.

Although clear assignments are not given for all signals, those that have been assigned confirm the structure of the product. Moreover, determination of signals corresponding to the aromatic protons is hindered by the presence of a small quantity of unreacted starting material, with the small peak at approximately 4.0 ppm, corresponding to the CH_2-OH group of (4-nitrophenyl)-[3-[N-(2-hydroxyethyl)carbazolyl]]diazene, clearly indicating this.

6.3. Homopolymerisation of (4-nitrophenyl)-[3-[N-[2-(methacryloyloxy)ethyl] carbazolyl]]diazene

6.3.1. Free-radical polymerisation of (4-nitrophenyl)-[3-[N-[2-(methacryloyloxy)ethyl]carbazolyl]]diazene

In order to determine whether (4-nitrophenyl)-[3-[N-[2-(methacryloyloxy)ethyl] carbazolyl]]diazene will polymerise by a free-radical mechanism, a conventional free-radical polymerisation initiated by α,α'-azobisisobutyronitrile (AIBN) was conducted in DMSO solution, according to the procedure described in section 2.6.3.1, where $[MOECarb]_0 = 0.222$ mol dm^{-3}, and $[AIBN]_0 = 0.00222$ mol dm^{-3}.

The resultant red precipitate was recovered and analysed by GPC, as described in section 2.7.1. The corresponding chromatogram is shown in figure 6.4. The analysis suggested that the polymer had a number average molecular weight of 2230 g mol^{-1} and a polydispersity index of 1.54. However, due to the probable differences between the solution properties of p(MOECarb) and the polystyrene calibrants, this is not an absolute value. The actual value may therefore differ considerably from this. Regardless of this, it is evident that MOECarb can be polymerised by a free-radical mechanism.

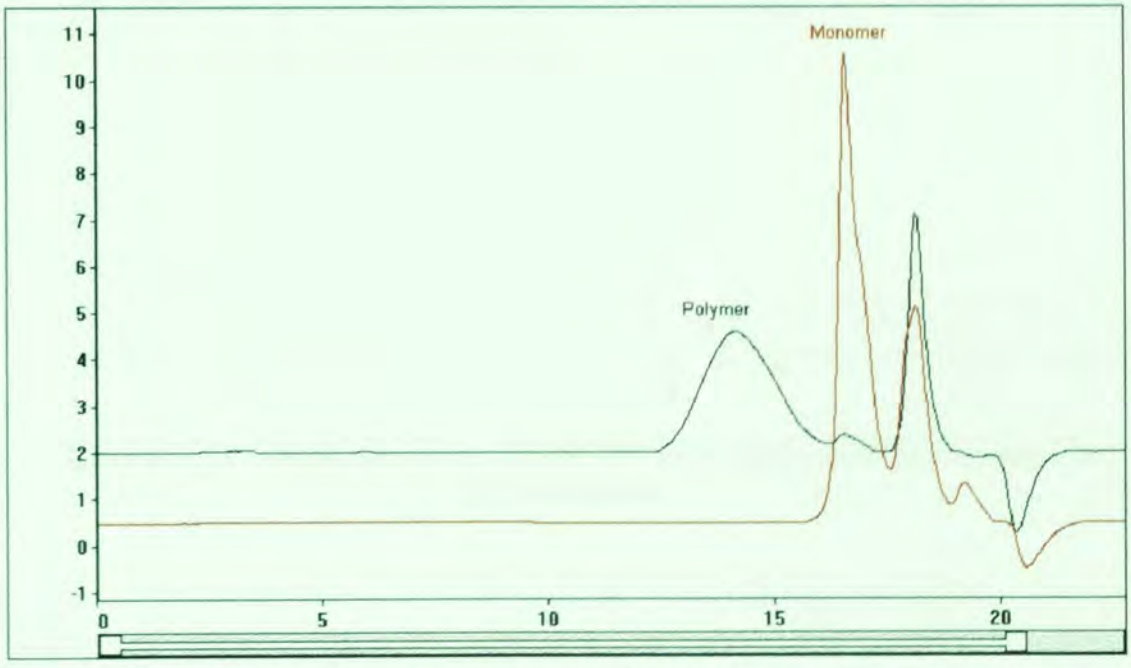

Figure 6.4. Gel permeation chromatogram of p(MOECarb) synthesised by free-radical polymerisation.

The ^{1}H N.M.R. spectrum of the polymer synthesised is shown in figure 6.5. The resolution of the spectrum is poor, owing to the limited solubility of p(MOECarb) in chloroform. However, typical resonances corresponding to the structure are still visible; aromatic protons (7-9 ppm), the NCH_2CH_2O group (3.7-4.7), the main-chain methylene protons (1.0-1.9 ppm), and the α-methyl group (0.25 ppm).

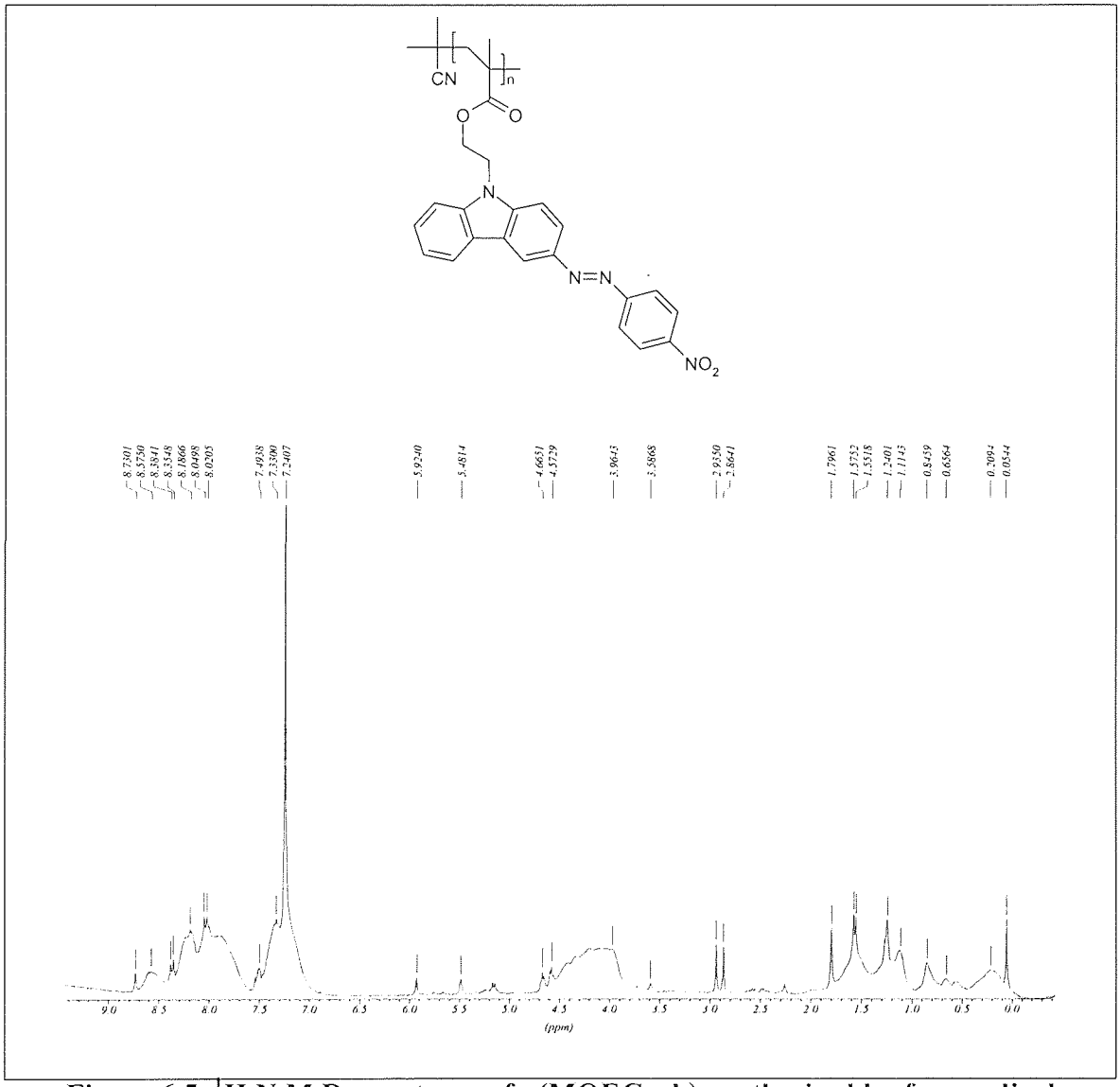

Figure 6.5. ^{1}H N.M.R. spectrum of p(MOECarb) synthesised by free-radical polymerisation.

6.3.2. ATRP of (4-nitrophenyl)-[3-[N-[2-(methacryloyloxy)ethyl]carbazolyl]] diazene

The ATRP of MOECarb was conducted in DMSO solution at 90°C, by the procedure described in section 2.6.3.2, where $[MOECarb]_0 = 0.222$ mol dm^{-3}, $[CuBr]_0 = 0.0264$ mol dm^{-3}, $[OPMI]_0 = 0.0792$ mol dm^{-3}, $[2\text{-EiBBr}]_0 = 0.0044$ mol dm^{-3}. The polymerisation was followed by periodic sampling of the reaction liquor.

Figure 6.6 shows the gel permeation chromatograms of the samples removed, as well as that of the monomer. It is evident from these results that the polymerisation was unsuccessful, with only low molecular weight polymer appearing to have been formed. Moreover, in each case it is apparent from the large peak corresponding to residual unreacted monomer, that the level of monomer conversion was low.

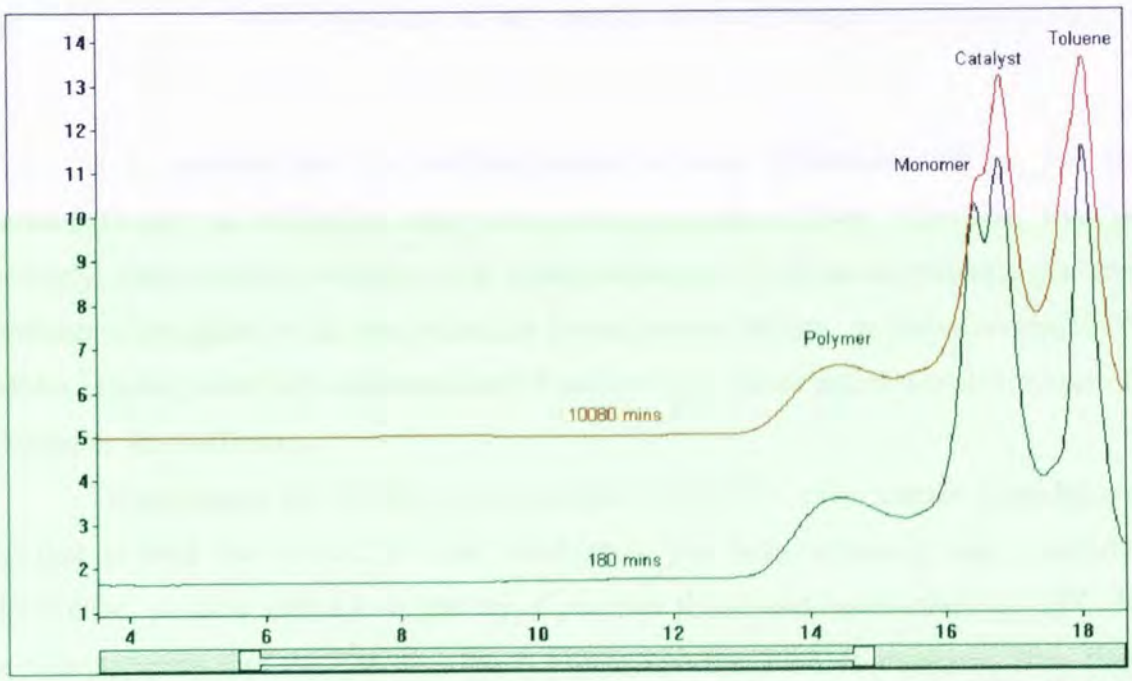

Figure 6.6. Gel permeation chromatograms of p(MOECarb) synthesised by ATRP.

An additional polymerisation was also conducted, utilising a much higher initial concentration of catalyst ($[CuBr]_0 = 0.286$ mol dm^{-3}), in an attempt to drive the polymerisation. However, as shown in figure 6.7, this did not furnish a similar effect to that observed for the polymerisation of MMA in polar solvents (section 5.6), yielding only low molecular weight chains and limited monomer conversion.

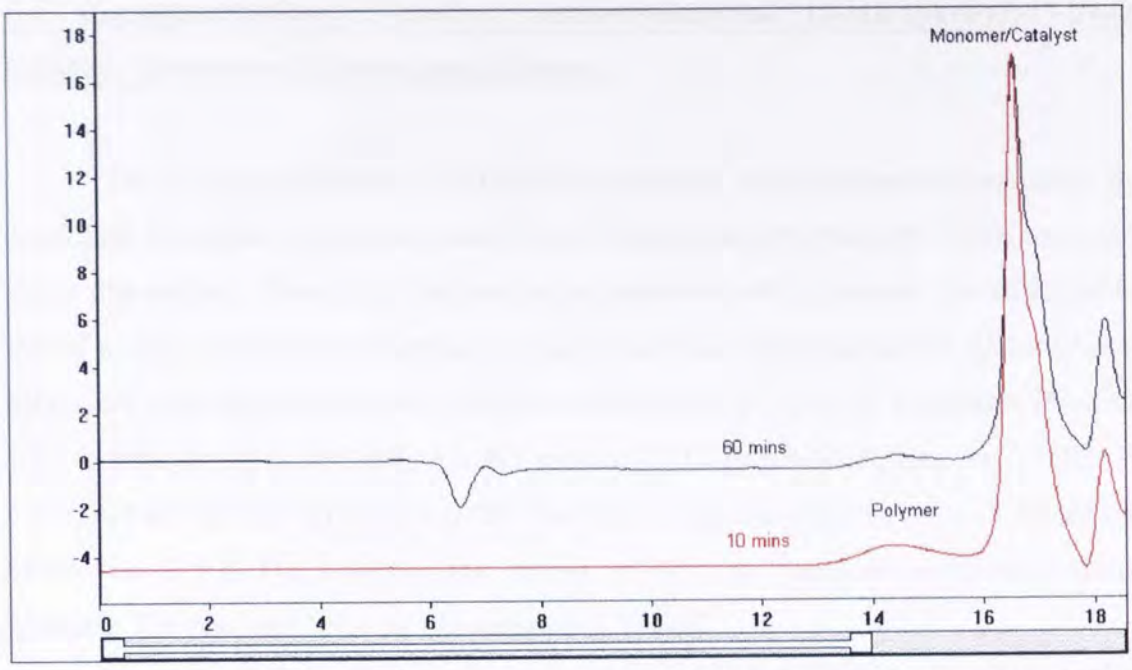

Figure 6.7. Gel permeation chromatogram of p(MOECarb) synthesised by ATRP utilising a high initial concentration of catalyst.

It is possible that the ineffectiveness of these polymerisations is due to incompatibility of MOECarb with the catalyst system utilised. However, this is unlikely, given that the initiation step appears operative. It is more probable that the problem arises from to the low monomer concentration utilised, as polymerisations of MMA utilising identical concentrations of catalyst, but much higher concentrations of monomer were effective.

To investigate this further, a polymerisation of MMA under identical conditions to that utilised for MOECarb was conducted. The polymerisation was similarly ineffective, yielding such a low quantity of polymer that it was undetectable by GPC. It is thus apparent that the use of a much higher concentration of monomer than that achievable for MOECarb is required for ATRP of methacrylic monomers in polar aprotic solvents. An exact reason for this behaviour is elusive, but it is probable that owing to the low monomer concentration, the ratio of propagation reactions to detrimental termination and side reactions is relatively low, and hence the destruction of active centres, and the consequent termination of chain growth processes, is prominent.

6.4. Copolymerisation of methyl methacrylate and (4-nitrophenyl)-[3-[N-[2-(methacryloyloxy)ethyl]carbazolyl]]diazene

The limited solubility of MOECarb precludes homopolymerisation under the conditions described, as it is not possible to increase the concentration of this monomer above that utilised. However, it is possible to raise the total monomer concentration by use of a more soluble comonomer. To this effect the copolymerisation of MMA and MOECarb was conducted by the procedure described in section 2.6.3.3, where $[MMA]_0$ = 2.749 mol dm^{-3}, $[MOECarb]_0$ = 0.161 mol dm^{-3}, $[CuBr]_0$ = 0.286 mol dm^{-3}, $[OPMI]_0$ = 0.858 mol dm^{-3} $[2\text{-EiBBr}]_0$ = 0.058 mol dm^{-3}, and the volume ratio of DMSO to MMA was 2.5:1. The solution was heated to 90°C and samples removed at timed intervals. The resultant residues were analysed by GPC.

The dependence of the number average molecular weight and polydispersity upon time is shown in table 6.1. The corresponding gel permeation chromatograms are shown in figure 6.8.

Time/Minutes	$\overline{M_n}$	$\overline{M_w}$	$\overline{M_w}/\overline{M_n}$
5	1950	2450	1.26
15	2840	3900	1.37
20	3120	4240	1.36
40	3720	5070	1.37
60	4290	6290	1.46

Table 6.1. Results of the copolymerisation of MMA and MOECarb.

It is evident from the results that the use of a higher monomer concentration, as expected, facilitates ATRP. However, it is notable that the molecular weight distributions of the final samples are relatively broad. It is possible that this may be due to the utilisation of non-optimal conditions.

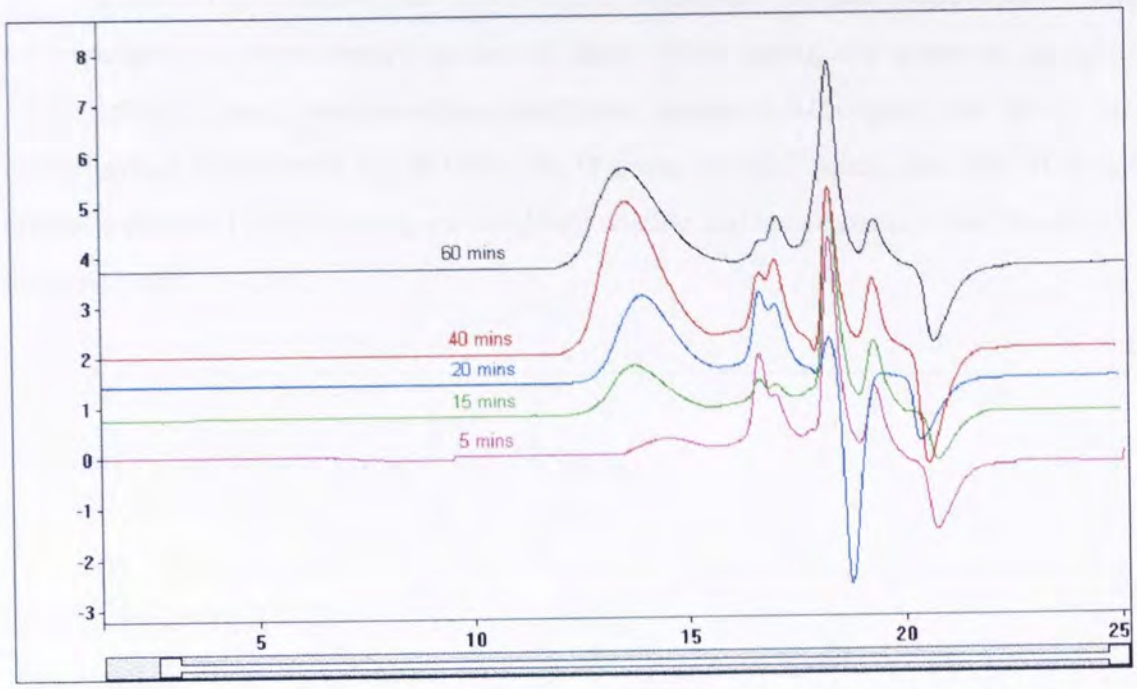

Figure 6.8. Gel permeation chromatograms of MMA/MOEcarb copolymers.

Poly(MOECarb) exhibits an intense absorption band at 428 nm, and hence the extent of MOECarb incorporation throughout the polymerisation was followed by G.P.C., using the U.V. detector. Figure 6.9 shows the resultant chromatograms, illustrating that MOECarb is incorporated steadily throughout the polymerisation.

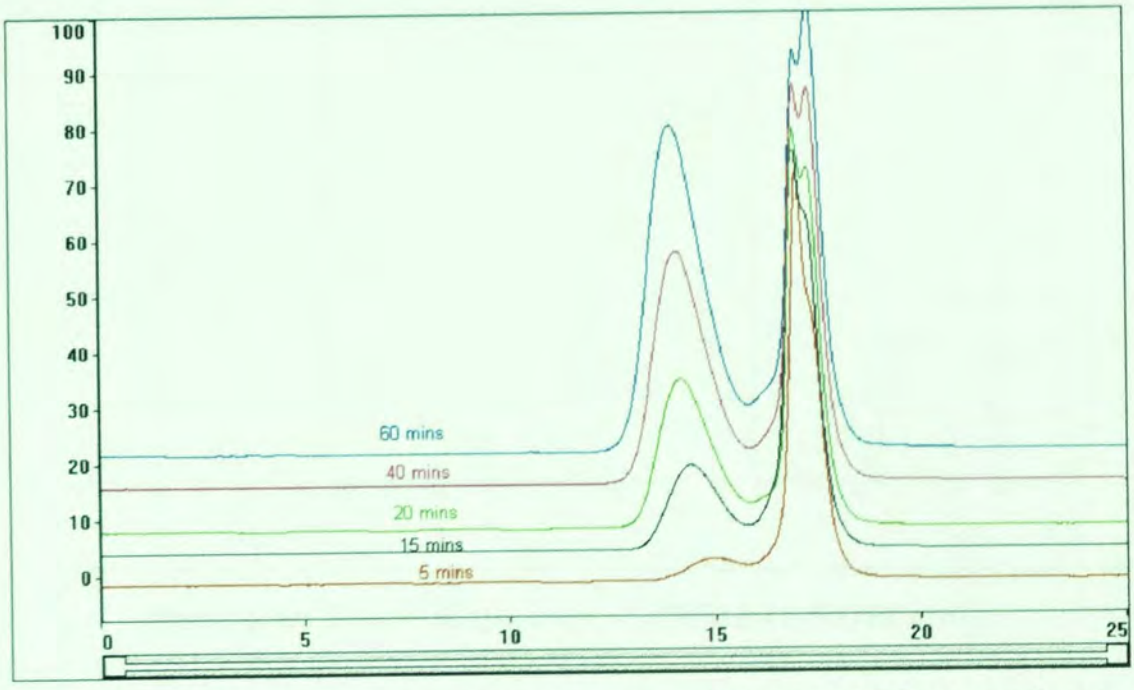

Figure 6.9. U.V. gel permeation chromatograms of MMA/MOECarb copolymer.

Figure 6.10 shows the ^{1}H N.M.R. spectrum of the copolymer. Peaks corresponding to the α-methyl group of MMA (0.05 ppm), the α-methyl group of MOECarb (0.25 ppm), the main-chain methylene groups (1.0-2.0 ppm), the MMA ester methyl group (2.59 ppm), the N-CH_2-CH_2-O group (4.0-4.7 ppm), and the MOECarb aromatic protons (7.0-9.0 ppm), are all clearly visible and hence confirm the structure of the copolymer.

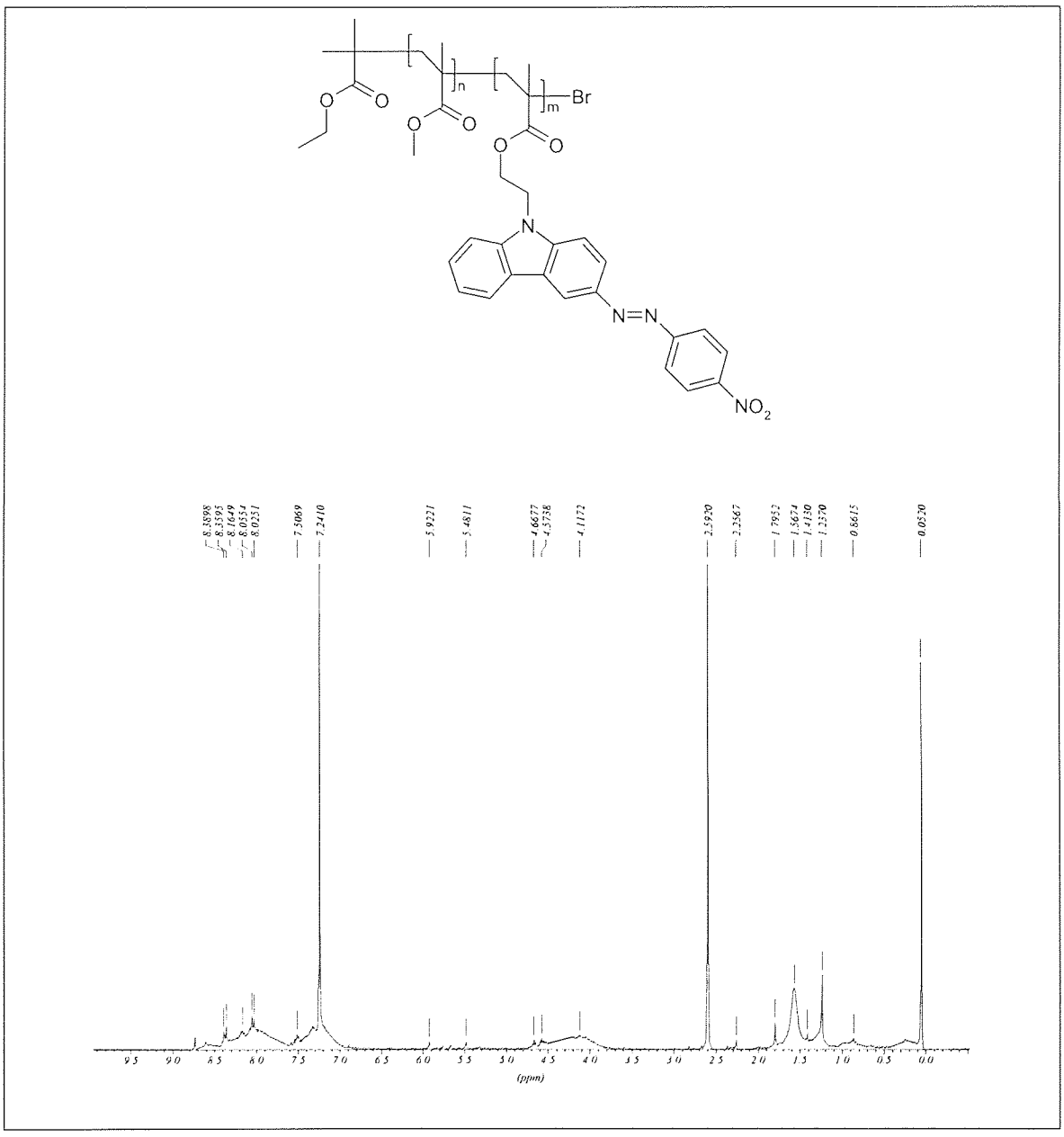

Figure 6.10. ^{1}H N.M.R. spectrum of p(MMA-co-MOECarb).

7. Conclusions and further work

7.1. Conclusions

The atom transfer radical polymerisation of styrene in xylene solution initiated with 1-PEBr and mediated by CuBr/N-propyl-2-pyridinemethanimine catalyst complex was studied. The polymerisation yielded polymers with broad molecular weight distributions (PDi > 1.5) and values of number average molecular weight that were considerably higher than the theoretical values calculated from 100% initiator efficiency. The low level of control afforded over the polymerisation is attributed to the heterogeneous nature of the CuBr/PPMI catalyst complex.

It was found that the solubility of the catalyst complex in xylene solution can be improved by extending the length of the alkyl chain on the ligand from propyl to octyl. This enabled the production of polymers of narrower molecular weight distribution (PDi < 1.25) having values of number average molecular weight close to the theoretical values. However, it is noteworthy, that increasing the solubility of the catalyst complex led to a decrease in the rate of polymerisation.

The solubility of the catalyst complex and the inherent level of control over the polymerisation of styrene was further enhanced by changing the solvent to a more polar system, diglyme, in which case polymers with PDi = 1.1 – 1.2 were produced and the catalyst system generated appeared amenable to kinetic study. Moreover, the improvement in the solubility of the catalyst complex again resulted in a decrease in the rate of polymerisation, relative to the observed rate of polymerisation in xylene solution, similar to that induced by extension of the alkyl chain on the ligand. It is probable that this phenomenon corresponds to an increase in the effective concentration of deactivating species.

The sigmoidal nature of the semilogarithmic plots for the ATRP of styrene mediated by CuBr/OPMI in xylene and diglyme solution is a result of the formation of steady-state conditions. It is perceived that during the incipient stages of the polymerisation control is evolved via the persistent radical effect, by formation of an excess of deactivator. However, this is inconsistent with the observed rate acceleration during the initial period of the polymerisation. It is thus probable that the excess

deactivator generated is converted to activating species via a process other than the assumed equilibrium. Moreover, it is evident that the rate of this reaction is dependent upon the polarity of the solvating medium, decreasing with increasing solvent polarity. Hence, it is possible to intimate that this is the principal cause of the solvent dependency of the rate of polymerisation.

The ATRP of MMA at 100°C in diglyme solution initiated with 1-PEBr and mediated by $Cu^{(I)}Br$/OPMI was inefficient, yielding polymers having broad molecular weight distributions ($1.5 < PDi < 2.0$) and values of number average molecular weight greatly in excess of the theoretical values calculated from 100% initiator efficiency. This is a direct consequence of the slow rate of initiation in comparison to the rate of propagation. This problem was circumvented by use of 2-EiBBr, which generates an initiator fragment analogous to a p(MMA) chain radical, increasing the ratio of the rate of initiation to the rate of propagation. The resultant polymers possess narrow molecular weight distributions ($PDi < 1.3$) and number average molecular weight values in agreement with the calculated values. Furthermore, the utilisation of one of the samples isolated as a macroinitiator for the polymerisation of MMA, resulted in chain-extension. Moreover, the corresponding gel permeation chromatogram (figure 4.4.) indicates that none of the macroinitiator remained unused, suggesting that the polymers possess a high degree of chain-end functionality.

Investigation of the effect of temperature upon the ATRP of MMA in diglyme solution revealed that the level of control afforded over the polymerisation is unaffected by temperature, over the range studied (100–35°C). All resultant polymers displayed narrow molecular weight distributions ($PDi < 1.3$) and values of number average molecular weight in agreement with calculated values. The rate of polymerisation decreases with decreasing temperature, as expected. The linearity of the corresponding semilogarithmic kinetic plots in each case, indicates that the concentration of propagating species was constant and low ($\approx 10^{-8}$M) throughout each polymerisation, which is consistent with controlled polymerisation.

The temperature dependence of the apparent rate constant of polymerisation of MMA in diglyme solution was found to be non-linear and distinctly unlike a typical Arrhenius plot. It is possible that this is due to a non-linear temperature dependence of the equilibrium constant, K_{eq}, where $K_{eq} = k_{act}/k_{deact}$. However, it is evident from the non-linearity of the semilogarithmic plot for polymerisation conducted in the presence

of an initial excess of deactivator (20% relative to $[Cu^{(I)}Br]_0$), that the equilibrium is more complex than initially assumed. Indeed, the magnitude of the rate acceleration observed for this experiment clearly suggests the operation of a process converting $Cu^{(II)}$ deactivating species to $Cu^{(I)}$ activating species in addition to the assumed equilibrium. Hence, the non-linear temperature dependence of the apparent rate constant of polymerisation may be manifested due to a non-linear temperature dependence of the rate constant of this process, k_c.

The temperature dependence of the apparent rate constant of polymerisation of MMA in xylene solution, initiated with 2-EiBBr and mediated by CuBr/OPMI catalyst complex, is also non-linear. However, it is of note that the observed rates of polymerisation are in excess of those corresponding to identical polymerisations conducted in diglyme solution. This is consistent with that observed for the ATRP of styrene, again illustrating the solvent dependency of the rate of polymerisation. It is suspected that this dependency arises owing to the effect of solvent polarity upon k_c, with increasing solvent polarity decreasing the rate of this reaction. Hence, the greater the polarity of the solvent, the higher the persistent concentration of deactivator and accordingly the lower the rate of polymerisation. However, it is of note that protic solvents such as water and alcohols have been reported to accelerate the rate of polymerisation. It is probable that this is manifested as a result of such compounds consuming $Cu^{(II)}$ deactivating species, or promoting their conversion to Cu(I) activating species.

The kinetic relationships between the apparent rate constant of polymerisation of MMA in diglyme solution at 90°C and the initial concentrations of catalyst, initiator and monomer were investigated. From plots of $\ln k_{app}$ versus $\ln[CuBr]_0$ and $\ln k_{app}$ versus $\ln[2\text{-EiBBr}]_0$, the rate of polymerisation was estimated to be first order with respect to the initial concentrations of catalyst and initiator respectively. The linearity of plots of $\ln([M]_0/[M]_t)$ against time, suggests that the rate of polymerisation is also first order with respect to monomer concentration.

Study of the effect of the ratio of the initial concentrations of CuBr:OPMI revealed that the kinetically optimum ratio of catalyst to ligand was 1:1. It is possible to speculate from this that the active catalytic complex is a 1:1 CuBr:OPMI complex. However, considering the evidence in combination with current reports in the literature, it is probable that the active catalyst is in fact a 1:2 CuBr/OPMI cationic complex having a $CuBr_2^-$ counteranion, which approximates to the observed phenomenon.

The role of the persistent radical effect in the establishment of steady-state conditions during the incipient stages of the ATRP of MMA was illustrated using gel permeation chromatography. It is evident from this data that the appropriate concentration of excess deactivator is generated via irreversible radical termination reactions during the initial 15 minutes of the polymerisation.

ATRP of MMA in polar aprotic solvents, such as DMF and DMSO, at 90°C utilising the same concentrations of reactants used for polymerisations in non-polar solvents, were found not to proceed beyond 40% monomer conversion. Further investigation of this phenomenon revealed that the formation of a high persistent concentration of deactivator is the basis of this problem. Moreover, it is suspected that the polar aprotic solvents utilised are the principal cause of this effect, suppressing the conversion of $Cu^{(II)}$ deactivating species to $Cu^{(I)}$ activating species. This is again consistent with the trends observed previously for the effect of solvent polarity upon the rate of this reaction.

Increasing the initial concentration of ligand, such that it was in an 8-fold excess of that conventionally utilised, was found to accelerate the rate of polymerisation of MMA and increase the level of monomer conversion achievable, in DMSO solution. It is therefore suspected that the conversion of $Cu^{(I)}$ activating species to $Cu^{(II)}$ deactivating species, by the process other than the assumed ATRP equilibrium, is mediated by the ligand. It is probable that this is owing to the preferential stabilisation of the lower oxidation state by this ligand. However, a precise mechanism for this process is unknown.

Increasing the initial concentration of catalyst complex in the ATRP of MMA conducted in polar aprotic solvents was found to increase the maximum level of monomer conversion achievable. Moreover, the inherent level of control afforded over the polymerisation was also found to increase with increasing initial catalyst concentration. Utilisation of an initial 5-fold excess of catalyst, over that conventionally used, was found to impart a high level of control over the polymerisation, comparable to that observed for polymerisations conducted in xylene or diglyme solution. It is believed that this enhancement arises as a result of the maintenance of a rapid exchange process between dormant and active species over a more substantial proportion of the polymerisation period.

A methacrylic monomer bearing a pendant bifunctional charge-conducting NLO chromophore, (4-nitrophenyl)-[3-[N-(2-methacryloyloxy)ethyl]carbazoloyl]]diazene,

was synthesised in high yield (72%), via a three stage process. This monomer was found to be susceptible to free-radical polymerisation, although only oligomeric material was produced.

ATRP of (4-nitrophenyl)-[3-[N-(2-methacryloyloxy)ethyl]carbazoloyl]]diazene in DMSO solution was ineffective, yielding only low molecular weight material and a low level of monomer conversion. It is suspected that this is owing to the low monomer concentration used, as polymerisation of MMA under identical conditions was also found to be ineffective. The low level of solubility of MOECarb in DMSO precludes any attempts to overcome this problem by increasing the concentration of this monomer. However, it was found that this problem could be circumvented by conducting a copolymerisation of this monomer with a more soluble monomer, such as MMA.

The atom transfer radical copolymerisation of MOECarb with MMA was found to proceed in a controlled manner. G.P.C using a U.V. detector at 428nm, illustrated that MOECarb was incorporated steadily throughout the polymerisation. However, the molecular weight distributions of the polymers ($1.25 < PDi < 1.50$) were notably broader than those observed for p(MMA) homopolymers synthesised under similar conditions ($1.2 < PDi < 1.3$). It is probable that this is due to utilisation of non-optimal conditions.

7.2. Further work

There are several limitations of the research conducted during the course of this project. Thus future work should address these deficiencies. In particular, the kinetics of the polymerisation require more thorough investigation, to facilitate the development of a more precise understanding of the processes and pathways involved in ATRP.

Although the observed results for the relationship between the apparent rate constant of polymerisation and the initial concentrations of monomer, initiator and catalyst are in agreement with those reported in the literature, a more in-depth study than that conducted may reveal significantly more information. A series of experiments should be conducted investigating the effect of the initial concentration of each reagent upon the polymerisation, over a wider range of concentrations than that studied.

The effect of the ratio of the initial concentration of $Cu^{(I)}Br$:OPMI upon the polymerisation should also be more thoroughly investigated. It would be particularly interesting to study the effect upon the polymerisation of MMA in diglyme solution, of raising the concentration of the ligand above that typically used.

This study has revealed some evidence suggesting the operation of a process converting $Cu^{(II)}$ deactivating species to $Cu^{(I)}$ activating species, in addition to the assumed ATRP equilibrium. This phenomenon should be studied in much greater detail, as substantial evidence concerning the mechanism of copper halide/α-diimine mediated ATRP would probably be revealed. Moreover, it is evident that the generation of a suitable persistent amount of deactivator is of paramount importance for the evolution of control over the polymerisation. Hence, a more precise understanding of the dynamics of the equilibria involved would allow optimisation of the appropriate reaction variables.

The effect of the initial concentration of deactivator upon the rate of polymerisation should be studied. This data could be used in conjunction with the corresponding GPC data from the incipient period of polymerisation for the series of experiments, to determine the persistent level of deactivator required to control the polymerisation of a given monomer. When the concentration of deactivator is sufficient to afford a high level of control from the initiation of polymerisation, avoiding in situ generation of deactivator by the persistent radical effect (i.e. near 100% initiator efficiency), only a single peak should appear on the gel permeation chromatograms throughout the course of the polymerisation, unless the resolution of the GPC apparatus is extraordinarily high.

The temperature dependence of the rate of conversion of $Cu^{(II)}$ to $Cu^{(I)}$ species by the process outside of the confines of the assumed ATRP equilibrium could be studied by UV spectroscopy, as these species have distinctly different absorption bands. This would allow clarification of the effect of temperature dependency of this phenomenon upon the temperature dependency of the apparent rate of polymerisation.

The effect of additives upon the rate of this process, as well as the rate of polymerisation, should also be investigated. Particular attention should be paid to protic compounds, such as alcohols and water. It may also prove interesting to determine whether such additives can be utilised to promote polymerisation in aprotic solvents.

This knowledge could then be used to optimise the conditions of polymerisation for monomers such as MOECarb.

References

1. **Gunter, P; Huignard, J. P.;** Eds. *"Photorefractive materials and their applications."*; Volumes 1 and 2, Springer-Verlag: Berlin, (1988).

2. **Yu, L.; Chan, W. K.;Peng, Z.; Gharavi, A.;** *"Multifunctional polymers exhibiting photorefractive effects."*, Acc. Chem. Res., 29, 13, (1996).

3. **Kipelen, B.; Merrholz, K.; Sandalphon; Volodin, B. L.; Peyghambarian, N.;** *"Photorefractive polymers and their applications."*, Molecular crystals and liquid crystals science and technology, section A-molecular crystals and liquid crystals, 283, 109, (1996)

4. **Halvorson, C.; Kraabel, B.; Heeger, A. J.; Volodin, B. L.; Meerholz, K.; Sandalphon; Peyghambarian, N.;** *"Optical computing by use of photorefractive polymers."*, Optics letters, 20, 1, 76, (1995).

5. **Kippelen, B.; Marder, S. R.; Hendrickx, E.; Maldonado, J. L.; Guillemet, G.;** *"Infrared photorefractive polymers and their applications for imaging."*, Science, 279, 5347, 54, (1998).

6. **Steele, D. D.; Volodin, B. L.; Savina, O.; Kippelen, B.; Peyghambarian, N.;** *"Transillumination imaging through scattering media by use of photorefractive polymers."*, Optics Letters, 23, 3, 153, (1998).

7. **Ashkin, A.; Boyd, G. D.; Dziedzic, J. M.; Smith, R. G.; Ballmann, A. A.; Nassau, K.;** *"Optically induced refractive index inhomogeneities in $LiNbO_3$ and $LiTaO_3$."*, Appl. Physics Lett., 9, 1, 72-74, (1966).

8. **Chen, F. S.;** *"A laser-induced inhomogeneity of refractive indices in KTN."*, J. Appl. Phys., 38, 3418-3420, (1967).

9. **Ducharme, S.; Scott, J. C.; Twieg, R. J.; Moerner, W. E.;** *"Observation of the photorefractive effect in a polymer."*, Phys. Rev. Letts., 66, 14, 1846-1849, (1991).

10. **Ducharme, S.; Jones, B.; Takacs, J. M.; Zhang, L.;** *"Electric-field stabilisation and competition of gratings in a photorefractive polymer."*, Opt. Letts., 18, 2, 152-154, (1993).

11. **Silence, S. M.; Walsh, C. A.; Scott, J. C.; Moerner, W. E.;** *"C_{60} sensitisation of a photorefractive polymer."*, Appl. Phys. Lett., 61, 25, 2967-2969, (1992).

12. **Silence, S. M.; Scott, J. C.; Hache, F.; Ginsburg, E. J.; Jenkner, P. K.; Miller, R. D.; Twieg, R. J.; Moerner, W. E.;** *"Poly(silane)-based high-mobility photorefractive polymers."*, J. Opt. Soc. Am. B – Opt. Phys., 10, 12, 2306-2312, (1993).

13. **Silence, S. M.; Donckers, M. C. J.; Walsh, C. A.; Burland, D. M.; Twieg, R. J.; Moerner, W. E.;** *"Optical-properties of poly(N-vinyl carbazole)-based guest-host photorefractive polymer systems."*, Appl. Opt., 33, 11, 2218-2222, (1994).

14. **Moerner, W. E.; Silemce, S. M.; Hache, F.; Bjorklund, G. C.;** *"Orientationally enhanced photorefractive effect in polymers."*, J. Opt. Soc. Am. B – Opt. Phys., 11, 2, 320-330, (1994).

15 **Bolink, H. J.; Krasnikov, V. V.; Malliaras, G. G.; Hadziioannou, J.;** *"Effect of plasticisation on the performance of a photorefractive polymer."*, J. Phys. Chem. 100, 40, 16356-16360, (1996).

16 **Bittner, R.; Daubler, T. K.; Neher, D.; Meerholz, K.;** *"Influence of glass-transition temperature and chromophore content on the steady-state performance of poly(N-vinylcarbazole)-based photorefractive polymers."*, Adv. Mater., 11, 2, 123-127, (1999).

17 **Meerholz, K.; Volodin, B. L.; Sandalphon; Kippelen, B.; Peyghambarian, N.;** *"A photorefractive polymer with high-optical gain and diffraction efficiency near 100%."*, Nature, 371, 6497, 497-500, (1994).

18 **Volodin, B. L.; Kippelen, B.; Meerholz, K.; Javidid, B.; Peyghambarian, N.;** *"A polymeric optical pattern-recognition system for security verification."*, Nature, 383, 6595, 58-60, (1996).

19 **Zobel, O.; Eckl, M.; Strohriegl, P.; Haarer, D.;** *"A polysiloxane-based photorefractive polymer with high optical gain and diffraction efficiency."*, Adv. Mater., 7, 11, 911, (1995).

20. **Poga, C. Lundquist, P. M.; Lee, V.; Shelby, R. M.; Twieg, R. J.;Burland, D. M.;** *"Polysiloxane-based photorefractive polymers for digital holographic data storage."*, Appl. Phys. Lett., 69, 8, 1047-1049, (1996).

21. **Hendrickx, E.; Volodin, B. L.; Steele, D. D.; Maldonado, J. L.; Wang, J. F.; Kippelen, B.; Peyghambarian, N.;** *"Phase stability of guest/host photorefractive polymers studied by light scattering experiments."*, Appl. Phys. Lett, 71, 9, 1159-1161, (1997).

22. **Grunnet-Jepsen, A.; Thompson, C. L.; Twieg, R. J.; Moerner, W. E.;** *"High performance photorefractive polymer with improved stability."*, Appl. Phys. Lett., 70, 12, 1515-1517, (1997).

23. **Yu, L. Chan, W.; Bao, Z.;** *"Photorefractive polymers. 2. Structure design and property characterisation."*, Macromolecules, 26, 9, 2216-2221, (1993).

24. **Chan, W. K.; Chen, Y.; Peng, Z.; Yu, L.;** *"Rational designs of multifunctional polymers."*, J. Am. Chem. Soc., 115, 11735-11743, (1993).

25. **Chen, Y. M.; Peng, Z. H.; Chan, W. K.; Yu, L. P.;** *"New photorefractive polymer based on multifunctional polyurethane."*, Appl. Phys. Lett., 64, 10, 11951197, (1994).

26. **Zhang, Y.; Wada, T.; Wang, L.; Aoyama, T.; Sasbe, H.;** *"Photorefractive polymers containing a single multifunctional chromophore."*, Chem. Commun., 2325-2326, (1996).

27. **Peng, Z. H.; Gharavi, A.; Yu, L. P.;** *"Hybridised approach to new polymers exhibiting large photorefractivity."*, Appl. Phys. Lett., 69, 26, 4002-4004, (1996).

28. **Peng, Z. H.; Gharavi, A.; Yu, L. P.;** *"Synthesis and characterisation of photorefractive polymers containing transition metal complexes as photosensitiser."*, J. Am. Chem. Soc., 119, 20, 4622-4632, (1997).

29. **Wang, Q.; Wang, L.; Yu, L. P.;** *"Synthesis and unusual physical behaviour of a photorefractive polymer containing tris(bipyridyl)ruthenium(II) complexes as a photosensitiser and exhibiting a low glass-transition temperature."*, J. Am. Chem. Soc., 120, 49, 12860-12868, (1998).

30. **Ho, M. S.; Barrett, C.; Paterson, J.; Esteghamatian, M.; Natasohn, A.; Rochon, P.;** *"Synthesis and optical properties of poly{(4-nitrophenyl)-[3-[N-[2-(methacryloyloxy)ethyl]carbazolyl]]diazene}."*, Macromolecules, 29, 4613-4618, (1996).

31. **Carothers, W. H.;** *"Studies on polymerisation and ring formation. I. An introduction to the general theory of condensation polymers."*; J. Am. Chem. Soc., 51, 2548-2559, (1929).

32. **Allen, G.; Bevington, J. C.;** Eds, *"Comprehensive Polymer Science"*, Vols. 3 and 4, Pergamon Press, Oxford, (1989).

33. **Bywater, S.;** *"Anionic polymerisation."*, Encyclopedia of Polymer Science and Engineering 2nd edition, 2, 1-43, John Wiley and Sons, New York, (1985).

34. **Cheradame, H.; Gandini, A.;** *"Cationic polymerisation."* Encyclopedia of Polymer Science and Engineering 2nd edition, 2, 729-814. John Wiley and Sons, New York, (1985).

35. **Danusso, F.; and Natta, G.;** *"Stereoregular polymers and stereospecific polymerisation."*, Pergamon Press, Oxford, (1967).

36. **Ivin, K. J.;** *"Metathesis polymerisation."*, Encyclopedia of Polymer Science and Engineering 2nd edition, 9, 634-668. John Wiley and Sons, New York, (1985).

37. **Farnham, W. B.; Hertler, W. R.; Rajanbabu, T. V.; Sogah, D. Y.; Webster, O. W.;** *"Group-transfer polymerisation. 1. A new concept for addition polymerisation with organosilicone initiators."*, J. Am. Chem. Soc., 105, 5706-5708, (1983).

38. **Cutler, D. J.; Hendra, P. J.; Cudby, M. E. A.; Willis, H. A.;** *"Chain branching in high pressure polymerised polyethylene."*; Polymer, 18, 1005-10008, (1977).

39. **Cowie, J. M. G.;** *"Polymers: Chemistry and physics of modern materials."*, 3, 66, 2nd Edition, Blackie academic and professional, Glasgow, (1991).

40. For a comprehensive review see: **Colombani, D.; Chaumont, P.;** *"Addition-fragmentation processes in free-radical polymerisation."*, Prog. Polym. Sci., 21, 439-503 , (1996).

41. **Bevington, J. C.;** in *"Comprehensive Polymer Science"*, 3, 6, 78-80; Eds. Allen, G.; Bevington, J. C.; Pergamon Press, Oxford, (1989).

42. **Peebles, L. H. Jr.;** *"Molecular weight distributions in polymers."*, J. Am. Chem. Soc., 62, 1561, (1940).

43. **Szwarc, M.;** *"Living polymers."*, Nature, 178, 1168, (1956).

44. **Szwarc, M.;** *"Living polymers and mechanisms of anionic polymerisation."*, Adv. Polym. Sci., 49, 1-187, (1983).

45. **Kroner, H.; Ingrisch, S.; Nuyken, O.; Oh, S.; Riess, G.;** *"Recent developments in living cationic polymerisation."*, Macromol. Symp., 101, 29-42, (1996).

46. **Webster, O. W.;** *"Group transfer polymerisation."*, Encyclopedia of Polymer Science and Engineering 2nd edition, 7, 580-588, John Wiley and sons, New York, (1987).

47. **Bianchi, J. P.; price, F. P.; Zimm, B. H.;** " *"Monodisperse" polystyrene."*, J. Polym. Sci., 25, 27, (1957).

48. **Farina, M.; Silvestro, G. D.; J.;** *"Stereoregular block copolymers obtained by a radical process in inclusion compounds."*, Chem. Soc., Chem. Commun., 842, (1976).

49. **Yatsu, T.; Ohno, T.; Maki, H.; Fujii, H.;** *"Polymerisation of ethylene by trialkylaluminium-Lewis base-peroxide catalyst."*, Macromolecules, 10, 243-248, (1977).

50. **Kabanov, V.;** *"Living chain radical polymerisation and micro-association phenomena in homogeneous polymerisation systems."*, J. Polym. Sci., Polym. Symp., 50, 71 (1975).

51. **Otsu, T.; Yoshida, M.;** *"Role of initiator-transfer agent-terminator (iniferter) in radical polymerisations: Polymer design by organic disulfides as iniferters."*, Makromol. Chem., Rapid Commun. 3, 127-132, (1982).

52. **Otsu, T.; Yoshida, M.; Tazaki, T.;** *"A model for living radical polymerisation."*, Makromol. Chem., Rapid Commun. 3, 133-140, (1982).

53. **Chang, V. S. C.; Ivan, B.; Kennedy, J. P.; Smith, R. A.;** *"New telechelic polymers and sequential co-polymers by polyfunctional initiation-transfer agents (inifers). V. Synthesis and characterisation of α-tert-butyl-ω-isopropenylpolyisobutylene and α,ω-di(isopropenyl)polyisobutene."*, Polym. Bull.; 1. 575-580, (1979).

54. **Bledzki, A.; Braun, D.; Titzschkau, K.;** *"Polymerisationsauslosung mit substituierten ethanen, 5. Polymerisation von verschiedenen methacrylmonomeren."* Makromol. Chem. 184, 287-294, (1983).

55. **Otsu, T.; Kuryama, A.;** *"Living radical polymerisation through the use of iniferters: Controlled synthesis of polymers."*; Eur. Polym. J., 25, 643, (1984).

56. **Endo, K.; Murata, K.; Otsu, T.;** "Living radical polymerisation of styrene with tetramethylene disulfide.", Macromolecules, 25, 5554-5556, (1992).

57. **Fischer, H.;** *"The persistent radical effect in "living" radical polymerisation."*, Macromolecules, 30, 5666-5672, (1997).

58. **Kothe, T.; Marque, S.; Martscke, R.; Popov, M.; Fischer, H.;** *"Radical reaction kinetics during homolysis of N-alkoxyamines: verification of the persistent radical effect."*, J. Chem. Soc., Perkin Trans., 2, 1553-1559, (1998).

59. **Fischer, H.;** *"The persistent radical effect in controlled radical polymerisation."*, J. Polym. Sci., A, Polym. Chem., 37, 1885-1901, (1999).

60. For a comprehensive review see: **Gridnev, A.;** *"The 25th anniversary of catalytic chain transfer."*, J. Polym. Sci. A: Polym. Chem., 38, 1753-1766, (2000).

61. **Heuts, J. P. A.; Forster, D. J.; Davis, T. P.;** *"Reversible cobalt-carbon bond formation in catalytic chain transfer polymerisation."*, Macromolecules, 32, 2511-2519, (1999).

62. **Solomon, D. H.; Rizzardo, E.; Cacioli, P.;** U.S. Patent 4,581,429.

63. **Rizzardo, E.;** Chem. Aust., 54, 32, (1987).

64. **Georges, M. K.; Veregin, R. P. N.; Kazmaier, P. K.; Hamer, G. K.;** "Narrow molecular weight resins by a free-radical polymerisation process.", Macromolecules, 26, 2987-2988, (1993).

65. **Georges, M. K.; Veregin, R. P. N.; Kazmaier, P. K.; Hamer, G. K.;** *"Taming the free-radical polymerisation process."*, TRIP 2, 2, (1994).

66. **Veregin, R. P. N.; Georges, G. K.; Kazmaier, P. M.; Hamer, G. K.;** *"Free-radical polymerisations for narrow polydispersity resins: Electron spin resonance studies of the kinetics and mechanism."*, Macromolecules, 26, 5316-5320, (1993).

67. **Veregin, R. P. N.; Georges, G. K.; Kazmaier, P. M.; Hamer, G. K.;** *"Mechanism of living free-radical polymerisations with narrow polydispersity: Electron spin resonance and kinetic studies."*, Macromolecules, 28, 4391-4398, (1995).

68. **Veregin, R. P. N.; Odell, P. G.; Michalak, L. M.; Georges, G. K.;** *"The pivotal role of excess nitroxide radical in living free-radical polymerisations with narrow polydispersity."*, Macromolecules, 29, 2746-2754, (1996).

69. **Greszta, D.; Matyjaszewski, K.;** *"Living radical polymerisation: kinetic results – comments."*, Macromolecules, 29, 15, 5239 – 5240, (1996).

70. **Fukuda, T.; Terauchi, T.;** *"Mechanism of "living" radical polymerisation mediated by stable nitroxyl radicals."*, Chemistry Letters, 4, 293-294, (1996).

71. **Davenport, W.; Michalak, L.; Malmstrom, E.; Mate, M.; Kurdi, B.; Hawker, C. J.; Barclay, G. G.; Sinta, R.;** *" "Living" free-radical polymerisations in the absence of initiators: controlled autopolymerisation."*, Macromolecules, 30, 7, 1929-1934, (1997).

72. **Buzanowski, W. C.; Graham, J. D.; Priddy, D. B.; Shero, E.;** *"Spontaneous polymerisation of styrene in the presence of acid: further confirmation of the Mayo mechanism."*, Polymer, 33, 14, 3055, (1992).

73. **Georges, G. K.; Veregin, R. P. N.; Kazmaier, P. M.; Hamer, G. K; Saban, M.;** *"Narrow polydispersity polystyrene by a free-radical polymerisation process - rate enhancement."*, Macromolecules, 27, 7228-7229, (1994).

74. **Odell, P. G.; Veregin, R. P. N.; Michalak, L. M.; Brousmiche, D.; Georges, M. K.;** *"Rate enhancement of living free-radical polymerisations by an organic acid salt."*, Macromolecules, 28, 8453-8455, (1995).

75. **Veregin, R. P. N.; Odell, P. G.; Michalak, L. M.; Georges, M. K.;** *"Mechanism of rate enhancement using organic acids in nitroxide-mediated living free-radical polymerisations."*, Macromolecules, 29, 4161-4163, (1996).

76. **Moad, G.; Rizzardo, E.;** *"Alkoxyamine-initiated living radical polymerisation: Factors affecting alkoxyamine homolysis rates."*, Macromolecules, 28, 8722-8728, (1995).

77. **Grimaldi, S.; Finet, J.-P.; Zeghdaoui, a.; Tordo, P.; Benoit, D.; Gnannou, Y.; Fontamille, M.; Nicol, P.; Pierson, J.-F.;** *"Synthesis and applications to "living" free-radical polymerisation of a new class of nitroxyl radicals."*, Am. Chem. Soc., Polym. Div., Polym. Prepr., 38, 651-652, (1997).

78. **Yamada, B.; Miura, Y.; Nobukane, Y.; Aota, M.;** *"Styrene polymerisation by five-membered cyclic nitroxides."*, Am. Chem. Soc., Polym. Div., Polym. Prepr., 38, 725-726, (1997).

79. **Benoit, D.; Grimaldi, S.; Finet, J. P.; Tordo, P.; Fontanille, M.; Gnanou, Y.;** *"Controlled free-radical polymerisation in the presence of a novel asymetric nitroxyl radical."*, Am. Chem. Soc., Polym. Div., Polym. Prepr., 38, 729-730, (1997).

80. **Moroni, M.; Hilberer, A.; Hadziioannou, G.;** *"Synthesis of a functional polymer with pendent luminescent phenylenevinylene units through nitroxide-mediated free-radical polymerization."*, Macromol. Rapid Commun., 17, 693-702, (1996).

81. **Gabaston, L. I.; Armes, S. P.; Jackson, R. A.;** *"Synthesis of water soluble homopolymers and block copolymers by living free-radical polymerisation."*, Am. Chem. Soc., Polym. Div., Polym. Prepr., 38, 719-720, (1997).

82. **Benoit, D.; Chaplinski, V.; Braslau, R.; Hawker, C. J.;** *"Development of a universal alkoxyamine for "living" free-radical polymerisations."*, J. Am. Chem. Soc., 121, 3904-3920, (1999).

83. **Chiefari, J.; Chong, Y. K.; Ercole, F.; Krstina, J.; Jeffery, J.; Le, T. P. T.; Mayadunne, R. T. A.; Meijs, G. F.; Moad, C. L.; Moad, G.; Rizzardo, E.; Thang, S. H.;** *"Living free-radical polymerisation by reversible addition-fragmentation chain transfer: The RAFT process."*, Macromolecules, 31, 5559-5562, (1998).

84. **Mayadunne, R. T. A.; Rizzardo, E.; Chiefari, J.; Chong, Y. K.; Moad, G.; Thang, S. H.;** *"Living radical polymerisation with reversible addition-fragmentation chain transfer (RAFT polymerisation) using dithiocarbamates as chain transfer agents."*, Macromolecules, 32, 6977-6980, (1999).

85. **Hadad, C. H.; Rablen, P. R.; Wilberg, K. B.;** *"C-O and C-S bonds: Stability, bond dissociation energies and resonance stabilistaion."*, J. Org. Chem., 63, 8668-8681, (1998).

86. **Chong, Y. K.; Le, T. P. T.; Moad, G.; Rizardo, E.; Thang, S. H.;** *"A more versatile route to block copolymers and other polymers of complex architecture by living radical polymerisation: The RAFT process."*, Macromolecules, 32, 2071-2074, (1999).

87. **Curran, D. P.;** *"Comprehensive Organic Synthesis."*, 4, 715 and 779, Pergamon press, Oxford, , (1991).

88. For a comprehensive review see: **Matyjaszewski, K.;** *"New (co)polymers by atom transfer radical polymerisation."*, Macromol. Symp., 143, 257-268, (1999).

89. **Kato, M.; Kamigaito, M.; Sawomoto, M.; Higashimura, T.;** *"Polymerisation of methyl methacrylate with the carbon tetrachloride/dichlorotris(triphenylphospine) ruthenium(II)/methylaluminiumbis(2,6-tert-butylphenoxide) initiating system: Possibility of living radical polymerisation."*, Macromolecules, 28, 1721-1723, (1995).

90. **Kotani, Y.; Kato, M.; Kamigaito, M.; Sawamoto, M.;** *"Living radical polymerisation of alkyl methacrylates with ruthenium complex and their block copolymers."*, Macromolecules, 29, 6979-6982, (1996).

91. **Nishikawa, T.; Kamigaito, M.; Sawamoto, M.;** *"Living radical polymerisation in water and alcohols: suspension polymerisation of methyl methacrylate with $RuCl_2(PPh_3)_3$ complex."*, Macromolecules, 32, 2204-2209, (1999).

92. **Takahashi, H.; Ando, T.; Kamigaito, M.; Sawomoto, M.;** *"$RuH_2(PPh_3)_4$: an active catalyst for living radical polymerisation of methyl methacrylate at or above room temperature."*, Macromolecules, 32, 6461-6465, (1999).

93. **Matyjaszewski, K.; Wei, M. L.; Xia, J. H.; Mcdermott, N. E.;** *"Controlled/"living" radical polymerisation of styrene and methyl methacrylate catalysed by iron complexes."*, Macromolecules, 30, 26, 8161-8164, (1997).

94. **Kotani, Y.; Kamagaito, M.; Sawamoto, M.;** *"$FeCp(CO)_2I$: A phosphine-free half-metallocene-type Iron(II) catalyst for living radical polymerisation of styrene."*, Macromolecules, 32, 6877-6880, (1999).

95. **Granel, C.; Dubois, P.; Jerome, R.; Teyssie, P.;** *"Controlled radical polymerisation of methacrylic monomers in the presence of a bis(ortho-chelated) arylnickel(II) complex and different activated alkyl halides."*, Macromolecules, 29, 8576-8582, (1996).

96. **Moineau, G.; Minet, M.; Dubois, P.; Teyssie, P.; Senninger, T.; Jerome, R.;** *"Controlled radical polymerisation of (meth)acrylates by ATRP with $NiBr_2(PPh_3)_2$ as catalyst."*, Macromolecules, 32, 27-35, (1999).

97. **Uegaki, H.; Kotani, Y.; Kamagaito, M.; Sawamoto, M.;** *"$NiBr_2(Pn\text{-}Bu_3)_2$-mediated living radical polymerisation of methacrylates and acrylates and their block and random copolymers."*, Macromolecules, 31, 6756-6761, (1998).

98. **Lecomte, P.; Drapier, I.; Dubois, P.; Teyssie, P.; Jerome, R.;** *"Controlled radical polymerisation of methyl methacrylate in the presence of palladium acetate, triphenylphosphine and carbon tetrachloride."*, Macromolecules, 30, 7631-7633, (1997).

99. **Moineau, G.; Granel, C.; Dubois, P.; Jerome, R.; Teyssie, P.;** *"Controlled radical polymerisation of methyl methacrylate initiated by an alkyl halide in the presence of the Wilkinson catalyst."*, Macromolecules, 31, 542-544, (1998).

100. **Kotani, Y.; Kamagaito, M.; Sawamoto, M.;** *"Re(V)-mediated living radical polymerisation of styrene: $ReO_2I(PPh_3)_2$/R-I initiating system."*, Macromolecules, 32, 2420-2424, (1999).

101. **Wang, J-S.; Matyjaszewski, K.;** *"Controlled/"living" radical polymerisation. Atom transfer radical polymerisation in the presence of transition metal complexes."*, J. Am. Chem. Soc., 117, 5614-5615, (1995).

102. **Wang, J-S.; Matyjaszewski, K.;** *"Controlled/"living" radical polymerisation. Halogen atom transfer radical polymerisation promoted by a Cu(I)/Cu(II) redox process."*, Macromolecules, 28, 23, 7901-7910, (1995).

103. **Percec, V.; Barboiu, B.;** *""Living" radical polymerisation of styrene initiated by arenesulphonyl chlorides and $Cu^I(bpy)_nCl$."*, Macromolecules, 28, 23, 7970-7972, (1995).

104. **Percec, V.; Barboiu, B.; Neumann, A.; Ronda, J. C.; Zhao, M.;** *"Metal-catalysed "living" radical polymerisation of styrene initiated with arenesulphonyl chlorides. From heterogeneous to homogeneous catalysis."*, Macromolecules, 29, 10, 3665-3668, (1996).

105. **Matyjaszewski, K.; Patten, T. E.; Xia, J.;** *"Controlled/"living" radical polymerisation. Kinetics of the homogeneous atom transfer radical polymerisation of styrene."*, J. Am. Chem. Soc., 119, 4, 674-680, (1997).

106. **Grimaud, T.; Matyjaszewski, K.;** *"Controlled/"living" radical polymerisation of methyl methacrylate by atom transfer radical polymerisation."*, Macromolecules, 30, 7, 2216-2218, (1997).

107. **Haddleton, D. M.; Jasieczek, C. B.; Hannon, M. J.; Shooter, A. J.;** *"Atom transfer radical polymerisation of methyl methacrylate initiated by alkyl bromide and 2-pyridinecarbaldehyde imine copper(I) complexes."*, Macromolecules, 30, 7, 2190-2193, (1997).

108. **Haddleton, D. M.; Crossman, M. C.; Dana, B. H.; Duncalf, D. J.; Heming, A. M.; Kukulj, D.; Shooter, A. J.;** *"Atom transfer polymerisation of methyl methacrylate mediated by Alkylpyridylmethanimine type ligands, copper(I) bromide, and alkyl halides in hydrocarbon solution."*, Macromolecules, 32, 7, 2110-2119, (1999).

109. **Destarac, M.; Bessiere, J-M.; Boutevin, B.;** *"Transition metal catalysed atom transfer radical polymerisation(ATRP): from heterogeneous to homogeneous catalysis using 1,10-phenanthroline and its derivatives as new copper(I) ligands."*, Macromol. Rapid Commun., 18, 967-974, (1997).

110. **Cheng, G. L.; Hu, C. P.; Ying, S. K.;** *"Kinetics of the heterogeneous atom transfer radical polymerisation of styrene by using bis(1,10-phenanthroline)copper bromide."*, Macromol. Rapid Commun., 20, 6, 303-307, (1999).

111. **Xia, J.; Matyjaszewski, K.;** *"Controlled/"living" radical polymerisation. Atom transfer radical polymerisation catalysed by copper(I) and picolyl amine complexes."*, Macromolecules, 32, 8, 2434-2437, (1999).

112. **Xia, J.; Matyjaszewski, K.;** *"Controlled/"living" radical polymerisation. Atom transfer radical polymerisation using multidentate amine ligands."*, Macromolecules, 30, 25, 7697-7700, (1997).

113. **Yu, B.; Ruckenstein, E.;** *"Controlled radical polymerisation catalysed by copper(I)-sparteine complexes."*, J. Polym. Sci, A, Polym. Chem., 37, 4191-4197, (1999).

114. **Percec, V.; Barboiu, B.; Kim, H-J.;** *"Arenesulphonyl halides: A universal class of functional initiators for metal-catalysed "living" radical polymerisation of styrene(s), methacrylates, and acrylates."*, J. Am. Chem. Soc., 120, 2, 305-316, (1998).

115. **Kicklebick, G.; Reinohl, U,; Ertel, T. S.; Bertagnolli, H.; Matyjaszewski, K.;** *"Copper catalyst in atom-transfer radical polymerisations: structural observations."*, Am. Chem. Soc., Polym. Div., Polym. Prepr., 334-335, (1999).

116. **Kajiwara, A.; Matyjaszewski, K.; Kamachi, M.;** *"Simultaneous EPR and kinetic study of styrene atom transfer radical polymerisation (ATRP)."*, Macromolecules, 31, 17, (1998).

117. **Ohno, K.; Goto, A.; Fukuda, T.; Xia, J.; Matyjaszewski, K.;** *"Kinetic study on the activation process in an atom transfer radical polymerisation process."*, Macromolecules, 31, 8, 2699-2701, (1998).

118. **Xia, J.; Matyjaszewski, K.;** *"Controlled/"living" radical polymerisation. Homogeneous reverse atom transfer radical polymerisation using AIBN as the initiator."*, Macromolecules, 30, 25, 7692-7696, (1997).

119. **Haddleton, D. M.; Kukulj, D.; Duncallf, D. J.; Heming, A. M.; Shooter, A. J.;** *"Low-temperature living "radical" polymerisation (atom transfer polymerisation) of methyl methacrylate mediated by copper(I) N-alkyl-2-pyridylmethanimine complexes."*, Macromolecules, 31, 16, 5201-5205, (1998).

120. **Arehart, S. V.; Matyjaszewski, K.;** *"Atom transfer radical copolymerisation of styrene and n-butyl acrylate."*, Macromolecules, 32, 7, 2221-2231, (1999).

121. **Haddleton, D. M.; Clark, A. J.; Crossman, M. C.; Duncalf, D. J.; Heming, A. M.; Morsley, S. R.; Shooter, A. J.;** *"Atom transfer radical polymerisation (ATRP) of methyl methacrylate in the presence of radical inhibitors."*, Chem. Commun., 1997-1998, (1997).

122. **Bagdasarian, K. S.; Sinitsina, Z. A.;** *"Polymerisation inhibition by aromatic compounds."*, J. Polym. Sci, 52, 31-38, (1961).

123. **Greenwood, N. N.; Earnshaw, A.;** *"Chemistry of the elements."*, Pergamon press, Oxford, 137877-1378, (1984).

124. **Wang, J-L.; grimaud, T.; Matyjaszewski, K.;** *"Kinetic study of the homogeneous atom transfer radical polymerisation of methyl methacrylate."*, Macromolecules, 30, 21, 6507-6512, (1997).

125. **Matyjaszewski, K.; Coca, S.; Jasieczek, C. B.;** *"Polymerisation of acrylates by atom transfer radical polymerisation. Homopolymerisation of glycidyl acrylate."*, Macromol. Chem. Phys., 198, 4011-4017, (1997).

126. **Coca, S.; Jasieczek, C. B.; Beers, K. L.; Matyjaszewski, K.;** "Polymerisation of acrylates by atom transfer radical polymerisation. Homopolymerisation of 2-Hydroxyethyl acrylate.", J. Polym. Sci., A, Polym. Chem., 36, 1417-1424, (1998).

127. **Ohno, K.; Tsujii, Y.; Fukuda, T.;** *"Synthesis of a well-defined glycopolymer by atom transfer radical polymerisation."*, J. Polym. Sci., A, Polym. Chem., 36, 2473-2481, (1998).

128. **Marsh, A.; Khan, A.; Haddleton, D. M.; Hannon, M. J.;** *"Atom transfer polymerisation: Use of uridine and adenosine derivatised monomers and initiators."*, Macromolecules, 32, 8725-8731, (1999).

129. **Wang, X-S.; Lascelles, S. F.; Jackson, R. A.; Armes, S. P.;** *"Facile synthesis of well-defined water-soluble polymers via atom transfer radical polymerisation in aqueous media at ambient temperature."*, Chem. Commun., 1817-1818, (1999).

130. **Ashford, E. J.; Naldi, V.; O'Dell, R.; Billingham, N. C.; Armes, S. P.;** *"First example of the atom transfer radical polymerisation of an acidic monomer: direct synthesis of methacrylic acid coplymers in aqueous media."*, Chem. Commun., 1285-1286, (1999).

131. **Matyjaszewski, K.; Jo, S. M.; Paik, H-J.; Gaynor, S. G.;** *"Synthesis of well-defined polyacrylonitrile by atom transfer radical polymerisation."*, Macromolecules, 30, 6398-6400, (1997).

132. **Matyjaszewski, K.; Jo, S. M.; Paik, H-J.; Shipp, D. A.;** *"An investigation into the CuX/2,2'-bipyridine (X = Br or Cl) mediated atom transfer radical polymerisation of acrylonitrile."*, Macromolecules, 32, 6431-6438, (1999).

133. **Xia, J.; Zhang, X.; Matyjaszewski, K.;** *"Atom transfer radical polymerisation of 4-vinylpyridine."*, Macromolecules, 32, 3531-3533, (1999).

134. **Teodorescu, M.; Matyjaszewski, K.;** *"Atom transfer radical polymerisation of acrylamides and methacrylamides."*, Am. Chem. Soc., Div. Polym. Chem., Polym. Prepr., 40, 2, 428-429, (1999).

135. **Teodorescu, M.; Matyjaszewski, K.;** *"Controlled polymerisation of (meth)acrylamides by atom transfer radical polymerisation."*, Macromol. Rapid Commun., 21, 190-194, (2000).

136. **Haddleton, D. M.; Heming, A. M.; Dax Kukulj; Duncalf, D. J.; Shooter, A. J.;** *"Atom transfer polymerisation of methyl methacrylate. Effect of acids and effect with 2-bromo-2-methylpropionic acid initiation."*, Macromolecules, 31, 2016-2018, (1998).

137. **Zhang, X.; Xia, J.; Matyjaszewski, K.;** *"Atom transfer radical polymerisation of protected methacrylic acids."*, Am. Chem. Soc., Div. Polym. Chem., Polym. Prepr., 40, 2, 440-441, (1999).

138. **Nakagawa, Y.; Matyjaszewski, K.;** *"The syntheiss of well-defined allyl end-functionalised polystyrene by atom transfer radical polymerisation with an allyl halide initiator."*, Polymer Journal, 30, 2, 138-141, (1998).

139. **Haddleton, D. M.; Waterson, C.; Derrick, P. J.; Jasieczek, C. B.; Shooter, A. J.;** *"Monohydroxy terminally functionalised poly(methyl methacrylate) from atom transfer radical polymerisation."*, Chem. Commun., 683-684, (1997).

140. **Coessens, V.; Matyjaszewski, K.;** *"Synthesis of polymers with hydroxyl end groups by atom transfer radical polymerisation."*, Macromol. Rapid Commun., 20, 3, 127-134, (1999).

141. **Haddleton, D. M.; Waterson, C.;** *"Phenolic ester-based initiators for transition metal mediated living polymerisation."*, Macromolecules, 32, 8732-8739, (1999).

142. **Alkan, S.; Toppare, L.; Hepuzer, Y.; Yagci, Y.;** *"Block copolymers of thiophene-capped poly(methyl methacrylate) with pyrrole."*, J. Polym. Sci, A, Polym. Chem., 37, 4218-4225, (1999).

143. **Nakagawa, Y.; Gaynor, S. G.; Matyjaszewski, K.;** *"The synthesis of end functional polymers by "living" radical polymerisation."*, Am. Chem. Soc., Div. Polym. Chem., Polym. Prepr., 37, 1, 577-578, (1996).

144. **Ivan, B.; Fonagy, T.;** *"Chain end functionalisation of polystyrene obtained by quasiliving atom transfer radical polymerisation."*, Am. Chem. Soc., Div. Polym. Chem., Polym. Prepr., 40, 2, 356-357, (1999).

145. **Coessens, V.; Nakagawa, Y.; Matyjaszewski, K.;** *"Synthesis of azido end-functional polyacrylates via atom transfer radical polymerisation."*, Polymer Bull., 40, 2-3, 135-142, (1998).

146. **Matyjaszewski, K.; Nakagawa, Y.; Gaynor, S. G.;** *"Synthesis of well-defined azido and amino end-functionalised polystyrene by atom transfer radical polymerisation."*, Macromol. Rapid Commun., 18, 1057-1066, (1997).

147. **Heuts, J. P. A.; Davis, T. P.;** *"Atom transfer radical copolymerisation kinetics."*, Macromol. Rapid Commun., 19, 371-375, (1998).

148. **Roos, S. G.; Muller, A. H. E.; Matyjaszewski, K.;** *"Copolymerisation of n-butyl acrylate with methyl methacrylate and pMMA macromonomers: Comparison of reactivity ratios in conventional and atom transfer radical copolymerisation."*, Macromolecules, 32, 8331-8335, (1999).

149. **Haddleton, D. M.; Crossman, M. C.; Hunt, K. H.; Topping, C.; Waterson, C.; Suddaby, K. G.;** *"Identifying the nature of the active species in the polymerization of methacrylates: Inhibition of methyl methacrylate homopolymerizations and reactivity ratios for copolymerization of methyl methacrylate n-butyl methacrylate in classical anionic, alkyllithium/trialkylaluminum-initiated, group transfer polymerization, atom transfer radical polymerization, catalytic chain transfer, and classical free radical polymerization."*, Macromolecules, 30, 3992-3998, (1997).

150. **Arehart, S. V.; Matyjaszewski, K.;** *"Atom transfer radical copolymerisation of styrene and n-butyl acrylate."*, Macromolecules, 32, 2221-2231, (1999).

151. **Jiang, X.; Xia, P.; Liu, W.; Yan, D.;** *"Atom transfer radical copolymerisation of styrene and N-cyclohexylmaleimide."*, J. Polym. Sci., A, Polym. Chem., 38, 1203-1209, (2000).

152. **Arehart, S. V.; Greszta, D.; Matyjaszewski, K.;** *"Gradient copolymers of styrene and n-butyl acrylate through stom transfer radical polymerisation."*, Am. Chem. Soc., Div. Polym. Chem., Polym. Prepr., 38, 1, 705-706, (1997).

153. **Chen, G.-Q.; Wu, Z.-Q.; Wu, J.-R.; Li, Z.-C.; Li, F.-M.;** *"Synthesis of alternating copolymers of N-sustituted maleimides with styrene via atom transfer radical polymerisation."*, Am. Chem. Soc., Div. Polym. Chem., Polym. Prepr., 40, 2, 360-361, (1999).

154. **Shipp, D. A.; mcmurry, G. P.; Gaynor, S. G.; Qiu, J.; Matyjasewski, K.;** *"Water-borne block copolymer synthesis and effective one-pot syntheis of acrylate-*

methacrylate block copolymers by atom transfer radical polymerisation.", Am. Chem. Soc., Div. Polym. Chem., Polym. Prepr., 40, 2, 448-449, (1999).

155. **Matyjaszewski, K.; Shipp, D. A.; Wang, J. L.; Grimaud, T.; Patten, T. E.;** *"Utilising halide exchange to improve control of atom transfer radical polymerisation.*", Macromolecules, 31, 20, 6836-6840, (1998).

156. **Haddleton, D. M.; Heming, A. M.; Kukulj, D.; Jackson, S. G.;** *"Halogen exchange during atom transfer polymerisation of methyl methacrylate mediated by copper(I) N-alkyl-2-pyridylmethanimine complexes.*", Chem. Commun., 16, 1719-1720, (1998).

157. **Shipp, D. A.; Wang, J.-L.; Matyjaszewski, K.;** *"Synthesis of acrylate and methacrylate block copolymers using atom transfer radical polymerisation.*", Macromolecules, 31, 8005-8008, (1998).

158. **Jo, S. M.; Gaynor, S. G.; Matyjaszewski, K.;** *"Homo and ABA block polymerisations of acrylonitrile, n-butylacrylate and 2-hexyl acrylate using ATRP.*", Am. Chem. Soc., Div. Polym. Chem., Polym. Prepr., 37, 2, 272, (1996).

159. **Cassebras, M.; Pascual, S.; Polton, A.; Tardi, M.; Vairon, J.-P.;** *"Synthesis of di and triblock copolymers of styrene and butyl acrylate by controlled atom transfer radical polymerisation.*", Macromol. Rapid Commun., 20, 261-264, (1999).

160. **Coca, S.; Matyjaszewski, K.;** *"Block copolymers by transformation of "living" carbocationic into "living" radical polymerisation.*", Macromolecules, 30, 2808-2810, (1997).

161. **Coca, S.; Matyjaszewski, K.;** *"Block copolymers by transformation of "living" carbocationic into "living" radical polymerisation. 2. ABA-type block copolymers comprising rubbery polyisobutene middle segment.*", J. Polym. Sci., A, Polym. Chem., 35, 16, 3595-3601, (1997).

162. **Chen, X.; Ivan, B.; Kops, J.; Batsberg, W.;** *"Polystyrene-b-polyisobutene-b-polystyrene block copolymers by combining living cationic and "Living" free-radical polymerisation.*", Am. Chem. Soc., Div. Polym. Chem., Polym. Prepr., 38, 1, 715-716, (1997).

163. **Acar, M. H.; Matyjaszewski, K.;** *"Block copolymers by transformation of living anionic polymerisation into controlled/"living" atom transfer radical polymerisation.*", Macromol. Chem. Phys., 200, 1094-1100, (1999).

164. **Coca, S.; Paik, H.-J.; Matyjaszewski, K.;** *"Block copolymers by transformation of living ring-opening metathesis polymerisation into controlled/"living" atom transfer radical polymerisation.*", Macromolecules, 30, 6513-6516, (1997).

165. **Gaynor, S. G.; Matyjaszewski, K.;** *"Step-growth polymers as macroinitiators for "living" radical polymerisation: synthesis of ABA block copolymers.*", Macromolecules, 30, 14, 4241-4243, (1997).

166. **Bednarek, M.; Biedron, T.; Kubisa, P.;** *"Synthesis of block copolymers by atom transfer radical polymerisation of tert-butyl acrylate with poly(oxyethylene) macroinitiators."*, Macromol. Rapid Commun., 20, 59-65, (1999).

167. **Kops, J.; Chen, X.; Jankova, K.; Truelsen, J. H.; Batsberg, W.;** *"Atom transfer radical polymerisation of p-acetoxy styrene for the synthesis of amphiphilic block copolymers."*, Am. Chem. Soc., Div. Polym. Chem., Polym. Prepr., 40, 2, 374-375, (1999).

168. **Nakagawa, Y.; Miller, P.; Pacis, C.; Matyjaszewski, K.;** *"Synthesis of block and graft copolymers from poly(dimethylsiloxane) macroinitiators by atom transfer radical polymerisation."*, Am. Chem. Soc., Div. Polym. Chem., Polym. Prepr., 38, 1, 701-702, (1997).

169. **Destarac, M.; Boutevin, B.;** *"Cu-catalysed ATRP of styrene initiated by vinyl acetate telomers."*, Am. Chem. Soc., Div. Polym. Chem., Polym. Prepr., 40, 2, 401-408, (1999).

170. **Paik, H.-J.; Teodorescu, M.; Xia, J.; Destarac, M.; Matyjaszewski, K.;** *"Block copolymers of vinyl acetate by atom transfer radical polymerisation using halogen terminated (macro) initiators."*, Am. Chem. Soc., Div. Polym. Chem., Polym. Prepr., 40, 2, 438-439, (1999).

171. **Zhang, Z.; Ying, S.; Shi, Z.;** *"Synthesis of fluorine-containing block copolymers via ATRP 1. Synthesis and characterisation of PSt-PVDF-PSt triblock copolymers."*, Polymer, 40, 1341-1345, (1999).

172. **Paik, H.-J.; Teodorescu, M.; Xia, J.; Matyjaszewski, K.;** *"Block copolymerisations of vinyl acetate by combination of conventional and atom transfer radical polymerisation."*, Macromolecules, 32, 7023-7031, (1999).

173. **Haddleton, D. M.; Waterson, C.;** *"Phenolic ester based initiators for transition metal mediated living polymerisation."*, Macromolecules, 32, 8732-8739, (1999).

174. **Matyjaszewski, K.; Miller, P. J.; Pyun, J.; Kicklebick, G.; Diamanti, S.;** *"Synthesis and characterisation of star polymers with varying arm number, length, and composition from organic and hybrid inorganic/organic multifunctional initiators."*, Macromolecules, 32, 6526-6535, (1999).

175. **Ueda, J.; Kamigaito, M.; Sawamoto, M.;** *"Calixarene-core multifunctional initiators for the ruthenium mediated living radical polymerisation of methacrylates."*, Macromolecules, 31, 6762-6768, (1998).

176. **Angot, S.; Murthy, S.; Taton, D.; Gnanou, Y.;** *"Atom transfer radical polymerisation of styrene using a novel octafunctional initiator: Synthesis of well-defined polystyrene stars."*, Macromolecules, 31, 7218-7225, (1998).

177. **Kraus, A.; Robello, D. R.;** *"Star polymers via atom transfer radical polymerisation from a simple, multifunctional initiator."*, Am. Chem. Soc., Div. Polym. Chem., Polym. Prepr., 40, 2, 413-414, (1999).

178. **Heise, A.; Hedrick, J. L.; Trollsas, M.; Miller, R. D.; Frank, C. W.;** *"Novel starlike poly(methyl methacrylate)s by controlled dendritic free radical polymerisation."*, Macromolecules, 32, 231-234, (1999).

179. **Maier, S.; Sunder, A.; Frey, H.; Mulhaupt, R.;** *"Synthesis of poly(glycerol)-block-poly(methyl acrylate) multi-arm star polymers."*, Macromol. Rapid Commun., 21, 226-230, (2000).

180. **Beers, K. L.; Gaynor, S. G.; Matyjaszewski, K.;** *"The synthesis of densely grafted copolymers by atom transfer radical polymerisation."*, Macromolecules, 31, 9413-9415, (1998).

181. **Matyjaszewski, K.; Pyun, J.; Gaynor, S. G.;** *"Preparation of hyperbranched polyacrylates by atom transfer radical polymerisation, 4[a]."*, Macromol. Rapid Commun. 19, 665-670, (1998).

182. **Frechet, J. M. J.; Leduc, M. R.; Weimer, M.; Grubbs, R. B.; Liu, M.; Hawker, C. J.;** *"Living free radical polymerisation and dendritic polymers."*, Am. Chem. Soc., Div. Polym. Chem., Polym. Prepr., 38, 1, 756-757, (1997).

183. **Matyjaszewski, K.; Gaynor, S. G.; Kulfan, A.; Podwika, M.;** *"Preparation of hyperbranched polyacrylates by atom transfer radical polymerisation. 1. Acrylic AB* monomers in "living" radical polymerizations."*, Macromolecules, 30, 17, 5192-5194, (1997).

184. **Matyjaszewski, K.; Gaynor, S. G.; Muller, A. H. E.;** *"Preparation of hyperbranched polyacrylates by atom transfer radical polymerisation. 2. Kinetics and mechanism of chain growth for the self-condensing vinyl polymerisation of 2-((2-bromopropionyl)oxy)ethyl acrylate."*, Macromolecules, 30, 23, 7034-7041, (1997).

185. **Matyjaszewski, K.; Gaynor, S. G.;** *"Preparation of hyperbranched polyacrylates by atom transfer radical polymerisation. 3. Effect of reaction conditions on the self-condensing vinyl polymerisation of 2-((2-bromopropionyl)oxy)ethyl acrylate."*, Macromolecules, 30, 23, 7042-7049, (1997).

186. **Buback, M.; Gilbert, R. G.; Hutchison, R. A.; Klumperman, B.; Kuchta, F.; Manders, B. G.; O'driscoll, K. F.; Russell, G. T.; Schweer, J.;** *"Critically evaluated rate coefficients for free-radical polymerisation. 1. – propagation rate coefficient for styrene."*, Macromol. Chem. Phys., 196, 3267-3280, (1995).

187. **Fischer, H.;** *"Unusual selectivities of radical reactions by internal suppression of fast modes."*, J. Am. Chem. Soc., 108, 14, 3925-3927, (1986).

188. IUPAC commission on polymer characterisation and properties. Pure Appl. Chem., 68, 1491, (1996).

189. **Qiu, J.; Pintauer, T.; Gaynor, S.; Matyjaszewski, K.;** *"Absorption spectroscopic studies of copper-based atom transfer radical radical reactions."*, Am. Chem. Soc., Div. Polym. Chem., Polym. Prepr., 420, (1999).

190. **Haddleton, D. M.; Clark, A. J.; Duncalf, D. J.; Heming, A. M.; Kukulj, D.; Shooter, A. J.;** *"Copperdiimine complexes: the synthesis and crystal structures of* $[Cu(C_{10}H_{14}N_{22})_2(MeOH)]$, $[Cu(C_{10}H_{20}N_2)_{2]}]Br$, $[\{(C_{10}H_{14}N_2)CuBr(\mu\text{-}Ome)\}_2(MeOH)]$ *and* $[\{(C_{10}H_{20}N_2)CuBr(\mu\text{-}Ome)\}_2]$*.",* J. Chem. Soc. Dalton Trans., 381-385, (1998).

191. Coleman, B. D.; Fox, T. G.; ***" General theory of stationary sequences with applications to the tacticity of polymers.", J. Polym. Sci. A, 1, 3183-3197, (1963).***

192. **Kitagawa, S.; Munakata, M.;** *"Binuclear copper(I) complexes which reversibly react with CO. 1. Di-μ-halogeno-bis(2,2'-bipyridine)dicopper(I) and its derivatives.",* Inorganic Chem., 20, 2261-2267, (1981).

193. **Munakata, M.; Kitagawa, S.; Asahara, A.; Masuda, H.;** *"Crystal structure of bis(2,2'-bipyridine)copper(I) perchlorate.",* Bull. Chem. Soc. Japan, 60, 1927-1929, (1987).

194. **Kajiwara, A.; Matyjaszewski, K.;** *"EPR study of the atom transfer radical polymerisation (ATRP) of (meth)acrylates.",* Macromol. Rapid Commun., 19, 319-321, (1998).

195. **Shipp, D. A.; Matyjaszewski, K.;** *"Kinetic analysis of the controlled/"living" radical polymerisations by simulations. 1. The importance of diffusion controlled reactions.",* Macromolecules, 32, 2948-2955, (1999).

196. **Pascual, S.;Coutin, B.; Tardi, M.; Polton, A.; Vairon, J.-P.;** *"Homogeneous atom transfer polymerization of styrene initiated by 1-chloro-1-phenylethane/copper(I) chloride/Bipyridine in the presence of dimethylformamide.",* Macromolecules, 32, 1432-1437, (1999).

197. **Klumperman, B.; Chambard, C.;** *"Recent advances in atom transfer radical copolymerisation.",* Am. Chem. Soc., Div. Polym. Chem., Polym. Prepr., 40, 2, 328-330, (1999).

198. **Matyjasewski, K.; Coca, S.; Gaynor, S. G.; Wei, M.; Woodworth, B. E.;** *"Zerovalent metals in controlled/"living" radical polymerisations.",* Macromolecules, 30, 7348-7350, (1997).

199. **Gaynor, S. G.; Wang, J.S.; Matyjaszewski, K.;** *"Controlled Radical polymerisation by degeneratuve transfer – Effect of the structure of the transfer agent.",* Macromolecules, 28, 24, 8051-8056, (1995).

Appendix 1. Infra-red spectra of N-alkyl-2-pyridinemethanimines

(a) BPMI

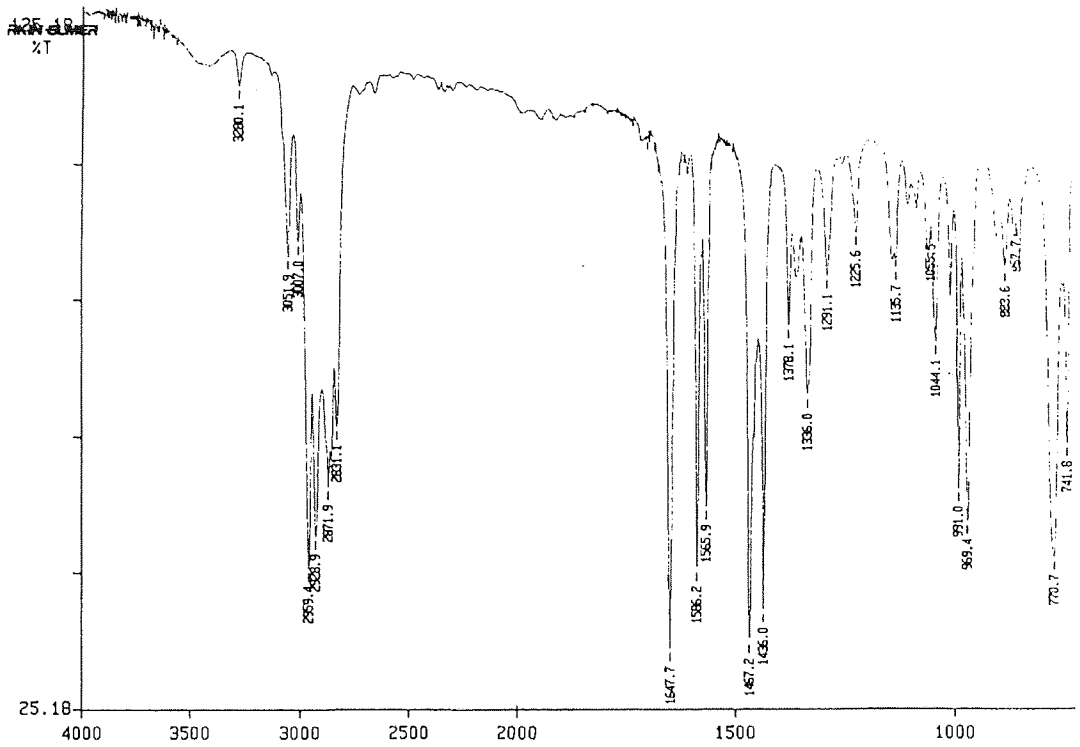

(b) OPMI

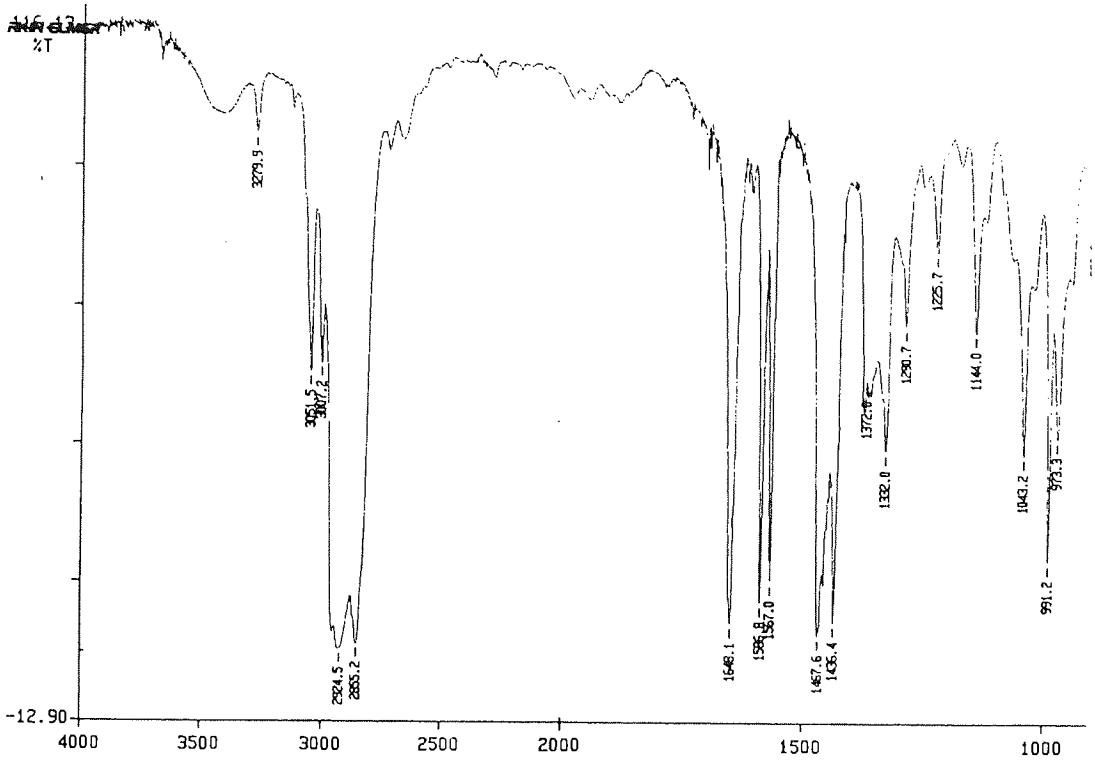
%T
3279.5
2924.5
2855.2
1648.1
1587.0
1467.6
1436.4
1372.9
1332.0
1290.7
1225.7
1144.0
1043.2
991.2
-12.90
4000
3500
3000
2500
2000
1500
1000

Appendix 2. ^{1}H NMRs of N-alkyl-2-pyridinemethanimines

(a) BPMI

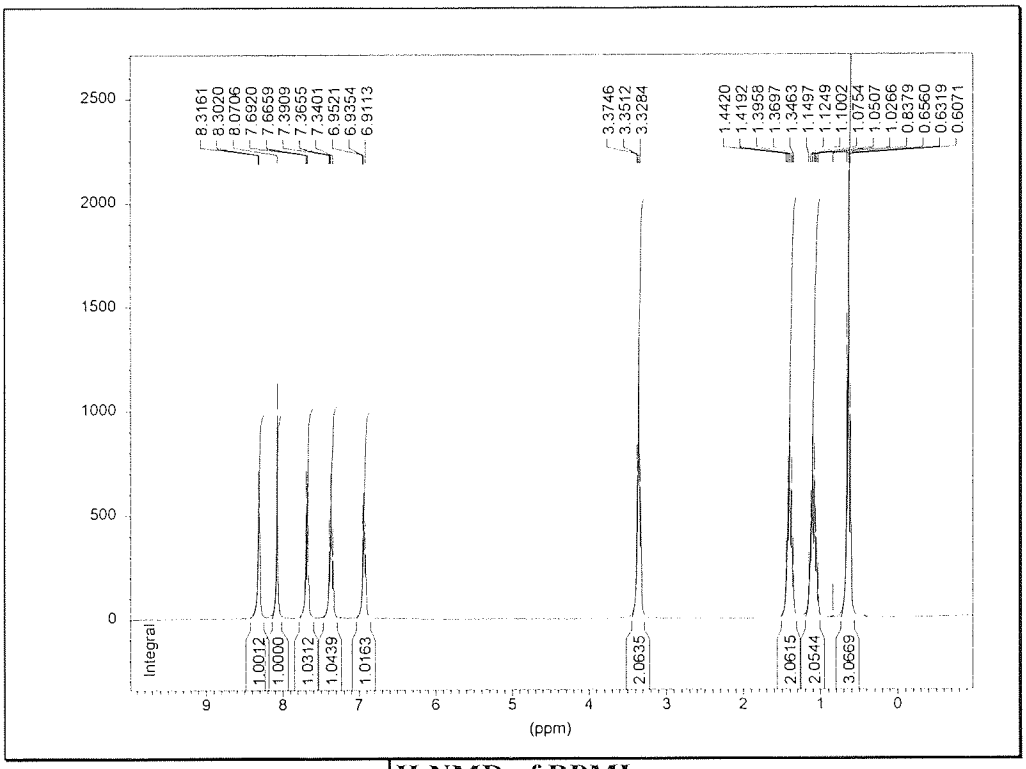

^{1}H NMR of BPMI.

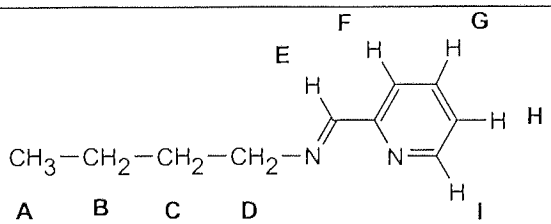

Assignment Label	Peak description and integral value	^{1}H NMR shift value/ ppm
A	triplet (3H)	1.00
B	sextet (2H)	1.12
C	quintet (2H)	1.40
D	triplet (2H)	3.35
E	singlet (1H)	8.07
F	doublet (1H)	7.69
G	triplet (1H)	6.90
H	triplet (1H)	7.36
I	doublet (1H)	8.30

^{1}H-NMR peak assignments for BPMI.

(b) OPMI

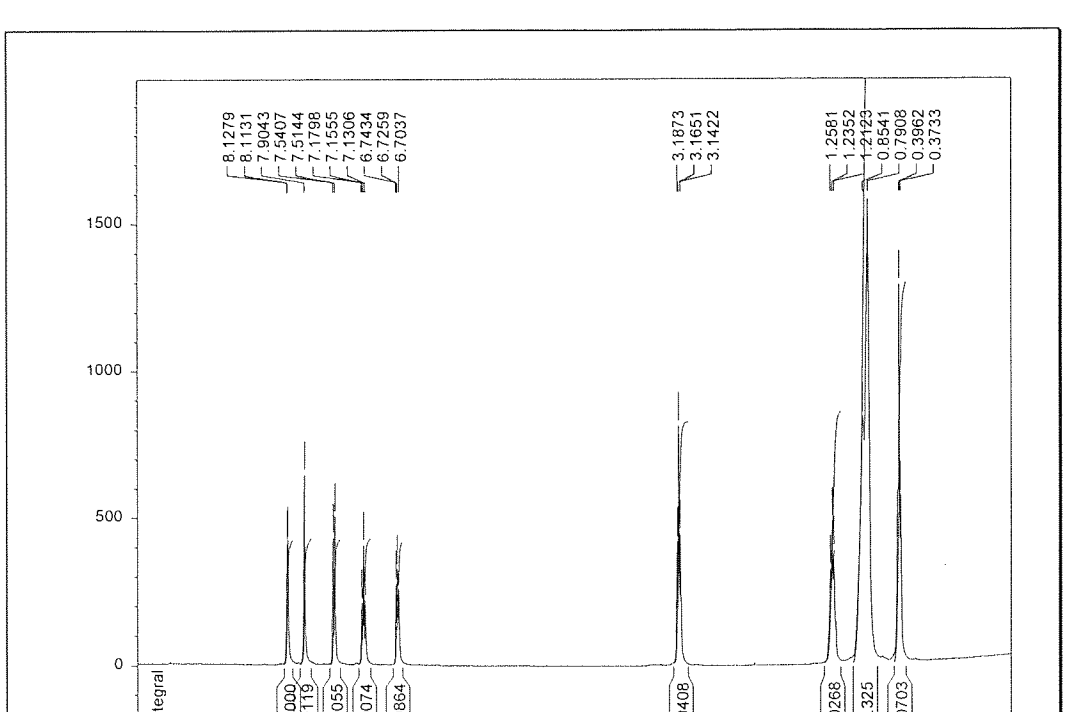

^{1}H NMR spectrum of OPMI.

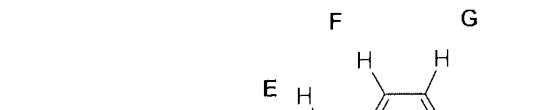

Assignment Label	Peak description and integral value	^{1}H NMR shift value/ ppm
A	Triplet(3H)	0.38
B	Doublet(10H)	0.82
C	Pentet(2H)	1.23
D	Triplet(2H)	3.16
E	Singlet(1H)	7.90
F	Doublet(1H)	7.51
G	Triplet(1H)	6.72
H	Triplet(1H)	7.15
I	Doublet(1H)	8.11

Peak assignments for the ^{1}H-NMR spectrum of OPMI.

Appendix 3. ^{13}C NMRs of N-alkyl-2-pyridinemethanimines

(a) BPMI

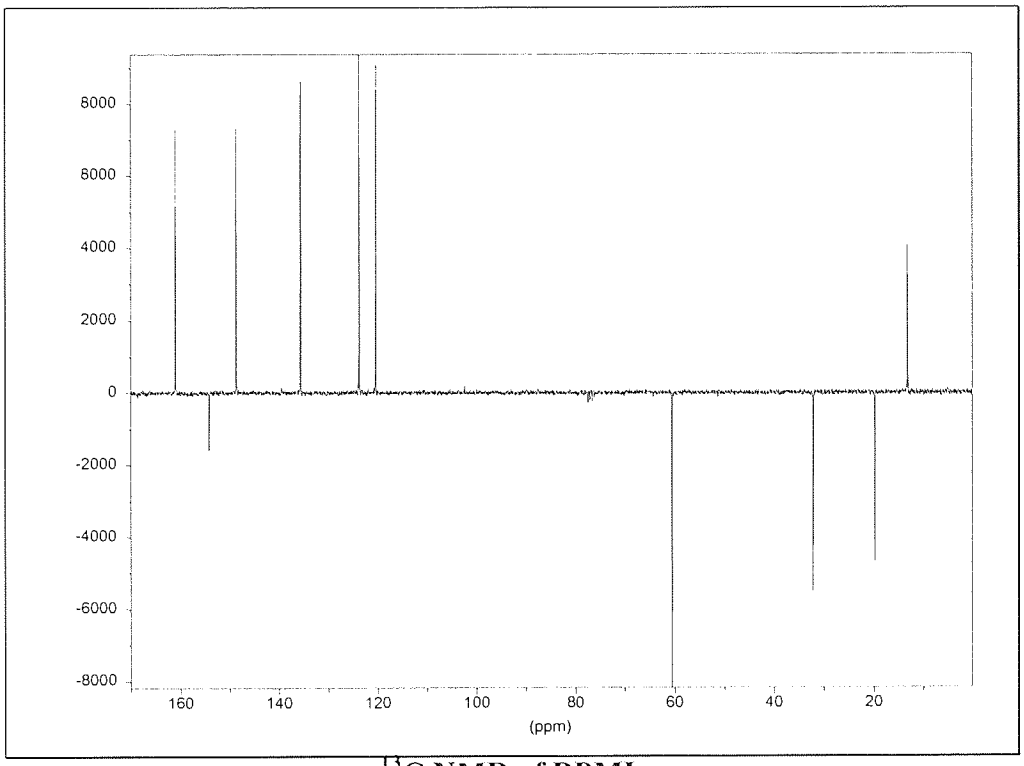

^{13}C NMR of BPMI.

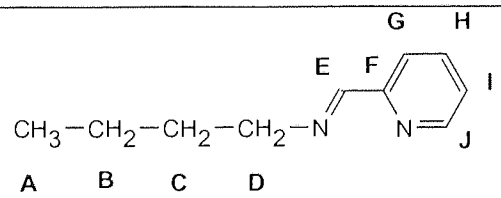

Assignment Label	^{13}C NMR chemical shift value/ppm
A	12.5
B	20
C	33
D	61.5
E	154
F	137
G	120.5
H	124
I	149
J	161

^{13}C-NMR peak assignments for BPMI.

(b) OPMI

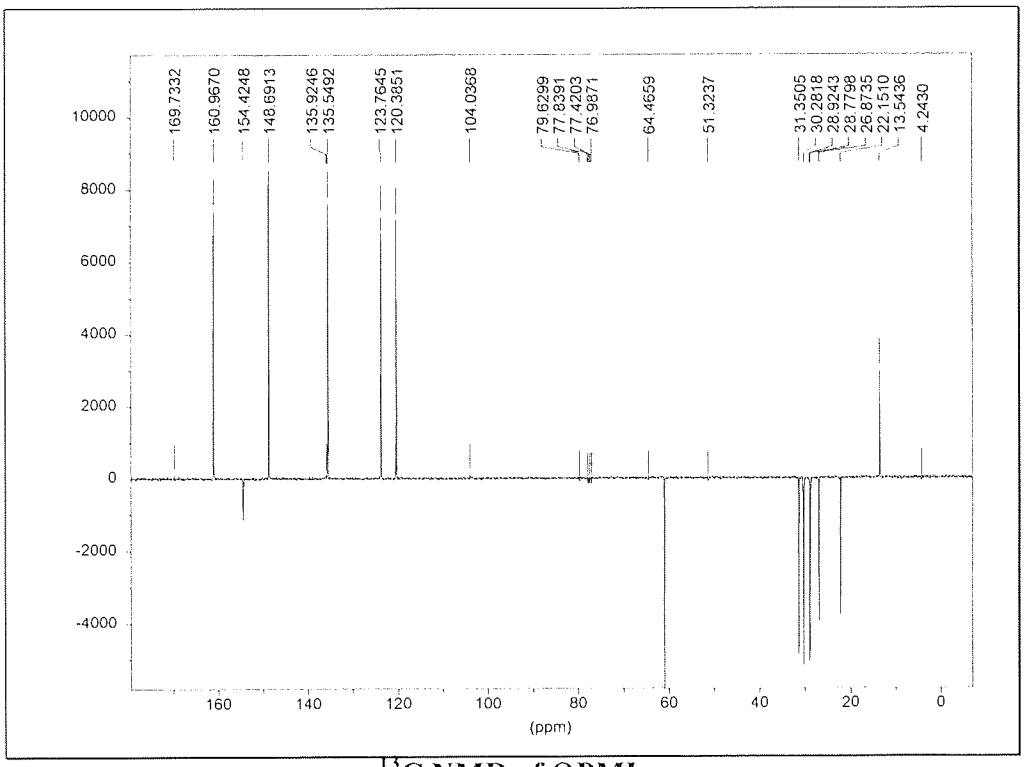

^{13}C NMR of OPMI.

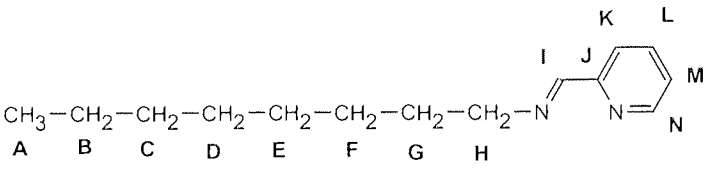

Assignment Label	^{13}C NMR chemical shift value/ ppm
A	13.54
B	22.15
C	26.87
D	28.78
E	28.92
F	30.28
G	31.35
H	64.47
I	160.97
J	154.42
K	135.55
L	120.38
M	123.76
N	148.69

Peak assignments for the ^{13}C NMR of OPMI.

Appendix 4(a). GPC overlays for the ATRP of MMA in diglyme

80°C

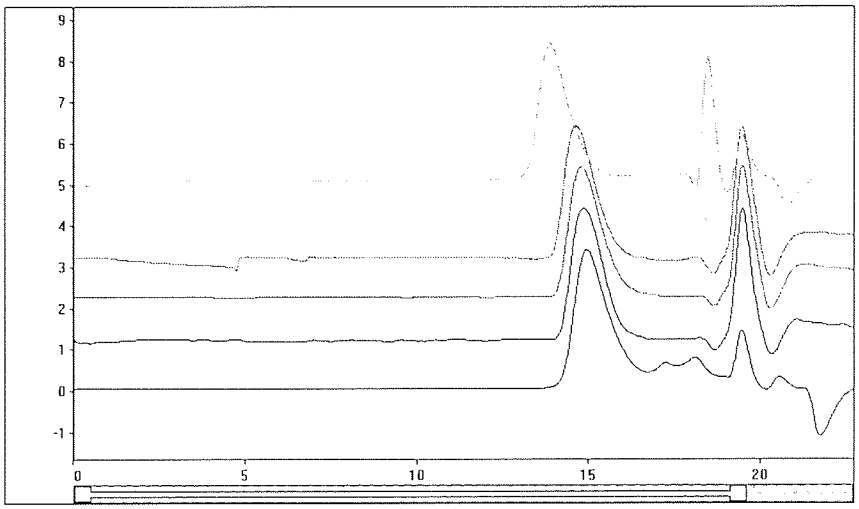

60°C

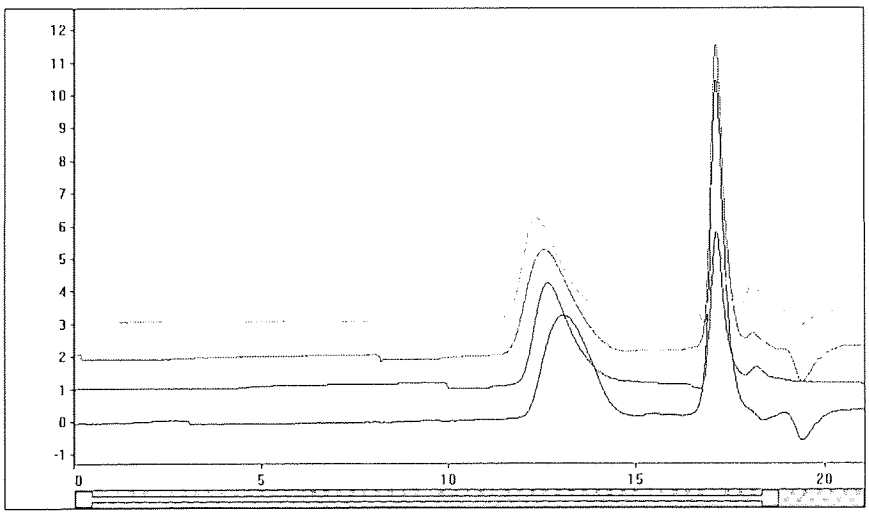

35°C

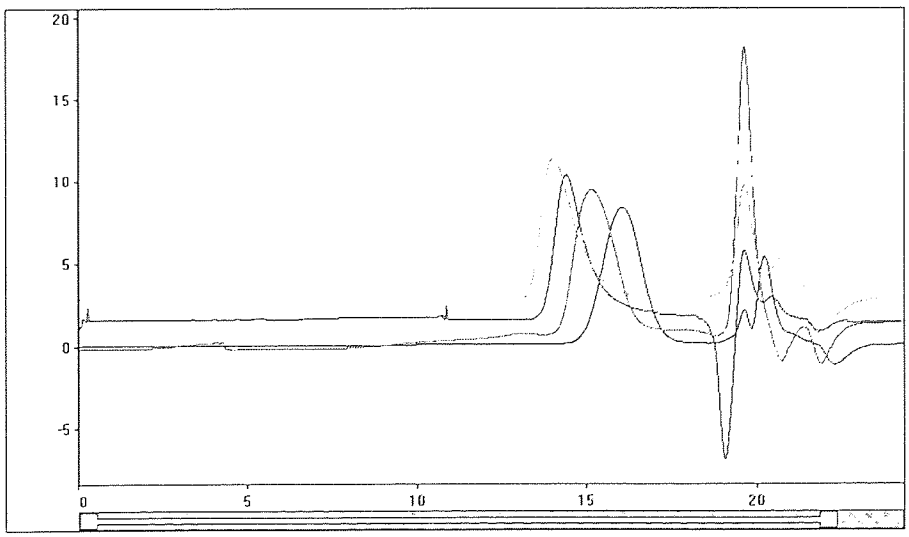

Appendix 4(b). Data sets for the repeat polymerisations of MMA in diglyme

90°C

Time/Minutes	%Conversion
30	10.6
60	24.2
90	38.1
120	49.5
180	64.7
240	83.9
300	88.9

60°C

Time/Minutes	%Conversion
30	10.1
60	15.0
90	16.8
120	20.4
150	24.3
200	36.0

35°C

Time/Minutes	%Conversion
60	16.2
240	28.4
1080	60.7
1275	63.1
1470	67.0
1665	72.2
2505	93.5

Appendix 5. Data sets for the ATRP of MMA in xylene solution

100°C

Time/Minutes	%Conv.	$\overline{M_n}$	$\overline{M_w}$	PDi.
15	14.3	1940	2480	1.28
30	34.7	3300	4350	1.32
45	53.9	5680	7270	1.28
60	73.7	7730	9970	1.29
75	87.4	8720	12210	1.40

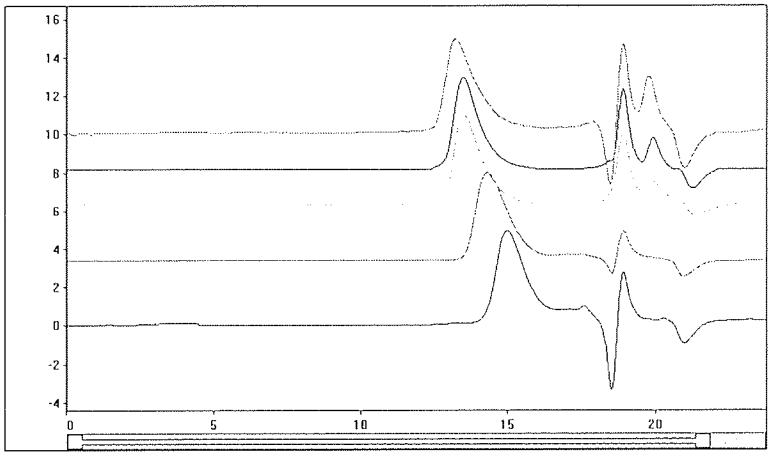

90°C

Time/Minutes	%Conv.	$\overline{M_n}$	$\overline{M_w}$	PDi.
30	18.7	2290	2840	1.24
60	48.0	5390	6790	1.26
90	64.8	6900	8690	1.26
185	80.6	8610	10590	1.23

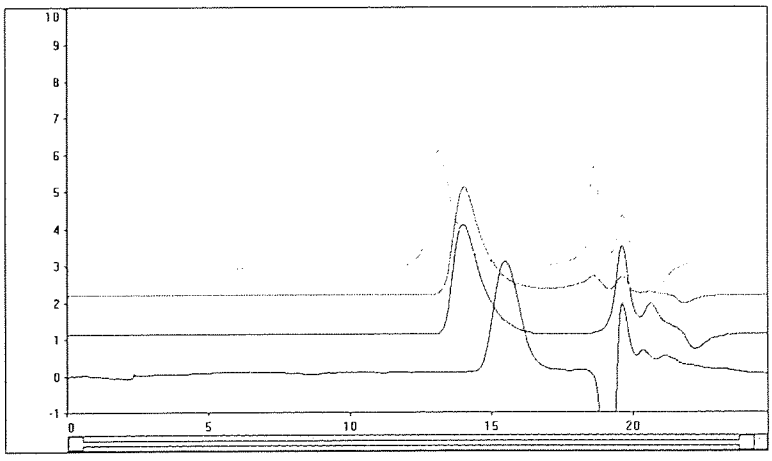

80°C

Time/Minutes	%Conv.	$\overline{M_n}$	$\overline{M_w}$	PDi.
30	10.4	1560	1920	1.23
60	19.9	2860	3570	1.25
80	34.5	4180	4910	1.18
140	51.7	7460	9530	1.24
210	66.3	7250	9080	1.25
240	74.4	8570	10640	1.24

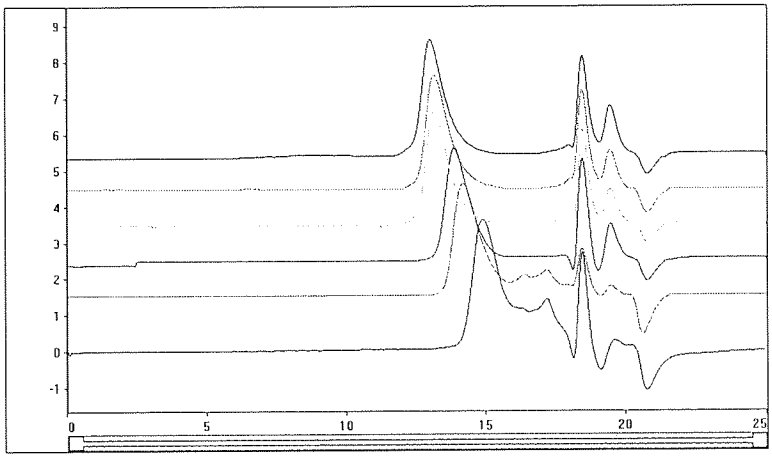

60°C

Time/Minutes	%Conv.	$\overline{M_n}$	$\overline{M_w}$	PDi.
60	15.8	2360	2740	1.16
160	34.3	4340	5130	1.18
225	48.0	5540	6360	1.15
285	50.2	5940	7170	1.21
365	60.0	6750	7860	1.16
465	70.5	6960	8120	1.17

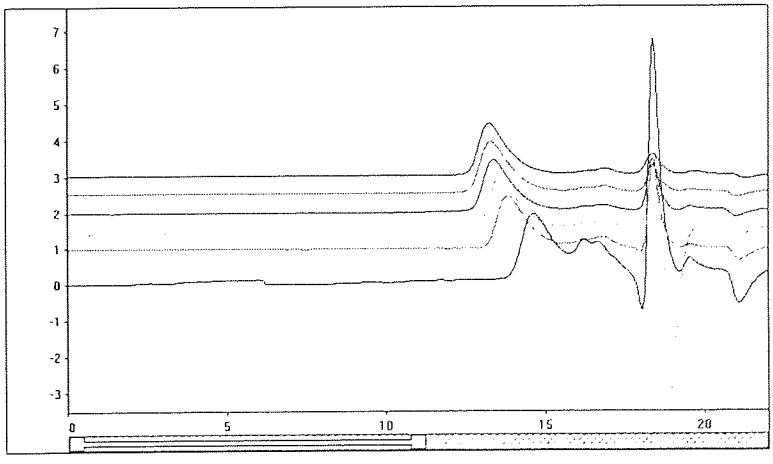

Appendix 6. Data sets for ATRP of MMA at various $[2\text{-EiBBr}]_0$

$[2\text{-EiBBr}]_0 = 0.0714$ mol dm^{-3}

Time/Minutes	%Conv.	$\overline{M_n}$	PDi.
30	35.6	2690	1.28
60	63.2	4510	1.25
90	79.4	5710	1.27
120	87.4	6140	1.29
150	92.0	6410	1.29

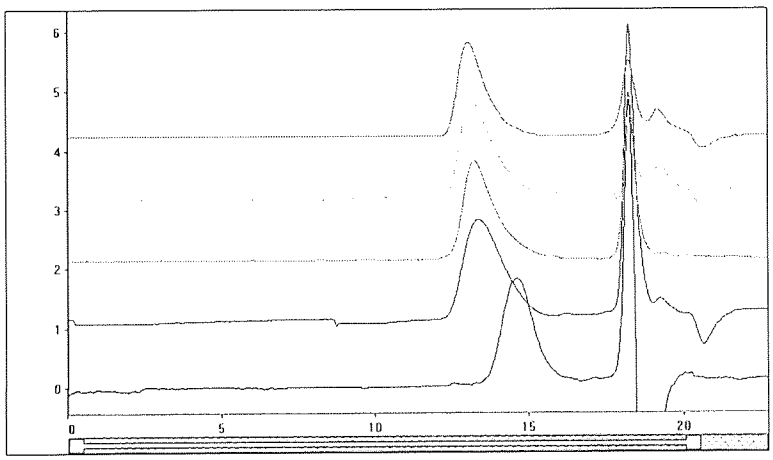

$[2\text{-EiBBr}]_0 = 0.0476$ mol dm^{-3}

See table 4.4 for results and figure 4.5 for G.P.C. overlays.

$[2\text{-EiBBr}]_0 = 0.0238$ mol dm^{-3}

Time/Minutes	%Conv.	$\overline{M_n}$	PDi.
15	10.4	2230	1.27
30	18.9	4010	1.25
60	30.2	6530	1.26
90	39.3	8500	1.24
120	47.3	10150	1.28
180	61.3	14320	1.29
240	73.8	16210	1.28

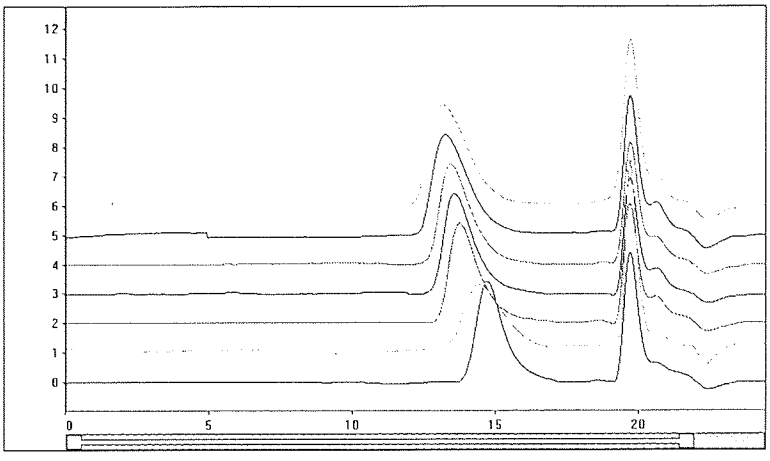
12
11
10
9
8
7
6
5
4
3
2
1
0
0
5
10
15
20

Appendix 7. Data sets for ATRP of MMA at various $[CuBr]_0$ at 90°C

$[CuBr]_0 = 0.0238$ mol dm^{-3}

Time/Minutes	%Conv.	$\overline{M_n}$	PDi.
30	22.2	2410	1.25
90	36.6	3750	1.22
120	57.0	5840	1.21
180	57.9	6640	1.19
240	75.3	7710	1.18
360	82.0	8990	1.19

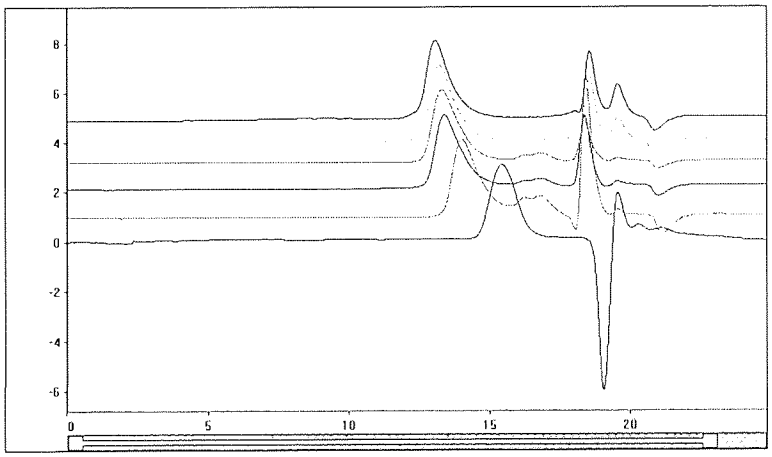

$[CuBr]_0 = 0.0476$ mol dm^{-3}

See Appendix 6; $[2\text{-EiBBr}]_0 = 0.0476$ mol dm^{-3}.

$[CuBr]_0 = 0.0952$ mol dm^{-3}

Time/Minutes	%Conv.	$\overline{M_n}$	PDi.
15	37.0	4100	1.28
30	67.6	7320	1.30
60	77.1	8530	1.29
90	84.7	9170	1.33

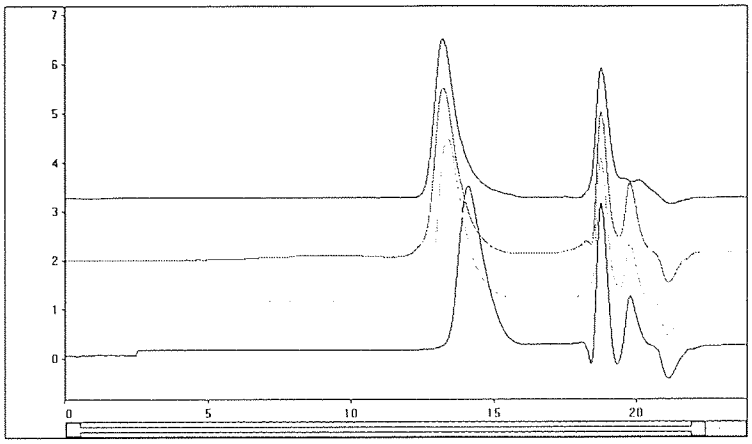
7
6
5
4
3
2
1
0
0
5
10
15
20

Appendix 8. Data sets for ATRP of MMA at various $[OPMI]_0:[CuBr]_0$, at 90°C

$[OPMI]_0:[CuBr]_0 = 0.5$

Time/Minutes	%Conversion
30	5.8
90	27.3
150	37.4
270	52.9
390	69.6

$[OPMI]_0:[CuBr]_0 = 1.0$

Time/Minutes	%Conversion
30	6.7
60	14.7
120	36.5
180	65.4
240	71.5
300	85.7

$[OPMI]_0:[CuBr]_0 = 1.5$

Time/Minutes	%Conversion
30	22.9
60	40.7
90	51.9

$[OPMI]_0:[CuBr]_0 = 2.0$

Time/Minutes	%Conversion
30	10.6
60	24.2
90	38.1
120	49.5
180	64.7
240	83.9
300	88.9

$[OPMI]_0:[CuBr]_0 = 3.0$

See appendix 6; $[2\text{-EiBBr}]_0 = 0.0476$ mol dm^{-3}.

Appendix 9. Data sets for the ATRP of MMA in polar solvents at 90°C

(a) DMSO

Time/Minutes	%Conversion	Mn	PDi.
30	23.5	3070	1.22
60	24.1	3280	1.22
120	29.3	3580	1.27
210	32.5	3760	1.24
240	33.0	3650	1.28
330	24.5	3530	1.30
390	35.2	3620	1.30

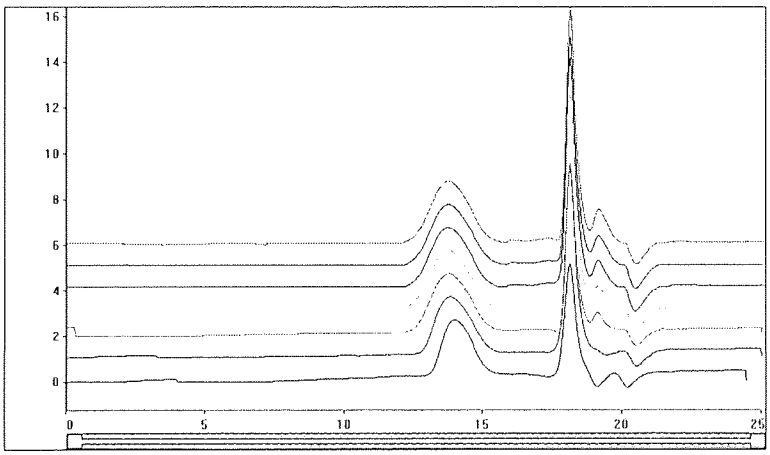

(b) DMF

Time/Minutes	%Conversion	Mn	PDi
20	8.0	2070	1.26
60	11.5	2340	1.31
90	20.3	2490	1.33
120	23.4	2530	1.37
195	24.0	2680	1.39
255	28.0	2990	1.42
315	28.7	3420	1.45
385	34.9	4210	1.59

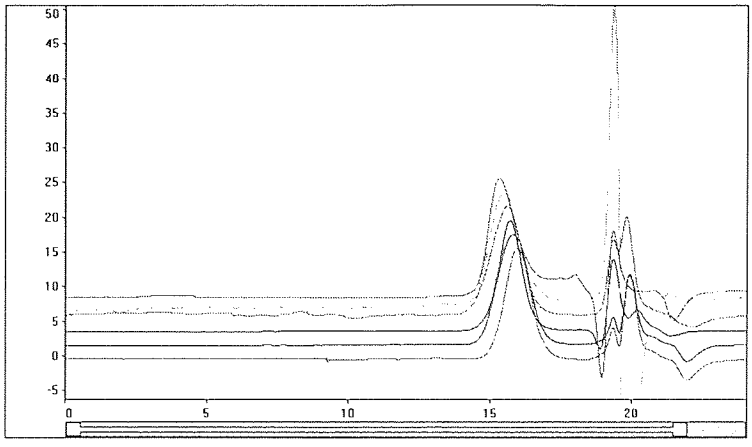
50
45
40
35
30
25
20
15
10
5
0
-5
0
5
10
15
20

Appendix 10. Data sets for the ATRP of MMA in polar solvents at various $[CuBr]_0$

(a) DMSO

$[CuBr]_0 = 0.0476$ mol dm^{-3}

See appendix 9(a).

$[CuBr]_0 = 0.0952$ mol dm^{-3}

Time/Minutes	%Conversion	Mn	PDi
15	36.1	4200	1.21
30	42.5	4620	1.28
45	53.9	4980	1.29
60	62.7	5070	1.30
90	60.3	5090	1.34
120	63.9	5190	1.32
180	56.8	5070	1.35
240	61.6	5110	1.34
300	63.4	5120	1.33

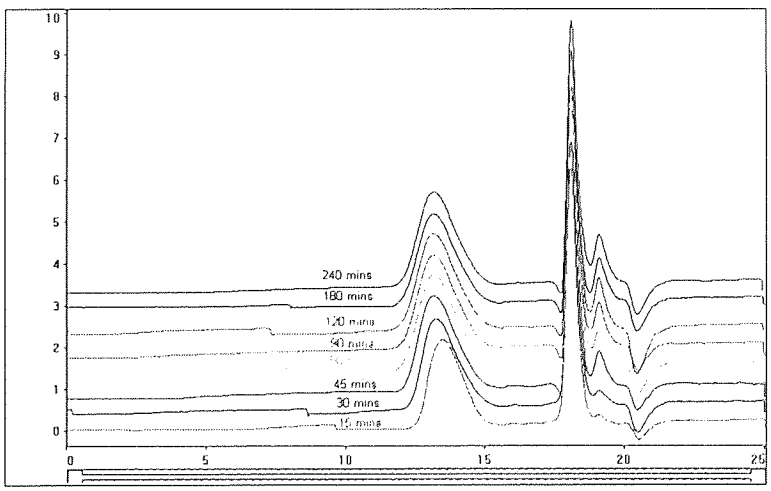

$[CuBr]_0 = 0.143$ mol dm^{-3}

Time/Minutes	%Conversion	Mn	Pdi
10	33.7	3880	1.21
20	69.1	6750	1.24
30	73.9	6930	1.28
60	72.3	7130	1.32
90	69.1	7200	1.34
185	79.0	7400	1.37

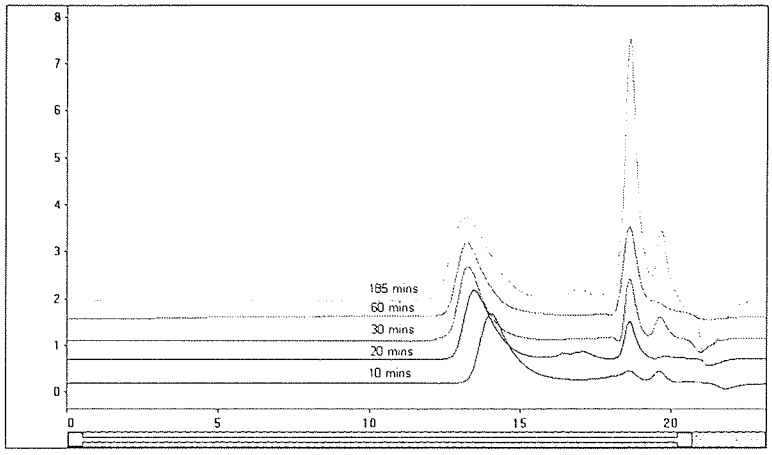

$[CuBr]_0 = 0.238$ mol dm^{-3}

Time/Minutes	%Conversion	Mn	PDi
10	48.8	6180	1.20
20	72.5	8390	1.22
30	78.6	9410	1.24
45	81.2	9950	1.27
60	85.6	10370	1.31
75	88.6	11220	1.33
90	91.0	11410	1.34

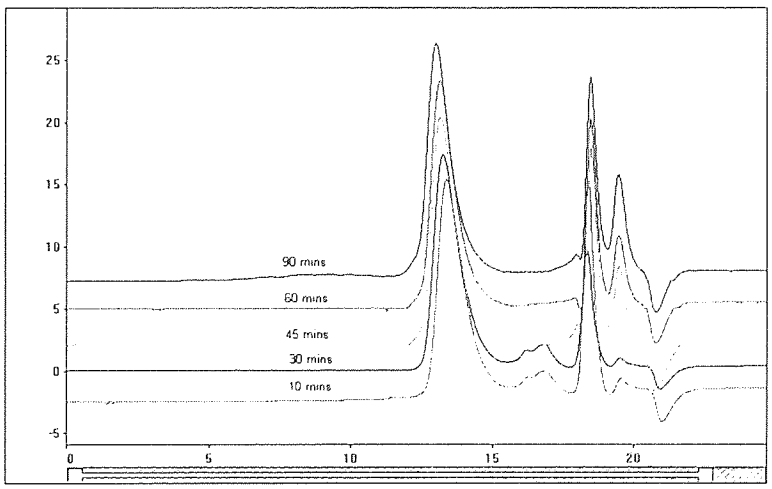

(b) DMF

$[CuBr]_0 = 0.0476$ mol dm^{-3}

See appendix 9(b).

$[CuBr]_0 = 0.0952$ mol dm^{-3}

Time/Minutes	%Conversion	Mn	PDi
10	20.7	3340	1.43
20	45.3	4060	1.39
45	61.4	5640	1.40
60	59.6	5720	1.36
90	65.0	6180	1.34
150	69.0	6290	1.43
180	71.1	6390	1.43

$[CuBr]_0 = 0.143$ mol dm^{-3}

Time/Minutes	%Conversion	Mn	PDi
10	26.3	2920	1.28
20	49.4	4320	1.33
30	62.5	5300	1.34
45	66.7	6120	1.37
60	83.3	7300	1.38
90	91.7	7600	1.60

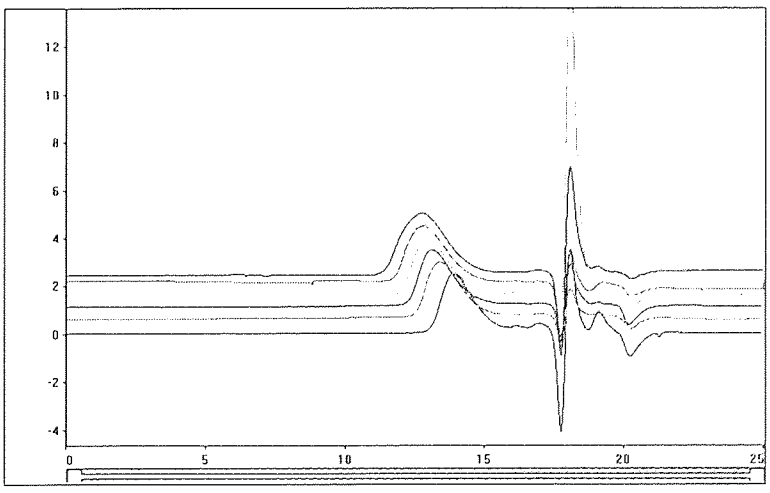

$[CuBr]_0 = 0.238$ mol dm^{-3}

Time/Minutes	%Conversion	Mn	PDi
10	49.3	4650	1.25
20	70.6	6860	1.28
30	71.4	6930	1.31
45	78.4	7210	1.33
60	84.6	8720	1.38
75	90.2	9460	1.41

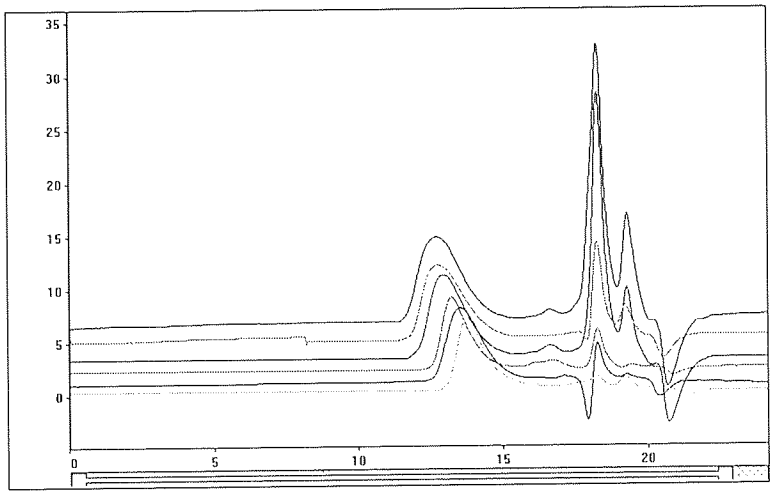

$[CuBr]_0 = 0.286$ mol dm^{-3}

Time/Minutes	%Conversion	Mn	PDi
5	31	2870	1.22
10	53	5680	1.23
20	76	7240	1.25
30	82	8400	1.27
45	89	9140	1.28
60	93	9530	1.28
75	96	9610	1.28